NUCLEATE POOL BOILING OF LIQUIDS AND THEIR MIXTURES ON COATED HORIZONTAL TUBES

Bibliography for Ph.D. Thesis

Submitted by

Chandra Kishore

Supervised by

Dr. V.K. Agarwal
Dr. Ravindra Bhargava

DEPARTMENT OF CHEMICAL ENGINEERING

INDIAN INSTITUTE OF TECHNOLOGY, ROORKEE

ROORKEE – 247667 (INDIA)

DECEMBER – 2013

ABSTRACT

The present investigation pertains to an experimental study on nucleate pool boiling of liquid and their binary and ternary mixtures on plain as well copper coated brass heating tubes at atmospheric and subatmospheric pressures. Basically, it deals with the effect of operating variable, namely heat flux, pressure and composition of mixture on heat transfer coefficient for the boiling of iso-propanol, methanol and distilled water and their binary and ternary mixture on a brass heating tube surface. Further, it also includes the effect of coating thickness along with other parameter for boiling of these liquids on brass heating tube surface coated with copper. Finally, a semi-empirical correlation for calculation of heat transfer coefficient of ternary mixture which is free from surface liquid combination factor has been developed.

Experiment has been carried out for saturated boiling of iso-propanol, methanol and distilled water and their binary and ternary mixtures on an electrically heated horizontal plain as well as copper coated brass heating tube surfaces. The heating tube is a brass cylinder having 18mm I.D., 30.02mm O.D. and 150 mm effective length it is heated by placing a laboratory made electric heater inside its wall and liquid temperature are measured by poly-tetrafluoro-ethylene (PTFE) coated 30 gauge copper-constantan calibrated thermocouples. The thermocouples are placed inside four holes drilled at a pitch circle diameter of 25mm in the wall thickness of heating tube for measurement of surface temperature. Similarly, thermocouple probes are placed in liquid pool corresponding to wall thermocouple positions in heating tube for the measurement of liquid temperature. A digital multimeter measures e.m.f of thermocouples. The composition of binary and ternary liquids mixtures and those of boiling liquid and vapour are measured by using HPLC system. A Novel Pack, C18 column of size 3.9 ×150 mm is used to measure the concentration of methanol and iso-propanol in the binary and ternary mixture. Power input to heater is increased gradually from 220 W- 500W in six steps and pressure from 45.40 kN/m^2 to 97.71 kN/m^2, three thickness of copper coating namely 15, 25 and 35 μm have been employed over a plain brass heating tube. The maximum uncertainity associate with the measured value of average heat transfer coefficient is of the order of ±1.12%

Experimental data for saturated boiling of distilled water on a plain as well as copper coated brass heating tube of various thicknesses at atmospheric and subatmospheric pressures

have been processed to obtain local as well as average heat transfer coefficient. Analysis of these experiment data show that surface temperature increases from bottom to side, side to top of heating tube for a given value of heat flux at atmospheric and subatmospheric pressures. However, liquid temperature remains uniformly constant at all values of heat flux for given pressure. Further, the local heat transfer coefficient increases from top to side, side to bottom position irrespective of heat flux and the variation in heat transfer coefficient is presented by $h_\phi \alpha q^{0.7}$. These observations are consistent for all the liquids of this investigation. Furthermore, average value of heat transfer coefficient of an uncoated heating tube vary according to the power law $h \alpha q^{0.7}$ at subatmospheric pressure of this investigation this in corroborated the finds of other investigators [A4, B6, B11, B12, C22, H6, K11, Y8] . A dimensional equation; $h = C_1 q^{0.7} p^{0.32}$ for the boiling of distilled water, methanol, iso-propanol on uncoated brass tube has been develop by regression analysis with a maximum error of ±8%, where C_1 is a constant whose values depends on the types of boiling liquid and heating surface characteristics. This dimensional equation has been modified to the following non dimensional form: $(h^* / h_1^*) = (P / P_1)^{0.32}$, it has been tested against data reported by various investigator [A2, B12, C12, C22, P8, V2, V12] for saturated boiling of other liquids on heating surfaces with different characteristics at various pressure and found to correlate them excellently with in error of -11 to +9%

Experimental data for pool boiling of methanol-distilled water, iso-propanol binary mixture at atmospheric and subatmospheric pressures on uncoated tube resulted in analogous behavior as that of pure liquids. The functional relationship of heat transfer coefficient with heat flux and pressures is same as observed for liquids and therefore a dimensional equation $h = C_2 q^{0.7} p^{0.32}$ for the boiling of binary mixture at atmospheric and subatmospheric pressures, has been developed. Further, this equation has also been reduced into non dimensional form $(h^* / h_1^*) = (P / P_1)^{0.32}$ alike, pure liquids and found to match the experimental data Pandey [P3], Alam [A2] with in error of -11 to +21%

Experimental data for pool boiling of distilled water-methanol-iso-propanol a ternary mixtures at atmospheric and subatmospheric pressure revealed similar boiling characteristics as that of pure liquids and their binary mixture. A functional relationship of heat transfer coefficient with heat flux and pressure has been developed by regression analysis which is a dimensional equation, $h = C_3 q^{0.67} p^{0.33}$. Further, above equation has been reduced into a non

dimensional form $(h^* / h_1^*) = (P / P_1)^{0.33}$ similar to, pure and binary mixture and found to match the experimental data of Nahar and Naess [N1] with in an error ranging from -12% to +9.5%.

A reduction in heat transfer coefficient has been observed for boiling of binary and ternary mixtures as compared to the weighted mean values of heat transfer coefficient of pure liquids present in the mixture. This behavior has been due to the occurrence of simultaneous heat and mass transfer in the process. Hence, and $(h / h_{id}) = (\Delta T_{id} / \Delta T) = [1 + | y_1 - x_1 | \sqrt{\alpha_1 / D_1} + | y_2 - x_2 | \sqrt{\alpha_2 / D_2}\,]^{-(0.73x1+0.36)}$ has been developed for the prediction of heat transfer coefficient of a ternary mixture. This equation correlates all the experimental data of this investigation within an error ±18% as well those obtained by other investigators [C22, F1, H8, S3, T5, T7] with an error of ±25%. Analysis of experimental data reveals that coating of copper on a brass tube enhances heat transfer for boiling distilled water at atmospheric and subatmospheric pressures. In fact enhancement is function of thickness of coating. It has also been found that for a given value of heat flux, heat transfer coefficient increases with increase in coating thickness and thereafter decreases. However, increase in heat transfer coefficient is not proportional to increase in coating thickness. A functional relationship amongst heat transfer coefficient, heat flux and pressure has been developed as $h = C_4 q^r p^s$, where the values of constant C_4 and exponents (r) and (s) depend upon heating surface characteristics and thickness of coating on brass heating tube surface. Further, enhancement on a 25 μm copper coated brass tube surface has been found to be maximum to the tune of 55% more than that of uncoated brass tube. Hence, a 25 μm thick copper coated tube has been selected to conduct experiment for the boiling of methanol, iso-propanol and their binary and ternary mixtures with distilled water. Boiling of iso-propanol, methanol on 25 μm thick coated heating tube resulted in same features as that of pure liquids. A correlation has been developed by regression analysis in dimensional form $h = C_4 q^v p^w$, where constant C_4 and (v) and (w) depend upon the boiling liquids. Further, boiling of methanol-distilled water and iso-propanol-distilled water, binary mixture on 25 μm thick copper coated tube at atmospheric and subatmospheric pressures, has also shown analogous behavior as observed on an uncoated tube. However, increase in magnitude of heat transfer coefficient has changed due to difference in physico-thermal properties of methanol, iso-propanol, distilled water and their binary mixture. A dimensional relationship $h = C_5 q^{0.57} p^{0.36}$ correlating heat transfer coefficient, heat flux and pressure, is of

the same form as obtained for liquid, where constant C_5 depend upon the composition in the mixture and heating surface characteristics. Furthermore, boiling of distilled water-methanol-iso-propanol ternary mixture on a 25 μm thick coated tube at atmospheric and subatmospheric pressure has shown similar trend as observed on a plain tube. A dimensional relationship $h = C_6 q^{0.59} p^{0.36}$ correlating heat transfer coefficient, heat flux and pressure is of the same form as obtain for liquids and their binary mixture, where constant C_6 depend upon the concentration of the highest component in the ternary mixture and the surface characteristics. In addition, it has been found that application of copper coating on brass heating tube surface does not change the highest composition (methanol) turnaround concentration. Hence, the correlation has been

$$(h / h_{id}) = (\Delta T_{id} / \Delta T) = [1 + | y_1 - x_1 | \sqrt{\alpha_1 / D_1} + | y_2 - x_2 | \sqrt{\alpha_2 / D_2}]^{-(0.73x1+0.36)}$$

developed for boiling of ternary mixture on a plain tube is also valid for boiling of those on a 25 μm thick copper coated heating tube as well. Further, this correlation has been compared against the experimental data for the boiling of ternary mixtures of this investigation on a 25μm thick copper coated tube and found to match with in an error of ± 18% and 20% at atmospheric and subatmospheric pressures, respectively.

ACKNOWLEDGEMENTS

I wish to express heartily deep sense of gratitude and indebtedness to my supervisors Dr. V.K Agarwal, professor and head of department. Dr. Ravindra Bhargava Associate professor. Department of Chemical Engineering, Indian Institute of Technology, Roorkee for their proper guidance, inspiration and encouragement throughout course of this work. Their efforts and immense care in going minutely through the manuscript thought provoking discussion and suggestions for its improvement are greatly acknowledged. In fact, I have no words to express my gratefulness towards my venerable supervisors for all the help received from time to time.

I am thankful to Prof. Shri Chand, Professor former Head of department, and Prof. Biskash Mohanty, Department of Chemical Engineering, IIT Roorkee for providing me the best of facilities during my research work. My sincere and grateful thanks are also due to Surendra Kumar, Professor, Prof.I.M Mishra, Prof. B. Prasad, Dr. R.P. Bharti, Assistant Professor, Dr. P. Mondal, Assistant Professor, Department of Chemical Engineering, IIT Roorkee for their kind assistance and encouragement.

Sincere thanks are due to Director, Institute Instrumentation centre, IIT Roorkee, and Mrs. Usha for their help during the acquisition of SEM photographs.

I would also like to thank M/S Anod Plasma Spray Limited, Kanpur (India). They provided copper coating over heating tubes and its coating thickness measurement.

A deep appreciation and enthusiastic association, cooperation and support provided by Praveen Pachuri, Dr. Mihir Kumar Das, M/S Mohammad Siraj Alam , former research scholar, for his help during my experimentation and fellow research scholars Somesh Bhambi, Umesh Kumar, Amit Rai, RaviKant , Richa gupta, , Praveen K.Toni, Nilambar, Vineet, for their help during correction and checking of manuscript.

I would like to express my sincere thanks to all staff members of all laboratories of Chemical Engineering department for their help provided from time to time during the entire period of this study. Mr.Raj Kumar, Vipin Ekka , Avind, Arvind Kumar, Vijay Singh, Satpal Singh, TaraChand, Bhatnagar, Akhilesh Sharma deserve special mention for their contributions during the experimentation.

My thanks are also due to my friends Mrs. & Mr.Surya Prakash, Mrs. & Mr. Somesh, for their help and moral support.

I express my sincere gratitude to Mrs. Suman Gupta and Mrs. Alka Agarwal for everlasting affection and encouragement during e ntire period o f the work.

I deeply express my heartiest regards to the ever ending heart felt affection to my reverend parents for their patience, love, encouragement and blessing without which it was not possible to complete my research work. Their faith in God and confidence make me to materialize their dream.

I am thankful to my, brother Dharemendra Kishore and sister in law for their affection and love.

Last but not the least I feel extremely grateful, to my wife, Sonia and my two little daughters nannu and mannu who bear all difficulties smiling during this doctoral programme and always stood along with me whenever required. Her patience, loving and caring nature made my work more effectively to complete this work. Her support is unforgettable.

I fully understand that the experience and knowledge gained during my research work of this doctoral program would be of immense utility for my carrier. This work was possible due to endless efforts of mine and also due to the blessings of my Almighty God, my parents, my guru and not the least my family and friends

Chapter – 1

INTRODUCTION

Nucleate pool boiling is a intensive area of heat transfer, and it finds wide applications in food, chemical, petrochemical, refrigeration, power generation, space and other allied industries. It is also becoming increasingly important in the modern era, where many intriguing problems imposed by scarcity of space, energy and materials etc. lead to the development of energy efficient and compact heat transfer equipment. One of the important factors which directly affect their design and economics is heat transfer coefficient. Hence, its precise determination is of vital significance.

Although numerous experimental and theoretical investigation covering various facets of nucleate pool boiling such as mechanism, design correlation, parameter effect on heat transfer rate etc. have been made during the 20^{th} century yet several problem still remains unsolved. One of them is the absence of generalized correlation which can be used for the design of boiling equipment irrespective of heating surface and liquid involved in the process. As a matter of fact, literature has some correlation which can be used for design of heat transfer equipment. However, each of them gives different values of heat transfer coefficient. This is quite natural as almost all of them are empirical or semi-empirical in nature and are valid for specific set of heating surface, liquids and operating condition for which they have been developed. Thus, there application to design is likely to provide erroneous results. Beside, some of them have been developed by using experimental data of flat plate surface which behave differently than tubular surface. In fact, boiling heat transfer on a flat surface is uniformly constant where as on cylindrical it is not so. Hence, the correlations based on flat surface cannot be directly applied for the design of boiling equipment containing tubular surfaces. In addition, most of the correlation does not include the effect of pressure as they are based on atmospheric pressure data only. Hence, their application to situation where heat sensitive liquids are boiled under vacuum to safe guard them against possible deterioration is not justified.

Due to advancement in technology in food processing and cryogenic industries, signal processing of micro electronics industries, exploitations of low heat flux non conventional energy sources and necessity to conserve material and energy resource, boiling heat transfer has become one of the most fascinating and dynamic field in thermal engineering research. The importance of enhanced boiling can be understood form its wide area of applicability. Its importance lies in the facts that it has been employed to augment performance of flooded evaporator in refrigeration system, in reboilers on distillation towers from non fouling service and in evaporator of cascade refrigeration system in refrigeration refineries and chemical process plant for cooling high power density components by improving cooling rate and there by lower start up and operational temperature of dissipating component to enhance their service life and reliability in the electronic industries, to augment heat transfer and to obtain compact design, air separation and gas processing industries and to reduce size and cost of new unit as well as energy related operating cost in heat exchanger. Accordingly many

techniques for enhancements of boiling heat transfer have been developed during last few decades. All of them may be classified into active, passive, compound technique. Active techniques include mechanical aids involving rotation, surface vibration, fluid vibration caused by ultrasound are oscillation in pressure, electrostatic field to the fluid, etc. and passive techniques include modified surfaces which refer to the coated, plated, painted or covered surface with another material; rough surfaces obtained by scoring, abrasive treatment rubbing with emery paper, pitting with corrosive chemical; then extended surfaces by the use of fins of different shape; displace device, swirled flow and coil tube and alike. Compound techniques include a combination of two or more active/ passive techniques simultaneously for enhancement of heat transfer rate such as coated over extended surfaces. Most of the active techniques are neither economic nor easy to implement outside the laboratory. Passive techniques seem to be of great significance for enhancement of heat transfer rate as fabrication of such surface is easy and do not require external energy for this purpose.

One of the important passive techniques involves modification of heating surface by altering their characteristics. These includes either /roughening or coating of metallic and non metallic materials over heating surfaces. Many investigators [B8, G1, G5, H4, M3, S1, V1, V12, W1] have used various non-metallic coating such as poly-tetrafluoro-ethyelne (PTFE), tetra-fluoro-ethylene (TFE), methane, paraffin carbon tetrachloride solution, etc, on heating surfaces and have reported substantial enhancement in boiling heat transfer rate. However, the surfaces coated with non-metallic materials have been found of limited durability because of their deterioration and surface's wetting characteristics. Therefore, such surfaces apparently do not seem to be suitable for commercial applications. On the other hand, the surfaces coated with metallic materials such as copper, silver, nickel, cadmium, bronze, zinc, tin, chromium, aluminum etc., as reported by various investigators [A1, B11, C5, C12, H5, N1, S7, T1, V10] have been found to last long to enhance heat transfer coefficient many folds as compared to non-metallic coated surfaces. Besides, it is also important to point out that the properties of coating material and techniques of coating influence heat transfer performance of the heating surface markedly. In fact, the heating surfaces coated with high thermal conductivity and high permeability materials provide better heat transfer performance than that of other coated materials. Another aspect is that, most of the investigations are confined to boiling of liquids- refrigerants, water, cryogenics and their mixtures at atmospheric pressure only. Therefore, it calls for an investigation to generate experimental data for boiling of industrially important liquids and mixtures at subatmospheric pressures on metallic coated heating surfaces and thereby to study the effect of various parameters on boiling heat transfer coefficient such as of heat flux, pressure, coating thickness and composition of liquid mixture and thereby, to develop a correlation free from surface liquid combination factor.

1.1 OBJECTIVES OF THE PRESENT STUDY

Keeping the above in view, an experimental investigation on nucleate pool boiling of saturated liquids and their binary and ternary mixtures on an electrically heated horizontal brass heating tube coated with various thickness of copper at atmospheric and subatmospheric pressures has been planned with the following objectives:

- To conduct experiments for nucleate pool boiling of saturated distilled water, methanol iso-propanol and their binary and ternary mixtures on a horizontal plain (uncoated) brass heating tube surface at atmospheric and subatmospheric pressures to determine the effects of operating parameters on local as well as average boiling heat transfer coefficients. Further, to develop a correlation of average heat transfer coefficient as a function of heat flux and pressures and thereby to recommend an equation, free from surface-liquid combination factor.

- To generate heat transfer data for nucleate pool boiling of distilled water on brass heating tube coated with various thickness of copper at atmospheric and subatmospheric pressure and to obtained the effect operating parameters heat flux, pressure, coating thickness on heat transfer coefficient and thereby to established correlation relating parameter with heat transfer coefficient for the identification of most suitable coated tube.

- To conduct experiments for saturated boiling of methanol, iso-propanol and various composition of methanol- distilled water, iso-propanol-distilled water binary mixture and methanol- iso-propanol- distilled water ternary mixture on a copper coated brass heating tube at atmospheric and subatmospheric pressures and thereby to obtain the effect of operating parameters- heat flux, pressures, and composition on heat transfer coefficient and to formulate correlations.

- To carry out a semi-theoretical analysis of nucleate pool boiling of liquids and their binary and ternary mixtures on both plain(uncoated) and copper coated surfaces for the prediction of heat transfer coefficient of binary and ternary liquid mixtures from that of pure liquids.

- To compare heat transfer coefficient of a coated heating tube surface with that of plain (uncoated) one to determine the percentage enhancement of heat transfer coefficient.

Chapter – 2

LITERATURE REVIEW

This chapter discusses literature pertaining to various aspects of nucleate pool boiling heat transfer and its enhancement. In fact, it includes important studies related to mechanism, dimensional and non-dimensional correlations developed by various investigators for saturated nucleate pool boiling of pure liquids and mixtures on uncoated and coated surfaces. It also briefly reviews enhancement of boiling heat transfer by the use of different passive techniques. Following sections are devoted to above aspects:

2.1 NUCLEATE POOL BOILING HEAT TRANSFER FROM A PLAIN HEATING SURFACE

Nucleate boiling heat transfer is an area of immense importance in academics as it finds wide application in industries involving vapour generating equipments. It has been an area of active research for nearly nine decades to understand its mechanism, the effect of operating and geometric parameters and to obtain empirical and semi-empirical correlations employed in design of boiling equipments. Probably, the systematic research in this area started with the pioneer work of Nukiyama [N8] who boiled distilled water on an electrically heated platinum wire submerged in it. He presented data in the form of a curve between heat flux and excess temperature (difference between temperature of platinum wire and temperature of liquid). The burning off the wire beyond a certain value of heat flux was observed and thus obtained a broken curve. However, he could not ascribe any reason for this behavior. Later, Drew and Mueller [D3] conducted experiments by using a temperature controlled heating surface and obtained a complete curve which is popularly known as boiling curve. Since then, many researchers [B11, K4, L3, W5] studied nucleate boiling and confirmed general shape of the boiling curve. They have also identified various regimes in it and governing mechanism to explain high rate of heat transfer associated with the boiling of liquids. As a result, large literature covering different aspects of nucleate

pool boiling has emerged. Some of the important investigations dealing with mechanism and design correlations are discussed here under:

2.1.1 Boiling heat transfer mechanism

Nucleate boiling is characterized by the formation of vapour-bubbles at preferred sites which are in the form of markings, cavities, depressions, etc. distributed randomly on the heating surface. The vapour-bubble grows in size on these sites and after attaining a maximum size detaches from the heating surface to travel in liquid pool and ultimately collapses at free surface of liquid. A void formed by the departure of vapour-bubble is immediately filled by the nearby cold liquid for the formation of next vapour bubble. This completes the ebullition cycle. A comprehensive work has been carried out by various researchers as discussed below on the factors involved in this cycle.

Madejski [M1] has shown analytically that nucleus of a vapour bubble is sphere only in the case of uniform superheat and flattened if there is a temperature gradient. Thus the liquid superheat at the wall needed for activation is greater than in case of uniform superheat.

Corty and Foust [C21] determined the relationship between the number of vapour nuclei which may expand into new bubbles and the superheat at which this may occur by experimentally studying the influence of the interface variables such as surface roughness, properties of the liquid and contact angle on nucleate boiling. He reported that the size and shape distribution of surface roughness, contact angle along with the properties of the liquid determine the relationship between the number of vapour nuclei which may expand into new bubbles and the superheat at which this may occur. Bankoff [B1] provided a quantitative procedure for determining the ability of a surface cavity of known shape and size to entrap gas or vapour in contact with a given liquid with a specified contact angle.

Griffith and Wallis [G5], Brown [B16] investigated the effect of different surface roughness values on the bubble nucleation. They agreed on the fact that diameter of cavity affects the degree of superheat required to initiate the boiling phenomenon and its shape affects the stability of boiling process. They recommended

the following correlation between superheat (ΔT_w) required and cavity nucleus radius r_c [B5, G1, G5]:

$$r_c = \frac{2\sigma T_{sat}}{\left(\frac{dp}{dT}\right)_s \Delta T_w} \tag{2.1}$$

However, Hsu [H10] and Han & Griffith [H4] argued that the value of superheat required for bubble initiation is far greater than that predicted by equation (2.1). They explained this phenomenon and supported their argument with their proposed model which is based on the hypothesis that nucleation sites cavities are activated principally due to transient conduction and subsequent replacement of superheated thermal layer around it. Hsu [H10] , Han & Griffith [H4], Griffith & Wallis [G5] and Rallis & Jawurek [R2] have developed criteria for size distribution of active nucleation sites. Han & Griffith [H4] gave the simplest and most useful expression of cavity radius as a function of surface temperature, liquid properties and the thermal layer thickness for bubble initiation which is reproduced below:

$$r_c = \frac{\delta (T_w - T_{sat})}{3 (T_w - T_\infty)} \left[1 \pm \sqrt{1 - \frac{12 (T_w - T_\infty)\, T_{sat}\, \sigma}{(T_w - T_{sat})^2\, \delta\, \rho_v\, \lambda}} \right] \tag{2.2}$$

This shows that there are two possible values of cavity radius which is capable of nucleation if filled with gas for any value of thermal layer thickness (δ). The above equation requires knowledge of thickness of superheated layer which was lacking at the time of formulation of equation.

Hsu & Graham [H11] and Cole [C18] reported that liquid must be superheated for nucleation. They have proposed the thermodynamic limit of superheat as upper boundary limit and kinetic limit of superheat as the lower boundary limit for the nucleation. They also observed that the initial superheat required to activate a cavity depends on the radius of the curvature of the interface within the cavity and the partial pressure of any non-condensable gas. In fact, when the initial radius of curvature is greater than or equal to cavity radius, the value of initial superheat can be determined by the cavity mouth radius. On the other hand, when the initial radius of curvature is less than the cavity radius, the value of initial superheat depends on the amount of vapour initially present, which can be obtained by the cavity geometry and the contact angle.

2.1.2 Nucleation Site Density

The phenomenon of boiling greatly depends upon the density of nucleation sites over the heating surface, the frequency of bubble formation at a given centre, the contact time of the bubbles and the magnitude and the shape of the bubbles have a great effect on the boiling phenomenon. It is now widely accepted that nucleation site density depends upon the surface physical properties, surface finish, wall superheat and liquid physical properties. Some notable studies on nucleation site density are discussed here.

Jakob [J3] & Leiner [L3] were apparently the first to study and find a linear relationship between the nucleation site density and the heat flux for boiling of water at low heat fluxes by usually counting the number of nucleation sites. However, later studies [D1, G1, G2, G5, K10, K17, N5, R7, S8, W6, W2, Y1] on relationship between nucleation site density and heat flux reveals that a non-linear relationship exists between these two quantities. The results of various investigators on non-linear relationship between nucleation site density and heat flux are listed in **Table 2.1.**

Mikic & Rohsenow [M7] were the first to relate active nucleation site density with the size of the cavities present on the commercial heating surface and expressed the functional dependence of active nucleation site density on cavity size as :

$$Na \sim \left[\frac{D_s}{D_c}\right]^m \tag{2.3}$$

Where D_s is the diameter of the largest cavity present on the surface, m is an empirical constant (= 6.5) and D_c is given by

$$D_c = \frac{4\sigma T_{sat}}{\rho_v h_{fg} \Delta T_w} \tag{2.4}$$

Table 2.1 presents the results from the literature for nucleation site density. The power of (Na) is different for the different correlation obtained by different researchers, since boiling is a surface phenomenon and nucleation site density depend upon surface properties (like roughness of surface, size of cavity and shape of cavity). As different researchers use different surfaces for the nucleate pool boiling, hence, it seems that difference in power of Na is bound to occur. Similar observations have been made by Hsu and Graham in their book' Transport Processes in Boiling and Two-Phase Systems: Including Near-Critical Fluids'.

Table 2.1 Important correlations of nucleation site density

Investigator	Relationship	Remark
Jakob [J3]	$q \propto Na$	$q < 56.783$ kW/m^2, Stainless steel-water
Gaertner [G1]	$q \propto Na^{0.47}$ $= 1400\ Na^{0.47}$	Nickel-Water solution on copper, $q < 94.638$ kW/m^2
Kurihara [K16]	$h \propto Na^{1/3}$	$q < 59.937$ kW/m^2, Copper/Glass-Water, Acetone, Carbon tetrachloride
Nishikawa & Urakawa [N6]	$h \propto Na^{1/3}$	Brass-Water, $q < 34.875$ kW/m^2
Gaertner [G2]	$Na \propto \exp(-k / T_w^{\,2})$	Copper-Water, $q < 184.799$ kW/m^2
Semeria [S8]	$Na \propto 0.012 q^2 p$	Water-Platinum, Stainless steel n in m^2, q in kW/m^2 pressure 3.04 to 101 bar
Gaertner [G2]	$q \propto Na^{2/3}$	$q < 184.799$ kW/m^2, Copper-Water
Kirby [K10]	$q \propto Na^{1/2}$ $q \propto Na^{0.73}$	Copper-Water, Glass-Water, $q < 310.943$ kW/m^2
Danilova & Tikhonov [D2]	$q \propto Na^{b}$	b = 4/9 for Freon-113, Stainless steel, b = 1/3 for Water, Stainless steel
Wang & Dhir [W2]	$q \propto Na^{1/2}$	Copper-Water, $q < 290$ kW/m^2

Kopp [K12] estimated the number of nucleation sites from a statistical description of a real surface, which compared well with his Na (Nucleate site density) data of mercury on a stainless steel surface with different roughness values.

Bier et al. [B14] obtained an expression for active nucleation site density from heat transfer data as:

$$\ln Na_{\max} = \ln(Na)\left[1-\left(\frac{D_c}{D_s}\right)^m\right] \tag{2.5}$$

Where, Na_{max} is the maximum value of Na occurring at $D_c = 0$. It was observed that the value of m was dependent on the procedure followed in preparing the surface. The value of 'm' was 0.42 and 0.26, respectively for chemically etched surface and on a turned surface with boiling of Freon-115 and Freon-11.

Studies were carried by Cornwell & Houston [C20] and Brown [B16] on active nucleation sites of copper surfaces for boiling of water at 1.013 bar and at low heat fluxes. The nature of the surface condition was varied from smooth to a scratched rough surface and the relation was established for the dependence of active site density on wall superheat as

$$Na \sim \Delta T_w^{4.5} \tag{2.6}$$

The proportionality constant in equation (2.6) increased with surface roughness. From the cavity size data obtained by electron microscope they also gave a relation between cavity size to total number of cavities present on the surface. The relation is given as under:

$$N_s \sim \frac{1}{D_c^2} \tag{2.7}$$

By taking the assumption that only conical cavities existed on the surface and that a minimum value of trapped gas was needed for nucleation they justified qualitatively the observed functional dependence of active site density on wall superheat by assuming that only conical cavities existed on the surface and that a minimum value of trapped gas was needed for nucleation.

Kocamustafaogullari & Ishii [K11] and Hibiki & Ishii [H5] correlated active nucleation site density data from literature by means of parametric study. They

assumed that both the surface conditions and thermo-physical properties of the liquid influences the active nucleation site density in pool boiling and developed following dimensionless correlation based on the data of water

Yang et al. [Y3] & Kim et al. [K7] predicted quantitatively the active nucleation sites from the knowledge of size and cone angle of the cavities actually present on the surface. They measured the probability density function of the cavity diameter and it was found to lie in the range of 0.65 to 6.2 μm by them and cone angle was determined using a scanning electron-microscope and a differential interference contrast microscope. They found the cavity size distribution fit satisfying the Poisson distribution where as half cone angle (ϕ_C) fits to normal distribution. They used Bankoff's [B1] criteria, i.e., $\beta > 2\phi_c$ for determination of cavities to trap gas. By combining the probability distribution function and criteria to trap gas, they related Na to average $\overline{N}_s$ on the surface as

$$Na = \overline{N}_S \int_0^{\beta/2} [(2\pi)^{1/2}]^{-1} \exp[-(\phi_C - \overline{\phi_C})^2/(2s^2)]\, d\phi_C \times \left(\int_{D_c}^{D_s} \lambda e^{-(\lambda D_c/s)} dD_c \right) \qquad (2.8)$$

Where $\overline{N}_s$ average density of cavities present on the surface, D_s is the diameter of largest cavity present on the surface, and λ and s are statistical parameters.

Barthau [B3] devised a simple optical method for counting the active nucleation sites. The method is found to be suitable for plain horizontal tube and for all transparent liquids. The method had been employed to measure active site density in pool boiling of R-114 at pressure of 1.50, 1.91 and 2.47 bar and heat fluxes up to 7×10^4 Wm^{-2} and succeeded in measuring up to 5000 sites per cm^2.

Wang & Dhir [W2] and Dhir & Liaw [D2] proposed an empirical correlation based on their experimental data to study the effect of contact angle on active nucleation site density. They carried out experiments on boiling of saturated water at atmospheric pressure on vertical copper surfaces with contact angle varying from 18^o to 90^o. The wetability (contact angle) of the surface was varied by controlling the degree of oxidation of the surface. The copper surfaces were prepared by following a well defined procedure and an electron microscope was employed to measure the cumulative number density of cavities and their shape were measured with an electron microscope. They found that the cavities that nucleate were mostly reservoir type rather

than the conical type. The actual cavity size was corrected by multiplying it with a shape factor $f_d\,(=0.89)$ to account for the irregular shape of the cavities. They correlated Na with corrected D_c for surfaces with $18^o \le \beta \le 90^o$ as

$$Na = 5.0 \times 10^5\,(1-\cos\beta)\,D_c^{-6.0} \tag{2.9}$$

Where the units of Na is in sites/cm^2 and D_c is in μm. The above equation is found to vary for $D_c < 5.8\ \mu m$, which corresponds to $\Delta T_w > 11.2\ ^oC$ for water at atmospheric pressure.

Benjamin & Balakrishnan [B5] investigated experimentally the surface-liquid interaction and its effect on nucleation site density during boiling of water, acetone, carbon tetrachloride and n-butanol at atmospheric pressure on aluminum and stainless steel surfaces with different surface finish obtained by polishing the surface with different grades of emery paper. They found that nucleation site density depends on the surface micro-roughness, the surface tension of the liquid, thermo-physical properties of the heating surface and the liquid and the wall superheat temperature. They proposed following correlation for nucleation site density.

$$Na = 218.8\ \mathrm{Pr}^{1.63}\left(\frac{1}{\gamma}\right)\Theta^{-0.4}\ \Delta T_W^3 \tag{2.10}$$

Where, $\gamma = \sqrt{\dfrac{k_s\ \rho_s\ C_{ps}}{k_c\ \rho_c\ C_{pl}}}$ and Θ, the dimensionless surface roughness parameter,

$$\Theta = 14.5 - 4.5\left(\frac{R_a P}{\sigma}\right) + \left(\frac{R_a P}{\sigma}\right)^{0.4}$$

Where, R_a is arithmetic average roughness in μm. They also validated above equation with their own data and that of other investigators [G1, G5, W1, Z5, Z6] within the following range of parameters:

$1.7 < Pr < 5$; $4.7 < r < 93$; $0.02\ \mu m < Ra < 1.17\ \mu m$;

$5k < \Delta T < 25k$; $13 \times 10^{-3}\ N/m < \sigma < 59 \times 10^{-3}\ N/m$; $2.2 < \Theta < 14$

Basu et al. [B4] studied the effect of contact angle on the active nucleation site density during sub-cooled flow boiling of water at atmospheric pressure on a vertical surface and proposed an empirical correlation based on their experimental data. They

used mirror-finished copper surfaces prepared by following a well defined procedure and changed the contact angle β to obtain the following relations:

$$Na = 0.34\,(1-\cos\beta)\,\Delta T_w^{2.0}, \quad \Delta T_{ONB} < \Delta T_w \le 15\,K \tag{2.11 a}$$

$$Na = 3.4\times10^{-5}\,(1-\cos\beta)\,\Delta T_w^{5.3}, \quad \Delta T_w \ge 15\,K \tag{2.11 b}$$

Where, units of Na and ΔT_w are site/cm^2 and K, respectively. The proposed correlation reproduced almost all their data on active nucleation site densities on surfaces having contact angle between 90^o and 30^o within $\pm 40\%$. The range of parameters covered for the flat plate test surfaces were

124 kg/(m^{2}s) < G < 886 kg/(m^{2}s), 6.6 < $\Delta T_{sub,in}$ < 52.5

$2.5\,W/m^2 < q_w < 96\,W/m^2$; $30^o < \theta < 90^o$

Recently, Hibiki & Ishii [H5] reviewed literature and presented a mechanistic model for active nucleation site density of knowing the size and cone angle distributions of cavities that are actually present on the surface. The proposed correlation of active nucleation site density was found to be a function of critical cavity size and contact angle as follows:

$$Na = \bar{N}a\left\{1-\exp\left(-\frac{\beta^2}{8\mu^2}\right)\right\}\left[\exp\left\{f(\rho^t)\frac{\lambda'}{r_c}\right\}-1\right] \tag{2.12}$$

Where,

$\bar{N}_a$ = average cavity density = 4.72 x 10^5 sites/m^2

μ and λ' are statistical parameter whose values are 0.722 rad and 2.50 x 10^{-6} m, respectively

r_c = critical cavity radius = $\dfrac{2\sigma\{1+(\rho_v/\rho_l)\}/p_l}{\exp\{h_{fg}(T_v-T_{sat})/(\bar{R}T_vT_{sat})\}-1}$

$f(\rho^t) = -0.01064 + 0.48246\,\rho^t - 0.22712\,\rho^{t^2} + 0.05468\,\rho^{t^3}$

non-dimensional density difference $\rho^t = \log(\rho^*)$

and $\rho^* = \dfrac{\rho_v - \rho_l}{\rho_v}$ and $\bar{R}$ is the gas constant based on molecular weight.

The above developed correlation has been validated by various active nucleation site density data taken for pool boiling and convective flow boiling systems. It gives fairly good predictions over a wide range of flow conditions.

$0\ kg/(m^2 s) \le G \le 886\ kg/(m^2 s);\ 0.101\ MPa \le p \le 19.8\ MPa;$

$5^o < \phi_s < 90^o\ ;\ 1.00 \times 10^4\ \text{sites/m}^2 \le Na \le 1.51 \times 10^{10}\ \text{sites/m}^2$

Sakashita & Kumada [S3] recommended following semi-empirical equation for predicting nucleation site density for boiling of liquids on a heating surface at various pressures:

$$Na = C_{ls}\left[Ja^{3/10} r_c^{3/10}\left(\frac{1}{r_c}\right)\right]^s \quad \text{for reduced pressure, } P_r \le 0.2, \qquad (2.13\ a)$$

and $$Na = C_{lshp}\left[Ja^{3/20} r_c^{3/20}\left(\frac{1}{r_c}\right)\right]^s \quad \text{for } P_r \ge 0.2 \qquad (2.13\ b)$$

Where, constant, C_{ls}, C_{lshp} and exponent, s have been determined by using experimental data of Fujita & Nishikawa [F5].

2.1.3 Bubble departure diameter

Diameter of a vapor-bubble at the time of its departure from a heating surface plays vital role in the evaluation of heat transfer rate as the volume of bubble represents the amount of latent heat removed from a cavity on the heating surface. The growth and detachment of a bubble from a heating surface depends upon various forces such as buoyancy force; surface tension force ; excess pressure force ; inertia force and viscous drag force acting on it. So, a large number of expressions for bubble departure diameter are available in literature based on balancing of different forces acting on a bubble.

First expression for bubble departure diameter was given by Fritz [F4] he assumed a static balance between the buoyancy force and surface tension force while the inertia and drag forces were assumed to be negligible:

$$D_b = 0.0208\ \beta \sqrt{\frac{\sigma}{g(\rho_l - \rho_v)}} \qquad (2.14)$$

Where β is the contact angle in degree.

However, later on a modification was carried out in above equation by incorporating a growth rate term $(dR/dz)_d$ due to its inability to predict departure diameter of bubble having high growth rates. The modified equation is as follows:

$$D_b = 0.071\beta \sqrt{\frac{2\sigma g_c}{g(\rho_l - \rho_v)}} \left[1 + 0.239 \left(\frac{dR}{dz} \right)_d \right] \tag{2.15}$$

Zuber [Z6] obtained following expression for bubble departure diameter by equating buoyancy and surface tension force,

$$D_b = \left[\frac{6 g_c \sigma}{g(\rho_l - \rho_v) q} \right]^{1/3} \tag{2.16}$$

Roll and Myers [R8] developed following equation for the calculation of bubble departure diameter by considering buoyancy, liquid inertia and viscous drag forces

$$D_b = (\pi Ja^2 \alpha_i)^{2/3} \left[3 \left(C_d - \frac{11}{12} \right) \right]^{1/3} \tag{2.17}$$

Semeria [S8] suggested separate expressions for bubble departure diameter which are valid for a definite range of pressure, as follows:

$$D_b = 0.241 P^{-0.5} \qquad \text{for } 2 < P < 20 \text{ atm} \tag{2.19 a}$$

and $$D_b = 26.8 P^{-1.5} \qquad \text{for } 20 < P < 110 \text{ atm} \tag{2.19 b}$$

Where D_b is in inches.

Nishikawa and Urakawa [N6] proposed following expression for bubble departure diameter for a pressure range of 300 to 760 mm Hg.

$$D_b = 0.672\ P^{-0.575} \tag{2.20}$$

Where D_b is in inch and P in lbf/in^2 (absolute).

Cole and Shulman [C17] obtained experimental values of departure diameters at atmospheric and sub-atmospheric pressures and tested these against available expressions for bubble departure diameter. They found that these expressions fail to correlate experimental data particularly at sub atmospheric pressures and therefore recommended following empirical expression

$$D_b = \frac{133.3}{P} \left[\frac{\sigma}{g(\rho_l - \rho_v)} \right] \tag{2.21}$$

Where P is in kN/m^2.

Cole [C18] proposed following expression for bubble departure diameter indicating that it is directly proportional to wall superheat

$$D_b = 4\times10^{-2}\ Ja\sqrt{\frac{\sigma}{g(\rho_l-\rho_v)}} \tag{2.22}$$

Cole and Rohsenow [C16] found that correlation proposed by Cole and Shulman [C17] and Cole [C18] failed to determine departure diameter at pressure greater than one atmosphere because value of Jakob number could not be calculated due to lack of wall superheat temperature at pressure greater than one atmosphere. Therefore, they proposed following expression for the determination of departure diameter with modified Jakob number.

$$D_b = C(Ja^*)^{5/4}\sqrt{\frac{\sigma}{g(\rho_l-\rho_v)}} \tag{2.23}$$

Where, $Ja^* = \dfrac{\rho_l\, C_{pl}\, T_{sat}}{\rho_v\, \lambda}$

The value of constant C in **Eq. (2.24)** has been found to be 1.5×10^{-4} for water and 4.65 x 10^{-4} for other liquids. Equation (2.24) has been found to correlate experimental data of and Gaertner [G1].

Saini et al. [S1] made an exhaustive evaluation of various forces for different values of Jakob number and recommended following equations of bubble departure diameter for various ranges of Jakob number:

i. For Ja $\leq$ 16,

i. $$D_b = \left(\frac{\alpha_l^{\,2}}{g}\right)^{1/3}\left(\frac{6.6C_{pl}\Delta T_W\sigma}{\alpha_l q}\right)^{1/3} \tag{2.24}$$

ii. For 16 < Ja < 100

i. $$D_b = \left(\frac{\alpha_l^{\,2}}{g}\right)^{1/3} 1.33\left(Ja\right)^{4/3}\left(1.22\pm\left[1+2.67\frac{C_{pl}\Delta T_W\sigma}{\alpha_l q\, Ja^4}\right]^{0.5}\right)^{2/3} \tag{2.25}$$

Equation (2.24, 2.25) has been obtained by considering buoyancy, surface tension, liquid inertia and viscous drag forces acting on the bubble.

iii. For Ja $\geq$ 100

$$\text{i.} \quad D_b = 9.18\,Ja\left(\frac{\alpha_l^{\,2}}{g}\right)^{1/3} \tag{2.26}$$

Equation (2.26) have been obtained by considering buoyancy, liquid inertia and viscous drag forces acting on the bubble.

Yang et al. [Y2] carried out experiments and recommended following equation for bubble departure diameter:

$$D_b = 3.0557\times10^{3}\,\frac{\rho_l}{\rho_v}\,\frac{\sqrt{C_{pl}T_s}}{\lambda}\,\frac{\alpha_l\,Pr_l^{3/5}}{\eta} \tag{2.27}$$

Where, $\eta = \psi Ja^{0.3}$,

ψ = modified factor for bubble growth $= \dfrac{C^2}{\phi^{0.4}\,[f(c)]^{2/3}}$, $C = \dfrac{R_b}{R}$

$$\phi = \left[\,1+\frac{1}{2}\left(\frac{\pi}{6\,Ja}\right)^{2/3}+\frac{\pi}{6\,Ja}\,\right]$$

and $$f(c) = 1-\frac{3}{4}\left(1-\sqrt{1-C^2}\right)^2+\frac{1}{4}\left(1-\sqrt{1-C^2}\right)^3$$

Where, R_b represents the radius of the liquid micro layer underneath the bubble.

Recently, Chen et al. [C8] conducted experiment for saturated boiling of propane and iso-butane on plain tube and propane on enhanced tube surface and gave separate expressions of bubble departure diameter for plain and enhanced surfaces, as follows:

i. For plain tube, the departure diameter has been obtained by considering buoyancy and surface tension force as follows:

$$D_b = C\left[\frac{\sigma}{g\,(\rho_l-\rho_v)}\right]^n$$

(2.28 a)

Where, C is an empirical coefficient depending on fluid and experimental conditions. For perfect spherical bubble the value of exponent n was taken as 1/2 and for non-spherical bubble this value was between 1/3 and 1/2.

ii. For enhanced tubes, the departure diameter has been obtained by taking buoyancy force, drag force and liquid inertia force

$$D_b = 0.86\left[\frac{\sigma}{g(\rho_l - \rho_v)}\right]^{\frac{1}{2}} \qquad (2.28\ b)$$

2.1.4 Bubble Emission Frequency

The computation of bubble emission frequency requires the knowledge of following parameters such as waiting period and growth period in an ebullition cycle. However, due to certain difficulties involved in the measurement of these parameters, bubble emission frequency has been expressed by the relationship between frequency and some other measurable parameters.

Jakob [J3] investigated bubble emission frequency in nucleate pool boiling of distilled water and carbon tetrachloride photographically for low to moderate range of heat flux and reported that product of bubble emission frequency and bubble departure diameter, (f & D_b) is constant at a given pressure. Subsequently, many equations for it have been developed. One of the common forms is:

$$fD_b^{\,n} = C \qquad (2.29)$$

The value of n has been found to vary and lies in between 0.5 to 3 whereas the value of constant, C depends upon the properties of liquid and vapour , system pressure and temperature difference.

Zuber [Z5] proposed following equation for the prediction of product of mean bubble emission and mean bubble departure diameter in terms of physical properties of liquid and vapour:

$$f\,D_b = 0.59\left[\frac{\sigma g\ (\rho_l - \rho_v)}{\rho_l^2}\right]^{1/4} \qquad (2.30)$$

However, Eq. (2.30) has been found to fit the experimental data only over a limited range of bubble diameters.

Rallis & Jawurek [R2] concluded that at a given value of heat flux and pressure, the product of bubble emission frequency and departure volume, ($f.\ V_b$) remains a constant for each bubble within a reasonable limit. They also showed that $f.V_b$ increases with heat flux.

2.2 BOILING HEAT TRANSFER CORRELATIONS

A review of literature on nucleate boiling heat transfer indicates that many researchers presented their work in the form of correlations to predict heat transfer coefficient for nucleate pool boiling of liquids. These correlations are either empirical or semi-empirical in nature and are presented in both dimensional and non-dimensional form. The correlation in dimensional form generally expresses heat transfer coefficient as a function of heat flux and system pressure through heating surface characteristic as represented in the following equation:

$$h = C\, q^m\, p^n \tag{2.31}$$

Where, the values of C and exponents m and n depend upon different surface-liquid combination used.

A thorough attempt has been made by various researchers to incorporate the set of non-dimensional group to correlate their experimental data. The works carried out by all these researchers lead to development of following general non-dimensional equation for boiling heat transfer coefficient

$$h = B\, Re^{n_1}\, Pr^{n_2}\, Ga^{n_3}\, k_p^{n_4}\, k_t^{n_5} \tag{2.32}$$

Where, the value of constant B and exponents of various non-dimensional group depends upon the system conditions used in the investigation.

2.2.1 Dimensional heat transfer correlations:

Jakob [J2] and Leiner [L2] were probably the first to introduce an empirical correlation for boiling heat transfer coefficient of liquids. They proposed following correlation by considering the effect of turbulence caused by bubble nucleation, growth and detachment from heating surface:

$$\frac{h\, D_{b,1}}{k_1} = \phi\left[\left(\frac{n\, A_{b1}}{A}\right)\left(\frac{V_{b2}}{V_{b1}}\right)\right] \tag{2.33}$$

Where $D_{b,1}$ is the bubble departure diameter at one atmosphere pressure, $A_{b,1}$ is the area accepted by each bubble, A is the total area of heating surface, $V_{b,1}$ is the volume of bubble at the time of its departure from heating surface and $V_{b,2}$ is the volume of bubble at the time of break off at free liquid surface. Later, they modified above

equation by assuming the shape of vapour bubble to be spherical and introducing the term bubble frequency as given below:

$$\frac{h D_{b,1}}{k_1} = \phi\left[\left(\frac{q}{\rho_v \lambda}\right)\left(\frac{1}{f D_{b,1}}\right)\right] \tag{2.34}$$

A further photographic study carried out by Jakob [J4] indicated that the value of $f D_{b,1}$ remains nearly same for the liquids used in the investigation. Jakob & Linke [J2] also modified Fritz gave equation and presented the above correlation in the following modified form:

$$\frac{h}{k_l}\sqrt{\frac{\sigma}{\rho_l}} = 30\left[\frac{q}{\rho_v \lambda D_{b,1} f}\right]^{0.8} \tag{2.35}$$

The above equation is not applicable for other than atmospheric pressure because the bubble departure diameter and emission frequency were calculated at 1 atm pressure only. Therefore, Jakob [J3] further modified above correlation to incorporate the effect of pressure and presented following correlation.

$$\frac{h}{k_l}\sqrt{\frac{\sigma}{(\rho_l - \rho_v)g}} = 31.6\,\frac{\nu_{l,a}}{\nu_l}\left[\frac{\rho_{l,a}}{\rho_l}\frac{\sigma}{\sigma_a}\frac{q}{\rho_{v,a}\lambda_a D_{b,a} f}\right]^{0.8} \tag{2.36}$$

Where subscript a refers to conditions at atmospheric pressure.

Cryder and Finalborgo [C22] boiled several liquids on a 1.5 inch brass tube at atmospheric and subatmospheric pressure. The liquid used by them were distilled water, methanol, n-butanol, carbon tetrachloride, kerosene and aqueous solution, e.g., 26.3% glycerol solution, 10.1% sodium sulphate solution and 24.2% sodium chloride solution. The heat flux was varied from 425 to 2360 Btu/h and pressure from 20 to 110 kPa. They correlated their experimental data by following equations

$$\log h = a + 2.5 \log \Delta t + bt \tag{2.37}$$

$$\log \frac{h}{h_n} = b\,(t - t_n) \tag{2.38}$$

Where, values of a and b are constants, which depends upon physico-thermal properties of liquid and their values are given in **Table 2.2**. It is the temperature of boiling liquid in ^{o}F, h is the heat transfer coefficient in Btu/hr ft ^{o}F and subscript n refers to atmospheric pressure.

Bonilla & Perry [B15] carried out experimental investigation for nucleate pool boiling of pure liquids namely water, ethanol, n-butanol, acetone and their mixture at different pressures. They correlate their experimental data by modifying the correlation given by Jakob [J3] and Lin, [L4] as follows

$$\frac{h}{k_l}\sqrt{\frac{\sigma}{\rho_l}} = 16.6\left(\frac{\nu_a}{\nu}\right)\left[\left(\frac{\sigma}{\sigma_a}\right)\left(\frac{\rho_{l,a}}{\rho_l}\right)\left(\frac{q}{\rho_{va}\,\lambda\, W}\right)\right]^{0.73}\left[\left(\frac{C_p\,\mu}{k_l}\right)\right]^{0.5} \qquad (2.39)$$

Where W is Jakob constant (= 918 ft/h).

Table 2.2 Values of constant (a) and (b) in Eq. (2.37 & 2.38)

Liquids	a	b
Water	-2.05	0.014
Methanol	-2.23	0.015
n-butanol	-4.06	0.014
Carbon tetrachloride	-2.57	0.012
Kerosene	-5.15	0.012
26.3% glycerine solution	-2.65	0.015
10.1% sodium sulphate solution	-2.62	0.016
24.2% sodium chloride solution	-3.61	0.017

Gupta and Varshney [G8] carried out a semi-empirical analysis for determining the nucleate pool boiling heat transfer coefficient from heated surface to saturated pure liquids at atmospheric and sub-atmospheric pressures. He used conceptual model of Nishikawa & Urakawa [N6] and recommended separate equation for distilled water and organic liquid for calculation of (h/h_0).

For distilled water

$$\frac{h}{h_o} = \left(\frac{p}{p_o}\right)^{-0.355}\left(\frac{\lambda}{\lambda_o}\right)^{4.5}\left(\frac{T_{so}}{T_s}\right)^{2.833}\left(\frac{k_{lo}}{k_{lo}}\right)^{0.7}\left(\frac{\rho_l}{\rho_{lo}}\right)^{0.25}\left(\frac{\rho_v}{\rho_{vo}}\right)\left(\frac{\sigma_o}{\sigma}\right)^{1.25}\left(\frac{C_{plo}}{C_{pl}}\right)^{2.133}\left(\frac{q}{q_o}\right) \qquad (2.40)$$

For organic liquids

$$\frac{h}{h_o} = \left(\frac{p}{p_o}\right)^{-0.194} \left(\frac{\lambda}{\lambda_o}\right)^{4.5} \left(\frac{T_{so}}{T_s}\right)^{2.833} \left(\frac{k_{lo}}{k_l}\right)^{0.7} \left(\frac{\rho_l}{\rho_{lo}}\right)^{0.25} \left(\frac{\rho_v}{\rho_{vo}}\right) \left(\frac{\sigma_o}{\sigma}\right)^{1.25} \left(\frac{C_{plo}}{C_{pl}}\right)^{2.133} \left(\frac{q}{q_o}\right) \quad (2.41)$$

Where, subscript 'o' refers to atmospheric condition. He correlated his own experimental data and those of other investigators excellently within an error approximation of $\pm 10\%$.

Cooper [C19] reviewed existing boiling correlations from literature and recommended following equation for predicting heat transfer coefficient in terms of reduced pressure, heat flux, surface roughness and molecular weight of liquid:

$$h = CP_r^{(0.12-0.2\log R_a)}(-\log P_r)^{-0.55} M^{-0.5} q^{0.67} \quad (2.42)$$

Where, R_a represents roughness of the heating surface. The value of constant, C is 55 for copper plate or stainless steel cylinders and 93.5 for copper cylinders. He also suggested that one can assume the value of R_a as 1 μm if this value is not available.

2.2.2 Non-dimensional heat transfer correlation

Rohsenow [R6] did carried out a comprehensive research investigation on pool boiling of liquids at atmospheric pressure to obtain a generalized correlation on pool boiling heat transfer. Using Jakob [J3] & Lin et al. [L4] assumption that product of frequency and bubble departure diameter is constant and he suggested following equation on the basis of their experimental data:

$$\frac{1}{St} = C_{sf}\ Re^r\ Pr^s \quad (2.43)$$

Where, C_{sf} is a constant and termed as surface-liquid combination factor. He obtained the values of exponent r and s as 0.33 and 1.7 respectively by validating his correlation with experimental data of Cichelli & Bonilla [C13] and Cryder & Finalborgo [C22]. Rohsenow [R6] pointed out that the value of exponent s is equal to one for water and for other liquids it varies between 1.3 to 0.8. The value of surface-liquid combination factor C_{sf} has been given by Vachon et al. [V1] & Pioro [P7] for various surface-liquid combinations used in experimentation. These are given in **Table – 2.3**. Rice and Calus [R4] obtained experimental data for heat transfer during pool boiling of saturated pure liquids and their binary mixtures on a nickel-aluminum wire of 0.0315 cm diameter and 8.9 cm effective length at atmospheric pressure. They took

the following pure liquids used in their investigation (water, toluene, carbon tetrachloride, methanol, iso-propanol and n-propanol). Based on their experimental data, following correlation was recommended by them for boiling heat transfer coefficient.

$$\frac{Nu}{K_p^{0.7}}\left[\frac{T_s}{T_{sw}}\right]^4 = E\,Pe_B^{0.7} \qquad (2.44)$$

Where, T_s is the absolute boiling temperature of the liquid, $T_{s,w}$ is the absolute boiling temperature of water of the system pressure and E is a constant whose value depends upon the heating surface characteristics of heating medium. The value of constant E in above equation as obtained by various investigators, are listed in **Table. 2.4.**

Table 2.3 Values of C_{sf} for various surface-liquid combinations

Liquid -surface combination	C_{sf}
Water on polished copper	0.0128
Water on ground and polished stainless steal	0.0080
Water on mechanically polished stainless steel	0.0132
Water on nickel	0.0060
Water on platinum	0.0130
Water on brass	0.0060
n-Pentane on polished copper	0.0154
n-Pentane on polished nickel	0.0127
n-Pentane on chromium	0.0150
Carbon tetrachloride on polished copper	0.0070
Benzene on chromium	0.0100
Ethyl alcohol on chromium	0.0027
Isopropyl alcohol on copper	0.0025

n-Butyl alcohol on polished copper	0.0030
35% K_2 CO_3 on copper	0.0054

Table 2.4 Value of constant E in Eq. (2.44)

Investigators	Heating surface	E x 10^4
Rice & Calus [R4]	Nickel-aluminium wire	6.30
Cichelli & Bonilla [C13]	copper polished with electroplated chromium	3.92

Gorenflo [G3] and Gorenflo et al. [G4] did modification in the Mostinski's [M8] modified dimensional correlation and presented it in non-dimensional form as follows:

$$\frac{h}{h_o} = F(P)\left(\frac{q}{q_o}\right)^n \left(\frac{R_a}{R_{ao}}\right)^{0.133} \qquad (2.45)$$

Where, subscript, o refers to the conditions of heat flux of 20 kW/m^2, reduced pressure of 0.1 and surface roughness of 0.4 μm. The expressions for F(P) and n are given below for different fluids:

$$\left.\begin{aligned} F(P) &= 1.2P_r^{0.27} + 2.5P_r + \frac{P_r}{1-P_r} \\ \text{and} \quad n &= 0.9 - 0.3P_r^{0.3} \end{aligned}\right\} \quad \text{for all liquids other than water and helium}$$

$$\left.\begin{aligned} F(P) &= 1.73P_r^{0.27} + \left(6.1 + \frac{0.68}{1-P_r}\right)P_r^2 \\ \text{and} \quad n &= 0.9 - 0.3P_r^{0.15} \end{aligned}\right\} \quad \text{for water and helium}$$

Later on further revision was carried out in Eq. (2.45) by Leiner & Gorenflo [L2] and Leiner [L3] further revised Eq. (2.45) and recommended following non-dimensional correlation which is applicable for all fluids and surfaces was given by them:

$$h^* = AF'(P)q^{*n}R^{*0.133} \tag{2.46}$$

Where, h^*, q^* and R^* are the non-dimensional form of heat transfer coefficient, heat flux and surface roughness, respectively which are given below along with other parameters:

$$h^* = \frac{h}{P_c(\overline{R}/MT_c)^{1/2}};\ q^* = \frac{q}{p_c(\overline{R}T_c/M)^{1/2}};\ R^* = \frac{R_{ap}}{(\overline{R}T_c/p_cN_{Av})^{1/3}}$$

and $$F'(P) = 43000^{(n-0.75)}\left[1.2P_r^{0.27} + (2.5 + \frac{1}{1-P_r})P_r\right]$$

The constant, A and exponent n is expressed as:

$$A = 0.6161C^{0.1512}K^{0.4894} \quad \text{and} \quad n = 0.9 - 0.3P_r^{0.15}$$

Where, $C = \frac{(\overline{C}_{pl})_{(P_r=0.1)}}{\overline{R}}$, $K = \frac{T_c \ln P_r}{(1-T_c)}$, $(\overline{C}_{pl})_{(P_r=0.1)}$ is the molar heat capacity at reduced pressure of 0.1, N_{Av} represent Avogadro number and R_{ap} is the arithmetic mean deviation of surface roughness.

Cornwell and Houston [C20] generated a correlation for pool boiling on tubes under conditions of fully developed nucleate boiling on normal engineering surfaces. The correlation can only be applied to water, refrigerants and organic liquids boiling on tubes of 8.50 mm in diameter. They used regression analysis on experimental data points of earlier investigators to obtain following correlation:

$$Nu = A\ F(P)\ Re_b^{0.67}\ Pr^{0.4} \tag{2.47}$$

Where, $A = 9.7\ P_c^{0.5}$ with critical pressure P_c in bars and $F(P)$ is given by a pressure term used by Mostinski [M9] as follows:

$$F(P) = 1.8\,P_r^{0.17} + 4\,P_r^{1.2} + 10\,P_r^{10}$$

Where, $P_r = \frac{P}{P_c}$

Some of the important non-dimensional empirical correlations developed by different investigators for heat transfer coefficient during nucleate boiling of liquids are listed in **Table – 2.5.**

2.3 BOILING HEAT TRANSFER ON ENHANCED SURFACES

The study of boiling phenomenon was not restricted to plain surfaces but was further moved a step ahead. The development of enhanced heat transfer surfaces is based on the improved understanding of boiling phenomena on plain surfaces which led to the ideas about modification of certain aspects of the process to increase boiling heat transfer coefficient. Thus, earlier works, in an attempt to enhance boiling heat transfer rate, firmly established that nucleate pool boiling heat transfer is dependent on the micro-geometry of the boiling surface. This realization gave rise to the development of special surfaces to enhance boiling heat transfer rate owing to space limitation, to conserve the material of construction and to operate equipment at higher heat fluxes with low wall superheat. Consequently, a number of techniques have been developed to enhance the boiling heat transfer either by altering the surface characteristics or by means of external aids. Bergles [B9], Webb [W4] and Thome [T5] have proposed eleven classifications to categorize various enhancement techniques for nucleate boiling under active, passive and compound techniques.

- Passive techniques include modified surfaces which refer to the coated, plated, painted or covered surfaces with another material; rough surfaces obtained by scoring, abrasive treatment, rubbing with emery paper, pitting with corrosive chemicals; extended surfaces by the use of fins of any shape; surface tension devices which involve wicks and slots in surface wall to transport liquid to the evaporation zone; additives to the liquids; displaced enhancement devices; swirl flow devices and coiled tubes.
- Active techniques include introduction of mechanical aids involving rotation, scraping or wiping of the heated surfaces; surface vibration; fluid vibration caused by ultrasound or oscillation in pressure; electrostatic field by the application of A.C. or D.C. fields to the boiling liquids; water jet impingement for cooling of hot fluid and suction or injection by the introduction of gas to the evaporating fluid through a porous surface.
- Compound techniques involves the utilization of both active and passive techniques simultaneously for the enhancement of heat transfer rate such as coating over extended surfaces.
- Among various techniques, passive technique which includes modified surfaces

has assumed significance for enhancement of heat transfer rate due to ease of fabrication, non requirement of external energy and simplicity associated as compared to other techniques. Consequently, enormous information is now available in literature on different facets of boiling of liquids from various modified surfaces. Following section provides a review of the literature concerning boiling on such surfaces:

Table 2.5 Non-dimensional correlations of nucleate pool boiling of liquids by various investigators

Name of investigator	Correlation
Cryder & Finalborgo[C22]	$Nu*_b = 0.38\,(\mathrm{Pr})^{0.425}\left(\frac{\Delta T\, S^2\, d^2\, k_l}{\mu_l^3}\right)^{2.34}\left(\frac{\mu^2}{S\, d\, \sigma}\right)^{1.65}$ where S = specific gravity
McNelly [M5]	$Nu*_b = 0.255\left(\frac{qd}{\mu\lambda}\right)^{0.69}\left(\frac{Pd}{\sigma}\right)^{0.31}(Bu)^{0.33}\,\mathrm{Pr}^{0.69}$
Bliss et al. [B14]	$\frac{h\sqrt{\sigma}}{\sqrt{k_L}\,\rho_l^{0.82}} = 4J^{0.41}\,g^{-0.09}(10)^{-3.2}\left(\frac{q^{0.68}\,c_L^{0.5}}{\rho_v^{0.5}\,\lambda^{0.27}}\right)$
Kruzhilin and Averin[K13]	$Nu*_b = 0.082\,(Pe_b)^{0.7}\,(\mathrm{Pr})^{-0.5}\,(K_t)^{0.377}$
Kutateladze [K17]	$Nu*_B = 7.0\times10^{-4}(Pe_B)^{0.7}(\mathrm{Pr})^{-0.35}(K_p)^{0.7}$
Alam and Varshney [A4]	$Nu*_B = 0.084(Pe_B)^{0.6}(K_{sub})^{-0.5}(K_t)^{0.37}$
Tolubinskii and Kostanchuk [T8]	$Nu*_B = 75\,K^{0.7}\,\mathrm{Pr}^{-0.2}$
Gupta et al. [G7]	$Nu*_b = 1.391\left(Pe\right)_b^{0.7}\left(\frac{\rho_v}{\rho_l}\right)(\mathrm{Pr})^{-0.32}$

2.3.1 Boiling on roughened surfaces

Jacob [J1] and Fritz [F4] were apparently the first to study the effect of surface finish on nucleate pool boiling heat transfer. They boiled water at atmospheric pressure

over a sand blasted surface and a surface having cross-hatched pattern. It has groves 0.172 mm wide and 0.152 mm deep at spacing of 0.447 mm. They reported that the sand blasted surface increased the boiling heat transfer coefficient up to about 25% at a fixed heat flux and at fixed wall super heat; performance could be increased more than four fold. The machined groove surface yielded boiling coefficient about 3 times higher than that of a smooth chrome plate surface. However their final observation indicated that boiling performance of these surfaces diminished quite rapidly with time, tending towards the smooth chrome plate's boiling curve. Later it was observed that similar results of enhancement and subsequent deterioration for a tube with 0.4 mm square grooves cut at 1.6 mm spacing.

Corty and Foust [C21] worked extensively to study the effect of surface roughness on nucleate boiling heat transfer performance. They prepared the nickel surfaces by rubbing emery paper, which resulted in scratches over the surface ranging from 0.254 to 25.4 μm across by 0.05 to 0.635 μm deep. Their result indicated that although roughness resulted in higher heat transfer rates but higher roughness has little effect on boiling process.

In a similar investigation, Berenson [B7] boiled n-pentane on a copper plate, whose surface was roughened using different grades of emery paper. He reported a large enhancement in boiling heat transfer with increased roughness.

Kurihara and Myers [K16] studied the relationship between the boiling site density and the boiling heat transfer coefficient for water and several organic fluids boiling on a surface roughened with emery paper. Using successive grades of grit size, they also investigated the effect of surface roughness on the nucleation site density. Their results for five test fluids showed that $h \propto (Na)^{0.43}$. Thus, they concluded that boiling heat transfer coefficient increases with the increase in surface roughness and boiling site density increased concurrently.

Marto and Rohsenow [M3] boiled sodium on a horizontal stainless steel disk and studied the effect of surface roughness and system pressure on pool boiling heat transfer. They came to conclusion that wall superheat decreases with increase in roughness owing to increased number of nucleation sites. Also, increased pressure resulted in lower wall superheat for nucleation.

Chowdhury and Winterton [C12] carried out experiment using a simple quenching technique on 18 mm diameter and 40 mm long with aluminum copper cylinder immersed in saturated water or methanol. They had given particular emphasis on the role of surface roughness, measured by centre line average (CLA), and surface energy, measured by contact angle, on nucleate boiling heat transfer. Their result showed that for copper cylinder quenched in methanol, nucleate boiling heat transfer improved steadily with increased roughness. But for aluminum cylinder that were first roughened and then anodized, when quenched in water, become virtually independent of measured roughness in spite of the fact that anodizing process did not affect the roughness. They came to conclusion that it is not only the surface roughness in itself that influences nucleate boiling but the number of active nucleation site. They also reported that low contact angle increases the heat flux at a given superheat.

Luke [L6] conducted experiments with propane boiling on copper and mild steel tube to study the influence of surface roughness on heat transfer coefficient. The copper tube of 8 mm diameter was roughened with 400 grade emery paper whereas the mild steel tube of 7.6 mm diameter was sand blasted to get fine or sand blasted surface. Number of experiments were carried out for a wide range of heat fluxes and saturation pressures (10% to 80% of the critical pressure). The activation of nucleation sites, the bubble departure diameter D_b and frequency f, site density Na, were also examined by high speed video technique. He reported that the effect of surface roughness on heat transfer decreases with increasing pressure and with increasing heat flux. He also found that production of densities of active nucleation site using the theoretical model could be improved for high heat fluxes at low pressures by incorporating the additional heat transfer $Q_{\delta V}$ by evaporation into the bubbles sliding along the tube surfaces.

Chun and Kang [C11] in an effort for improvement in the thermal design of passive residual heat removal system of advanced light water reactor carried out number of experiments to determine the combined effects of tube diameter, surface roughness and tube orientation on nucleate pool boiling heat transfer. They performed the experiments for boiling of water at atmospheric pressure over tubes of four different diameters (9.7, 14.0, 19.06 and 25.4 mm) having roughness 15.1, 26.2 and 60.9 nm and with two different orientations (horizontal and vertical). They reported that with increase in surface roughness heat transfer coefficient increases for both horizontal and

vertical tubes. However, the effect of surface roughness on nucleate boiling heat transfer for vertical tube was observed to be more than for that for horizontal tubes. Also, for a given surface roughness of the tube, the effect of the tube diameter on the nucleate pool boiling heat transfer for vertical tube is more than that for horizontal tubes.

Stephan & Preusser [S16] has experimental study for heat transfer in nucleate boiling for various compositions for binary and ternary mixtures of acetone, methanol and water. The horizontal tube of nickel of 14mm O.D., 550 mm length and mean roughness of about 0.25 μm. The experimental data observed a reduction in heat transfer for the boiling of mixtures as compared to that with pure liquids. Further, this effect explained by that more readily evaporation for the volatile component fraction in binary mixtures which creates a concentration difference between the liquid and the vapor bubble building the diffusion resistance in addition to the thermal resistance. The heat transfer coefficient varies withthe mole fraction present in both phases. It increases with the difference in the mole fractions and vanishes at azeotropic points.

They further recommended that the data of corresponding binary mixtures can be used in the expanded formulation of the correlation of Stephan & Korner [S15] for the rough estimation of the heat transfer coefficient in the boiling of ternary mixtures. Further, an equation is derived for determining the heat transfer coefficient in the boiling of mixtures, in which non-linear variation of the material properties has been taken into consideration.

Stephan & Abdelsalam [S14] made an attempt to put forward the guidelines for predicting the heat transfer coefficient during natural convection boiling. Method of regression analysis was applied over 5000 experimental data points for natural convection boiling in order to establish the correlation with wide application. As observed from the analysis, these data can be represented by subdividing the substances into four groups based on their physico-thermal properties. The four groups were water, hydrocarbons, cryogenic fluids and refrigerants. Each set of groups employed a different set of dimensionless numbers to correlate the data for the calculation of approximate value of heat transfer coefficient.

In a recent study, Kang [K6] performed experiments for the saturated boiling of water at atmospheric pressure to determine the effect of surface roughness on pool

boiling heat transfer. In his study, he took three different diameter (9.7, 19.05 and 25.4 mm) tubes having different lengths (100, 300 and 530 mm) and two different surface roughnesses (15.1 and 60.9 nm) to obtain the heat flux (q'') versus wall superheat (ΔT) data for various combinations of test parameters. He also studied the effect of tube orientation at horizontal $\theta = 0^o$, inclined $\theta = 45^o$ and vertical $\theta = 90^o$ on boiling heat transfer coefficient. The main outcomes of his study are as follows:

i. Increased surface roughness gives no reasonable change in pool boiling heat transfer for horizontal tubes in high heat flux region. However, its effect magnified with the change in orientation of the tube from horizontal to the vertical.

ii. The increase in the ratio of a tube length to its diameter magnified the effect of surface roughness on pool boiling heat transfer for vertically installed tubes.

Based on his work he suggested that the net effect of surface roughness on pool boiling heat transfer can be observed if following parameters such as active nucleation site density, intensity of liquid agitation, bubble agglomeration on the surface and the formation of a rapid flow around the tube surface are considered.

2.3.2 Extended surfaces

During the late 1940s and early 1950s, extensive research work has been carried out on boiling on the outside of the integral low finned tube by Kajikawa et al. [K4], Robinson and Katz [R5], Meyers and Katz [M6]. In the first study, nucleate pool boiling curves were plotted for hexane, and isobutane boiling on a single horizontal tube with 14.5 fpi, fins per inch(fpi). In the subsequent studies, four horizontal low finned tubes arranged in a vertical array were tested. These copper tubes had 19.5 fpi with an 18.8 mm diameter over the fins and a base diameter of 16.00 mm, producing a wetted surface area on the finned tube 2.7 times that of a comparable plain tube with the same diameter as at the top of the fins. The common conclusion by all these researchers was that the fins not only increased the surface area but also modified the boiling process to increase the performance.

Kriby and Westwater [K10] carried out the studies on ways to improve the boiling performance of extended surfaces. They optimized the shape of a single spine for pool boiling by minimizing its volume. They considered the situation in which the

heated wall at the base of the fin was sufficiently hot to be in the film boiling regime. Due to the large variation in boiling heat transfer coefficient with wall superheat over the entire range of the pool boiling curve, turnip-shaped fins were found to be the most effective. However, they found that this is not the optimum shape when only nucleate pool boiling occurs on the fin, or when fins are in close proximity to one another.

Webb [W6] generated and patented a simple and effective method to augment the boiling performance by rotating the low finned tube in a chuck and running a bending or rolling tool over the fins. Due to this action the fins were deformed and a continuous reentrant channel was made. The tip of the tool was designed to produce the desired degree of bending and a controlled gap size from the tip of one fin to the back of the next one. He found that when R-11 boiled over the surface, the heat transfer performance falls down rapidly with a gap size beyond the range from 0.0254 to 0.127 mm (0.001 to 0.005 inch) and that the preferable gap size was between 0.038 and 0.089 mm (0.0015 and 0.0035 inch). He also noted that a tube with whose fins were 0.76 mm high and 0.254 mm thick produced essentially the same performance as another tube with twice the fin density and fins half as high and half as thick.

Danilova and Tikhonov [D2] attempted to explore an optimum low finned tube for boiling R-12 and R-22 using single tube tests. They found that tubes having dimension 27.7 fpi outperformed a 12.5 fpi tube by about 20%. The subsequent bundle tests carried out by them, however, showed only marginal improvement, i.e., about 5%. In addition, the optimum fin density for one fluid at one pressure is probably not optimum at another pressure for a different fluid. From the experimental studies carried out by them it is concluded that optimum fin density of a low finned tube have less importance than similar studies of the higher performance boiling tubes, which tend to have high single tube performance than one similar to their bundle boiling values.

Bergles [B8] investigated the effect of gap size between fin tips of tubes with T-shaped fins. They carried out experiments with water and R-113 for copper tubes with gap sizes of 0.15, 0.25, 0.35 and 0.55 mm. The copper tubes tested were of diameter ranging between 25.4 mm to 26.00 mm with fin density of (18.8 fpi) and a fin height of 1.1 mm. They found that for R-113, maximum performance occurred at a gap width of about 0.25 mm and for water, the maximum performance was obtained with a gap width of 0.40 mm. They also investigated the liquid flows around the tube by injecting

a blue dye into the liquid around the circumference of the tube with hypodermic needle and syringe and observed that there were distinct locations where liquid tends to enter the reentrant channel, namely at the bottom at both sides and at the top dead centre.

Kumar [K15] did work on boiling of distilled water, and iso-propanol on finned heating tube having different fin spacing (8, 12, 16, 19 and 24 fpi) at various heat flux and pressures. He found that heat transfer coefficient increases with increase in fpi and became maximum at 19 fpi and thereafter decreases due to interference between fins.

Fantozzi et al. [F1] made an experimental and theoretical evaluation on boiling heat transfer from finned surfaces to dielectric fluids. They reported that for a finned surface made up of aluminum alloy having fin height of 10 mm, a thermal dissipation equivalent to the value of boiling water at atmospheric pressure was obtained when the surface was coupled with pool boiling controlled return. They also theoretically proposed method to estimate critical heat flux related to finned surface and an approach to perform a nearly optimum design of fins and fin array in pool boiling.

2.3.3 Boiling on Non- Metallic Coated Surfaces

Griffith & Wallis [G5] for the first time reported that a thin coating of non-metallic material (wax) improves the nucleation characteristics. Water was boiled on a single conical cavity of 0.08 mm diameter, formed by piercing a phonograph needle into the heating surface. They observed that this type of coating has no effect on the temperature at which cavity nucleates. They also found that it is easy to maintain boiling and get reproducible results from paraffin cavity than from a clean metal surface and thus concluded that un-wetted cavities are more stable than wetted surface.

Young and Hummel [Y8] utilized spray coated Teflon stainless steel surface having 30-60 spots/m^2 with each spot of 0.25 mm diameter or less for the boiling of water. They found an enhancement in boiling heat transfer with a nucleation occurring at $\Delta T < 0.5$ K. Their study showed that the performance of the pitted surface has been marginally better than the smooth surface when both surfaces have Teflon spots. They argued that it is undesirable to have Teflon coat over the entire surface as blanket formation of vapour took place over a large area of the surface and thereby results in reduction in the heat transfer coefficient.

Gaertner [G2] in a similar type of work, performed experiment by covering the inside surface of artificial nucleation site with a non-wetting material. He boiled water

on different surfaces having closely spaced nucleation sites formed with the help of needle sharp punches and parallel scratches. The surface containing the artificial sites was coated over with the low surface energy material and then removed from the flat surface by abrasion, leaving a thin film of the material deposited in each cavity. He found that coated surface promotes boiling at lower superheat and remained active for much longer time. On the other hand, heat transfer coefficient reduced considerably when the coating was left on the entire surface owing to the same reason as explained by Young and Hummel [Y8].

Bergles et al. [B9] argued that Teflon spotting method is effective only for surface-liquid combinations that have high interfacial surface energy, e.g., when the liquid normally wets the surface. They confirmed this in their tests with refrigerants, which have low surface tension and large contact angles (e.g., 40 ^{o}). Their result showed that the Teflon spotting method did not favourably affect the boiling performance of the refrigerants.

Marto and Rohsenov [M3] boiled liquid nitrogen on a flat copper heating surface coated with grease and Teflon. The coating done by grease significantly decreases heat transfer coefficient while coating with teflon material show very little effect on heat transfer coefficient.

Vachon et al. [V1] carried out experiments for nucleate pool boiling of water at atmospheric pressure on a stainless steel surface coated with Teflon of 7.6, 30.4 and 35.6 μm thickness using green enamel. Coating of stainless steel surface is carried out using spray technique. Results indicate a considerable enhancement in heat transfer coefficient for 7.6 μm thick coating. However, heat transfer coefficient decreases with increase in coating thickness because of their insulating effect. Further, they have also correlated their experimental data by **Eq. (2.43)**, Rohsenow correlation. **Table 2.6** lists the values of constant, C_{sf} and exponents, r and s of **Eq. (2.43)** as obtained by them for different Teflon coating thikness as well as uncoated surface.

Table 2.6 Values of constant, C_{sf} and exponents, r and s of Eq. (2.43) due to Vachon et al. [V1]

Liquid-surface combination	C_{sf}	r	s

Water-stainless steel	0.0141	0.25	1.0
Water-7.6 μm teflon coat	0.0071	0.26	1.0
Water-30.4 μm teflon coat	0.0269	0.71	1.0
Water-35.6 μm teflon coat	0.0523	0.87	1.0

Warner et al. [W3] investigated the effect of plasma deposited tetrafluoroethylene (TFE) coating over copper surface for the boiling of liquid nitrogen Their result reveals that heat transfer coefficient of coated surface is five times more than that over an uncoated surface for the same temperature difference. Thicker coating provides higher heat transfer rate as it has many nucleation sites for activating bubbles. It is also found that transition from nucleate to film boiling is much slower for TFE coated surface than that for an uncoated one.

Hinrichs et al. [H6] used plasma deposited polymers on copper heating surface for the boiling of water under atmospheric pressure. Copper surface coated with Tetrafluoroethylene (TFE) and methane were used by them. Their findings showed that an 18 nm thick coating of TFE enhances heat transfer rate while 150 nm thick coating reduces heat transfer rate. The enhancement of heat transfer rate was explained by surface energy effect. They explained this phenomenon saying that the chemical potential of the liquid in the cavity increases due to high interfacial surface energy which results in the reduction of wall superheat required for incipience of nucleation. On the basis of above argument and contact angle data for water over TFE and methane coated surface, they showed that 18 nm thick coated heating surface enhances nucleation as observed by the experimental results. However, 15 nm methane coated surface reduces nucleation due to attainment of lower interfacial surface energy and unable to alter the chemical potential of the liquid in cavity enough to enhance the boiling. Further, they also stated that as the coating thickness increases there is a decrease in the nucleation sites due to deactivation of some of boiling sites and concluded that enhanced boiling is a strong function of surface energy.

Vittala et al. [V11] carried out work on nucleate pool boiling of distilled water on brass heating tubes having surface coated with PTFE at atmospheric and sub-atmospheric pressures. The tube surface coating was done with PTFE for different

thicknesses viz. 21, 39 and 51μm. The significant enhancement in heat transfer coefficient due to PTFE coating on tube surface was observed. However, enhancement in heat transfer coefficient was found to be a function of heat flux, pressure and coating thickness. Similar results were obtained during the boiling of alcohols (ethanol, methanol and isopropanol) on PTFE coated tubes.

Bhaumik [B12] recently carried out work on distilled water, benzene and toluene at atmospheric and sub-atmospheric pressure over plain and PTFE coated stainless steel heating tubes. Five coating thicknesses, e.g., 14, 27, 30, 45 and 50 μm were used. He reported an increase in boiling heat transfer coefficient for tube having 14 μm thick coating at all pressures. However, plain tube outperforms all PTFE coated tube for boiling of benzene and toluene at atmospheric as well as sub-atmospheric pressures.

2.3.4 Boiling on metal coated surfaces

Alam et al. [A2] carried out experimental study for pure and binary liquid mixture of methanol, methanol- distilled water on stainless steel tube coated with various thickness of copper coating and effect of various parameter heat flux, concentration of volatile component at atmospheric and sub-atmospheric pressure. He reported an increase in boiling heat transfer coefficient for tube having 43 μm thick copper coating heating tube at all pressures.

Bonilla & Perry [B15] used gold /chromium plated copper surface and aged copper surface for boiling ethanol, water, acetone & their mixtures. They found that the plating of chromium /gold on copper surface results in higher heat transfer coefficient than that on aged surface.

Cichelli & Bonilla [C13] studied the effect of chromium coating on copper surface for boiling of water, ethanol, benzene, propane, n-heptane, n-pentane and their mixtures. Electroplating technique was used to obtain thickness of 0.002 inch of chromium on copper surface. They found power law, $h \propto q^{0.7}$ to hold good. However experiments depicts the lower value of heat transfer coefficient on scaled surfaces than on cleaned surface.

Milton [M8] at union carbide carried out work on boiling of liquid oxygen at atmospheric pressure over the copper surface coated with a thin porous layer of nickel. This coating produced a large number of active boiling sites and gave a twenty times enhancement in the boiling heat transfer coefficient at atmospheric pressure. His work also shows that coating with copper material on the surface in comparison to nickel results in an additional improvement in heat transfer coefficient.

Bliss et al. [B14] in an attempt to investigate the effect of plating material observed that boiling behavior of different coated materials is not singly due to thermal properties of plated material and the base material has no impact over boiling from such coated surfaces. They boiled water under atmospheric condition over stainless steel tube coated with copper, zinc, tin, nickel, cadmium & chromium. Thickness of plated material for all specimens in the experiment was about 0.005 inch. Their work revealed that copper and chromium coatings have enhanced heat transfer coefficient by 200 – 300 % where as zinc, nickel, cadmium and tin plating results in a reduction in heat transfer coefficient.

Magrini & Nannei [M2] did work on the saturated boiling of water over epoxy-resin rods electroplated with copper, silver, zinc, nickel and tin under atmospheric pressure. The dimensions of the heating surface were of 10 mm in diameter and 190 mm in length and coating thickness of 5 to 250 microns was varied over it. The average surface roughness was of the order of 0.7 to 1.0 micron. Their work led to conclusion that heat transfer coefficient increases with decrease in thickness of coating in case of lower thermal conductivity coating material such as zinc, tin & nickel surfaces. The heat transfer coefficient enhancement was found to be 500 to 700 percent in case of nickel or tin and 100 percent for zinc. They further observed that when coating thickness exceeds a certain limiting value, the influence of coating thickness on the heat transfer coefficient become negligible. This limiting value is found to be approximately 70 μm for zinc and 15 μm for both nickel & tin. No appreciable effect of coating thickness on heat transfer coefficient was observed for higher thermal conductivity material such as copper & silver.

Nishikawa and Ito [N5] investigated the effect of particle size and coating layer thickness over porous surfaces for boiling of R-11 and R-113 on an 18 mm diameter horizontal tube. Sintered spherical shaped copper and bronze particles were used for the

coating of heating tubes. The particle size of bronze varied from 0.1 to 1 mm and the porosity of the surface ranges in between 38% to 71%.Particles of diameter 250 μm were found to depict better performance in comparison to particles of other diameters (100, 500, 750 and 1000 μm). When copper coating thickness was four times the particle diameter, highest heat transfer coefficient obtained in the region of $10<q<100$ kW/m^2. Further, coating of spherical bronze particles on heating tube demonstrates marginal effect on boiling heat transfer coefficient. However, when coating thickness was taken four times the particle diameter highest boiling heat transfer coefficient was observed for $q> 50$ kW/m^2.

Nakayama et al. [N2] investigated heat transfer performance of various structured enhanced surfaces composed of interconnected internal cavities in the form of tunnels and small pores connecting the pool of liquid and the tunnel. They carried out experiments for boiling of water, R-11 and liquid nitrogen at atmospheric pressure on these structured surfaces and found that surface structure having pore diameter of around 0.1 mm is highly efficient in bringing 80-90% reduction of wall superheat required to transfer same heat flux as that on plain surface. They observed that latent heat flux is a significant contributor to enhancement of heat transfer coefficient. An analytical model was also generated on the basis of interconnecting cavities that remain in contact with the liquid outside the porous matrix and found it to be in well agreement with experimental data.

In another work Nakayama et al. [N3] investigated the effect of pore diameter of porous surfaces and pressure on the saturated boiling of R-11. Surfaces having pore diameters of 50, 100 and 150 μm and pressures of 0.04, 0.1 and 0.23 MPa were taken for investigation. They investigated different combinations of pore diameter and pressure and observed that if pores of different sizes are present on the surface, the most populous pore govern the rate of heat transfer for heat flux greater than 30-40 kW/m^2. However, for low heat flux value, pore of largest size play important role in heat transfer. They postulated that intense bubble formation does not necessarily yield a high rate of heat transfer. Further, they also concluded that liquid suction and evaporation inside the cavities probable describe the mechanism of boiling with small temperature difference. They reported that surfaces having pores of diameter 100 or 150 μm with number density of 252/cm^2 have shown remarkably good heat transfer

performance at a system pressure of 0.23 MPa.

Kajikawa et al. [K4] studied heat transfer performances of metal fiber sintered stainless steel tubes for boiling of R-11. Stainless steel fiber was characterized based on the following parameters viz. metal fiber diameter, amount of metal fiber, web/area and porosity. Twenty six types of surface configurations were studied with diameter of fiber ranging from 4 to 50 mm, amount of metal fiber web/area ranging from 0.08 to 2.0 kg/m^2 and porosity ranging from 50 t0 80%. Experimental work indicates a ten-fold enhancement in heat transfer coefficient for sintered surfaces in comparison to that on a smooth surface. It was also observed that heat transfer coefficient varies with thickness of porous coating and an optimum value of thickness exists. Besides this, they also reported that apart from thickness, diameter of fiber used for sintering and porosity also influence heat transfer coefficient considerably. Further, metal fiber sintered surface clad with titanium film has shown an improvement over sintered surfaces and it was proposed to be suitable for Ocean thermal energy conversion system.

Afgan et al. [A1] carried out experiments to investigate heat transfer during boiling of water, ethanol and R-113 from porous surfaces at atmospheric pressure. Sintering process was employed for preparation of heating tubes of Cr-Ni Stainless Steel. Sintering process over a single Cr-Ni Stainless steel surface was carried with titanium porous layer. Dendrite shaped and spherical 63-100 μm particles were sintered. The porosity of the surface varied from 30% to 70% and porous layer thickness varied from 0.45 to 2.2 mm, respectively. They obtained boiling curves of different shapes depending on the mode of operation namely, bubble mode, transient mode and film formation mode. However, authors did not suggest any criterion for any mode of boiling. In bubble mode, boiling took place at small temperature difference. At high heat flux, a vapour film develops at the base of the porous layer. Thus, a qualitative change of mechanism of bubble boiling occurs. They found that for surfaces with thick porous layers, the transition to this new mode of boiling occurs at critical heat flux values 2 to 3 times greater than that for smooth surface.

Jung et. al. [J8] investigated the pool boiling heat transfer of a flat copper surface and two metal coated surface (UNB#1, UNB#2) in R-11 with surface orientations varying from horizontally facing upward (0^0), to vertical (90^0), to horizontally facing downward (180^0). A flat 7.8 cm diameter test surface was used. The

coarse emery paper was used for the preparation of plain copper surface by polishing where as the enhanced surfaces were prepared by depositing metal particles on plain mild steel plates. They found 2-3 times higher heat transfer coefficient for the enhanced surfaces (UNB#1 & UNB#2) at constant heat flux as compared to the plain copper surface in the fully developed nucleate boiling regime. For all surfaces under observation, the super heat decreases by 15-25 % as the inclination angle changes from 0^0 to 165^0 in the relatively low heat flux range i.e. 10-40 kW/m^2. Beyond this heat flux range, the super heat remains constant regardless of the surface orientation.

Lu & Chang [L5] investigated the problem of boiling heat transfer from a porous layer sintered on a horizontal heating surface for laminar to turbulent region. They determined the effect of various parameters such as porous layer particle diameter, pore size distribution porosity, and properties of liquid on boiling heat transfer rate. They employed Ergun equation for pressure drop in granular beds and solved for different cases of dry out of the bed. On the basis of this, they found that for thick porous bed, thickness does not alter the heat transfer coefficient whereas for thin bed, it plays an important role. Further, experiments were performed by boiling methanol over copper heating surface coated with porous matrix and validated their model with their experimental data.

Hongji & Li [H7] studied pool boiling of water and ethyl alcohol from porous surfaces prepared by sintering spherical bronze powder particles of 16 different sizes over the copper surface at atmospheric pressure. Their result revealed that heat transfer coefficient of prepared surfaces increases by 3 -10 times that on a plain surface. Also a model was proposed by them based on annular countercurrent two-phase flow in porous surface enabling explanation to enhanced boiling on porous surfaces. Their model can be expressed by the following equations:

For $3 < \left(\frac{\delta}{d_p}\right) < 10$

$$Nu = 34.34\left(\frac{Re}{We}\right)^{0.5089} (S_r)^{-0.4757} (Pr)^{0.4335} \left(\frac{\delta}{d_p}\right)^{-0.6913} \left(\frac{\rho_l}{\rho_v}\right)^{0.3427} \quad (2.53)$$

and for $10 < \left(\frac{\delta}{d_p}\right) < 40$

$$Nu = 0.3318 \left(\frac{Re}{We}\right)^{0.2253} (S_r)^{0.1309} (Pr)^{1.041} \left(\frac{\delta}{d_p}\right)^{-0.7993} \left(\frac{\rho_l}{\rho_v}\right)^{0.7583} \quad (2.54)$$

Where, S_r is the superheat ratio criteria which is equal to $\frac{(C_{pl}\,\Delta T)}{\lambda}$ and $\left(\frac{Re}{We}\right)$ is equal to $\frac{q\mu_l}{g\,\lambda\,\sigma\,\varepsilon}$.

Equations (2.55) & (2.56) have been validated by the experimental data for the boiling of distilled water and ethanol.

Tehvir [T1] studied the effect of coating aluminium particles onto the surface of aluminium rod of 22 mm diameter by plasma spraying method for the boiling of R-113 and liquid nitrogen at atmospheric pressure. Eight samples were taken by him for study and heat flux was varied from low value to burn out condition. Pore diameter varied from 6 to 14.2 μm, porosity from 26 to 37% and porous layer thickness varied from 0.15 to 1.5mm respectively. He concluded from the formation and vaporisation conditions of liquid macro layer at near burn out heat fluxes that the influence of porous coating on the condition of liquid suction is essential. Also the period of macro layer evaporation extended which in turn delays the boiling crisis due to liquid absorbed by porous coating during the contact period with bulk liquid was observed by him.

Tehvir et al. [T2] investigated and carried experiments on a wide range of porous surfaces to find the relationship between the effectiveness of heat transfer and structural parameters of a plasma sprayed coating for nucleate pool boiling of R-113 at atmospheric pressure. Base material of copper and aluminium was used by them for different porous surfaces. Coating combinations such as such as copper-bronze, aluminium-bronze, aluminium-copper, aluminium-corundum, copper-copper, and aluminium-aluminium using plasma spraying technique were employed for the coating of heating materials. The parameters such as porous layer thickness varies from 0.01 to 0.60 mm, mean pore diameter from 2 to 31.4 μm and porosity from 5 to 61%. They generated data up to burn out heat flux point. They found that the surface parameters

taken under consideration such as porosity, mean pore radius and porous layer thickness of porous coating have significant effect on heat transfer performance and found optimal values of these three parameters analytically. Their investigation also came to conclusion that these porous surfaces were capable of providing stable boiling. Further, they stated that porous coating material of higher thermal conductivity provides higher rate of heat transfer.

Zhang & Zhang [Z1] did work on the boiling heat transfer phenomena of distilled water, ethyl alcohol and R-113 from thin powder porous surfaces with low and moderate heat flux at atmospheric pressure. The heating surface was formed by sintering bronze powder over a cylindrical copper block. Particle size of bronze material varied from 0.105 mm to 0.392 mm and matrix thickness ranges from 0.94 to 4.6 mm. An analytical model was developed by them by utilizing their own boiling experimental data based on two phase flow and heat transfer in thin porous layers. Following correlation was proposed by them based on their model and found the model to fit experimental data within an error of $\pm 23.5\%$:

$$Nu = 1.6746\times10^{-5}\left(\frac{Fr}{We}\right)^{0.4254}\left(\frac{Re_l\,\rho_l}{\rho_v}\right)^{-0.6032} We_1^{\,1.1605} We_2^{\,-0.811}\left(\frac{\delta^2\varepsilon^3}{4d_p^{\,2}}\right)^{0.2626}\left(\frac{\nu_l}{\nu_v}\right)^{0.2999} \quad (2.55)$$

Where, $We_1 = \dfrac{\sigma}{d_p(\rho_l-\rho_v)g}$ and $We_2 = \dfrac{\sigma}{d_p\rho_l g}\dfrac{\delta}{d_p}$

Scurlock [S7] gave experimental results for saturated boiling of liquid nitrogen, argon and R-12 over enhanced porous surfaces at atmospheric pressure. Coating of the heating surfaces was done using plasma spray technique with pure aluminium or a mixture of aluminium/10% silicon powder and polyester on to a 5mm thick aluminium back plates. The thickness of the coating layer over the surface varied from 0.13 to 1.32 mm. They found heat transfer coefficient to rise by tenfold for smooth untreated surfaces. However, they pointed out that there is an optimum thickness of plasma sprayed coating for each liquid and selected heat flux in order to achieve maximum heat transfer coefficient. Also the effect of fouling by impurities was studied by them and concluded that smooth surfaces exhibit greater degradation in heat transfer performance than porous surfaces.

Chang & You [C3] conducted experiments to investigate the effect of coating

on pool boiling heat transfer performance of diamond coated particle surfaces immersed in saturated FC-72. Size of the diamond particles taken for study were 2, 10, 20, 45 and 70 μm were used for coating. The thickness of coating range in between 30 to 250 μm and porosity from 40 to 48%. For determining the activation of cavities during nucleation transient thermal boundary layer concept was used by them and coatings were classified into two groups microporous (coating thickness less than 100 μm) and porous (coating thickness greater than 100 μm). They observed that microporous coating on heating surface was found to show different boiling characteristics as compared to that on porous coating.

In another work, Chang & You [C4] experimentally investigated the boiling characteristics at atmospheric pressure for different enhanced surfaces immersed in FC-87 and R-123. Six different types of tube geometries i.e. plain, integral fin with 709 fins/m, micro-porous enhanced low fin, micro-porous enhanced, Turbo-B and High flux have been studied. They found that micro-porous (ABM coated) plain tube exhibits 200 – 380% enhancement of heat transfer coefficient of for FC-87 and 140-280% for R-123 over the uncoated one. The increased number of active nucleation sites as a result of creation of micro-porous structure lead to the enhancement of heat transfer coefficient. ABM coated low finned tube shows an increase in heat transfer coefficient by 220-270% for FC-87 whereas High flux surface results in an increase of 260-810% for FC-87 and 460-1500% for R-123 as compared to uncoated one. Turbo-B surface also exhibited a significant rise in boiling heat transfer coefficient.

Chang & You [C5] investigated the effect of various uncoated and coated heating surface orientation on critical heat flux by carrying out experiments for nucleate pool boiling of FC-72 at atmospheric pressure. Their surfaces included uncoated, copper particles (size ranging from 1-50 μm) coated and aluminium particles (size ranges in between 1-20 μm) coated surfaces. The surfaces thus formed have been identified as CBM and ABM. They reported that for microporous enhanced surface, incipient boiling superheat decreases by 80% and heat transfer coefficient enhances by 330% and critical heat flux rises by 100% as compared to that of an uncoated one. They also observed that the rotation of plain surface from horizontal to vertical position improves heat transfer in nucleate boiling regime. However, boiling superheats was found to be independent of tube orientation for micro-porous layer.

Hsieh and Weng [H9] conducted experiment on copper surface, coated with porous aluminum, copper, molybdenum & pitted coating, immersed in saturated R-34a & R-407c. The copper tubes dimensions were 350mm long and 19mm in outer diameter with an inner diameter of 11mm. The coating techniques adopted for the purpose of coating the copper surface were namely; plasma spraying, flame spraying and pitted coatings. Plasma spray technique was employed for coating the surface by Copper & molybdenum with a coating thickness of 35μm &100μm respectively. Aluminium & zinc were coated by flame spraying with a coating thickness of 150μm of zinc and 50-300μm of aluminum. Four different mesh sizes of the pitted particles were treated with pitted coating using a sand blasting technique. The coating thicknesses obtained by pitted coatings are 30, 18, 31&32 μm respectively for the four different mesh size of the pitted particles. The conclusion from their work was that their results were well in agreement with that of Bier et al. [B13] for the same trend; namely, the same log-log slope of 0.7 but the magnitude was much higher due to the enhanced tube used. At heat flux ($q > 10$ kW/m^2) the R-34a has better heat transfer performance than that of the corresponding coated surface in R-407c. The reason for such behavior as suggested was an improvement in the heat transfer coefficient at the nucleation site under certain coated surfaces occurs as the surface become more wettable in R-134a compared to that of R-407c at a higher heat flux. They also reported that pitted coating surfaces exhibits the best performance over a range of heat flux in R-134a, while the surface prepared by plasma spray technique performs well in R-407c. The authors also correlated their experimental data for plasma and flame spray coating surfaces by the following equation:

$$Ja = 0.137(Re)^{0.292}\left(\frac{d_o}{\delta}\right)^{-0.190}\left[N_{cf}\right]^{0.065} \qquad (2.56)$$

Where, N_{cf} = Constant heat flux number = $\mu_l^2 / d_o\, \rho_l\, \sigma$

Equation (2.52) holds true for

$$6.909\times10^{-3} \le Re \le 1.899\times10^{-1};\quad 6.667\times10^{-3} \le \left(\frac{d_o}{\delta}\right) \le 1.667\times10^{-1}$$

and $\quad 7.773\times10^{-3} \le N_{cf} \le 4.787\times10^{-2}$

Above equation has been found to fit 95% of the experimental data points within ± 20%.

Chien & Webb [C10] investigated experimentally the boiling characteristics of R-123 over five different structured enhanced surfaces at atmospheric pressure. They used a high speed camera to obtained bubble frequency, bubble diameter and nucleation site density for each surface-liquid combination. They concluded that bubble growth mechanism on enhanced surfaces was different from that on plain surface. According to them, a significant fraction of vaporization occurs at meniscus in the corner of the tunnels which control bubble frequency and nucleation site density. Further, evaporation and bubble growth take place after the bubble emerges from the surface pores. It was found that the frequency of smaller bubble formation on the enhanced surfaces is greater as compared to those on plain surface for the same heat flux condition. The enhanced surface has greater nucleation site density than that on plain surface. They observed that bubble growth frequency is mainly controlled by the liquid inertia. The nucleation site density depends on the latent heat generated inside the tunnels. The latent heat flux contributes approximately 20 to 50% of the total heat flux. The contribution of latent heat transport is greater in low heat flux region.

Rainey and You [R1] conducted experiments to investigate the effect of orientation of heating medium and size on the pool boiling performance of plain and micro-porous coated surfaces immersed in saturated FC-72. They used flush mounted copper surfaces having dimensions 2 cm x 2 cm and 5 cm x 5 cm and compared their performance with the previous work of Chang and You [C5] who studied a 1 cm x 1 cm surface. They observed following:

i. The boiling performance of plain surface increased slightly for the orientation ranging in between 0^0 to 45^0 and then decreased from 90^0 to 180^0. In addition, larger surfaces exhibited diminished enhancement for orientation from 0^0 to 45^0 in the lower heat flux region and increased enhancement from 0^0 to 45^0 in the higher heat flux region.

ii. Unlike plain surfaces, the boiling performance of microporous enhanced surfaces was found to be insensitive to both inclination angle and heater size due to the higher number of active nucleation sites.

iii. The CHF data for all heater sizes and surface orientations tested were found

to be in agreement with the empirical correlation obtained by Chang and You [C3]

iv. The plain and micro-porous coated surfaces showed similar CHF behavior with respect to heater size.

Kim et al. [K7] carried out experiments to study nucleate pool boiling heat transfer enhancement mechanism of micro-porous surface immersed in saturated FC-72 at atmospheric pressure. Consecutive photo method was employed for the measurement of bubble size, frequency and vapor flow rate from a plain and micro-porous coated (DOM) platinum wire having diameter 390 μm to determine the effect of the coating on the convective and latent heat transfer mechanisms. They concluded that:

i. Surfaces having micro-porous coating increases nucleate boiling performance through increased latent heat transfer in the low heat flux region and through increased convection heat transfer in the high heat flux region.

ii. The higher active nucleation site density of micro-porous coating results in increase in bubble frequency while bubble diameter

iii. The CHF for the micro-porous coated surface is significantly increased over the plain surface due to decreased latent heat transfer and/or increased hydrodynamic stability from increased vapor inertia.

Cieslinski [C14] performed experiments for saturated boiling of distilled water on electrically heated stainless steel tubes of various diameters and flat horizontal plates at atmospheric pressure. Different materials such as zinc, brass, aluminum, copper, molybdenum and stainless steel particles were used by them to form coatings. Various methods of deposition techniques such as plasma spraying, gas flame spraying, dispersive electrolytic treatment and modified gas flame spraying were brought into practice to form metal coatings on flat horizontal surfaces and on stainless steel tubes. Various surfaces were varied such as surface roughness from 0.3 to 4 μm, porosity from 10 to 65%, coating thickness from 0.08 to 2 mm and mean pore radius from 1.11 to 10.5 μm. They found that boiling begins at lower wall superheat temperature for all coated surfaces as compared to that on a smooth surface but the rate of enhancement decreases with the increase in heat flux. Further, surface having aluminum particles

deposited on them have shown superiority over other material coated surfaces in promoting nucleate boiling. However, the porosity and coating thickness of porous surface puts an impact on the boiling phenomenon irrespective of deposition technique used in the investigation. Burnout heat flux has been found essentially to be independent of surface finish.

Vasiliev et al. [V9] investigated experimentally the saturated boiling of propane on single horizontal stainless steel (1Kh18N9T) pipes with smooth and porous surfaces. They also examined the loop heat pipe evaporator wick structure made from aluminum oxide ceramic with heat generation inside the wick. The coating technique employed for the coating of stainless steel pipes was gas thermal spraying. The investigations were carried out in the range of heat flux densities q = 0.1 to 100 kW/m^2 and saturation pressure P_{sat} = 3.45 to 13.8 bar. The coating thickness varied from 0.1 to 0.3 mm while porosity ranges in between 4 to 17%. They found that heat transfer coefficient for porous surface enhances upto 3 to 5 times in the region of low heat flux (q < kW/m^2) and upto 2.3 to 3 times in the region of high heat flux (q > kW/m^2). They also stated that as the porosity increases an increase is observed in the heat transfer coefficient Further, for the same porosity , heat transfer coefficient for coating thickness 0.2 mm was found to be lower than that for with coating thickness of 0.1 and 0.3 mm.

Vemuri & Kim [V10] experimentally investigated the pool boiling heat transfer phenomenon from nano-porous surface immersed in saturated FC-72 at atmospheric pressure (101 kPa). A comparison was made in between plain reference heating surface made of aluminium of thickness about 105 µm and a plain surface attached with nano-porous coating of aluminium oxide of thickness about 70 µm. The nano-porous coating has been bonded to the plain surface using Omega-bond 200 high thermal conductivity epoxy (thermal conductivity 1.4 W/m -K). SEM images of the nano-porous coating over the surface was taken by them and found that diameter of pores to be in the range of 50 to 250 nm. They concluded that the incipient superheat for the nano-porous coated surface to fall by 30% as compared to that of a plain surface.

Recently Nahra & Ness [N1], performed an experimental work on binary and ternary non-azeotropic hydrocarbon mixtures in order to determine the heat transfer coefficient. The nucleate pool boiling of binary and ternary mixtures was carried out using a vertical electrically heated cylindrical carbon steel surface at atmospheric

pressure with several surface rough nesses. The fluids used were Methanol/1-Pentanol and Methanol/1-Pentanol 1, 2 Propandiol at constant 1,2-Propandiol mole percent of 30%. Heat fluxes were varied in the range of 25 to 235 kW/m^2 . Comparison of this experimental data with that predicted from other correlations showed that the correlations available in literature based on the boiling range are in better qualitative agreement than correlations based on the phase envelop. He also found that with increase in the surface roughness there is an enhancement in the heat transfer coefficient, and the effect was observed to be dependent on the heat transfer flux and fluid composition. The influence of the surface roughness in binary mixtures results in higher heat transfer coefficient at the same heat fluxes and the mixture composition.

At different surface roughnesses the heat transfer coefficients for the pure components were measured for determining the ideal heat transfer coefficient of the mixture. The experimental results were fitted using simple power law equation of the following form:

$$h = Cq^b \qquad (2.57)$$

The constants C and b in the above equation depends on the surface roughnesses and fluid composition and their values are reproduced in **Table 2.7** for ready reference.

Table 2.7 Values for Constant C and index b of **Eq.(2.57)**

Liquid	Ra=0.2		Ra=2.98		Ra=4.36	
Constant	C	b	C	b	C	b
Methanol	2.08	0.68	2.01	0.72	0.85	0.80
1-Pentanol	2.05	0.67	1.61	0.73	2.95	0.70
1,2-Propanediol	0.63	0.78	0.42	0.83		

Peyghambarzadeh et al. [P6] performed experiments to determine saturated nucleation pool boiling heat transfer coefficient of binary and ternary mixtures of MEA/water, DEA/ water and water/ MEA/DEA ternary mixtures respectively at atmospheric pressure over a wide range of heat fluxes, various concentration. Heat flux varies in 14 levels from 7 to 230 kW/m^2 and amines concentration varies in 10 values from zero to 84 wt% , which show reduction on the heat transfer coefficient as the mass

transfer interference in this phenomenon. Hence, the experiment data have compared with the most of correlations corresponding for calculating the RMS error, also find the impacts of existing parameters in these correlations like ideal heat transfer coefficient (h_{id})

2.4 MOTIVATION FOR PRESENT INVESTIGATION

A review on passive techniques, mentioned above, show that coating of metallic material over plain surfaces has resulted in several fold of enhancement in boiling heat transfer coefficient. In addition, it has also several advantages such as ease of fabrication, low cost, fouling retardation etc. over other passive techniques. Further, coating of high thermal conductivity and high permeability material has been found to offer additional enhancement in heat transfer coefficient. Unfortunately, as summarized in **Table - 2.8**, it has been found that most of the investigations on nucleate pool boiling of liquids on metal coated surfaces are limited to distilled water, refrigerants and cryogenics at atmospheric pressure. However, such situation found application in food processing, refinery and petrochemical industries where boiling of liquids on plain and coated surfaces is required to occur at sub-atmospheric pressure. Besides, these investigations have not considered the parametric effect of heat flux, pressure and coating thickness on heat transfer coefficient. Thus, it is imperative to investigate boiling heat transfer characteristics of a plain tube coated with metallic material of different thicknesses at atmospheric and sub-atmospheric pressure using various organic liquids.

The present work has been motivated by the research gaps in the above mentioned research gaps in passive techniques and thereby, it has been planned to investigate nucleate pool boiling of distilled water, methanol and iso-propanol as pure liquids, their binary and ternary mixtures of various compositions on brass heating tube surface coated with copper particles of various thicknesses at atmospheric and sub-atmospheric pressures.

Table-2.8 Summary of important investigations related to boiling of liquids on non-wetting surfaces

Investigator(s)	Substrate material	Coating materials	Coating thickness	Test fluid	Pressure Atm.
Bliss et al. [B14]	Stainless Steel	Copper, Tin, Zinc, Nickel, Cadmium and Chromium	127μm	Water	1
Magrini & Nannei [M2]	Epoxy resin	Copper, Tin, Zinc& Nickel	5 to 250 μm	Water	1
Afgan et al. [A1]	Chromium, Nickel Stainless Steel	Titanium & Cr-Ni	63 to 100 μm	Water, Ethyl alcohol & R-113	1
Scurlock [S7]	Aluminium	Pure Al & Al/Silica (10%)	0.13 to 1.32 mm	Liq. Nitrogen, Argon, Oxygen, & R-12	1
Zhang & Zhang [Z1]	Copper	Bronze powder	0.94 to 4.60mm	Distilled water, Ethyl alchohol & R-113	1
Chang & You [C5]	Copper	Diamond particles	30 to 250μm	FC-72	1
Cieslinski [C14]	Stainless steel	Cu, Al, Mo, Zn, Brass	0.08 to 2.0mm	Distilled water	1
Rainy & You [R1]	Copper	DOM	50 μm	FC-72	1
Kim et al. [K8]	Platinum wire	DOM	35 μm	FC-72	1
Vemuri & Kim [V10]	Aluminum	Aluminum oxide	70 μm	FC-72	1

Chapter – 3

EXPERIMENTAL SET-UP

To meet the objective of the present investigation an experimental setup was design and fabricated. The setup requires proper designing and fabrication in order to obtain consistent, precise and reproducible experimental data. The following sections discuss, the general design considerations and, details of experimental setup.

3.1 GENERAL DESIGN CONSIDERATIONS

- The experimental runs are performed for various compositions of liquids at atmospheric and sub-atmospheric pressures. At the time of experimental runs excessive hoop stresses and pressure are developed in the vessel so to withstand these conditions the shape of vessel is chosen cylindrical. The height of the vessel around two time of its diameter, so the adequate space above the liquid pool may be available for disengagement of vapour to the condenser.
- Present investigation is on the nucleate pool boiling of liquid and their mixtures. Hence, a provision was made in the vessel to place the heating tube at a vertical distance of 180 mm from the bottom. This was carried out so that a thick sheet of liquid may surround the heating tube.
- A provision for complete condensation of vapor formed during boiling and return of condensate, so formed, to liquid pool is made. Thus, a horizontal condenser is mounted over the test vessel. To overcome the possible error due to the disturbances created in the liquid present on and near the heating tube surface by the returned condensate also the returned condensate may affect the boiling phenomenon appreciably. Besides, adequate free space above liquid pool is necessary to ensure that vapor above pool liquid does not change pressure over pool which has reasonable effect on heat transfer, the vapor moving to condenser and condensate returning to liquid pool. This is necessary for maintaining liquid level constant in the vessel.
- A thick solid portion was kept at one end of the heating tube to meet the condition of unidirectional heat flow, i.e. radially from heating tube to liquid pool. Beside a thick sheet of PTFE (A low thermal conductivity material) in

form of a cap is also attached at the end of the heating tube to abate the possibility of any heat flow in longitudinal direction.

- For visualization of the nucleate pool boiling phenomena over heating tube surface, a provision of two view ports on diametrically opposite sides of the vessel body is incorporated.
- Since heating tube was inserted horizontally in the pool of liquid, the surface temperature may vary position to position, and provision has been made to measure surface temperature by locating thermocouple at circumferential position of heating tube. For this purpose axial hole were drilled in wall thickness of the heating tube. Four locations such as top, side, bottom and side of the tube were considered sufficient to represent the tube surface temperature distribution around the tube. In view of small diameter and length of the drill bit and further to avoid any error due to end effects, thermocouples are mounted up to the midway at the circumferential positions.
- In order to measure the liquid temperature corresponding to each position namely top, side, bottom and side positions around heating tube surface four thermocouple probes are inserted. Further, it is kept in mind that thermocouple probes be located at sufficient distance away from heating tube surface to obtain the bulk temperature of liquid.

3.2 DETAILS OF EXPERIMENTAL SET-UP

The schematic representation of the experimental setup used as shown in **Fig. 3.1** and photographic view in **Fig 3.2.** Its main components are, test vessel, heating tube, electric heater, horizontal condenser, separator, sampling arrangement, vacuum pump, control panels. The details of these components are discussed below.

3.2.1 Test Vessel

A cylinderical vessel (1) is used in present investigation is of cylindrical shape. It is made from AISI 304 stainless steel using sheet of 3.2 mm thickness. The vessel is of an internal diameter of 210 mm and a height of 400 mm. It is closed at both ends with dished cap of same material. The dished cap attached to bottom end of the vessel has fittings for a pipe with a valve (V1) used to drain out liquid from pool as well as for filling the vessel by liquids as when required. Similarly, the top cover for the test vessel has provision, to mount vacuum/pressure gauge (6), condenser (11), a pipe line

attached with a valve (V2) for the expulsion of air in bubbler (9) and a thermocouple probe (T_L) to measure the temperature of liquid pool above the heating tube. A socket (5) is welded to vessel body at a distance of 80 mm from the bottom of vessel to hold heating tube in horizontal orientation. Two view windows (7) of 75 mm diameter are welded at diametrically opposite side position of the vessel body for visual observation of bubble dynamics on and near the heating tube surface. A liquid level indicator (4) along with a graduated scale is fitted on one side of vessel to determine the height of liquid inside the vessel. Four thermocouple probes (T_L) are inserted through the body of the vessel at suitable positions to measure the temperature of liquid pool on opposite sides of heating tube. The liquid samples taken out directly with help of syringe from the liquid pool, an arrangement is made at the bottom of vessel through air tight valve and a septum.

To prevent the heat loss to the surrounding, the outer surface of vessel and pipe fittings is insulated by winding asbestos rope around it, followed by the application of a thick paste of a mixture of plaster of Paris, asbestos powder and magnesia powder.

3.2.2 Heating Tube

A photographic view of the heating tube used in this investigation is shown in **Fig 3.3** and the details of the heating tube along with the heater are shown in **Fig. 3.4.**

The heating tube is a brass cylinder of 32.01 mm outside diameter, 235 mm length. A provision for heater is made by drilling a central hole of 18 mm diameter in the brass rod up to a distance of 185 mm from its one end. A portion of 40 mm is left undrilled at the other end of the tube. Besides, undrilled end of tube is covered with a cap made of 10 mm thick solid sheet of PTFE, an inert material of very low thermal conductivity. This is required to minimize the possibility of any heat flow in longitudinal direction. In this work and in other works carried out on pool boiling on horizontal cylinders in this department, efforts had been made to study temperature variation in axial direction by moving thermocouples along the length. It was observed that there is negligible variation in axial direction. Hence during other runs, wall temperature was measured only at a fixed position for entire work. A 10 mm portion of it is cut and used as a sample for SEM studies. Further a length of 35 mm on the open end of heating tube to make provision for a hexagonal nut, a collar and a threaded portion. Thus, effective length of heating tube is 150 mm. The hexagonal nut of 10 mm length is made at the open end of heating tube surface. It is followed by a collar of 50

mm diameter and 5 mm length. The collar is used to tighten heating tube in the socket welded to the test vessel. Next to the collar is a threaded portion of 20 mm length. The threads are of 19 TPI. They are made so that heating tube can be fitted tightly in horizontal position with the socket. In order to measure wall temperature of the heating tube at top, side, bottom and side positions,

four holes, equi-spaced at 90^0, are made circumferentially in the wall thickness of heating tube. The holes are of 2 mm diameter and of 115 mm length measured from the open end of the heating tube. They are drilled on a pitch circle diameter of 25 mm. Their positions are clearly shown in **Fig. 3.4** by symbols a, b, c and d. The outer surface of the uncoated heating tube is made smooth by turning and rubbing against emery paper of 800 grit size and followed by a very fine emery paper of 1200 grit size. Finally, the surface is polished by 4/0 grade emery paper. Three numbers of uncoated heating tubes are coated by plasma spray coating technique which is used in this investigation. All of them are coated with various thicknesses of copper particles by using the following procedure:

The coating on heating tubes is carried out by plasma spraying technique at M/s Anod Plasma Spray Ltd. Kanpur (India). In this technique, copper powder particles are feed through spray gun. A Mixture of Argon gas and compressed air is used as a copper powder carrier gas. During the movement of spraying gun, around the nozzle Argon gas jet is used to avoid any oxidation during the plasma spraying of copper particles. The whole process is carried out in the closed chamber. When the spray of copper powder at high pressure bombarded on the heating surface, it melts and the fine molten droplets rapidly solidify forming a uniform coating over the surface. It is necessary to maintain continuous flow and the proper ratio of argon and copper particles in the spray gun and control the compressed air pressure to obtain correct atomization of metal spray. Thickness of coating over the heating tube is described in Annexure-A. The dimensions of all heating tubes used in present investigation are given in **Table 3.1.**

Table-3.1: Dimensions of Heating Tube

Heating Tube Nomenclature	Diameter of Tube before Coating d, (m)	Diameter of Tube after Coating d_o, (m)	Inner Diameter d_i, (m)	Pitch Circle Diameter d_h,(m)	Effective Length L ,(m)	Coating thickness (μm)
BT-0	0.032010	0.032010	0.01801	0.0250	0.1500	0
BT-15	0.032011	0.032041	0.01799	0.0250	0.1500	15
BT-25	0.032013	0.032063	0.01804	0.0250	0.1501	25
BT-35	0.032210	0.032280	0.01805	0.0250	0.1500	35

An electric heater (8), used to heat the tube, is placed inside the heating tube as shown in **Fig. 3.4**. It is prepared by winding 24 gauge nichrome wires having a current carrying capacity of 5A over a porcelain tube of 16 mm diameter. The length of the porcelain tube is equal to the effective length of heating tube. Both the terminals of nichrome wire are taken out through porcelain beads and connected to an autotransformer (12) via a connector. The heater is insulated by wrapping several layers of mica sheet and glass tape to prevent electric short circuiting.

3.2.3 Condenser

A condenser (11), made from AISI 304 stainless steel sheet, is used for the condensation of vapor formed during boiling of liquid inside the vessel. Essentially, the condenser is a double pipe heat exchanger having an inner pipe of 25 mm O.D. and outer pipe of 75 mm O.D. The length of condenser is 660 mm. The condenser is fitted horizontally over the vessel and connected to the separator, where the condensate collected and return to the pool vessel.

The vapor passes through the inner pipe whereas coolant (water) flows is the annular space formed between the pipes. The coolant flow is counter current to the vapor of liquids which ensure rapid condensation.

3.2.4 Separator

Separator is connected to the condenser by universal union with pipe fitting tangentially to the separator. At the top of separator outlet pipe fitting is provided which is connected to a surge tank. The main aim of installing a air-liquids separator (12), is provide additional facility to remove non-condensable gases which is passed to the surge tank. The condensate collected in the separator is used for sampling purpose to determine vapor composition. The condensate is returned to the pool vessel through pipe line provided at the bottom of separator.

3.2.5 Sampling Arrangements

Sampling arrangement are provided in the separator and the pool vessel for drawing out the samples of boiling liquids and the vapor of different concentration mixtures for their HPLC Analysis. The arrangements are made by combination of two

nut and cap type. It is made of stainless steel. An axial hole is drilled of 2mm diameter in nut and cap, a septum is placed between nut and cap to avoid any leakage. One of it is connected to bottom of separator with the help of valve (V3) and other is connected to pool vessel for liquid samples.

3.2.6 Vacuum Pump

The vacuum pump (14) used in this investigation is a two-stage oil sealed rotary pump driven by a 0.5 hp of class (B) motor having a speed of 1400 rpm. It is supplied by M/S G.E. Motors India Ltd., Faridabad (India). It has a suction capacity of 7.5 dm^3/min and an ultimate vacuum capacity of 0.003 mm Hg. The vacuum pump is connected to the vessel through a surge tank (13) and a needle valve (V6). The surge tank dampens fluctuations in pressure and also prevents liquid condensate to enter in to vacuum pump.

3.2.7 Control Panel Instrumentation

The determination of boiling heat transfer coefficient of liquids following parameters are to be measured:

- Measurement of power input to heating tube;
- Measurement of the temperatures of liquid and heating tube wall;
- Determination of vacuum / pressure inside the vessel

Consequently, the experimental set-up is suitably instrumented. The details of instrumentation for above parameters are described below:

The AC mains power is supplied with the help of a servo voltage stabilizer (18) manufactured by M/S Gargy Research Instruments, Delhi (India). The stabilizer is connected to a constant voltage stabilizer (17), manufactured by M/S Bhurji Electronics Pvt. Ltd. Gurgaon (India). The controlled voltage through stabilizer ensures the constant power input to heating coil of heater (8). Power supply to heating tube is controlled by an auto-transformer, manufactured by M/S Agro Transformer Company Ltd., Mumbai (India). The current is measured by calibrated ampere meter and power input to heating tube is measured by a calibrated digital wattmeter, supplied by M/S Electronics and Scientific Devices, New Delhi (INDIA) having an accuracy of ± 1%

Sub-atmospheric pressure in the vessel is measured using vacuum gauge (6) mounted over the test vessel. The vacuum gauge is calibrated against a standard McLeod gauge.

Polytetrafluoroethylene (PTFE) coated 30 gauge copper constantan thermocouple wires are used to measure liquid and heating tube wall temperatures. Thermocouples are made in the laboratory by passing DC current (12V) through one end of thermocouples wire whose junction is dipped in mercury solution, after passing current the junction of thermocouples wire turned into spherical bead. Thermocouples are suitably calibrated before their installation, Thermocouple probes are inserted at various positions in the pool boiling vessel body with appropriate fittings to measure liquid pool temperature around the heating tube. Thermocouples are placed inside the holes drilled 90^0 at the open end where the heater is fitted in heating tube. All thermocouples and probes are connected with help of lead wire to a digital multimeter through a 12 -point selector switch. The e.m.f generated in thermocouple circuit is measured with the help of a digital multimeter (KEITHLEY 177 Microvolt DMM made in USA, Line Voltage: 105-125 V, 210-250V having a least count of 0.1μv in 20 mv range). For reference temperature, a bath of ice and water mixture is used maintained at 0^0C.

The sample of liquid and vapor of binary and ternary mixtures are use to identify the composition of the mixture are measured using Waters Breeze HPLC system, supplied by M/s Waters (India) PVT. Ltd., Bangalore. The C-18 column of size 3.9 mm×150 mm was used as for measurement of methanol, iso-propanol concentration.

Degassed organic free water made through micro pore setup used as a solvent, while maintaining a flow rate of 1 cm^2/min, the procedure followed as per the given in manual of instruction. Before taking reading of actual composition, the instrument was calibrated for standard distilled water-methanol, distilled water-iso-propanol and their ternary mixtures at suitable wave length range of 210 μm to 300 μm.

The above sections described details of the setup used for experimental investigations in present work. A qualitative analysis of surface structure of heating tube surfaces with and without coating has been analysed using scanning electron microscope and the images are given Annexure A. Following chapter deals with the procedure followed during experimentation in detail.

Chapter – 4

EXPERIMENTAL PROCEDURE

The procedure followed in present work to obtain consistent experimental data has been discussed in this chapter. Also it includes details of tests conducted for examining the reliability of each component and of complete set-up. The reproducibility of the experimental data has been discussed here with.

4.1 INSPECTION OF MECHANICAL AND ELECTRICAL LEAKAGE

Each and every components of the experimental set-up is tested individually and then assembled according to set up design as depicted in **Fig.3.1**. A brief description of the tests conducted to ensure the proper functioning of the set-up is given as under

The whole assembly of setup checked for leakage testing of all the valves i.e. V1 to V7 and pipe fitting by passing of compressed air through Valve (V4) of 210 kN/m^2 pressure.

The condenser is checked against compressed air which ensure the proper functioning of condenser and to avoid the leakage of coolant (water). The procedure adopted is as follows:

The nozzles provided in outer pipe of the condenser are connected to water inlet and fittings and valves of the outlet pipelines are checked to ensure that there is no leakage. Pressure gauge is connected to one end of the inner pipe whereas the other end is connected to a compressor through a valve. Compressed air is filled into the condenser at a pressure of 210 kN/m^2. After this, all the end-valves are closed and soap solution is applied to the welded joints and other portions on outer surface of the condenser. Any leakage is detected by the appearance of air bubble on the surface. If leakage at any joint is detected it is rectified. This process is repeated until no air bubble appears. Now the condenser is considered to be leak-proofed.

A vacuum gauge is mounted on the vessel to have the reading of sub atmospheric pressures. The socket (4) used for fastening the heating tube is closed by a dummy nut and valves are connected to the openings of the vessel. Valve V_2 is kept open for the entry of liquid / compressed air while the remaining valves are kept closed.

The pressure in the set up is maintained at about 210 kN/m^2 pressure by admitting

compressed air through the inlet valve V_2. Thereafter valve V_2 is shut-off and the set up is monitored for a period of 24 hour to identify leakage, if any. The pressure drop indicated by pressure gauge reading verifies the existence of leakage in the set-up. To identify the leakage, careful examination of each joint is performed by applying the soap water solution at all the joints of the vessel, and pipeline and each joint is examined carefully. If any bubble formation is observed across the joints of the vessel the leakage should be attended immediately. The process is repeated until there is no bubble formation and all the joints are leak - proof. Thereafter, the set-up is again filled with compressed air of pressure of 210 kN/m^2 (g) and kept for a period of 48 hour. When it is observed that there is no alteration in the reading of pressure gauge, then the set-up is ready for experimentation.

After the set-up is tested successfully against pressure, it is now tested against vacuum by creating a vacuum. For this purpose, a vacuum gauge is mounted at the vessel. A vacuum of 45.0 kN/m^2(g) is created inside the vessel by the use of vacuum pump. No change in the reading of vacuum gauge over a period of 48 hour confirmed that the set-up is completely leak proof.

For operational safety, experimental setup is properly earthed to eliminate any possibility of electrical short-circuiting. For this purpose all wire joint are insulated by tape and screws are tightened, heating coil element is properly insulated against any electrical leakage. The points where sparking is observed are immediately repaired. For safe experimental run proper earthing of the setup is ensured.

4.2 PRELIMINARY OPERATIONS

In order to acquire precise, consistent and reproducible data a set of operations is to be repeated after every experimental run, it include cleaning and rinsing of vessel, charging of liquid, stabilization of heating tube and de-aeration of liquid pool. Details of the procedure is as follows:

- All pipelines and vessel are flushed with compressed air to remove foreign solid particle adhering to surface of tube, vessel, pipeline etc. This is carried out by introducing compressed air in the system through valve V_4 while keeping valve V_1 opened and valve V_2 closed. Thereafter, all valves except V_5 are closed and vacuum is created inside vessel by vacuum pump. The soap–water solution is filled with the help of flexible tube, solution is sucked due to pressure difference created by vacuum

pump through valve V_2.

- The vacuum is released during filling of soap solution and compressed air at a pressure of 210 kN/m^2 is admitted to vessel via flexible tube through the valve V_2. Compressed air impart a whirling motion to soap-water solution in vessel and this helps to loosen the adherence of dust and other foreign particles on inner surface of vessel. Now the solution is drained off from vessel through valve V_2. Consequently, distilled water is admitted into the vessel via flexible tube and after repeating above procedure liquid is drained off. This process is repeated several times till drained-off liquid is found to be completely liberated from dust and other foreign particles. Consequently heating tube surface is also cleaned with distilled water and acetone and finally with the test liquid before fitting the same in the vessel.
- After vessel is cleaned and rinsed properly, liquid is admitted in to it by developing vacuum inside it. The liquid is filled up to a height of 100 mm from top surface of heating tube. Now, water (coolant) is passed into the condenser and heater is energized by providing a power input of 550 W. Temperature of liquid increases and reaches saturation temperature. The condition of atmospheric pressure is maintained throughout the system by opening valve V_4. At this condition liquid is boiled for several hours. The prolonged submergence of heating tube followed by vigorous boiling of about 72 hour makes the surface aged and thermally stabilized due to the removal of entrapped gases from the cavities. This operation ensures accurate and reproducible experimental data. Further, this is confirmed by taking data at different intervals of time.

4.3 DATA ACQUISITION

After preliminary operations, series of experimental runs are performed by following the procedure given below:

Presence of disperse air in liquid pool affects boiling heat transfer rate. So, it is essential to remove them before experimentation. It is achieved by boiling of liquid and or their mixture for several hours and passing the disperse air into a bubbler which is connected by PVC flexible pipe to the vessel through valve V_2. During this process all valves except V_2 which is connected to the bubbler are closed. Continuous bubbling of air in the bubbler indicates de-aeration of liquid. This is carried out till bubbling in bubbler ceases, indicating no presence of dissolved air in liquid pool and the vapor space. At the end of de-aeration process valve V_2 is closed. This de-aeration procedure is carried out

every time before starting a given set of experimental runs.

After de-aeration process, setup is ready for experimentation. At first the vessel is subjected to atmospheric pressure by opening the valve V_4. Then, heating tube is energized with the lowest heat input of 220 W. As a result, temperature of liquid increases progressively until it reaches saturation temperature corresponding to atmospheric pressure. At saturation condition, the e.m.f readings of all thermocouples as indicated by DMM are kept under continuous observation. When no change in readings of thermocouples is noted, steady state condition is said to exist. Now e.m.f readings of all wall and liquid thermocouples are noted. The heat input rate is then adjusted to the next predetermined higher value and procedure as mentioned above is repeated. Heat input rate is increased from 220 W to 500 W in six steps. After completing experiments at atmospheric pressure, the system is maintained at sub-atmospheric pressure by creating vacuum in test vessel and above mentioned procedure is repeated to obtain boiling heat transfer data. Pressure in the test vessel is varied from 97.71 kN/m^2 to 45.11 kN/m^2. The liquids investigated in present investigation are distilled water, methanol, iso-propanol and their binary and ternary mixtures.

After conducting experimental runs for the boiling of above mentioned liquids on plain heating tube surface, three copper particles coated heating tubes of known thicknesses are placed in vessel one by one and experiments are conducted in the same manner for each tube as discussed above. Liquid and vapor samples are collected for all heat fluxes through liquid and vapor sampling arrangements, as shown in Fig. 3.2. The samples are analyzed through HPLC system in Instrumentation Laboratory of IIT Roorkee, where all condition is maintained as per requirement for HPLC analysis. To samples of binary and ternary mixture are tested for their peak areas for the volatile components in the mixture such as methanol and iso-propanol are measured. These values are plotted with the composition for binary and ternary mixture as shown **Fig.4.1** and **Fig.4.2.** This procedure is adopted for all experimental runs which performed on total of four number of heating tubes - one plain and three copper coated tubes having thicknesses of 15, 25, and 35 µm have been used in this investigation. The operating parameters used in this investigation are listed in **Table – 4.1**

4.4 THERMOCOUPLE INSTALLATION

The PTFE coated thermocouples made in the laboratory are wrapped with Teflon tape to make them a little bit firms, so that they can be inserted in the holes easily without any buckling. Each thermocouple is then inserted in holes made in wall thickness of

heating tube. While placing thermocouple, care is exercised to ensure perfect contact between thermocouple and wall surface at the end of the hole. It is worth-mentioning here that very little stagnant air exists between thermocouple and wall surface. Thus, there is absolutely no possibility of any heat loss by convection through air present in these holes. This ensures true measurement of surface temperature of the heating tube by the thermocouples at their locations.

For measurement of liquid temperature, thermocouple probes are used. They are inserted through fittings welded in the body at top, bottom and side positions of heating tube corresponding to wall thermocouple positions. All probes are positioned at a sufficient distance away from heating tube so that they are outside superheated boundary layer surrounding the tube. For this purpose, liquid is boiled and probes are moved away from tube gradually till they display no change in their e.m.f. values. This is essential for the measurement of bulk temperature of liquid pool.

4.5 REPRODUCIBILITY AND CONSISTENCY

Reproducibility and consistency of experimental data is most important for their accurate and reliable analysis. Reproducibility is examined by conducting experiments at different times under the same operating condition. As no discernable variation in the readings of wall thermocouples is noted, data are considered to be reproducible.

Also, the confirmation of homogeneity of heating tube surface during preliminary operations validates the consistency of experimental data. Besides, analysis of data for circumferential variation of wall temperature around heating tube shows that surface temperature increases continuously from bottom to side to top position. This conduct is in accordance to the literature available on variation of surface temperature of heating tube during nucleate pool boiling. Thus, above tests proves that data obtained in the present investigation are consistent.

Table 4.1 Operating parameters of present investigation

Sl. No.	Test liquid	Heating tube	Pressure (kN/m^2)	Power Input (W)
1	Distilled Water	BT-00	97.71, 85.39, 71.13, 57.71, 45.10	220, 300, 350, 400, 450, 500
2		BT -15	97.72, 84.89, 71.15, 57.68, 45.21	220, 300, 350, 400, 450, 500
3		BT -25	97.75, 84.79, 71.14, 57.69, 45.40	220, 300, 350, 400, 450, 500
4		BT -35	97.71, 84.39, 71.21, 57.77 , 45.40	220, 300, 350, 400, 450, 500
5	Distilled Water and Methanol	BT -00	97.76, 84.39, 71.23, 57.75, 45.40	220, 300, 350, 400, 450, 500
6		BT -25	97.77, 84.39, 71.13, 57.71, 45.40	220, 300, 350, 400, 450, 500
7	Distilled Water and Iso-Propanol	BT -00	97.70, 84.39, 71.17, 57.78 , 45.40	220, 300, 350, 400, 450, 500
8		BT -25	97.78, 84.39, 71.26, 57.76, 45.17	220, 300, 350, 400, 450, 500
9	Distilled Water, Methanol and Iso-Propanol	BT -00	97.79, 84.39, 71.16, 57.74, 45.21	220, 300, 350, 400, 450, 500
10		BT -25	97.74, 84.39, 71.96, 57.72, 45.13	220, 300, 350, 400, 450, 500

- Material of construction of heating tube Brass.
- BT-0 indicates plain heating tube, whereas BT -15, BT -25, and BT-35 µm stands for copper coated heating tubes having coating thicknesses of 15, 25, and 35 µm , respectively.

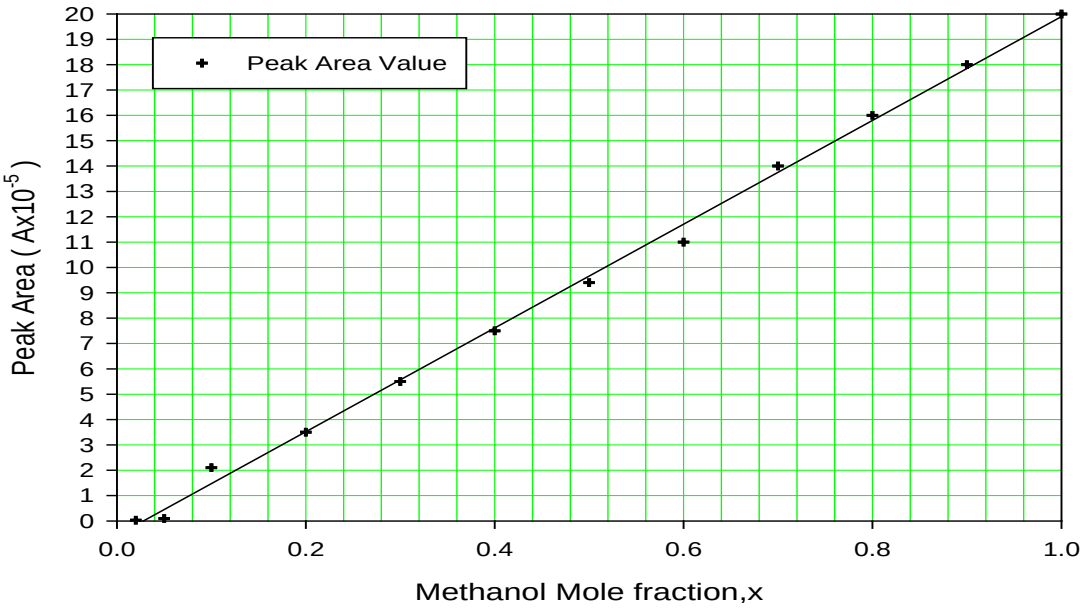

Figure 4.1 Calibration curve for measurement of methanol concentration using HPLC system

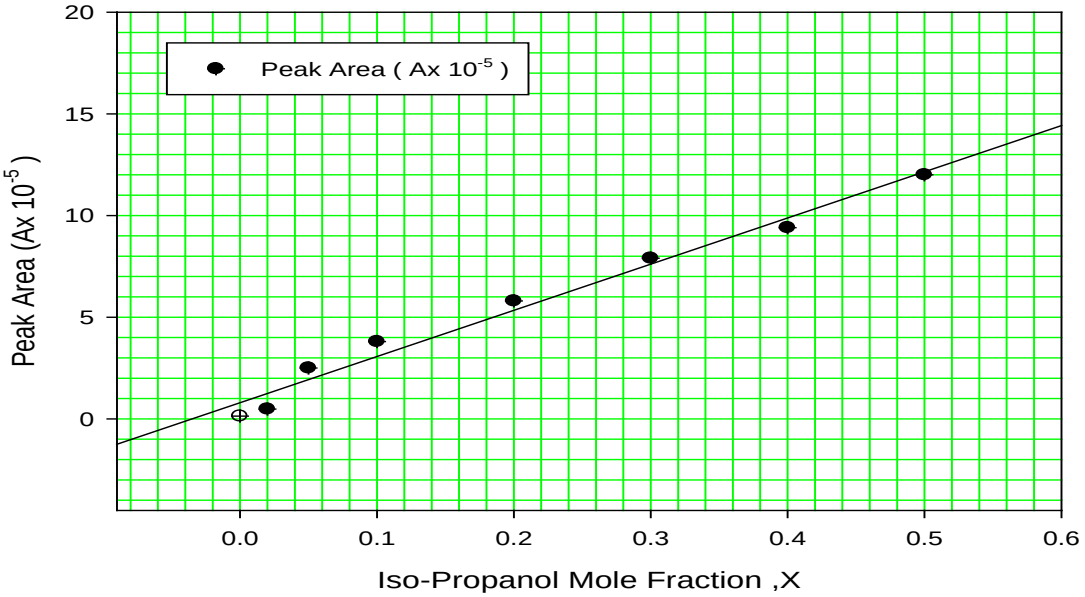

Figure 4.2 Calibration curve for measurement of methanol concentration using HPLC system

4.6 OPERATIONAL CONSTRAINT

The operating variables in present investigation are heat flux, pressure, coating thickness and liquids and their mixtures. Their ranges are determined by certain operation constraints which are described below:

The maximum power input given heating tube surface is limited by the current carrying capacity of wire used in the construction of electric heater. However, minimum heat input is decided by the value at which sustained nucleate boiling of liquid occurs. In present investigation 24-gauge nicrome wire having a maximum current carrying capacity of 5 amperes is used to make the heater. Accordingly, the maximum power input to the heater is limited to 550 W, which corresponds to a heat flux of 33156.9 W/m^2. The minimum power input at which sustained boiling of liquid occurs is 220 W, which is equivalent to a heat flux of 14588.8 W/m^2.

The minimum thickness of coating on heating tube surface is limited by the diameter of nozzle gun used for spraying. In the present investigation only one coating thickness of 15, 25 and 35 μm are used.

This chapter pertains to results of experiment conducted for saturated boiling of distilled water, methanol, iso-propanol and their binary and ternary mixture on horizontal copper coated brass heating tube (hereafter referred as coated tube) surface and their interpretation have been discussed. It also includes comparison between thermal effectiveness of coated and a plain tube (here after referred as uncoated tube) to bring out the usefulness and applicability of copper coating on an uncoated tube for enhance boiling of liquid and mixtures.

Experimental data of present investigation for boiling of saturated liquid and their mixture on an uncoated and coated are given in table B.1 and B.44. These includes heat flux, liquid and surface temperature at bottom, two sides and top position of heating tube and heat transfer coefficient. Heat flux varied from 14588.86 W/m^2 to 33156.5 W/m^2 in six steps and pressure from 45.40 kN/m^2 to 97.71 kN/m^2 in five steps. Saturated liquids – distilled water, methanol, iso-Propanol and their binary and ternary mixtures are used in this investigation. Three thicknesses of copper coating 15μm, 25μm and 35 μm have been used over uncoated brass heating tube

5.1 LIMITATIONS OF PRESENT ANALYSIS

The present investigation pertains to measurement of liquid and surface temperature of heating tube. For this purpose, copper-constantan thermocouples have been employed. They have been mounted at top, two sides and at bottom position of heating tube to measure the variation in surface temperature around tube circumference, if any. Further, thermocouples have been placed at a pitch circle diameter [$d_h = (d_i + d_o)/2$] in the wall thickness of heating tube. Thus, they did not measure the temperature of outer surface of the tube directly. So, a temperature drop, δT_w across the thickness between thermocouple location and outer tube surface has been calculated by the use of following equation for heat conduction in a thin cylinder:

$$\delta T_w = \frac{q d_o}{2k_w} \ln\left(\frac{d_o}{d_h}\right) \tag{5.1}$$

The temperature drop, δT_w so obtained, has been subtracted from the recorded wall temperature of heating tube measured by thermocouples to obtain the outer surface temperature. Further, it is assumed that the flow of heat is transmitted radially to liquid pool from heating to outer tube surface. This has also been substantiated by the fact that no significant variation in thermocouple's readings was noticed when wall thermocouples were moved longitudinally. Besides 10 mm thick plug, covered with a thick sheet of PTFE, provided at the closed end of the heating cylinder also diminished the possibility of any heat flow in longitudinal direction. This has been explained in detail in Chapter – 3. Arithmetic averaging has been employed to obtain the average temperature of heating surface. As variation in temperature is less than 2^oC and temperature plots are linear as shown in Figure 5.1. Thermocouple probes have also been mounted in the liquid pool at various circumferential positions corresponding to surface thermocouples i.e. at the top, at the two sides and at the bottom. All the probes have been placed in pool at a sufficient distance away from tube surface so as to monitor bulk temperature of liquid. An arithmetic averaging has also been used to obtain the average temperature of the liquid. Sample calculation as given in Annexure – C clearly describes the method of calculation for heat transfer coefficient. An uncertainty analysis of each experimental run has been carried out as per procedure outlined in Annexure – D. The maximum uncertainty associated with heat transfer coefficient has been found to be the order of ± 1.12 %.

It is important to mention here that the measured values of liquid temperature are slightly higher than saturation temperature corresponding to pressure prevailing in the unit. This can be attributed to superheated vapours entrapped in bubbles which when collapse results in higher temperature than saturation temperature of liquids. Besides, there is also an insignificant difference in the values of surface temperatures measured at the two side positions of the tube. Although difference is quite small, yet it has been taken into account while computing the value of local and average heat transfer coefficient. Physico-thermal properties of liquids have been taken at arithmetic mean of liquid and surface temperature of heating tube. The physico-thermal properties of binary and ternary mixture have been calculated at their saturation temperature corresponding to the prevailing pressure. The computated values of the properties for pure liquid, binary and ternary mixtures are given in Annexure –E.

The plasma spraying technique has been employed for coating copper powder over uncoated brass heating tube using the procedure given in Annexure –A. However, it has not

been possible to get thickness of coating of less than 15μm over uncoated heating tube due to various constraints involved in coating operation. It is worthwhile to mention here that temperature drop across thickness of copper coated layer has not been included in the determination of heat transfer coefficient. In other words, calculation of heat transfer coefficient on coated tube is based on substrate surface temperature only. This has enabled a comparison of heat transfer characteristics on coated tube with that of uncoated tube.

5.2 NUCLEATE POOL BOILING OF SATURATED LIQUIDS ON UNCOATED TUBE

Experimental data for nucleate pool boiling distilled water, methanol, iso-Propanol are given are given in table B.1, B.5 and B.7 of Annexure B. Using these data, Temperature distribution and thereby variation of heat transfer coefficient along the circumference of uncoated tube and average heat transfer coefficient for boiling of different liquid has been determined. It also discusses the effect of heat flux, pressure and liquids on local and average heat transfer coefficient and functional relationship between heat transfer coefficients have also been developed. These are discussed in the following subsections.

5.2.1 Circumferential variation of surface temperature

Figures 5.1(a) to 5.1(e) demonstrate plots representing variation of surface temperature along the circumference of an uncoated heating tube for saturated boiling of distilled water at atmospheric and subatmospheric pressures with heat flux as parameter. Each plot is for a distinct pressure specified therein. The variation of liquid temperature around the tube circumference is also including by dotted line. Close inspection of a plot reveals the following silent features:

i. At a given heat flux, surface temperature increases from bottom to side to top position of heating tube.
ii. For a given circumferential position, a rise in heat flux increases surface temperature.
iii. The liquid temperature remains constant irrespective of circumferential position and heat flux imposed on heating tube.

These features are consistent and can be explained by the following reasoning.

In nucleate pool boiling of liquids at given pressure vapor-bubbles from at active sites randomly distributed over the heating outer surface. They grow in size and depart from the surface after attaining maximum size, to travel in the pool of liquid. However, when

boiling occurs on a tube surface, growth of vapor- bubbles is not uniform throughout the circumference due to its cylindrical geometry. As a matter of fact, bubbles generated at top position have free access to travel upward whereas those formed at bottom and side positions do not have so. In fact, bubbles generated at top position and side positions do not have so. In fact, bubbles formed at bottom position slide upward along wall surface as their movement

gets continuously accelerated due to increase in buoyancy force. In doing so, they push the bubbles formed at adjoining circumferential positions on their way and carry them along the wall surface to reach to top position. Thus, frequency of bubble formation increases continuously as one moves from bottom to side to top position. Coalescence of vapor-bubbles leading to form agglomerates and thereby vapor clouding occurs in this thick layer of vapor-bubbles engulfing the tube circumference. The thickness of this layer increases along the circumference from bottom to side to top position. Since this layer obstructs the passage of heat from tube surface to liquid, heat removal rate decreases from bottom to side to top position. In other words, bottom position provides the highest heat removal rate followed by side and top position in decreasing order. As a consequence, wall temperature is found to increase continuously from bottom to side to top position.

Figures 5.2(a) to 5.2(e) and 5.3(a) to 5.3(e) represent plots for variation along the circumference of an uncoated heating tube for the boiling methanol and Iso-Propanol at atmosphere and subatmospheric pressures. Above plots have essentially the same features, as discussed above for distilled water.

On the basis of above, it can be concluded that a significant variation in surface temperature exists along the circumference of heating tube during boiling of liquids at atmospheric and sub-atmospheric pressures. In other words, boiling on a heating tube is a non-uniform phenomenon and therefore calls for an investigation to determine the extent of variation in heat transfer coefficient around heating tube.

5.2.2 Variation of local heat transfer coefficient

Figure 5.4 is a plot to show variation of local heat transfer coefficient with heat flux for boiling of distilled water on an uncoated heating tube at atmospheric pressure. Circumferential position is a parameter in this plot. A close examination of this plot reveals the following points:

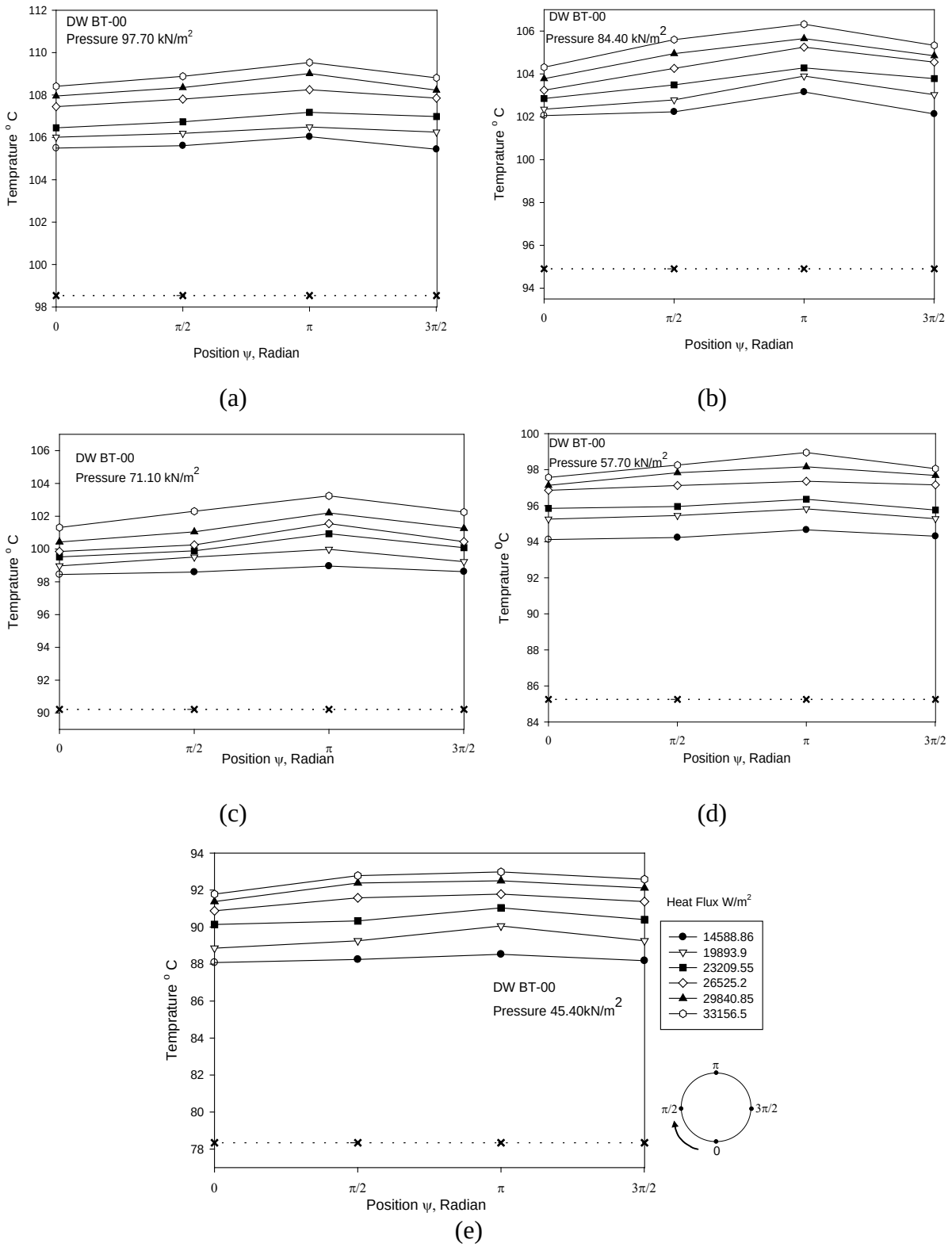

Figure 5.1. Variation of liquid and surface temperature along circumference at bottom, two sides and top position of an un coated heating tube with heat flux as a parameter for boiling of distilled water at atmospheric and subatmospheric pressures

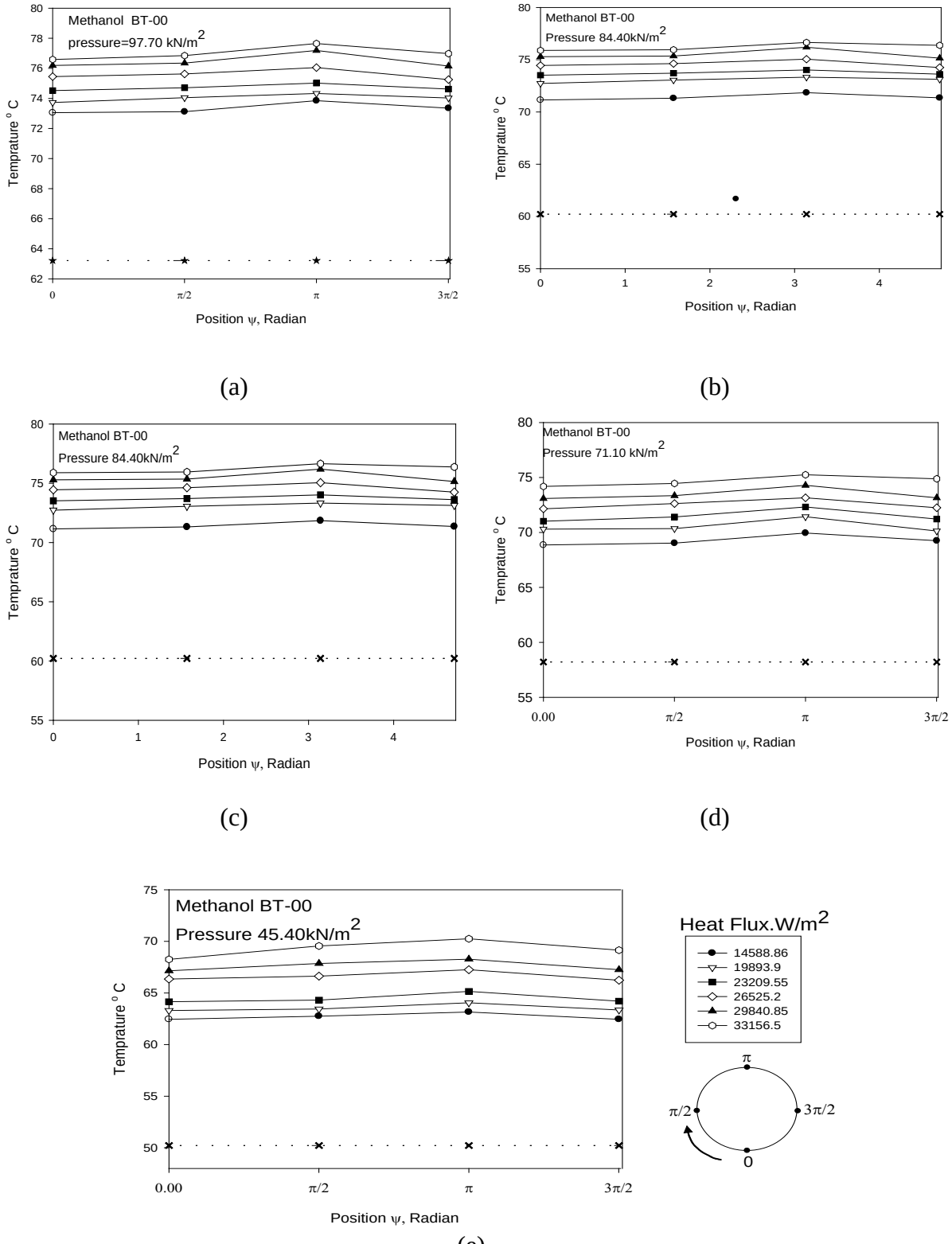

Figure 5.2 Variation of liquid and surface temperature along circumference at bottom, two sides and top position of an un coated heating tube with heat flux as a parameter for boiling of methanol at atmospheric and subatmospheric pressures

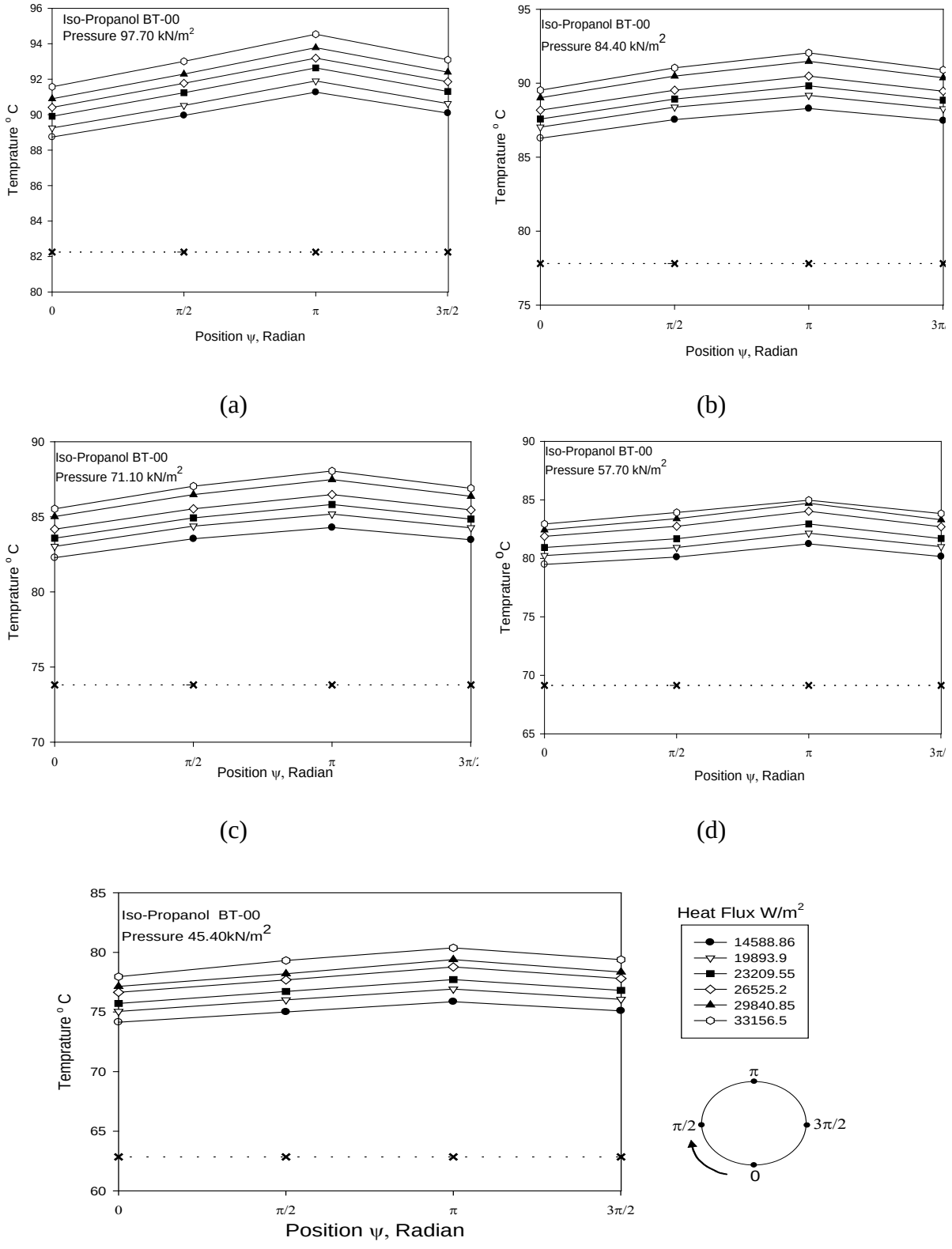

Figure 5.3. Variation of liquid and surface temperature along circumference at bottom, two sides and top position of an un coated heating tube with heat flux as a parameter for boiling of Iso-propanol at atmospheric and subatmospheric pressures

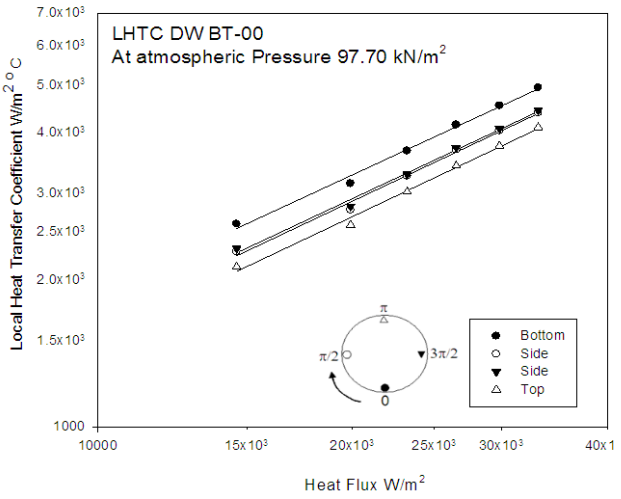

(a)

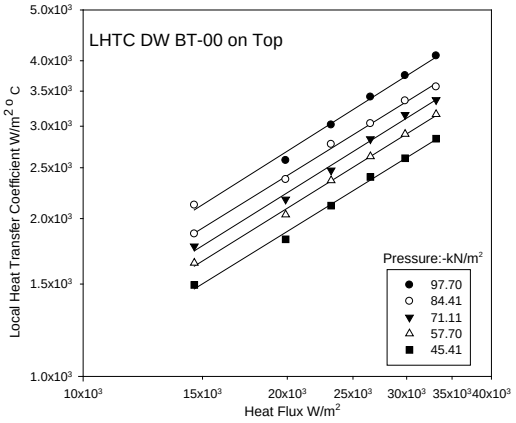

(b)

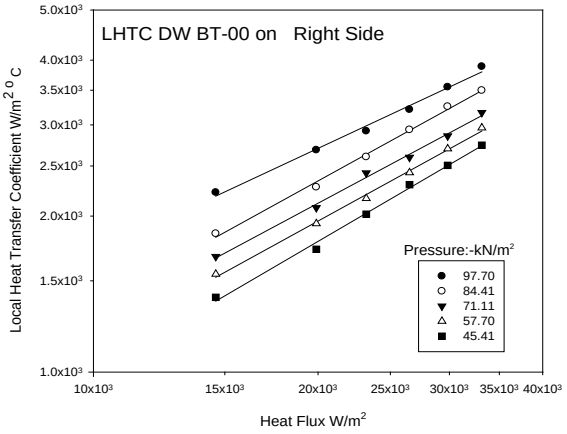

(c)

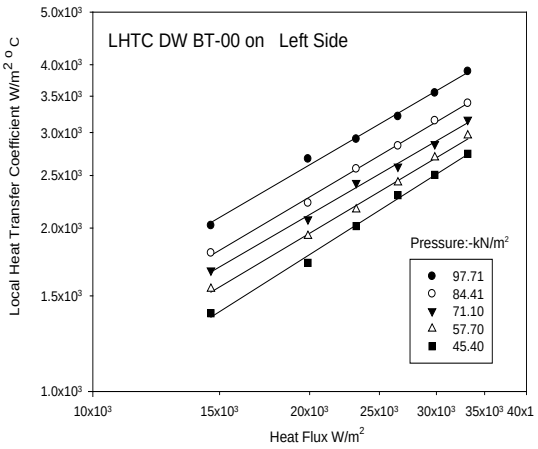

(d)

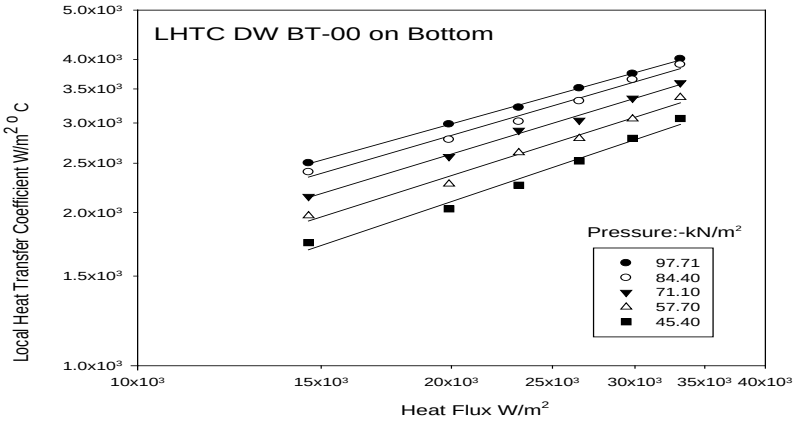

(e)

Figure 5.4 Variation of local heat transfer coefficient with heat flux and pressure along the circumference of an uncoated heat tube of boiling distilled water

a. At a given value of heat flux, local heat transfer coefficient increases from top to

side to bottom position on heating tube.

b. At a given circumferential position, value of local heat transfer coefficient increases with increase in heat flux and the variation between two can be represented by a power law, $h_\phi \propto q^{0.7}$.

These features are obvious and can be explained as follows: As mentioned in subsection **5.2.1** at a given heat flux, surface temperature increases continuously from bottom to side to top position of heating tube. So wall superheat $\Delta T_w (= T_w - T_s)$ increases in same order and therefore value of local heat transfer coefficient is found to decrease from bottom to side to top position on the heating tube. A rise in heat flux increases the surface temperature at a given circumferential position. This, in turn, increases the value of local wall superheat and thereby, according to following equation, value of minimum radius of nucleation site, at which vapour-bubble can originate, to decrease:

$$r_c = \frac{2\sigma}{\left(\frac{dp}{dT}\right)_s \Delta T_w} \tag{5.2}$$

As the population of small sized nucleation sites on a heating surface is more than that of larger sized ones, large number of vapour-bubbles forms, grow and detach from the surface to travel in the pool of liquid at high heat flux condition. All these increase intensity of turbulence and enhance heat removal rate. Consequently, local heat transfer coefficient is found to be higher at high value of heat flux.

Above features have also been observed during boiling of methanol and iso-propanol at atmospheric pressure as can be seen from the plots of **Figs. 5.5** and **5.6.**, respectively. At this stage it may be pointed out that although functional relationship between h_ϕ and q remains unaltered irrespective of the liquid boiled on uncoated heating tube surface, the magnitude of local heat transfer coefficient at a given circumferential position on uncoated heating tube is found to differ from liquid to liquid. This is due to difference in physico-thermal properties of liquids under consideration. Further, similar behavior has also been noticed during the boiling of distilled water, methanol and iso-propanol at sub-atmospheric pressures. However, a value of local heat transfer coefficient at a given circumferential position is found to vary with pressure. In fact, it increases with raising pressure.

This observation can be explained by fact that raising pressure changes the thermo physico properties, however, most significant change appear in the values surface tension, this cause minimum radius of nucleation site at which vapour bubbles originated to decrease, as can be seen from **Eq. (5.2)**. Consequently, large numbers of small sized vapour- bubbles forms and detached from the surface to travel in pool of liquid and there by intensity of turbulence increase. This, in turn, causes higher heat removal rate and therefore heat transfer coefficient increase.

From the above it is clear that local heat transfer coefficient for boiling of liquids on an uncoated heating tube is a function of heat flux, pressure and circumferential position. Hence, An empirical equation related to heat transfer coefficient with variable has been develop by using the least square method which follow;

$$h_{\Phi} = C_{\Phi} q^{0.7} p^{0.32} \tag{5.3}$$

Where C_{Φ} is constant whose values depends upon boiling liquid and circumferential position on a heating tube. These values are given **Table 5.1.**

Table 5.1 Values of C_{Φ} of **Eq. (5.3)** for various saturated liquids at various circumferential positions

Sl. No.	Liquids	Circumferential Positions			
		Top	Side	Bottom	Side
1	Distilled water	0.585	0.580	0.612	0.581
2	Methanol	0.445	0.491	0.561	0.453
3	Iso-propanol	0.365	0.383	0.435	0.373

Figure 5.7 Depicts of plot between experimental values of local heat transfer coefficients and those computated from **Eq. (5.3)** for boiling distilled water, methanol and Iso-propanol at the atmospheric and sub atmospheric pressures. This plot clearly indicates an excellent agreement between the values predicted by **Eq. (5.3)** and experimental values within a maximum error of ± 8%.Thus **Eq. (5.3)** can correlate experimental data of local heat transfer coefficient of various boiling liquids. In other words, above equation can be used to calculate local heat transfer coefficient at an circumferential position on heating tube from the knowledge of heat flux and pressure provided the value of constant $C_{\Phi}$is known. The value of constant C_{Φ} depend upon heating surface characteristics,

circumferential

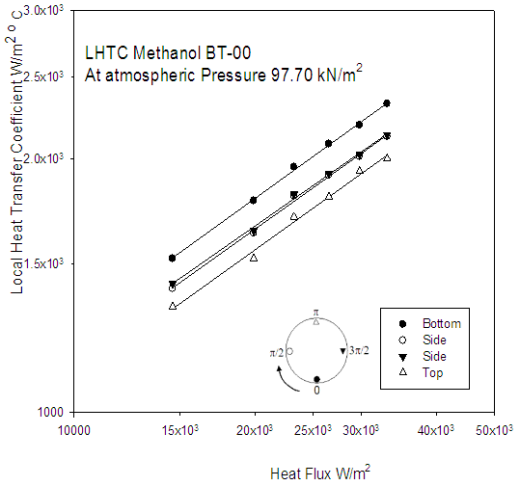

(a)

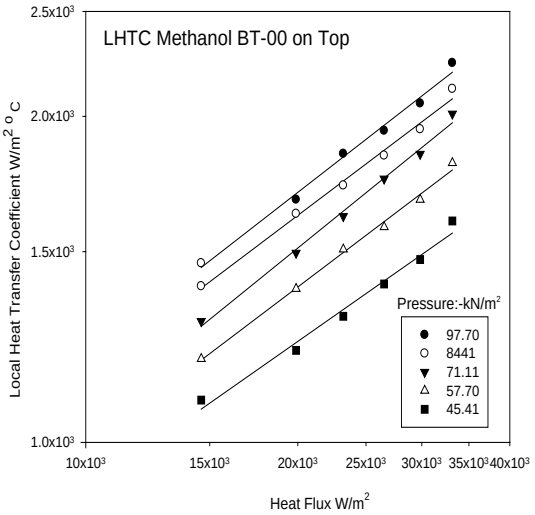

(b)

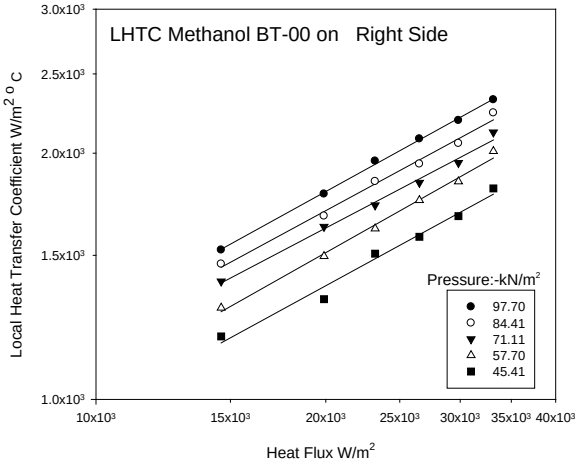

(c)

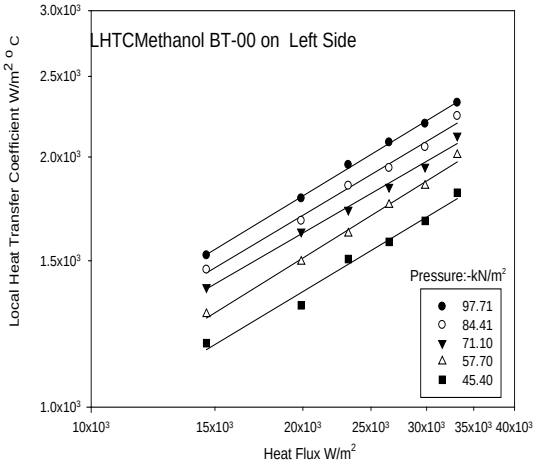

(d)

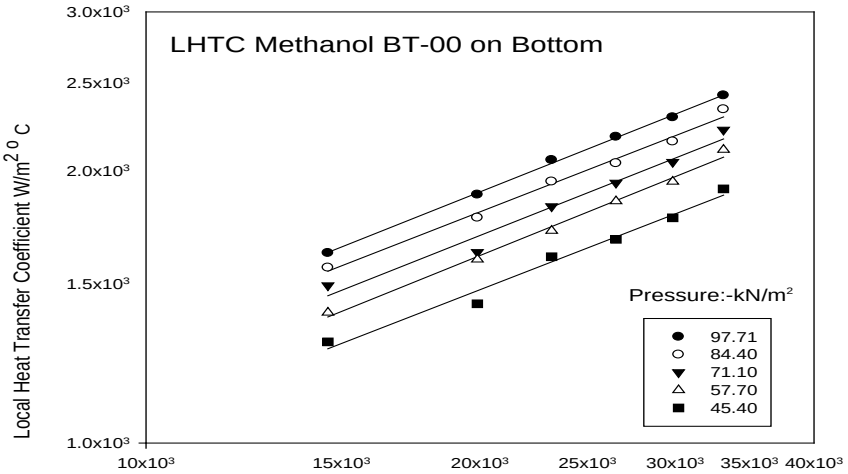

(e)

Figure 5.5 Variation of local heat transfer coefficient with heat flux and pressure along the circumference of an uncoated heat tube for boiling methanol

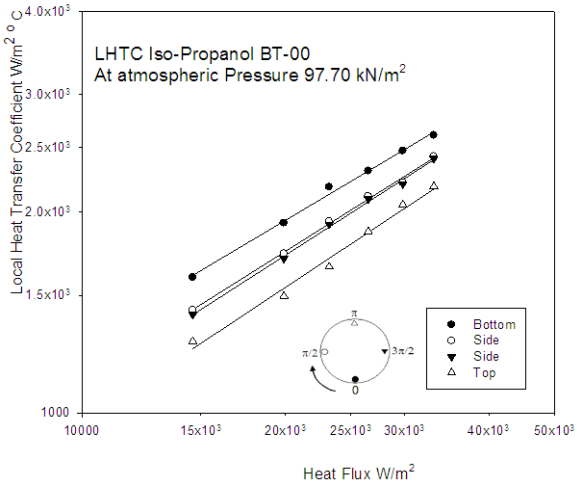

(a)

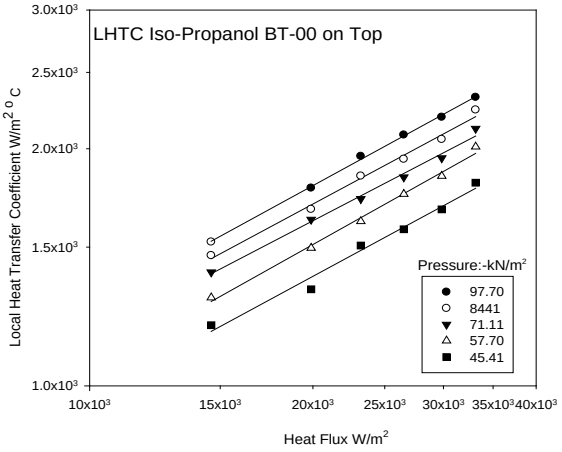

(b)

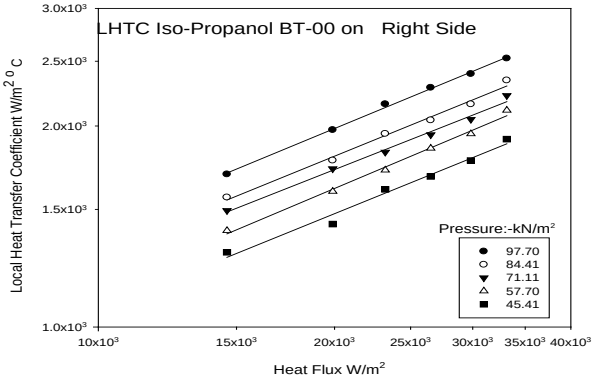

(c)

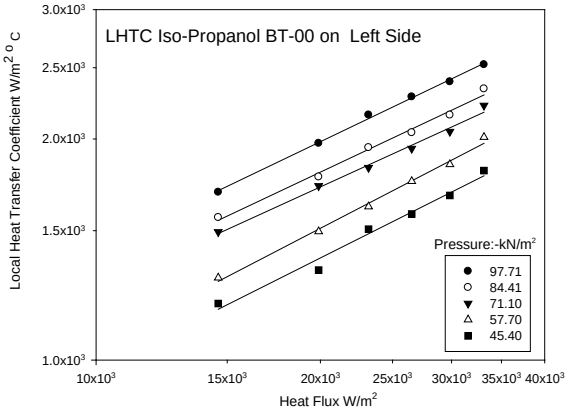

(d)

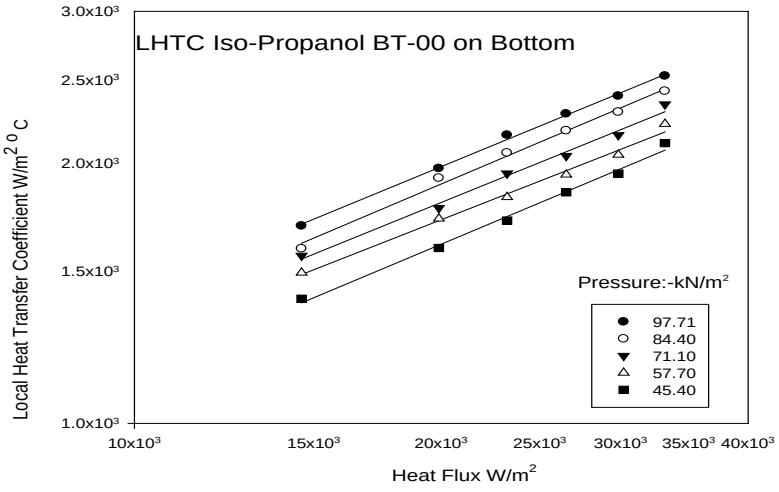

(e)

Figure 5.6 Variation of local heat transfer coefficient with heat flux and pressure along the circumference of an uncoated heat tube for boiling Iso-propanol

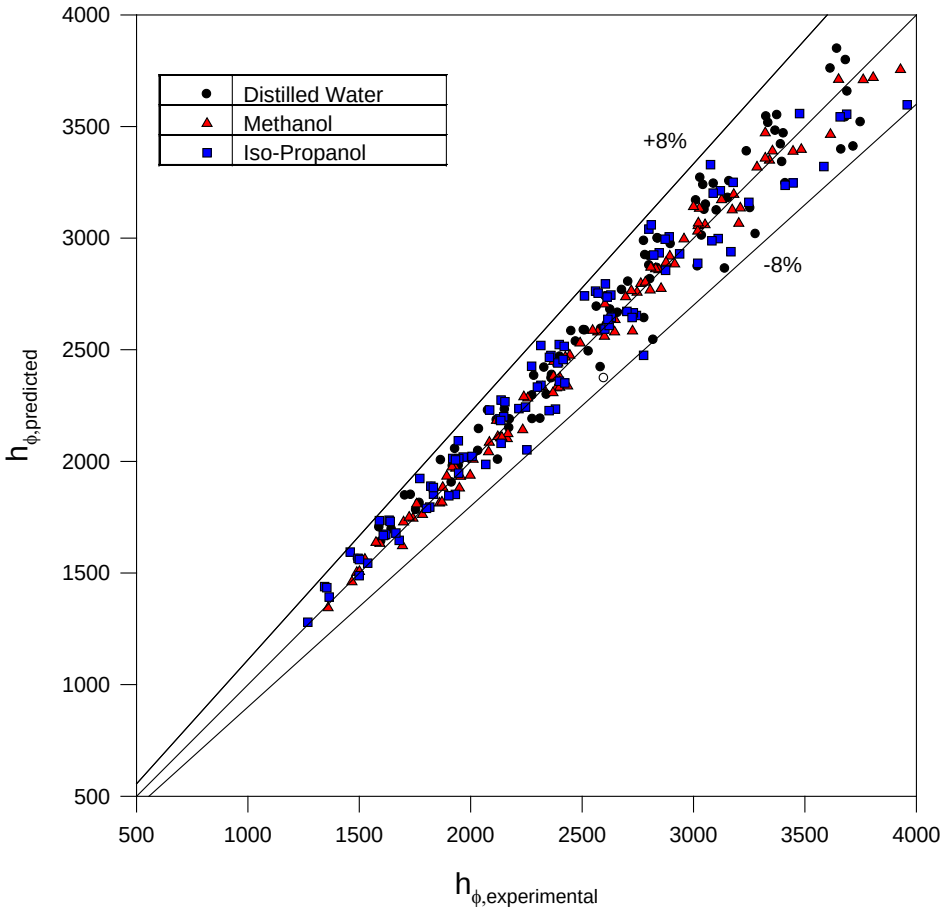

Figure 5.7 Comparison of experimental local heat transfer coefficient, W/m^2K with those predicted from **Eq. (5.4)** for pool boiling of distilled water, methanol and iso-propanol at atmospheric and subatmospheric pressures

position and boiling liquid.

The analytical calculation of constant C_Φ is highly improbable owing to variation in size, shape and number of irregularities present on a tube surface. Hence, **Eq. (5.3)** cannot be employed for the determination of local heat transfer coefficient of those heating surface-liquid combination whose value of constant C_Φ is not experimentally known. In other word, **Eq. (5.3)** is of limited applicability.

5.2.3. Average heat transfer coefficient

The value of surface temperature measured at various circumference position of the tube; show a significance variation as evident from the previous section. Therefore the values of various surface temperature measured at various circumferential position of tube have been averaged, to determine average surface temperature. Similarly, the average liquid temperature has been calculated and these values the average heat transfer coefficient (here after called as heat transfer coefficient) has been calculated corresponding to each heat flux, subjected to an uncoated tube for boiling of distilled water, methanol and Iso-Propanol, at atmospheric and subatmospheric pressures. Procedure used for computation is given in an Annexure C, Sample Calculation. The computed value of heat transfer coefficient, of each experimental run is given in the Table B.1, B.5 and B.7 of Annexure-B.

Figure 5.8 shows a plot between heat transfer coefficient flux or boiling distilled water at atmospheric pressure it also contains experimental data of earlier investigation namely alam.et al.[A4], Benjamin & Balakrishan [B6], Bhaumik et al. [B11,12], Borishanskii et al.[B16], Cryder & Finalborgo [C22], Dhir & Liaw [D2], Hirichs et al.[H6], Heish & Hsu[H8,H9], Kurihara& Myers[K17], Wang& Dhir[W2], and Young and Hummel[Y8] for the purpose of comparison. A close examination of this plot reveals the following features:

i. It can be seen that data of this investigation do not agree with those of any of investigations.
ii. Data of earlier investigators do not match amongst themselves. However, data points of an investigator forms a distinct group and obey the power law relationship $\boldsymbol{h} \propto \boldsymbol{q}^{0.7}$.

These features are consistent as heating surfaces used in these investigations have deferred in the surface characteristics owing to different surface employed and hence differed in their surface characteristics owing to differing roughness, material of construction, etc. Since boiling is a surface phenomena, above disagreement amongst data

of various investigators is bound to occur. On the basis of above, it can be said that it is difficult to compare boiling heat transfer data of an investigator conducted on a heating surface with the data of other investigators.

Figure 5.9(a) represents plots to show the variation of heat transfer coefficient with heat flux for saturated boiling of distilled water. Pressure is a parameter in this plot. Following key features have been drawn from this plot:

i. For a given pressure, heat transfer coefficient increases with an increase in heat flux and the variation between the two can be described by power law $\mathbf{h} \propto \mathbf{q}^{0.7}$.

ii. At a given heat flux, an increase in pressure enhances the value of heat transfer coefficient.

Both the above features are consistent and in accordance with the physics of boiling phenomena. Possible explanation for these features is as follows:

As explained earlier, an increase in heat flux raises local wall superheat which, in turn, leads to increase average wall superheat of heating tube. This according to equation, **Eq. (5.2)** causes the value of minimum radius of nucleation site at which vapor bubble can originate, r_c to decrease. Consequently, nucleation sites of smaller sizes present on heating surfaces get activated and generate vapor bubbles forms at enhanced value of heat flux. This increases the intensity of turbulence which in turns leads to higher rate of heat removal and thereby higher heat transfer coefficient.

An increase in pressure, as discussed in subsection 5.2.2, enhances intensity of turbulence caused by vapor – bubble dynamics due to the occurrence of large population of small sized vapor-bubbles. As a result high value of heat removal rate occurs and so heat transfer coefficient is found to be higher at an elevated pressure.

Boiling of methanol and iso-propanol provided the same features as observed above for the boiling of distilled water. This can be easily seen from **Fig. 5.9.(b)** and **Fig. 5.9.(c).** Which is a plot between heat transfer coefficient and heat flux for saturated boiling of methanol at atmospheric and subatmospheric pressures. It may be mentioned here that above features have also been observed by Cryder& Finalborgo [C22] for boiling of water , methanol and carbon tetrachloride, and n-butanol on a brass surface, Bonilla & Perry [B15, P5] for boiling of water ethanol, n- butanol and acetone on copper surface and Kurihara & Myers [K17] for boiling of water, carbon tetrachloride, acetone and n-hexane on a copper surface. Thus, this investigation has corroborated the findings of earlier

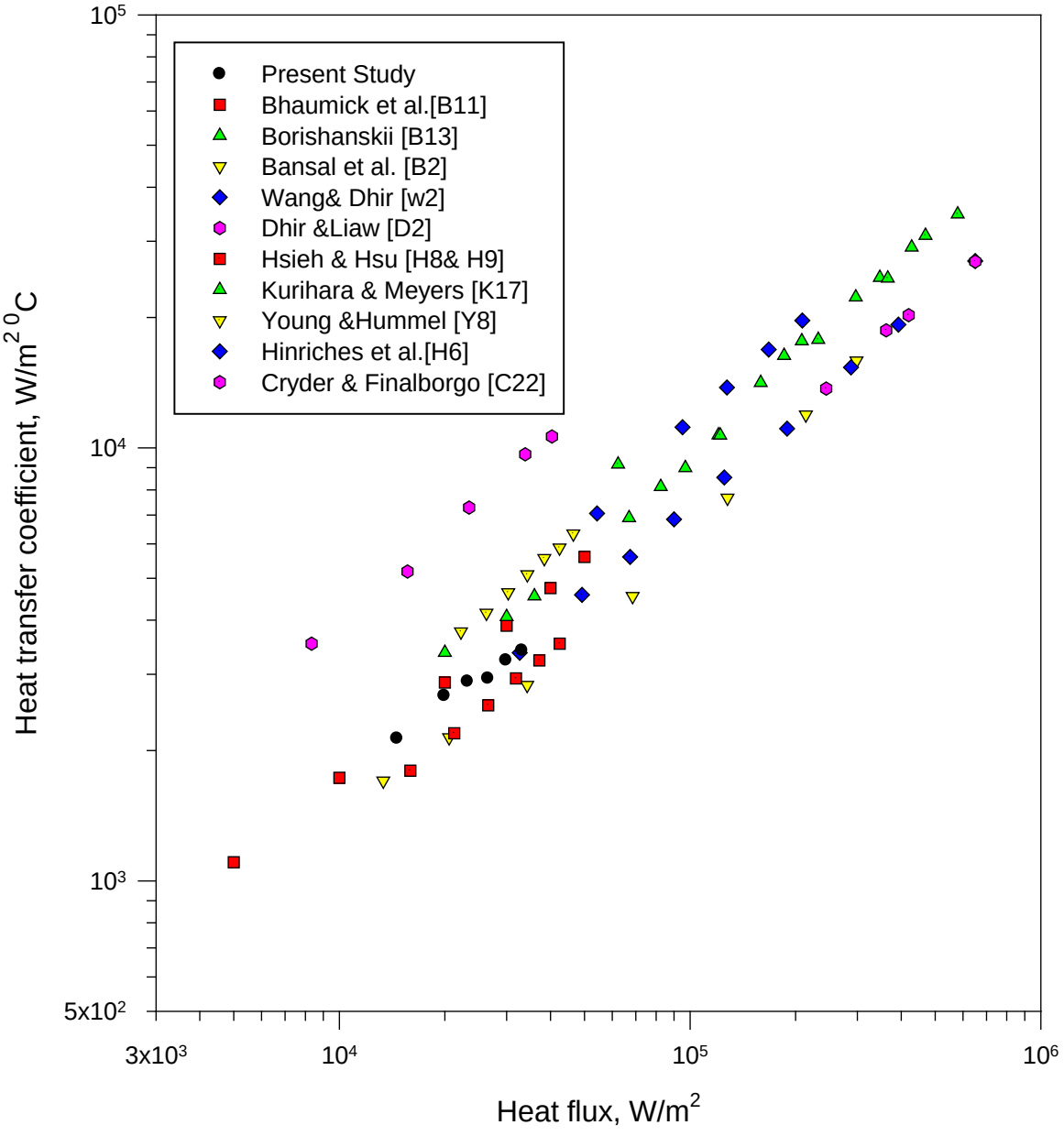

Figure 5.8 Comparison of experimental data of this investigation with those of earlier investigation for boiling of distilled water at atmospheric pressure

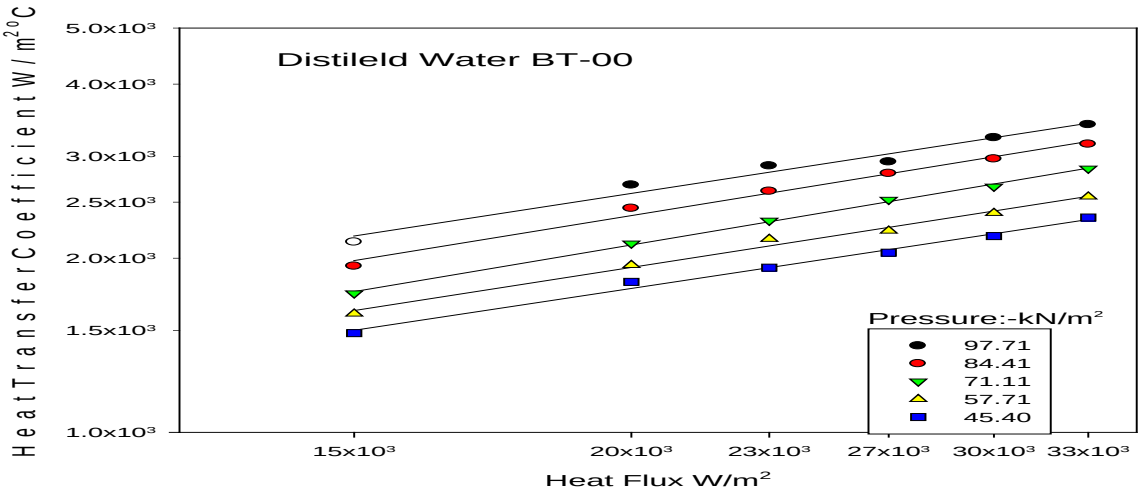

(a)

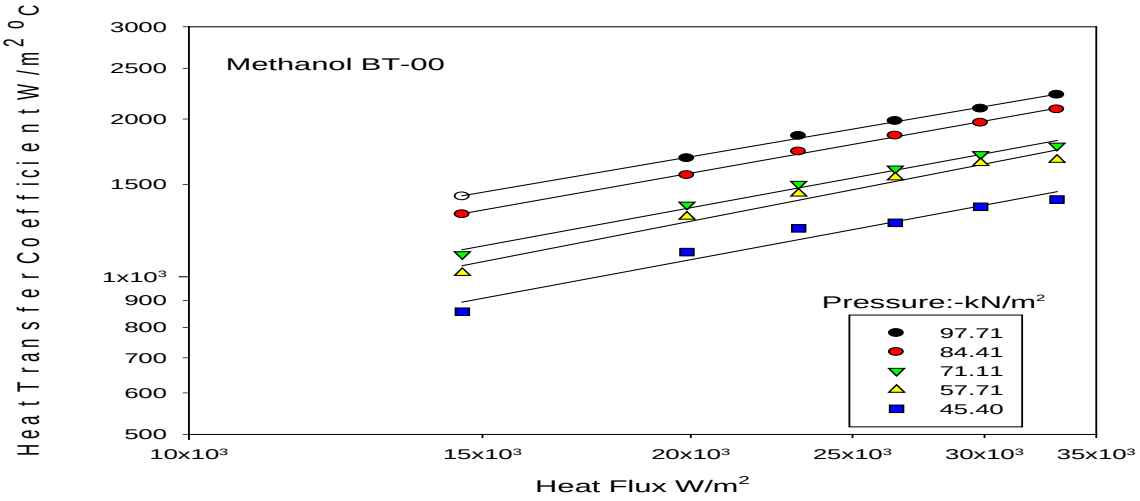

(b)

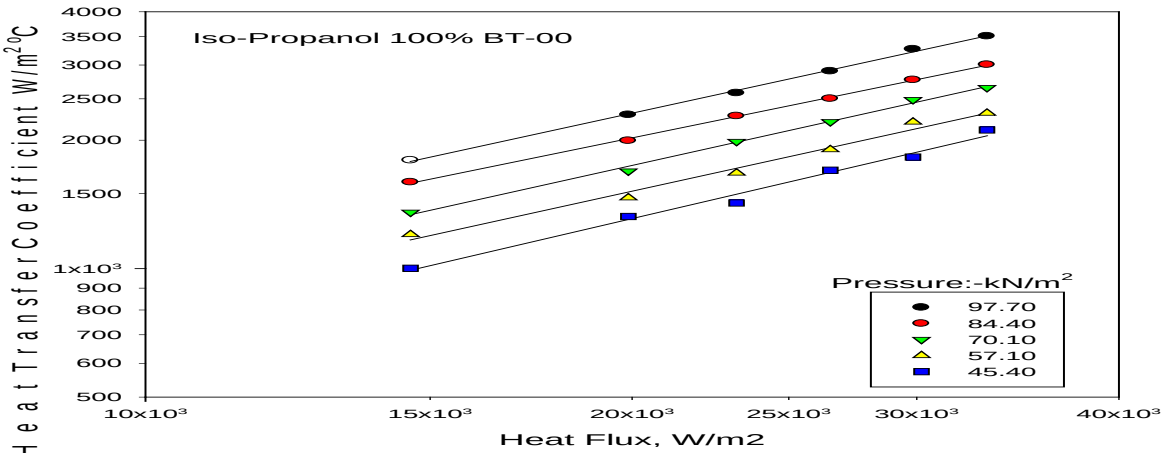

(c)

Figure 5.9 (a, b, c) Variation of heat transfer coefficient with heat flux for saturated boiling of distilled water, methanol and iso-propanol

investigators for saturated boiling of liquids on an uncoated heating surface at atmospheric and subatmospheric pressures.

5.2.4 Heat transfer correlation for boiling of liquids

On the basis of above, it can be said that heat transfer coefficient for boiling of a Liquid on an uncoated heating tube depends upon heat flux and pressure. Therefore, functional relationship amongst them has also been developed by the method of least squares using experimental data of this investigation for the boiling of distilled water, methanol and Iso-propanol. The functional relationship is as follows:

$$h = C_1 q^{0.7} p^{0.32} \tag{5.4}$$

Where, $\mathbf{C_1}$ is a constant whose value depends up on the type of boiling liquid and heating surface characteristics. The values of constant $\mathbf{C_1}$ are 0.5895, 0.4875 and 0.389 for distilled water, methanol and iso-propanol, respectively, in this investigation.

Figure 5.10 depicts a plot between experimentally determined values of heat transfer coefficient and those predicted from **Eq. (5.4)** for the boiling of distilled water, methanol, and iso-propanol at atmospheric and subatmospheric pressures on an uncoated heating tube. From this plot, it is noticed that predictions match excellently with experimental values within a maximum error of $\pm$ 6 %. Therefore, **Eq. (5.4)**, which is a simple and convenient one, can be used for the computation of heat transfer coefficient of a liquid boiling on an uncoated heating tube from the knowledge of heat flux and pressure provided the value of constant $\mathbf{C_1}$ is known.

Unfortunately the determination of $\mathbf{C_1}$ is highly improbable due to variation of irregularities present on a tube surface. Hence, **Eq. (5.4)** cannot be used to determine heat transfer coefficient of those heating surface-liquid combination whose value of constant $\mathbf{C_1}$ is not known.

In other word, it calls for the development of a method which may make **Eq. (5.4)** free from the constant $\mathbf{C_1}$**.** Hence, following strategy has been adopted as relation between heat transfer coefficient and heat flux remain unchanged for entire subatmospheric range. **Eq. (5.4)** may be written in following form

$$h^* = Cp^{0.32} \tag{5.5}$$

Where $h^* = \left(\frac{h}{q^{0.7}}\right)$

Eq. (5.5) can also be written in following dimensionless form, if one assumes that the value of constant C does not depends on pressure.

$$\frac{h^*}{h_1{}^*} = \left(\frac{p}{p_1{}^*}\right)^{0.32} \tag{5.6}$$

Equation (5.6) is tested against experimental data for the boiling of distilled water , methanol and iso-propanol on an uncoated heating surface of this investigation; water, methanol and carbon-tetrachoride and n-butanol on a brass tube surface by cryder & Finalborgo[C22];of n-heptane on a copper plate surface by Cicelli & Bonilla [C12]; of distilled water, methanol, ethanol and iso-propanol on a brass tube surface by vittala et al. [V12]; of distilled water on a stainless steel tube surface by Bansal[B2]; of distilled water, benzene and toluene on a stainless steel surface by Bhaumik [B12] ;of distilled water on mild steel heating tube surface by Alam et al. [A2]; of methanol on a mild steel heat tube surface by Prasad et al. [P8] ; and of iso-propanol on a mild steel heat surface by Prasad[P8]. The comparison between predictions due **Eq. (5.6)** and the experimental values is shown in **Figure 5.11**. As can be seen, the predictions are in excellent agreement with the experimental values within an error of -11% to +9%. Thus, **Eq. (5.6)** is capable of correlating experimental data for the boiling of various liquids irrespective of heating surface involved in the process. This also proves the correctness of the hypothesis that constant, $\mathbf{C_1}$ does not depend upon pressure. This corroborates the finding of Bhaumik et al. [B11], Dhir[D2], Pandey.[P3], Prasad[P8] and Vitala et al.[V12], they also obtained similar results .

An implication of **Eq. (5.6)** is that it enables one to generate heat transfer data for the boiling of liquids at subatmospheric pressures without resorting to experimentation from the knowledge of experimentally determined value of heat transfer coefficient at atmospheric pressure only. Another important point is that **Eq. (5.6)** can also be used to examine the consistency of heat transfer data taken for the boiling of various liquid on heating surfaces of differing surface characteristics of atmospheric and subatmospheric pressures.

Finally, it is concluded that this investigation has reaffirmed the relationship amongst heat transfer coefficient, heat flux and pressure. It has also established a dimensionless correlation which is free from surface liquid combination factor. So the correlation is applicable to the boiling of liquids on a surface irrespective of its characteristics for subatmospheric pressure only.

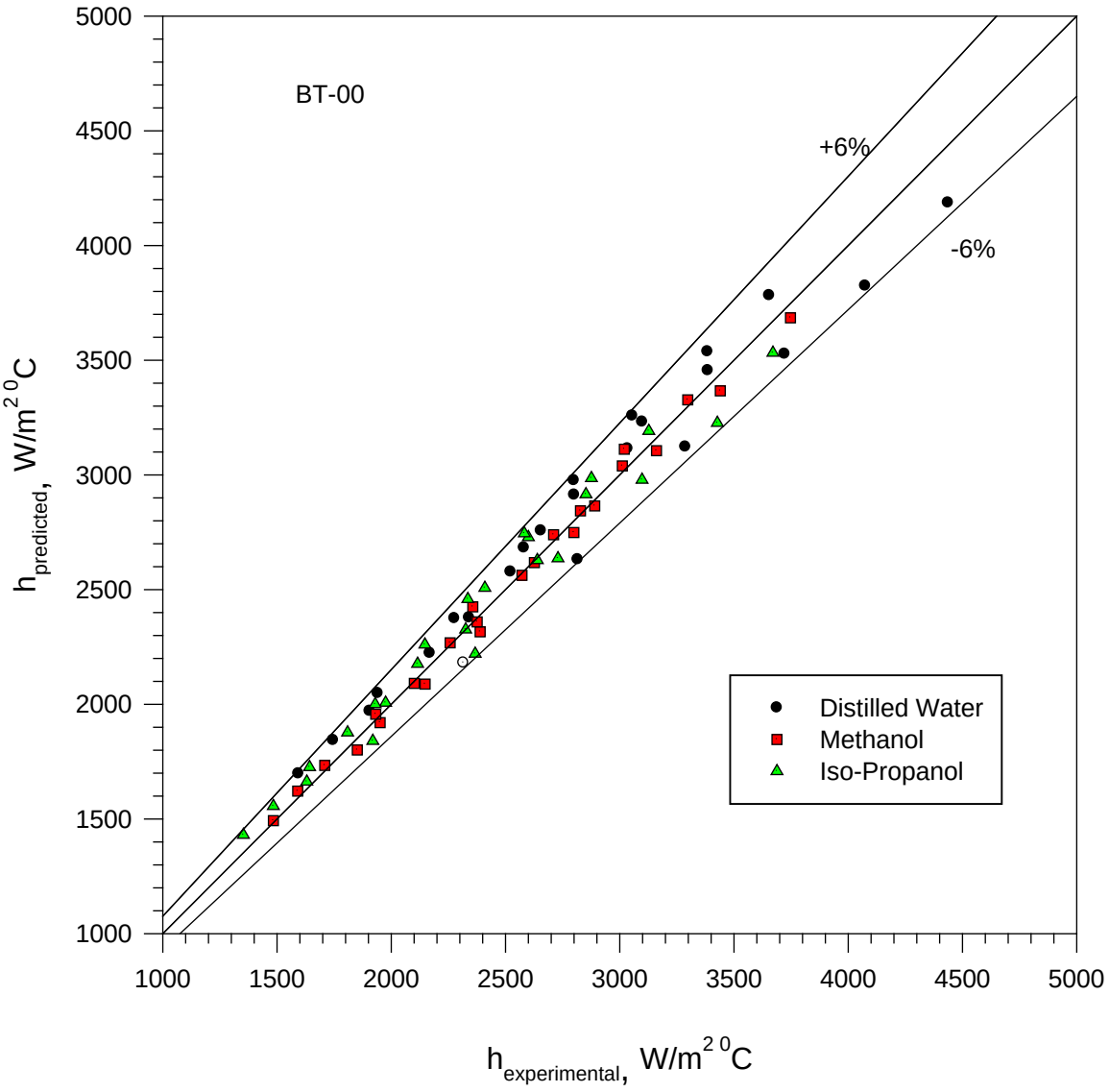

Figure 5.10 Comparison of experimental values of heat transfer coefficients with heat flux those predicted from **Eq.(5.4)** at atmospheric and subatmospheric pressures

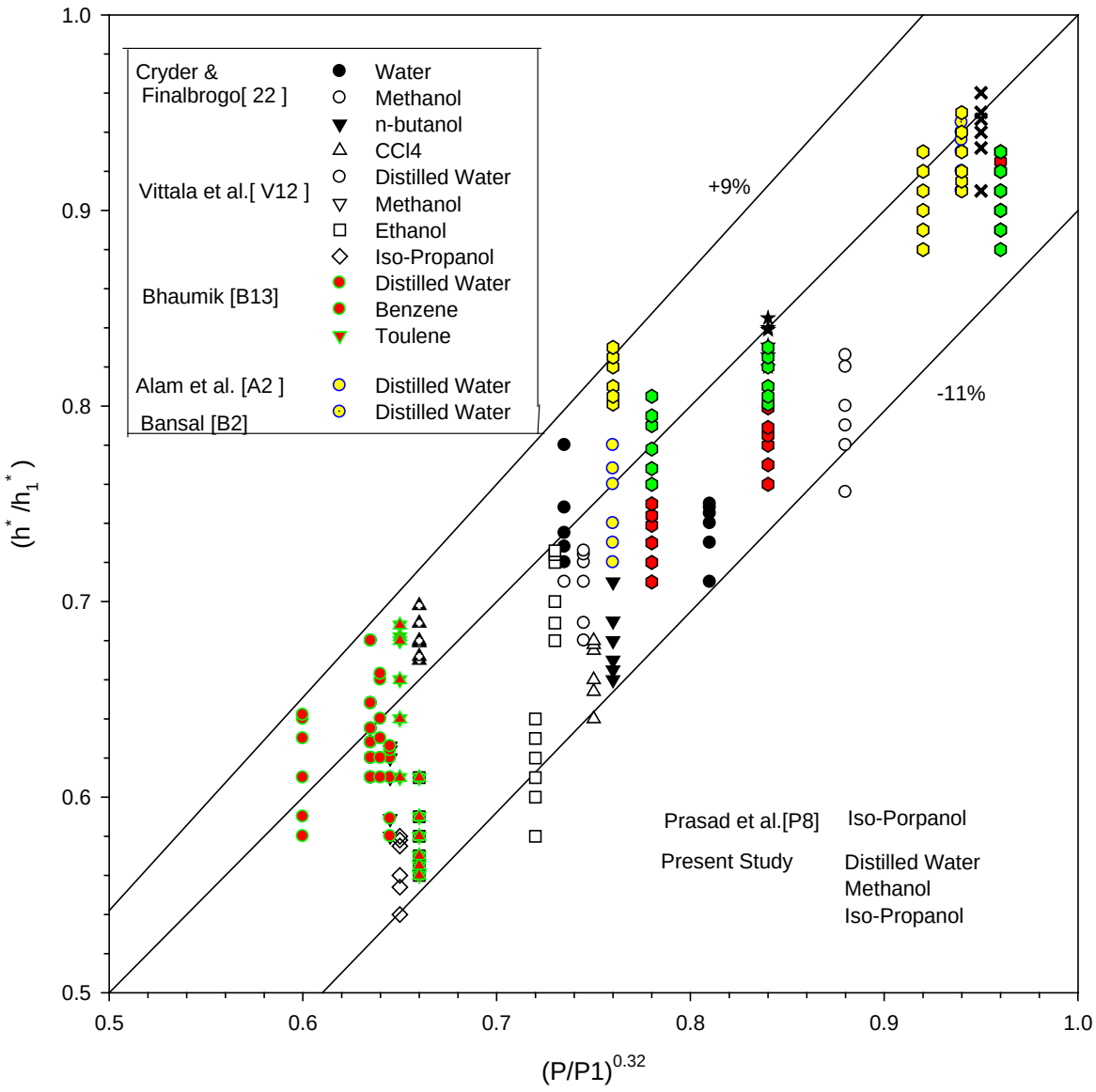

Figure 5.11 A plot between (h* /h1*) and $(P/P1)^{0.32}$ for the boiling of various liquid on an uncoated heating surface at atmospheric and subatmospheric pressures

5.3 NUCLEATE POOL BOILING OF BINARY MIXTURES ON A UNCOATED HEATING TUBE

Experimental data for the boiling of various compositions iso-propanol-distilled water and methanol-distilled water are tabulated in table's B.15, to B.20 and B.9 to B.15, respectively of Annexure B. It includes the measured value of temperature of heating surface as well as liquid pool at top, two side and bottom and heat flux. It also include the calculated

value of heat transfer coefficient of each composition at atmospheric and subatmospheric pressures, based on these data variation of surface temperature and heat transfer coefficient around the circumference of the heating tube and the effect of heat flux, pressure and composition on heat transfer coefficient for the boiling of iso-propanol-distilled water and methanol-distilled water have been studied. Following section discuss these in details:

5.3.1 Variation of heat transfer coefficient along circumference

Figure 5.12 and 5.13 depicts surface temperature profile for the boiling of various compositions of iso-propanol-distilled water and methanol-distilled water mixtures on an uncoated heating tube surface at atmospheric pressure. Heat flux is the parameter in each plot. Each plot contains a dotted line which represent boiling temperature of liquid mixture. A close examination of these plots reveals the following:

1. Surface temperature is found to increases continuously as moving from bottom, to side, side to top position of the tube at given heat flux.
2. An increase in heat flux increase the value of surface temperature for a given circumference position.
3. Saturation temperature remains unchanged irrespective of heat flux and circumference position.

Above features have also been found to true hold for various iso-propanol distilled water mixture at subatmospheric pressure as clearly shown in **Figs 5.14 to 5.15.**

Further, similar feature have also been obtained for various composition of methanol-distilled water mixtures at atmospheric and subatmospheric pressures shown in **Figs. 5.16 and 5.17.**

Above features are same as observed in case of boiling saturated liquids. It may be mentioned here that experimentally obtained saturation temperature of mixture was compared with the theoretical value calculate by NRTL in software Aspen-Plus [J4] This comparison indicates an indiscernible difference between the two, as evident from **Figs. 5.18** and **5.19.** These are plots between the experimentally obtained values of saturation

temperature with that of calculated values for iso-propanol distilled water and methanol-distilled water mixtures, respectively pressure is parameter in these plots.

Thus, it can be concluded that boiling characteristic of a given composition of iso-propanol distilled water and methanol-distilled water mixtures are same as of an individual liquids. Hence, local heat transfer coefficient of binary is likely to vary in the same way as that of liquids. Keeping this in view it has not been included here, but detail analysis of heat transfer coefficient with respect to heat flux, pressure and composition has been carried out.

5.3.2 Average Heat Transfer Coefficient for Binary Mixtures

The average value of surface temperature of heating tube has been determined by taking the arithmetic mean of local surface temperature. Similar procedure has also been adopted for taking the average values saturation temperature of binary liquid mixtures. Using these values of heat transfer coefficient for boiling of various composition of iso-propanol-distilled water and methanol-distilled water mixtures have been determined. The heat transfer coefficient of binary mixtures have been calculated as given in Annexure C, Sample Calculation.

Figure 5.20(a) describe a plot between heat transfer coefficient and heat flux for boiling 10 mol% iso-propanol-distilled water. In this plot pressure is a parameter and close examination of this plot reveals the following features:

1. Heat transfer coefficient increases with increase of heat flux irrespective of pressure.

   The variation between the two can be described by power law $\mathbf{h \propto q}^{0.7}$

2. At a given heat flux the values of heat transfer coefficient of a mixture increase with the increase of pressure.

Above features have also been observed for the boiling of other composition of iso-propanol – distilled water mixture at various pressures as can be evident from plots in **Figs. 5.20(b)**, **5.21** and **5.22**. Further, these features have also been observed for the boiling of methanol–distilled water mixture at atmospheric and sub atmospheric pressures as shown in **Figs. 5.23, 5.24, and 5.25.**

Above observed features are same as obtained for boiling of individual liquids. Hence, same explanation was given in section **5.2.3.** holds true in this case also. It may be pointed out that this also corroborates the findings of Pandey [P3,P4] for boiling of ethanol-water, methanol- water and iso-propanol- water mixtures at atmospheric and subatmospheric pressures, Alam and Varshney [A4] for boiling of glycerine-water,

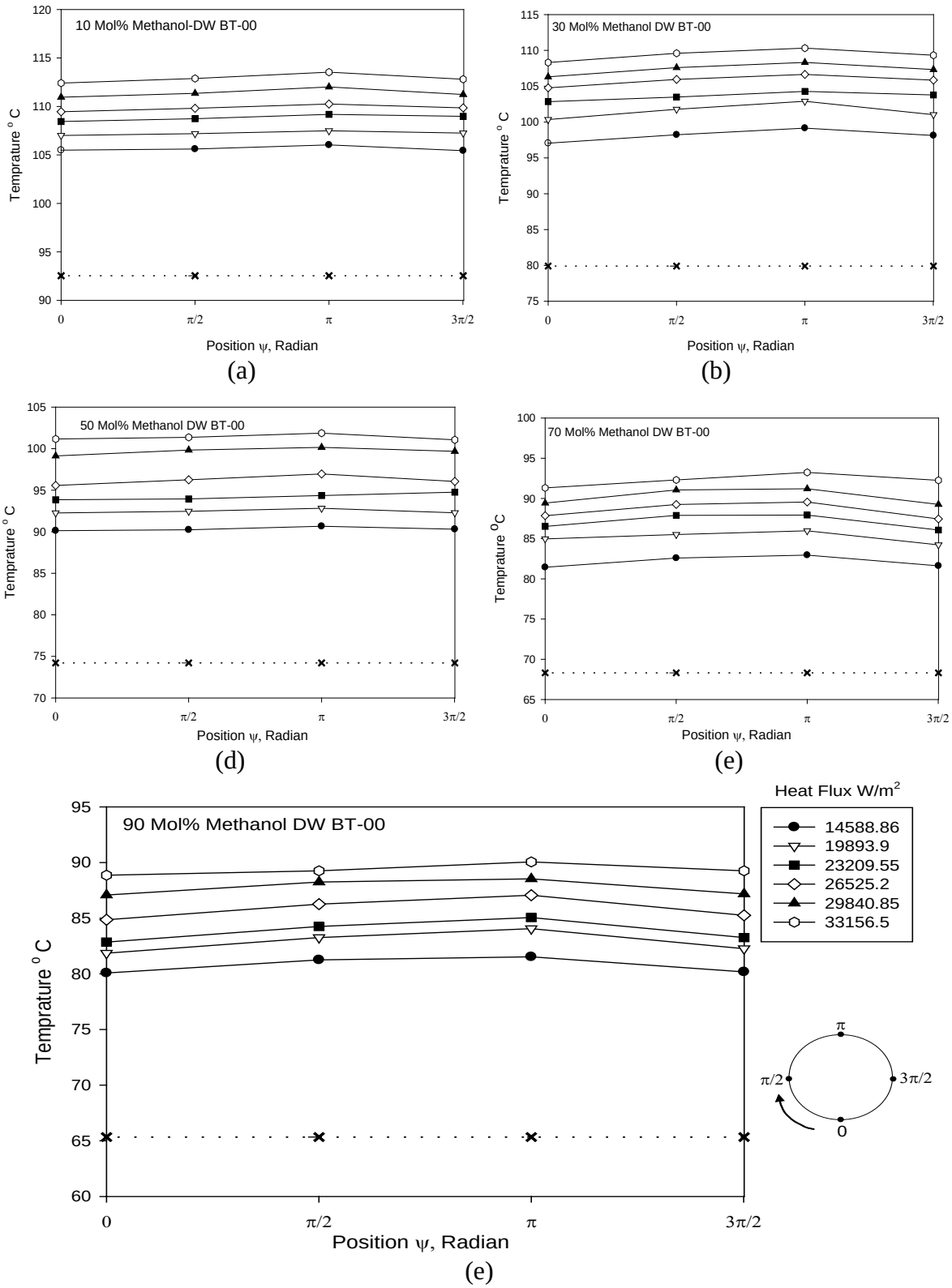

Figure 5.12 Variation of liquid and surface temperature along circumference at bottom, two sides and top positions of uncoated heating tube with heat flux as a parameter for boiling of methanol-distilled water mixtures at atmospheric pressure

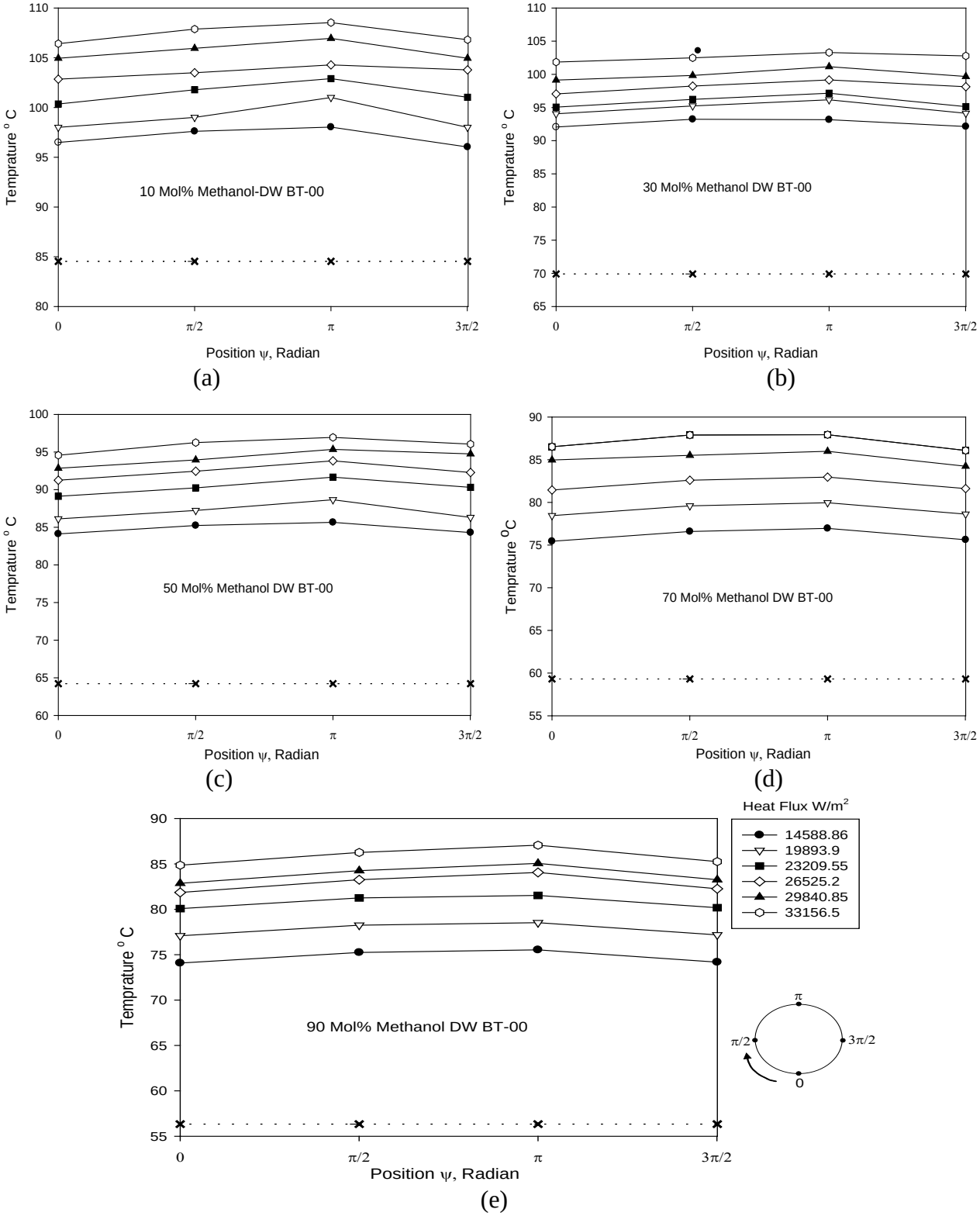

Figure 5.13. Variation of liquid and surface temperature along circumference at bottom, two sides and top positions of uncoated heating tube with heat flux as a parameter for boiling of methanol-distilled water mixtures at 70.10 kN/m^2 pressure

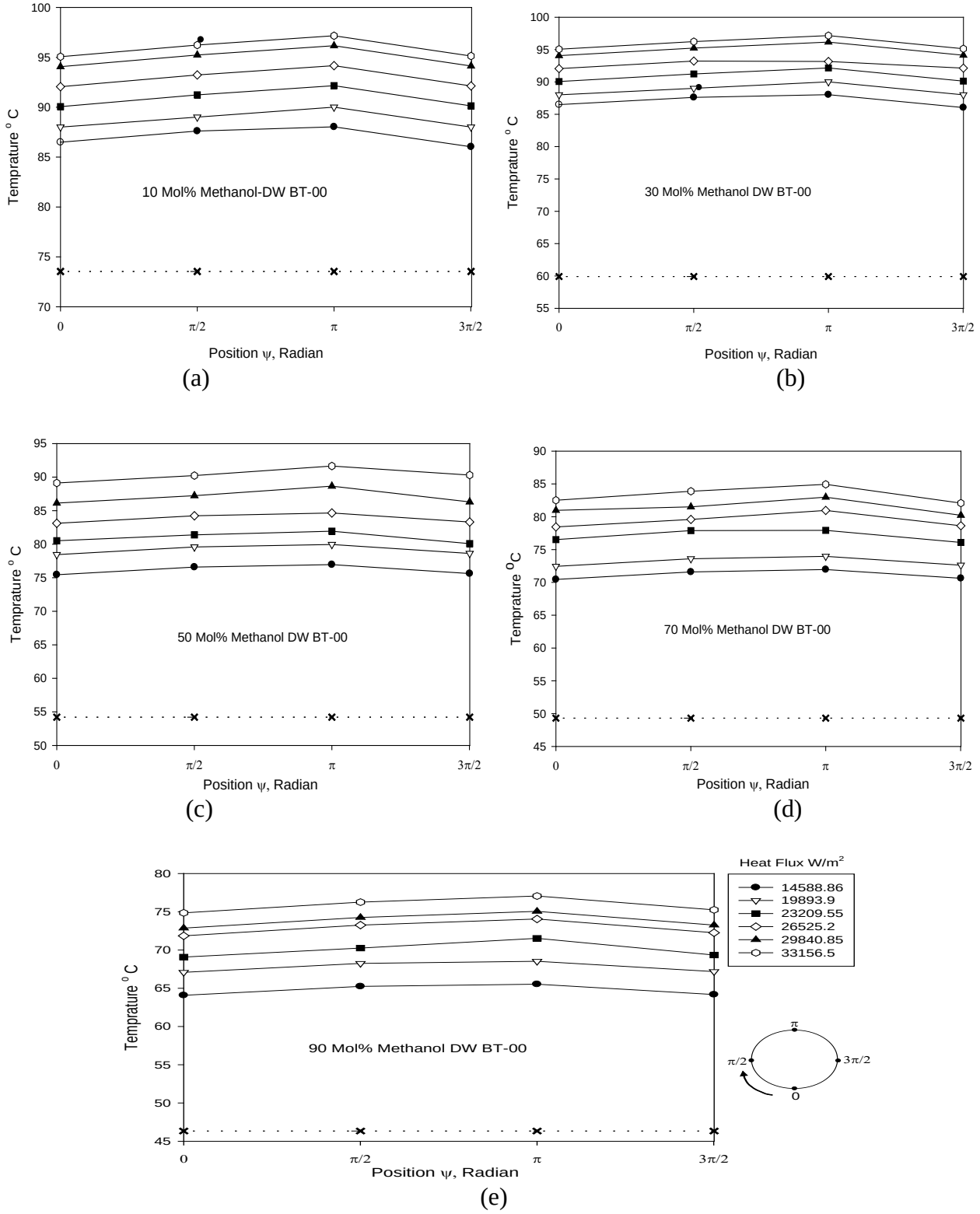

Figure 5.14. Variation of liquid and surface temperature along circumference at bottom, two sides and top positions of uncoated heating tube with heat flux as a parameter for boiling of methanol-distilled water mixtures at 45.40 kN/m^2 pressure

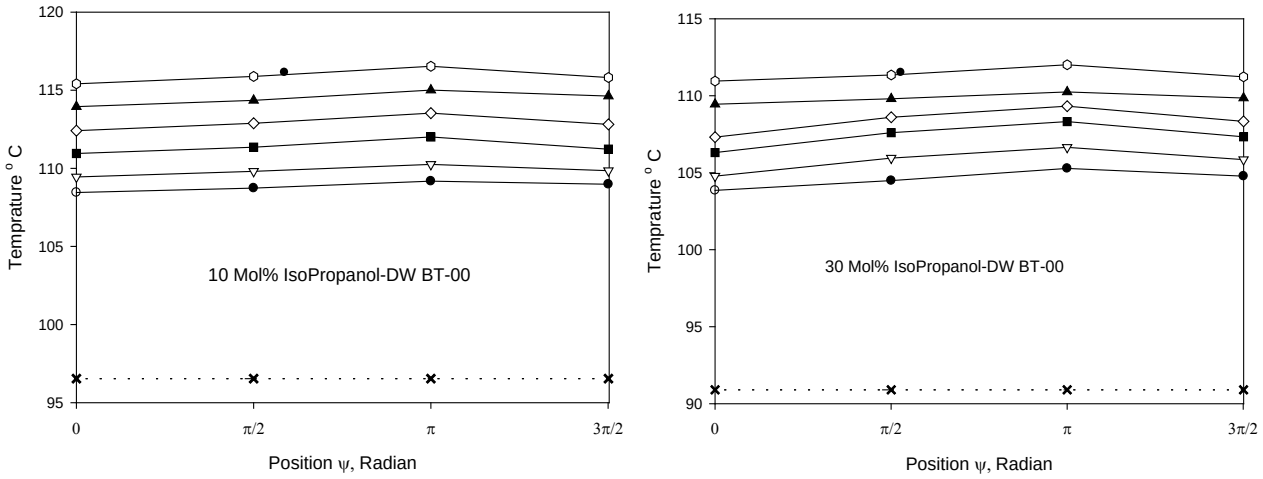

(a)

(b)

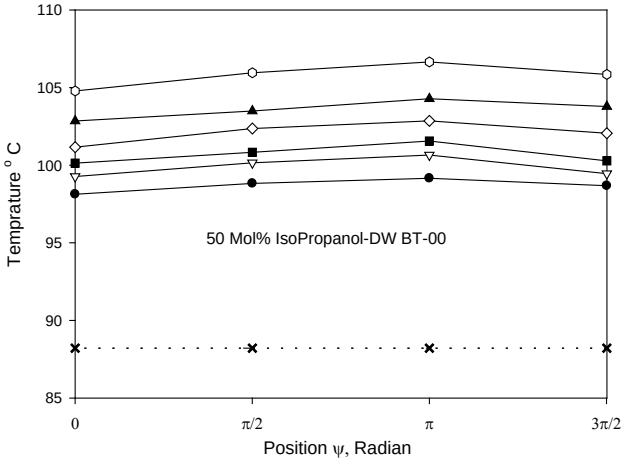

(c)

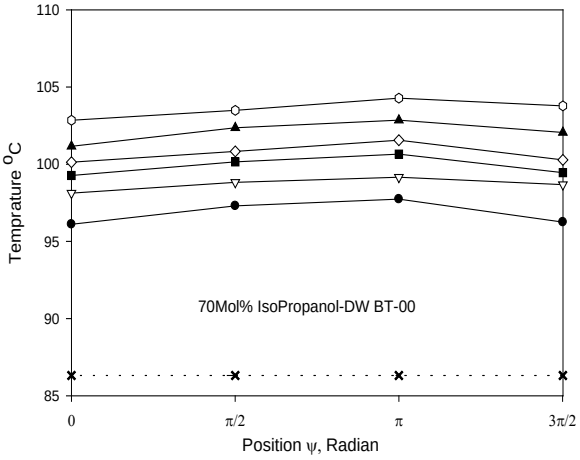

(d)

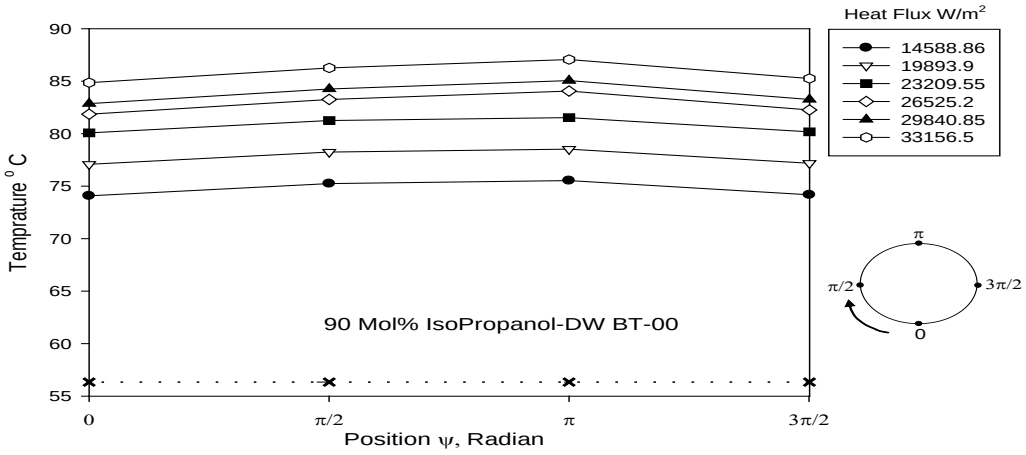

(e)

Figure 5.15 Variation of liquid and surface temperature along circumference at bottom, two sides and top positions of uncoated heating tube with heat flux as a parameter for boiling of Iso-Propanol- distilled water mixtures at atmospheric pressure

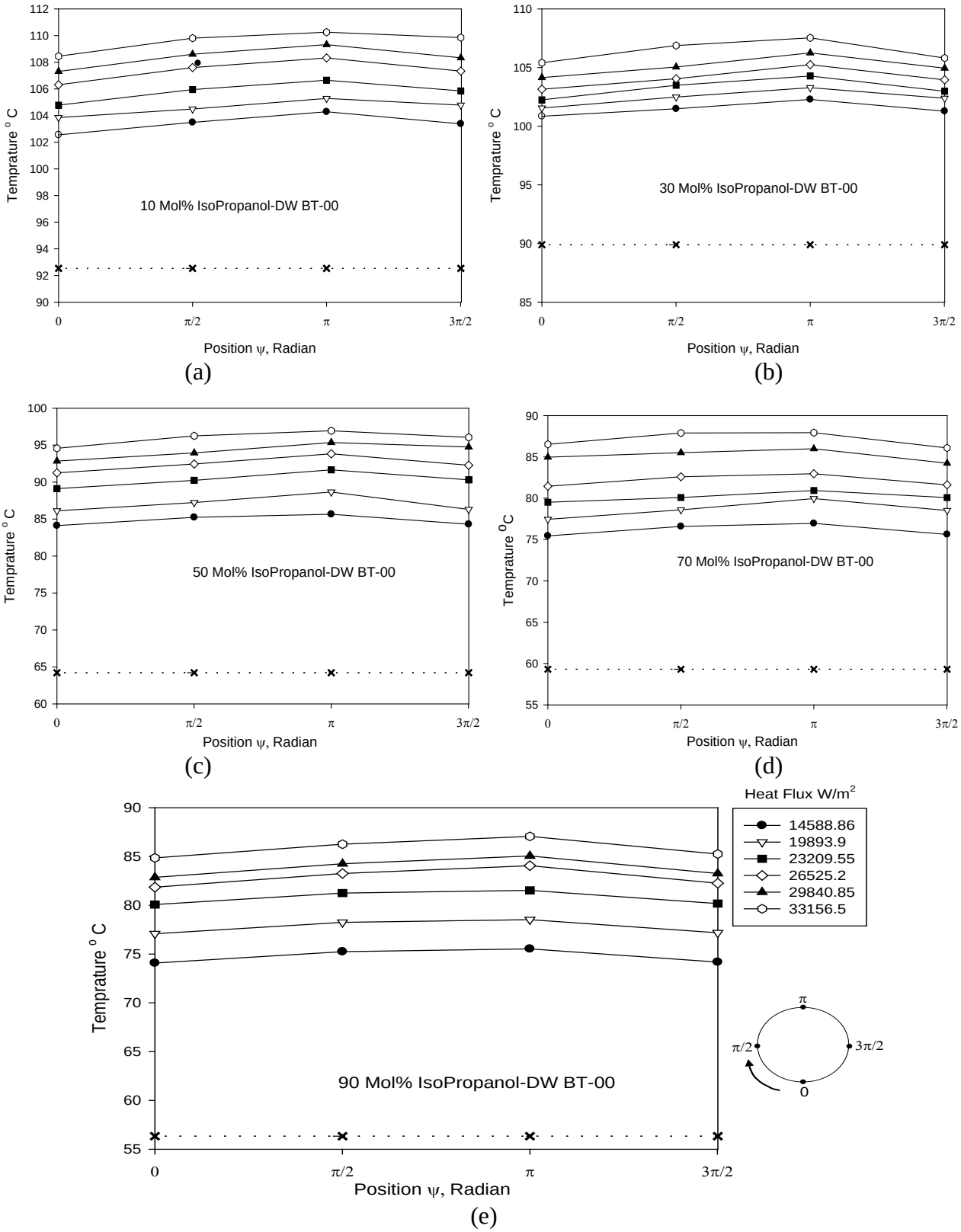

Figure 5.16. Variation of liquid and surface temperature along circumference at bottom, two sides and top positions of uncoated heating tube with heat flux as a parameter for boiling of Iso-Propanol- distilled water mixtures at 70.10 kN/m^2 pressure

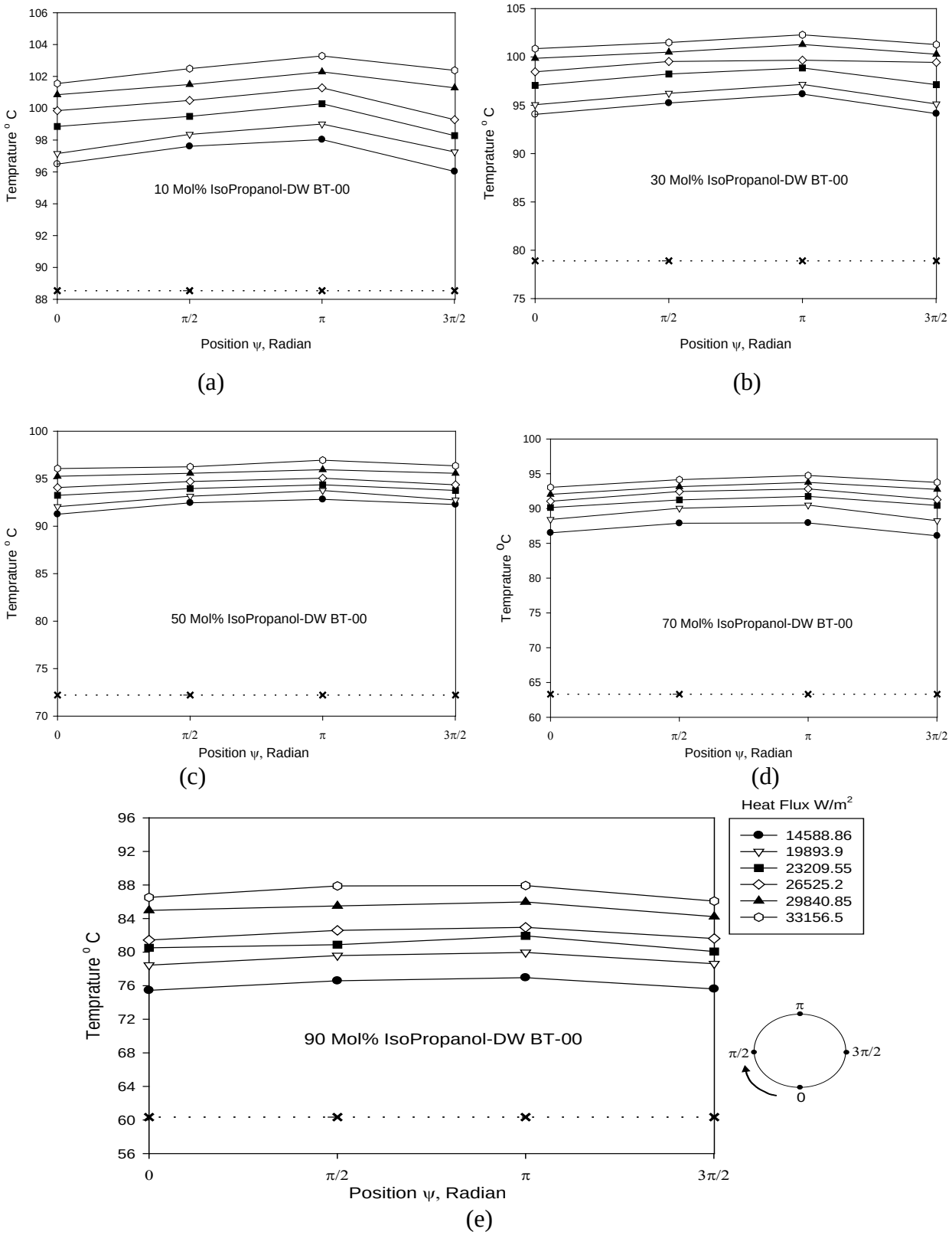

Figure 5.17. Variation of liquid and surface temperature along circumference at bottom, two sides and top positions of uncoated heating tube with heat flux as a parameter for boiling of Iso-propanol-distilled water mixtures at 45.40 kN/m^2 pressure

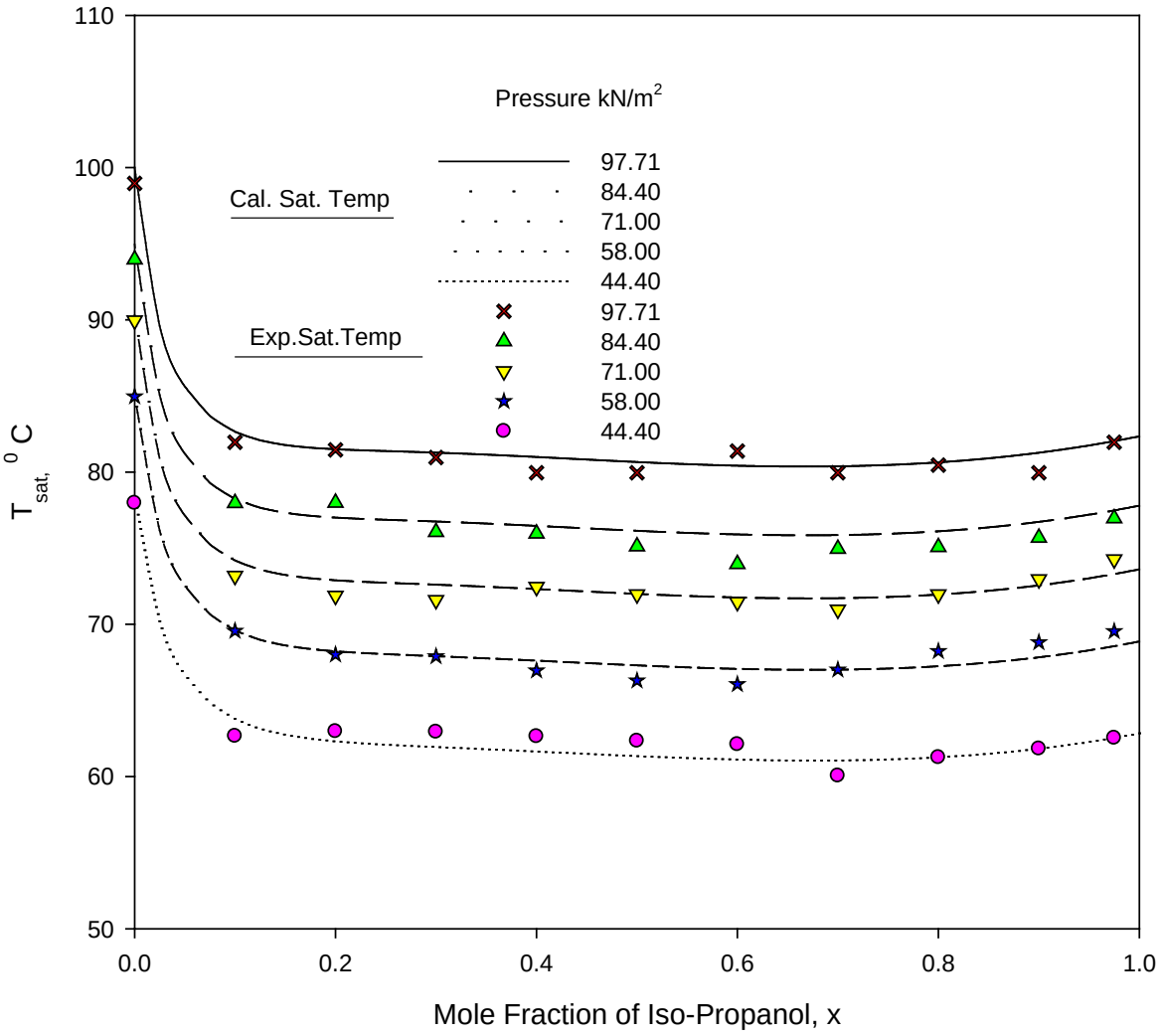

Figure 5.18 Comparison of experimental saturation temperature with those of calculated values of Iso-propanol – Distilled water at atmospheric and subatmospheric pressures

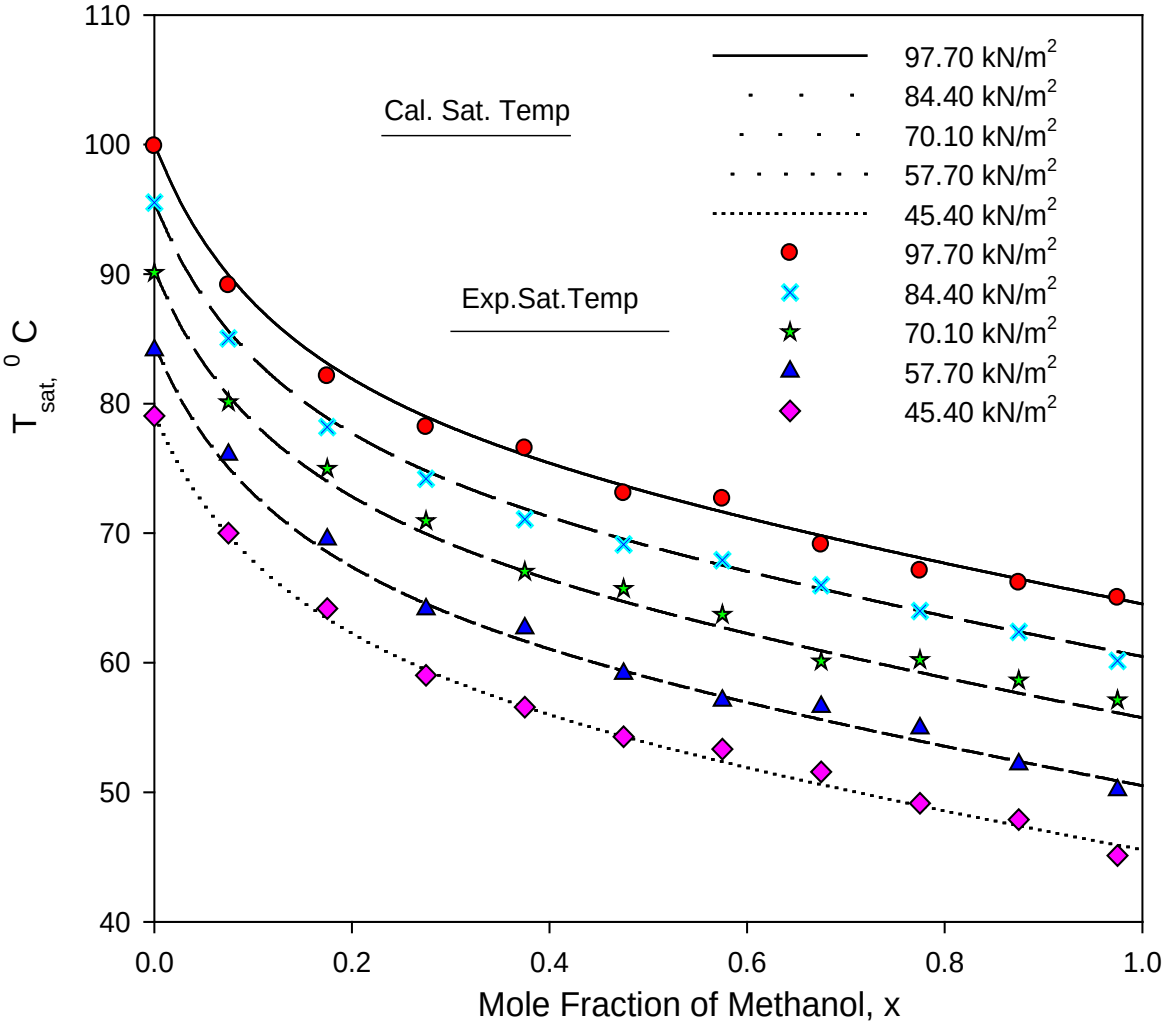

Figure 5.19 Comparison of experimental saturation temperature with those **o**f calculate values Iso-Propanol with Distilled water at atmospheric and sub atmospheric pressures

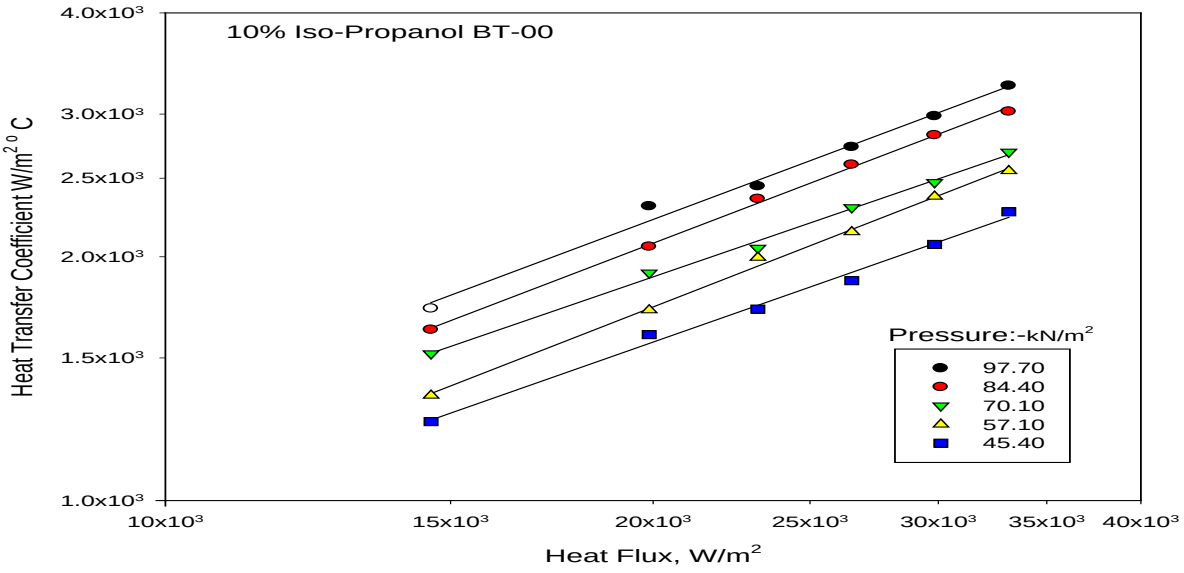

(a)

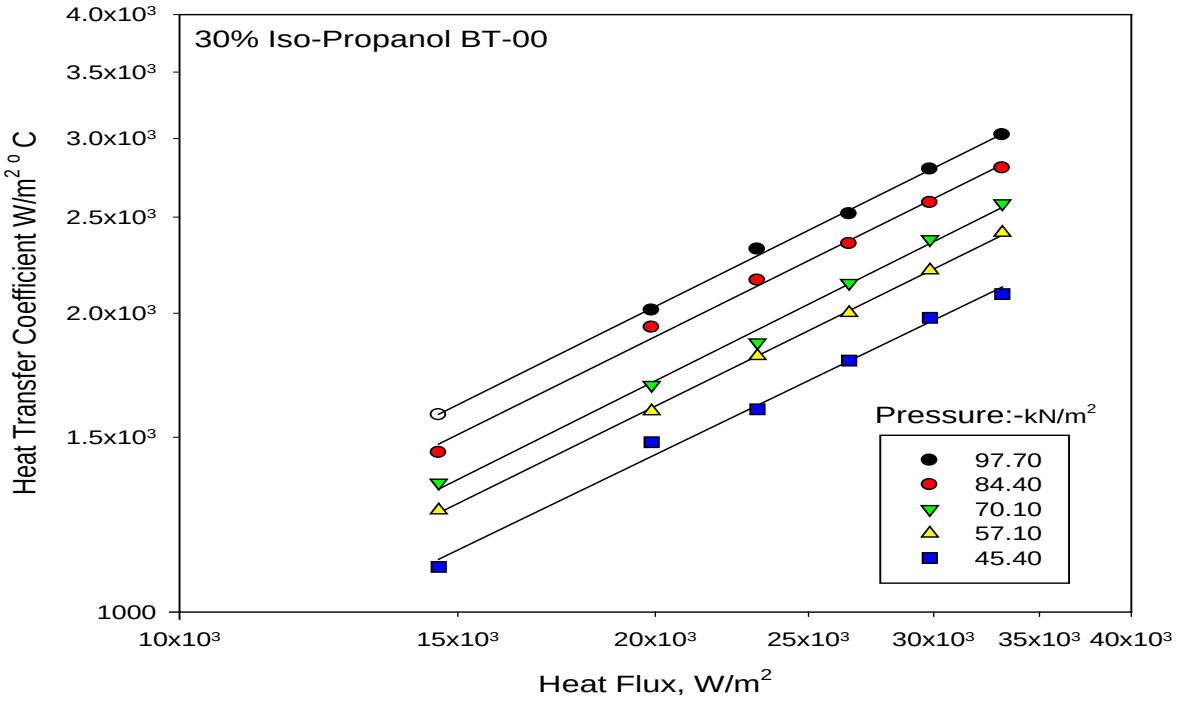

(b)

Figure 5.20 (a,b). Variation of heat transfer coefficient with heat flux for boiling of 10 and 30 Mol% Iso Propanol-distilled water mixture on an uncoated heating tube with pressure as a parameter

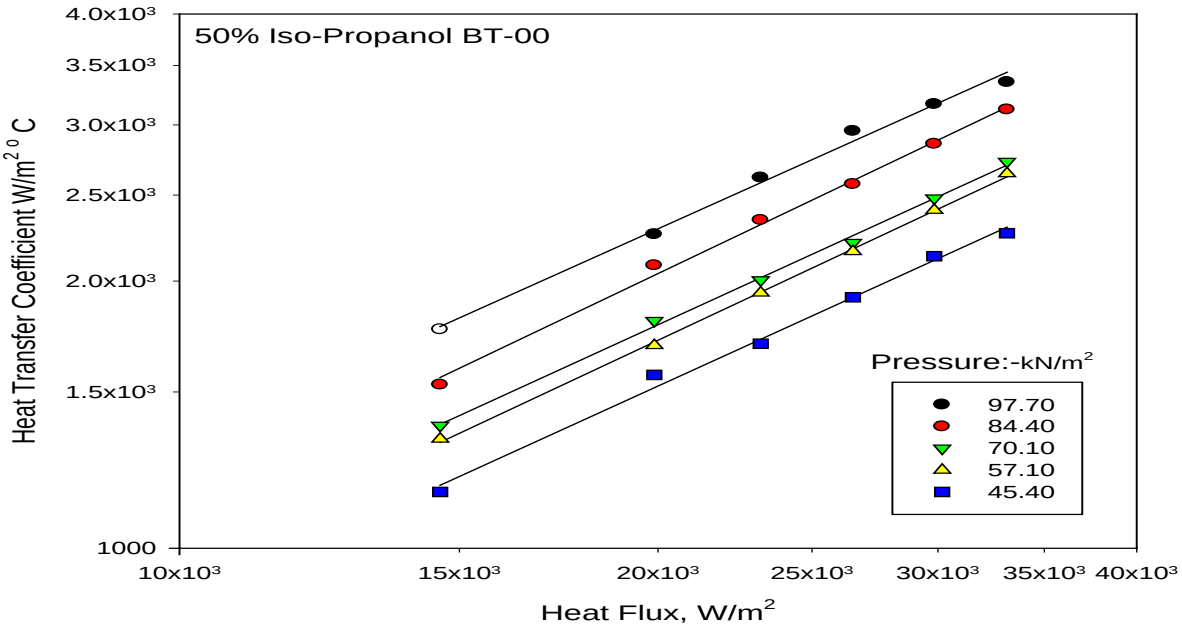

(a)

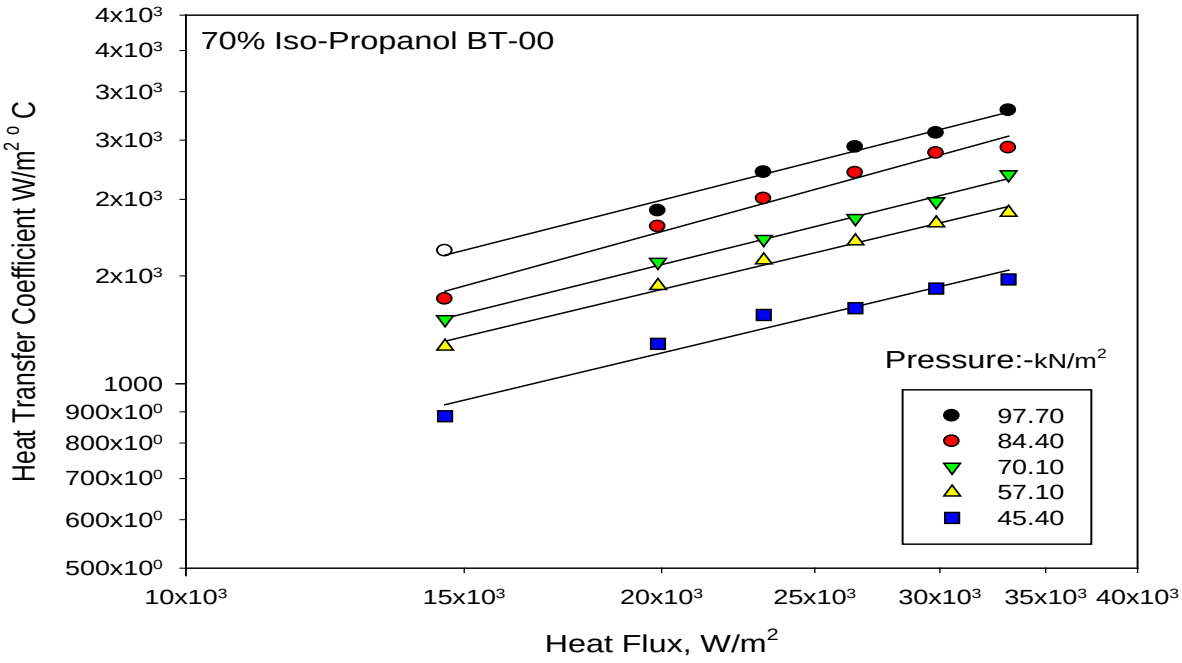

(b)

Figure 5.21(a,b). Variation of heat transfer coefficient with heat flux for boiling of 50 and 70 Mol% Iso Propanol distilled water mixture on an uncoated heating tube with pressure as a parameter

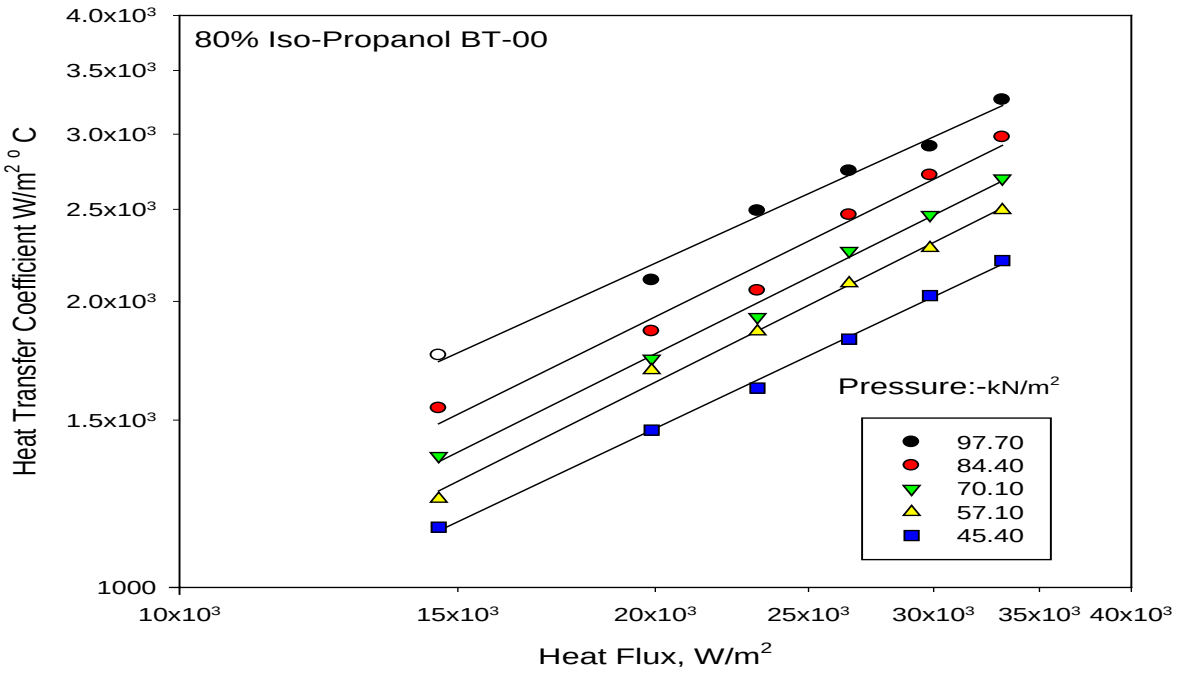

(a)

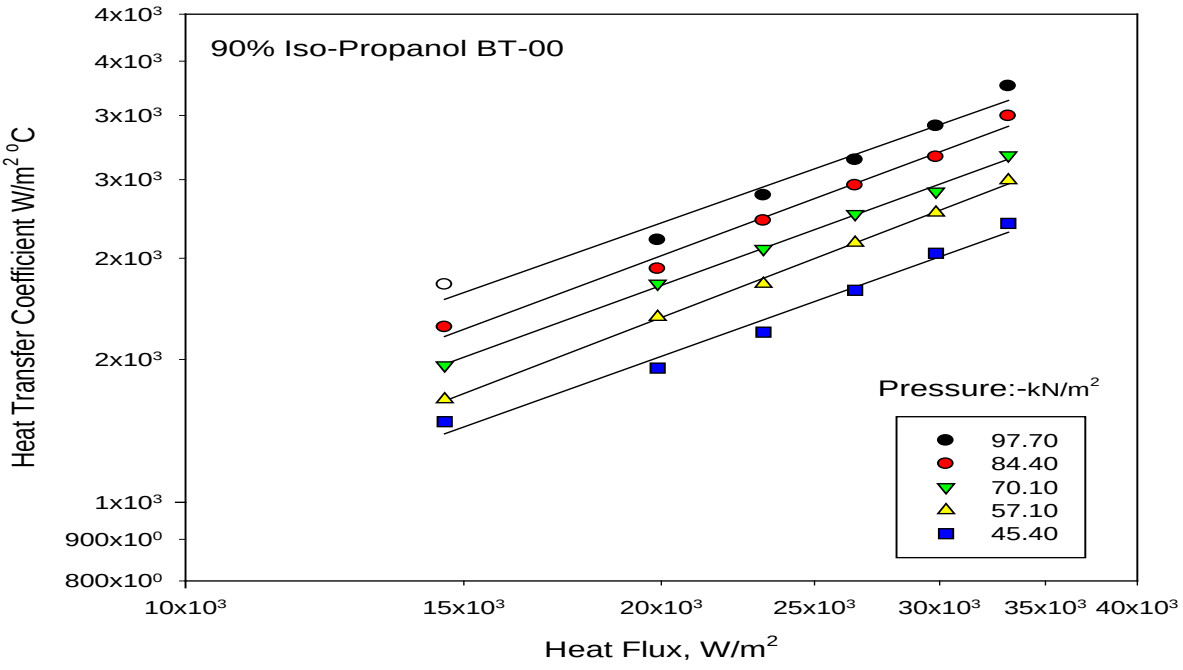

(b)

Figure 5.22(a,b). Variation of heat transfer coefficient with heat flux for boiling of 80 and 90 Mol% Iso Propanol-distilled water mixture on an uncoated heating tube with pressure as a parameter

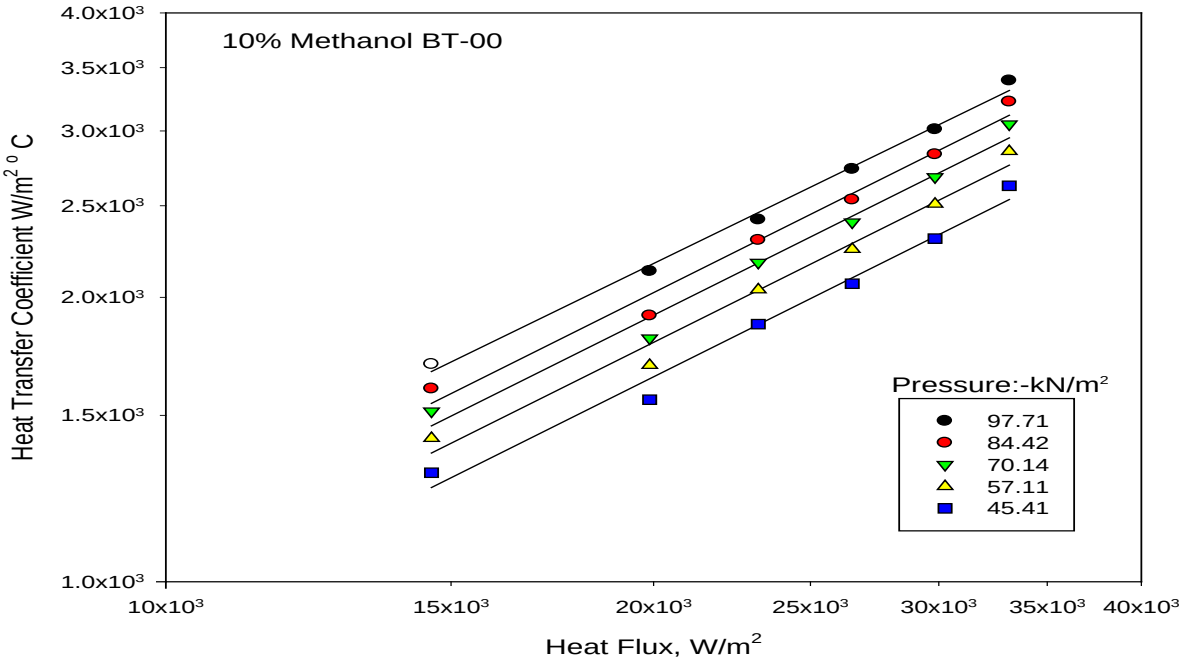

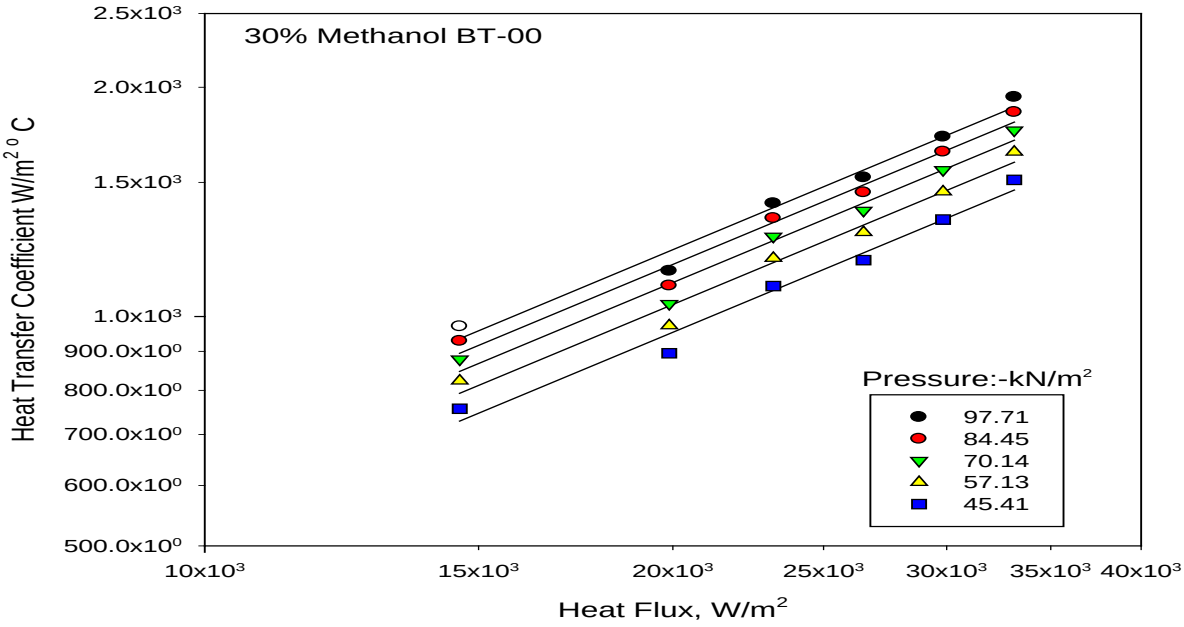

Figure 5.23(a,b). Variation of heat transfer coefficient with heat flux for boiling of 10 and 30 Mol% Methanol-distilled water mixture on an uncoated heating tube with pressure as a parameter

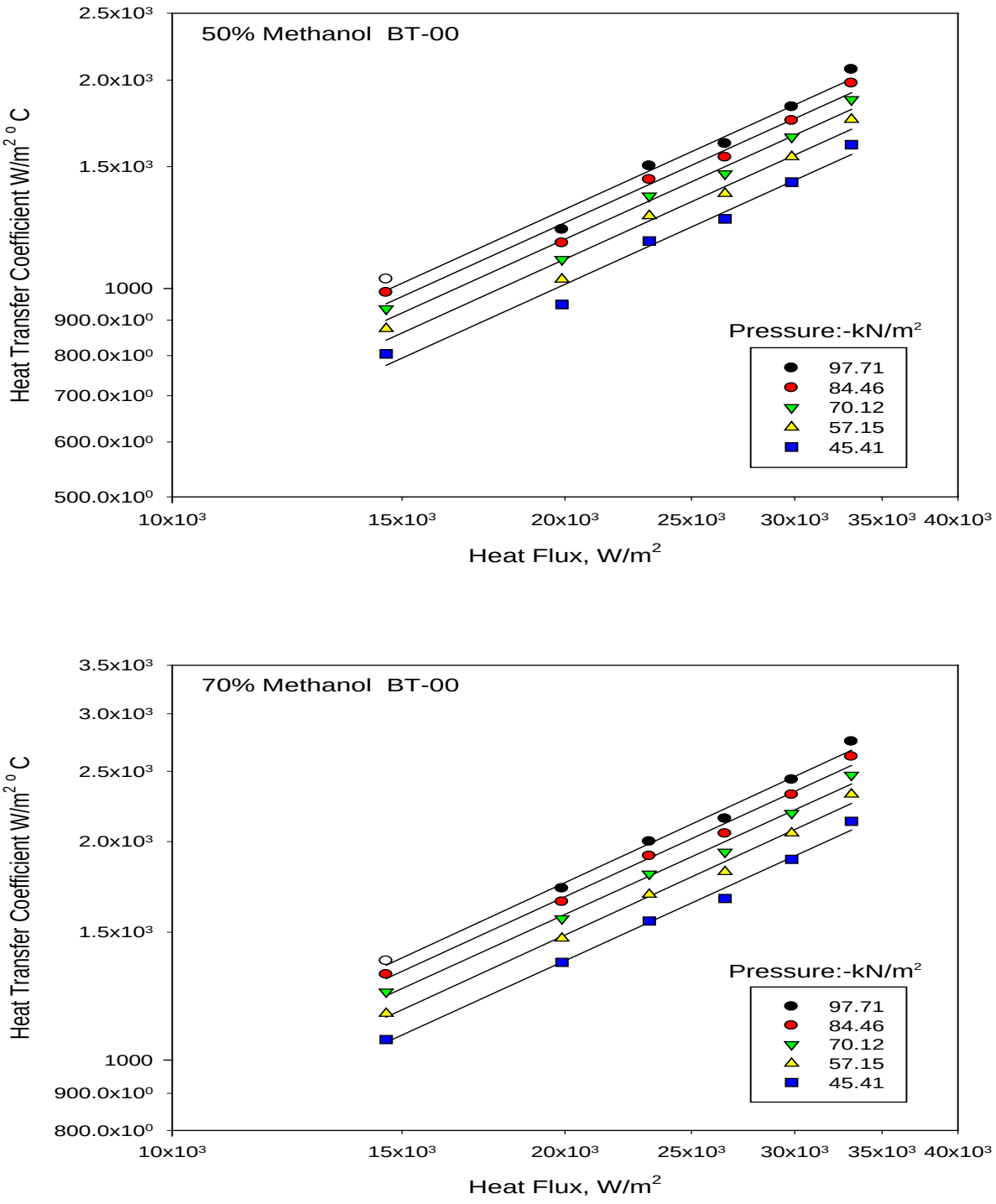

Figure 5.24 (a,b).Variation of heat transfer coefficient with heat flux for boiling of 50and 70 Mol% Methanol-distilled water mixture on an uncoated heating tube with pressure as a parameter

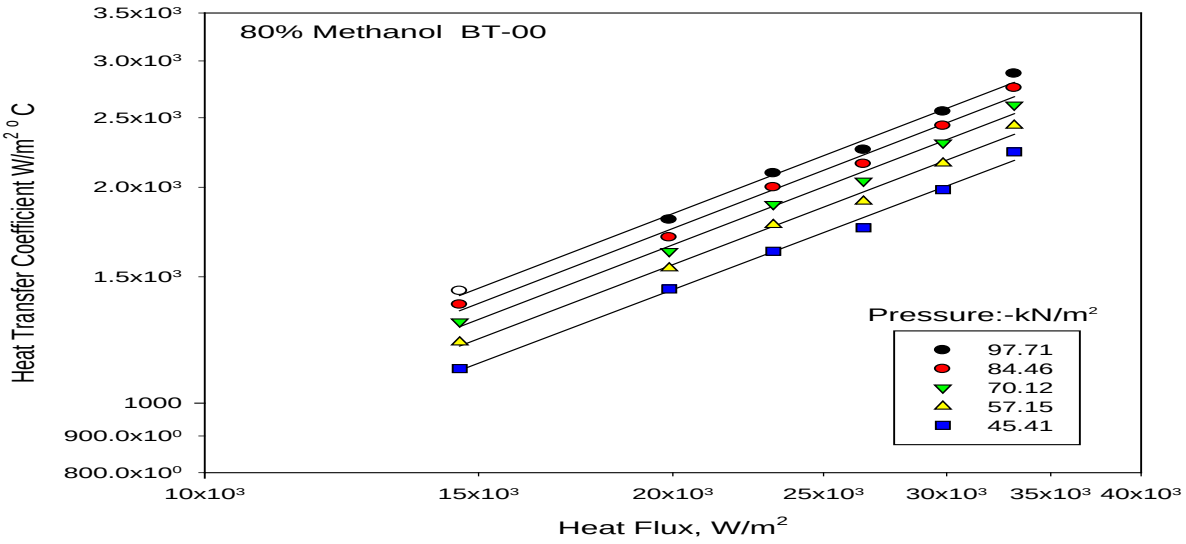

(a)

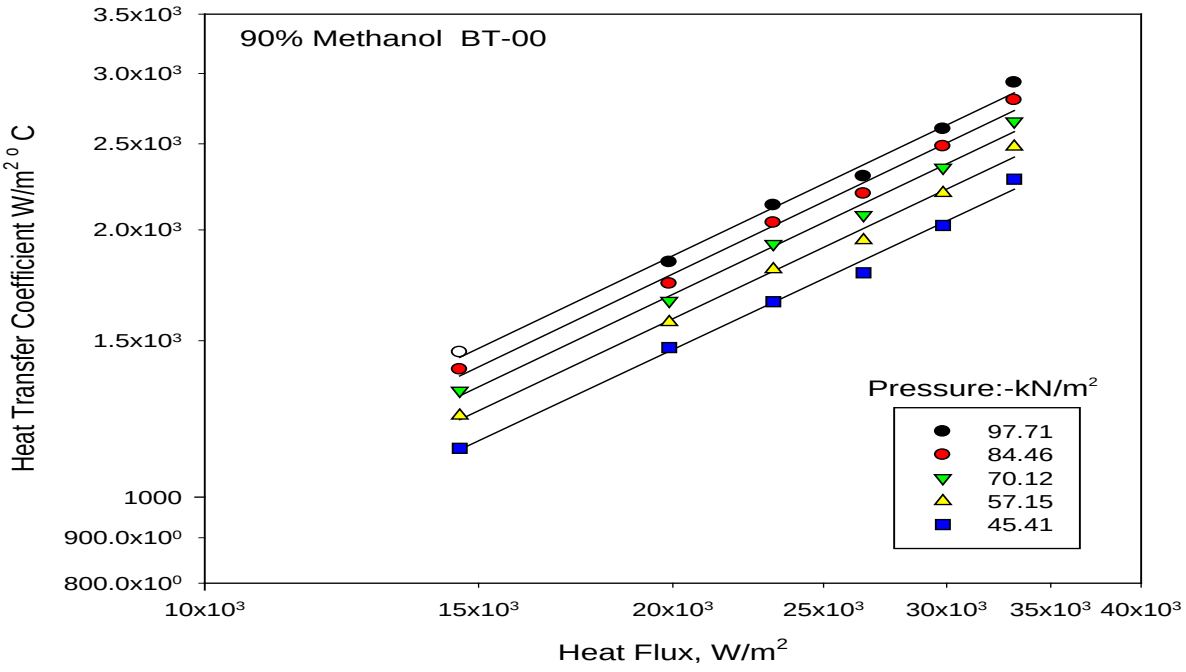

(b)

Figure 5.25(a,b). Variation of heat transfer coefficient with heat flux for boiling of 80 and 90 Mol% Methanol-distilled water mixture on an uncoated heating tube with pressure as a parameter

ethylene glycol-water, acetic acid water, and acetone-water mixtures at atmospheric and subatmospheric pressures, Fujita et al.[F7] for boiling of methanol-water, ethanol-water, methanol-ethanol, ethanol-butanol and methanol-benzene at atmospheric pressure, Alam et al. [A3] for boiling of methanol and methanol-distilled water mixture at atmospheric and subatmospheric pressure.

Hence, boiling characteristic representing the variation of heat transfer coefficient of a binary mixture with respect to heat flux and pressure remains the same as of individual liquids. It can be described by the following equation which has been obtained by regression analysis with an error of ± 7.25%

$$h = C_2 q^{0.7} p^{0.32} \quad \textbf{(5.7)}$$

Where, $\mathbf{C_2}$ is a constant whose value depends upon the percentage composition of the mixture, and their surface characteristics. The values of constant, $\mathbf{C_2}$ as determined for various compositions of iso-propanol-distilled water and methanol- distilled water are given in **Table 5.2.**

Table 5.2 Values of constant $\mathbf{C_2}$ of **Eq. (5.7)** for various compositions of iso-propanol-distilled water and methanol- distilled water mixtures

S.No.	Iso-Propanol- Distilled Water		Methanol-Distilled Water	
	Iso-Propanol Composition	$\mathbf{C_2}$	Methanol Composition	$\mathbf{C_2}$
1	10 Mol%	0.374	10 Mol%	0.471
2	30 Mol%	0.326	30 Mol%	0.421
3	50 Mol%	0.255	50 Mol%	0.351
4	70 Mol%	0.285	70 Mol%	0.385
5	80 Mol%	0.301	80 Mol%	0.401
6	90 Mol%	0.329	90 Mol%	0.429

An important implication of **Eq. (5.7)** is that heat transfer coefficient of a given composition of iso-propanol distilled water and methanol-distilled water can be calculated from the knowledge of heat flux, (q) and pressure, (p) provided the value of constant, $\mathbf{C_2}$ appearing in **Eq. (5.7)** is experimentally known. **Figure 5.26** and **Figure 5.27** represent plots between experimentally determined values of heat transfer coefficient and those calculated from **Eq. (5.7)** for the boiling of various iso-propanol distilled water and methanol-distilled water mixtures at atmospheric and subatmospheric pressures on an uncoated heating tube. These plots clearly reveal that the predicted values of heat transfer coefficient match excellently with experimental values within a maximum error of ± 8%.

Equation (5.7) is quite analogous to **Eq. (5.4)** which holds true for the boiling of pure saturated liquids. This equation also requires the experimentally determined values of constant, $\mathbf{C_2}$ for its applicability to determine heat transfer coefficient of a given composition of a binary mixture from the known values of heat flux, (q) and pressure, (p). The constant, $\mathbf{C_2}$ is quite similar to constant, $\mathbf{C_1}$ of **Eq. (5.4)**. Hence, the strategy which has been followed to get rid of the constant in case of liquid is also used herewith. Hence, $h^* = (\frac{h}{q^{0.7}})$ is defined and following dimensionless correlation is obtained:

$$\frac{h^*}{{h_1}^*} = (\frac{p}{{p_1}^*})^{0.32} \qquad \textbf{(5.8)}$$

Where, Subscript, 1 refers to atmospheric pressure condition.

Figure 5.28 is a plot between $(\frac{h^*}{{h_1}^*})$ vs $(\frac{p}{{p_1}^*})^{0.32}$ for the boiling of various composition of iso-propanol distilled water and methanol-distilled water mixtures on an uncoated heating surface at atmospheric and subatmospheric pressures. It also contains experimental data for the boiling of methanol-distilled water mixtures, ethanol-water mixtures and iso-propanol water mixtures due to Pandey [P3], methanol-distilled water due to Alam [A2], on a plain stainless steel surface at atmospheric and subatmospheric pressures. As can be noticed from this plot, all the data points of this investigation as well as those of Pandey [P3] lie around a 45^0 diagonal line with the maximum deviation ranging from -11 to 21%. This indicates the validity of **Eq. (5.8)**. In this way **Eq. (5.8)** has been found to hold good for the boiling of a given composition of a binary liquid mixture.

A close scrutiny of **Eq. (5.8)** inferred that it is free from surface-liquid mixture combination factor $\mathbf{C_2}$. Therefore, it is applicable to any liquid mixture boiling on a surface. Further, it can be used to generate boiling heat transfer data of liquid mixture at subatmospheric pressures from the knowledge of experimental data of one atmosphere

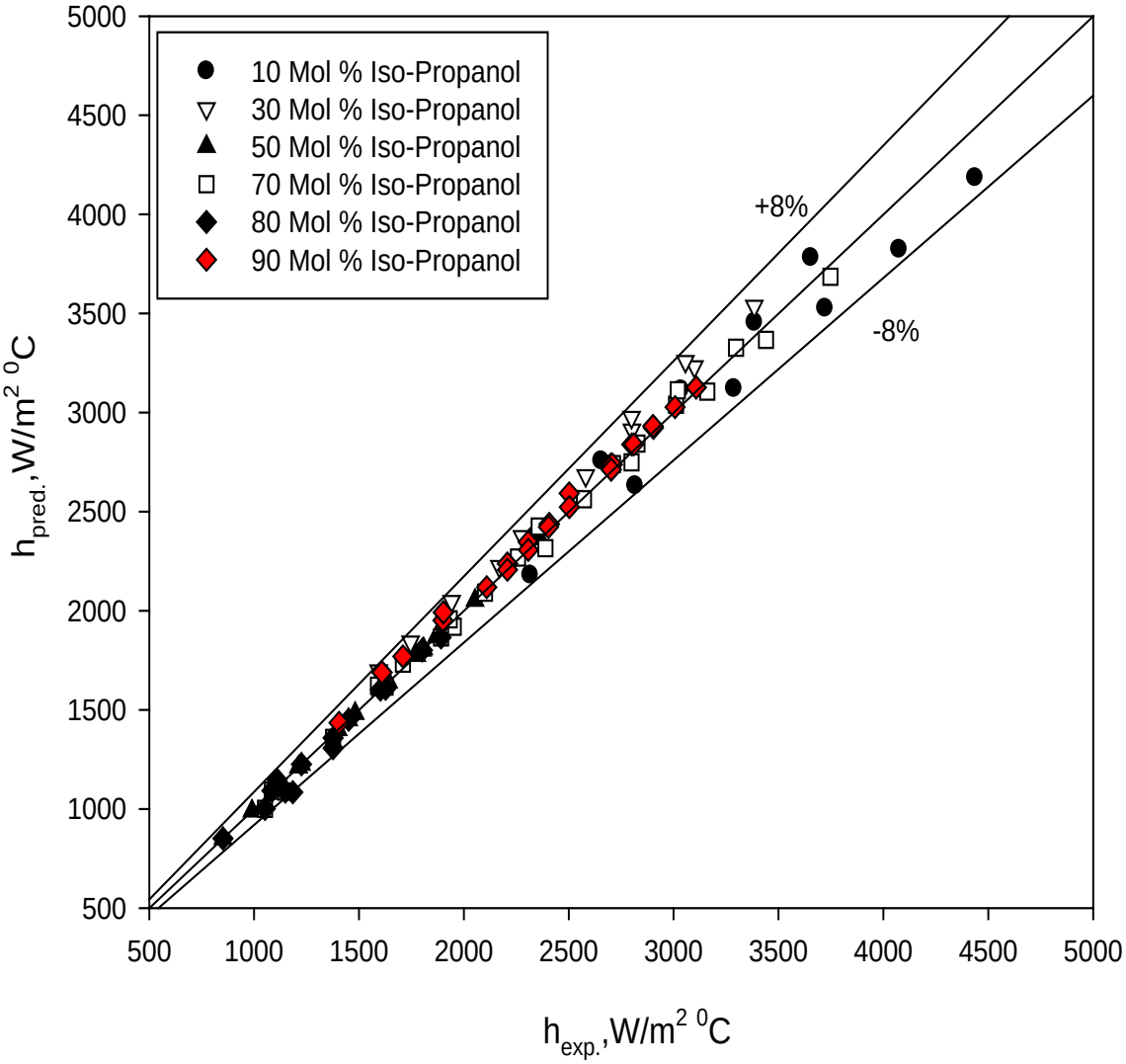

Figure 5.26 Comparison of experimental heat transfer coefficient with those predicted from **Eq.(5.7)** for boiling of iso-propanol-distilled water mixtures on an uncoated heating tube surface at atmospheric and subatmospheric pressures

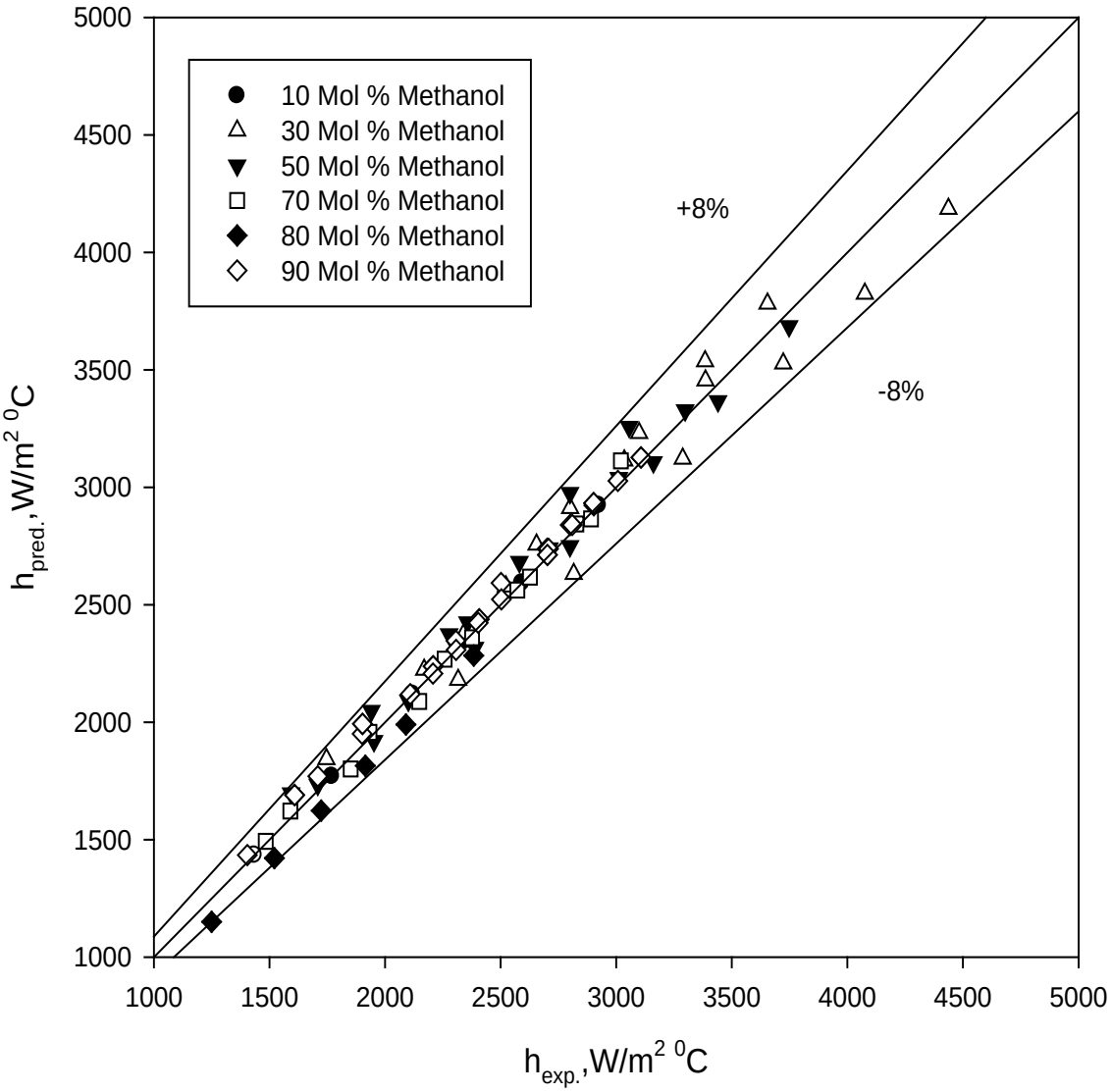

Figure 5.27 Comparison of experimental heat transfer coefficient with those predicted from **Eq.(5.7)** for boiling of methanol- distilled water mixtures on an uncoated heating tube surface at atmospheric and subatmospheric pressures

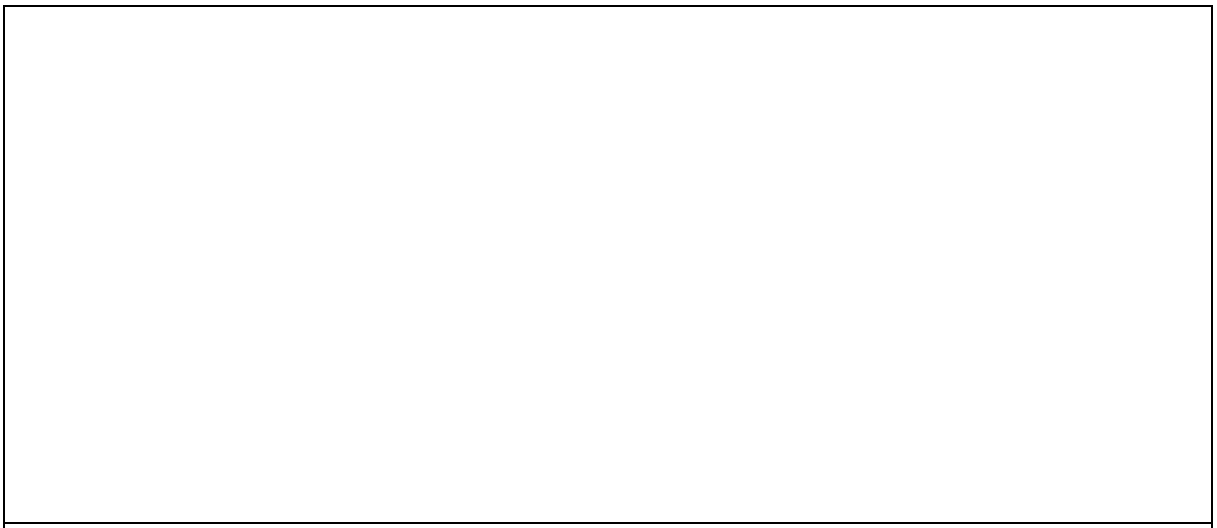

Figure 5.28 A Plot between (h^*/h^*_1) and $(P/P_1)^{0.32}$ a for the boiling of various composition of binary mixtures on an uncoated heating surface ant atmospheric and subatmospheric pressures

pressure only. In other words, it requires experimentation only at atmospheric pressure. Another implication of above equation is that it can be used to test the consistency of experimental data of boiling heat transfer of binary liquid mixture conducted on heating surfaces of varying characteristics at subatmospheric pressures.

5.3.3 Variation of heat transfer coefficient of binary mixtures with composition

In the previous section, discussion has been restricted to the boiling of a given composition of a binary liquid mixture at atmospheric and subatmospheric pressures. However, it has also been found that the salient features during boiling of liquid mixtures

during boiling of liquid mixtures remain the same as those of a pure liquid. So it is quite logical to determine boiling heat transfer coefficient of a given mixture from the knowledge of individual components boiling heat transfer coefficients. Keeping this in view, heat transfer coefficient of a boiling binary mixtures have been computed by the following equation which represents the weighted mean of individual components heat transfer coefficient.

$$\frac{1}{h_{id}} = \frac{x}{h_1} + \frac{(1-x)}{h_2} \qquad \textbf{(5.9)}$$

Where, subscripts 1 and 2 denote high and low volatile components, respectively in the mixture.

Computations of heat transfer coefficient have been made for various compositions of iso-propanol distilled water and methanol-distilled water at atmospheric and subatmospheric pressures using **Eq. (5.9)**. The computed values, so obtained, are compared with the experimentally determined one, as shown in **Fig. 5.29(b)**. As it is clear from this plot, the computed values, represented by dotted curves. This disagreement is quite obvious due to distinct differences between the inherent nature of the boiling mixture and a single component liquid. **Figs. 5.29(b),** and**. 5.30(b),** are plots between experimental and predicted heat transfer coefficients with mole fraction of high volatile component (methanol or iso-propanol) in distilled water mixture at an atmospheric pressure. Heat flux is parameter in these plots:

Following points emerged out from this plot:

i. At a given heat flux, heat transfer coefficient of a given composition of the boiling mixtures is lower than those of its components. In other words, heat transfer coefficient of a binary mixture cannot be predicted by interpolation of heat transfer

coefficient of its components.

ii. Left hand ordinate indicates boiling heat transfer coefficient of distilled water. At given heat flux, an addition of high volatile component (methanol, or iso-propanol) to distilled water reduces the value of boiling heat transfers coefficient. This trend continues till the mole fraction of methanol mixture reaches to 0.30 and 0.2 in the case of methanol-distilled water and iso-propanol- distilled water mixtures, respectively. Thereafter, any further addition of methanol and iso-propanol results in turnaround and thereby heat transfer coefficient rises to reach ultimately to the value of methanol or iso-propanol.

iii. An increase in heat flux makes the appearance of the region depicting lowest heat transfer coefficient in the curve to the more pronounced. Further, it also enhances the value of heat transfer coefficient of a given mole fraction methanol or Iso-Propanol in the mixture.

Figures 5.31(b), **5.32(b), 5.33(b), and 5.34(b)** show similar plots of heat transfer coefficient verses high volatile component mole fraction at 70.10 kN/m^2 and 45.40 kN/m^2 pressures, respectively. These plots have essentially the same features as described above. Thus, it is clear that pressure does not change the nature of h verses x (mole fraction) curve. Above observations are consistent and in agreement with the findings of many earlier investigators [A1, B6, C1, C13, F6, F7, J6, J7, P4, S17, T5, T8].

A binary mixture is composed of two component having different volatilities. They as single component liquids boil at different temperatures. So, a binary mixtures boils over a range of temperature spanning from the boiling temperature of the high volatility components to that of low volatility one. It can be understood easily by vapor-liquid phase equilibrium diagrams from methanol-distilled water and iso-propanol distilled water mixture at atmospheric and subatmospheric pressures, as shown in **Figs 5.29(a), and 5.30(a)**. The upper curve in these plots represents the vapour temperature whereas the lower on indicates liquid boiling temperature as a function of methanol or iso-propanol mole fraction in the mixtures. As can be seen from these plots, equilibrium vapour mole fraction, $\mathbf{y}^*$ is higher than that of the surrounding liquid mole fraction, x for the mixture vaporizing at a given temperature. Van Wijk et al. [V8] have also noted this phenomenon in bubbles growing on heated surfaces. So, in order to maintain equilibrium between phases more amount of high volatile component present in liquid mixture to vapourize to provide

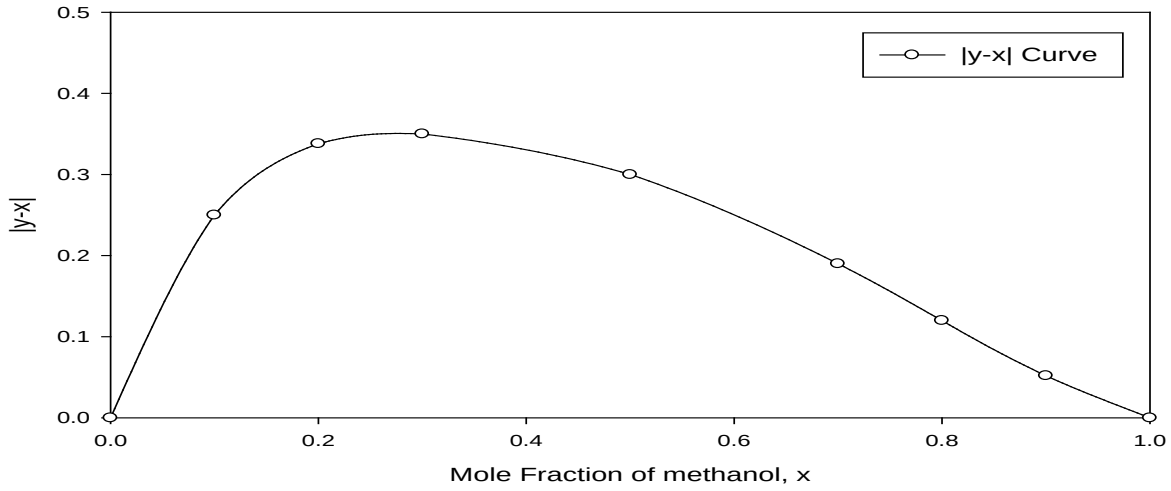

(a)

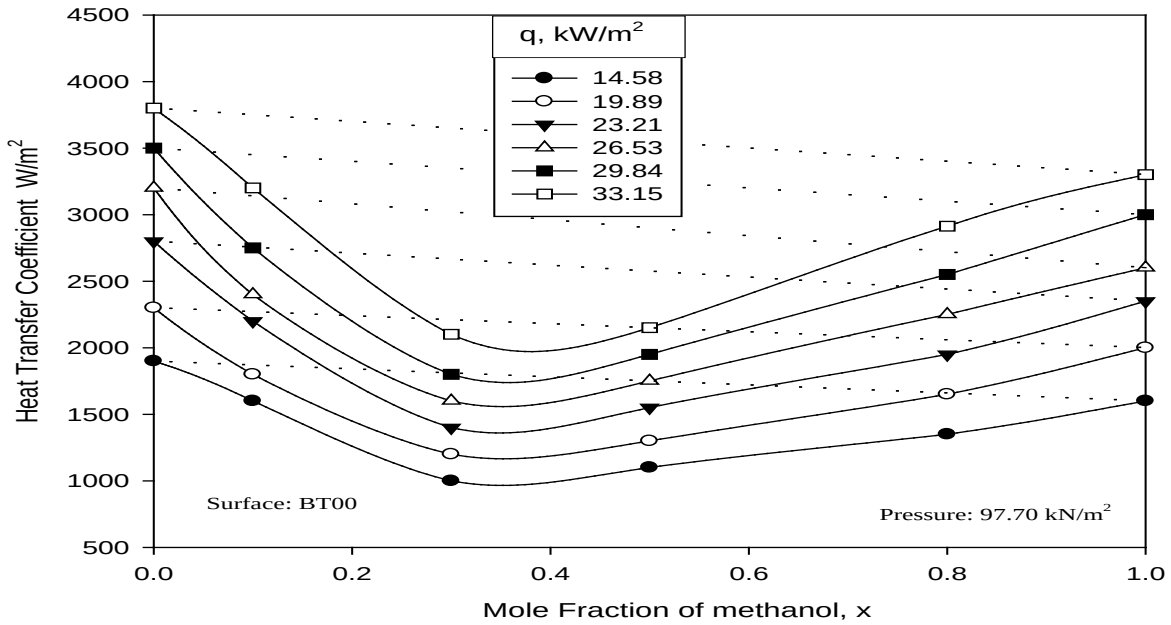

(b)

Figure 5.29 Variation of heat transfer coefficient, and |y-x| with mole fraction of methanol for methanol-distilled water mixtures on uncoated tube at atmospheric pressure

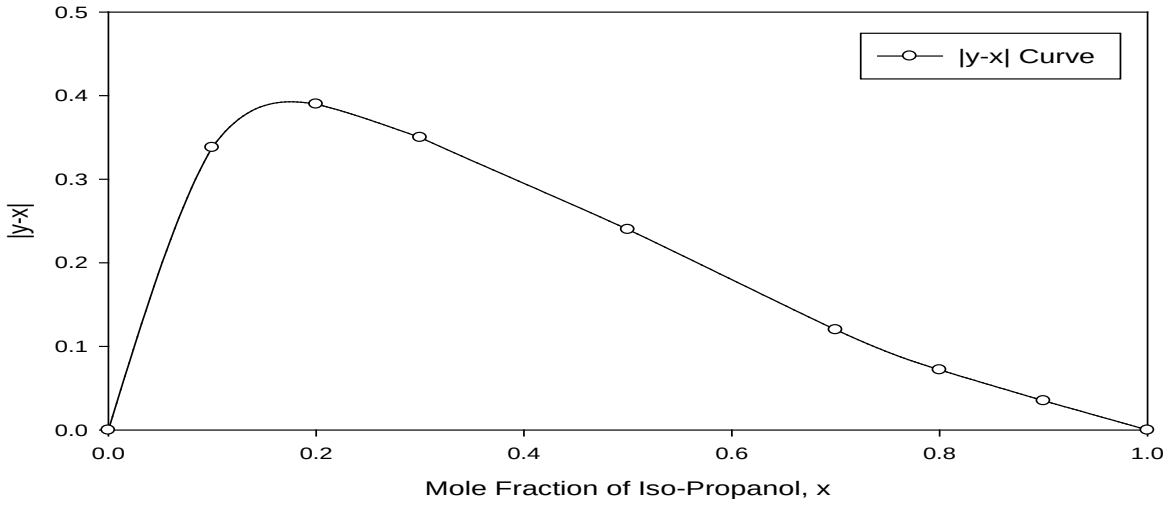

(a)

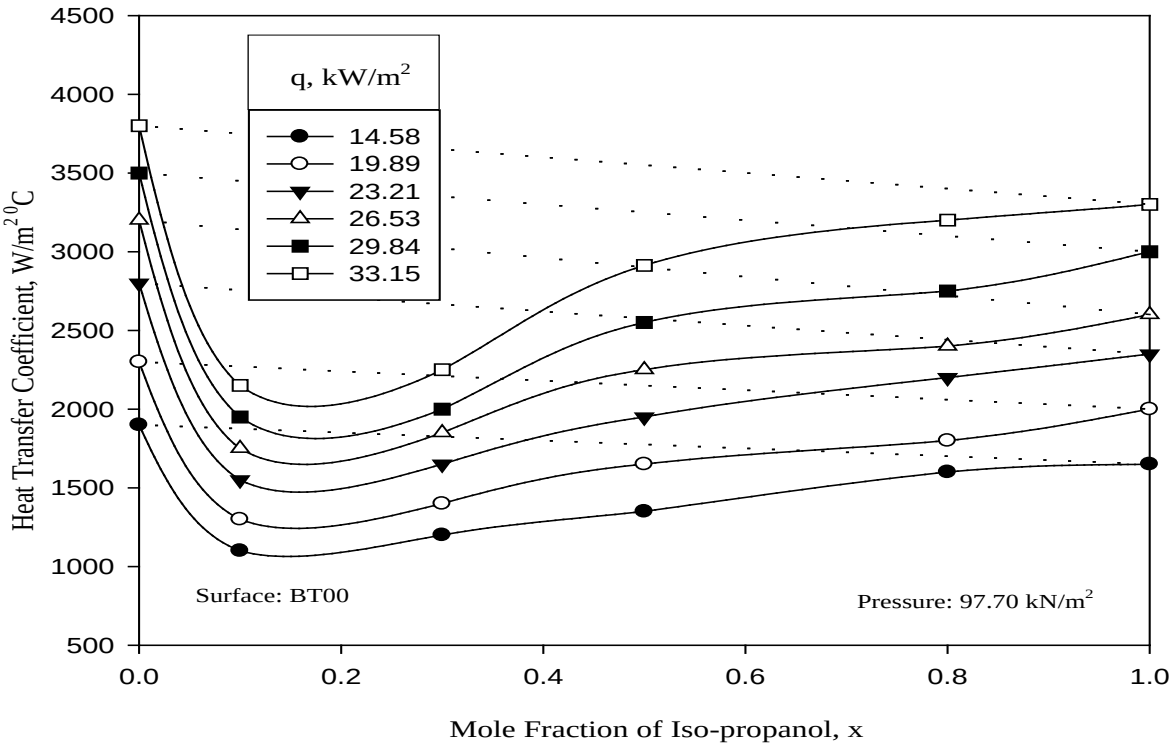

(b)

Figure 5.30 Variation of heat transfer coefficient, and |y-x| with mole fraction of Iso-propanol for Iso-propanol-distilled water mixtures on uncoated tube at atmospheric pressure

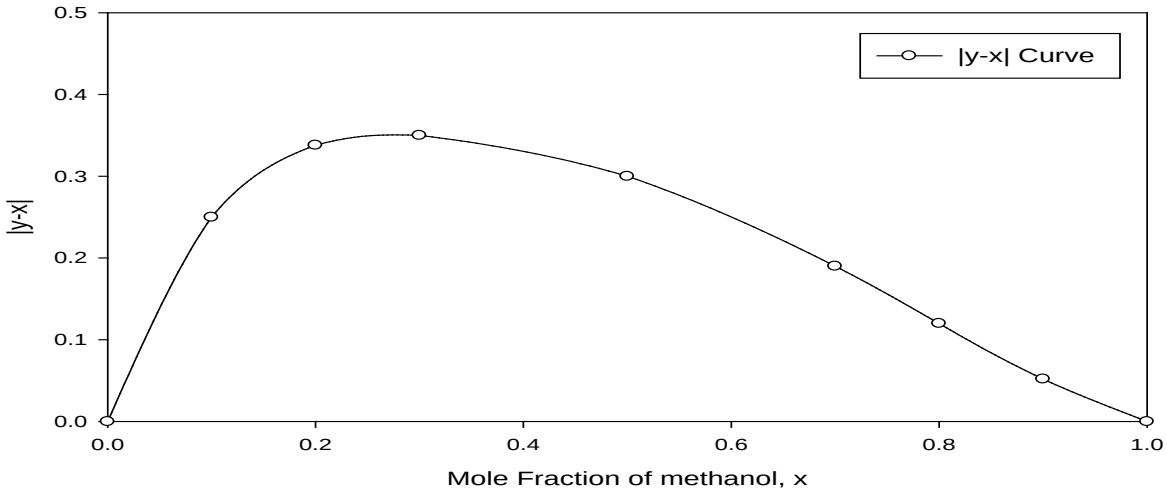

(a)

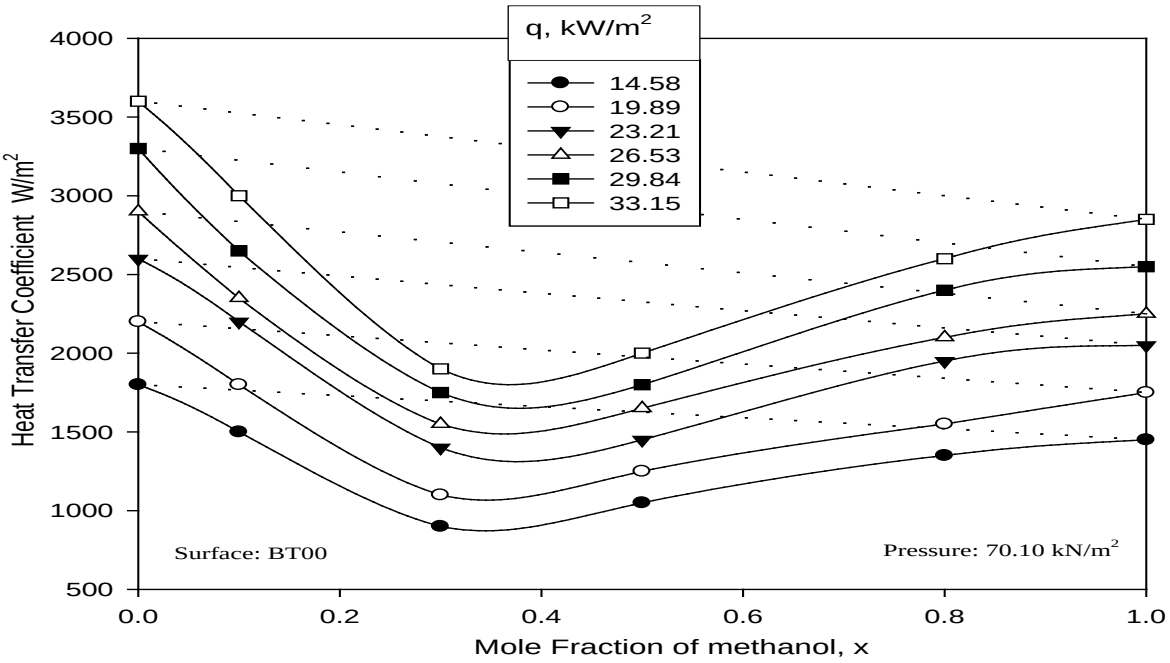

(b)

Figure 5.31 Variation of heat transfer coefficient, and |y-x| with mole fraction of methanol for methanol-distilled water mixtures on uncoated tube at 70.10 kN/m^2 pressure

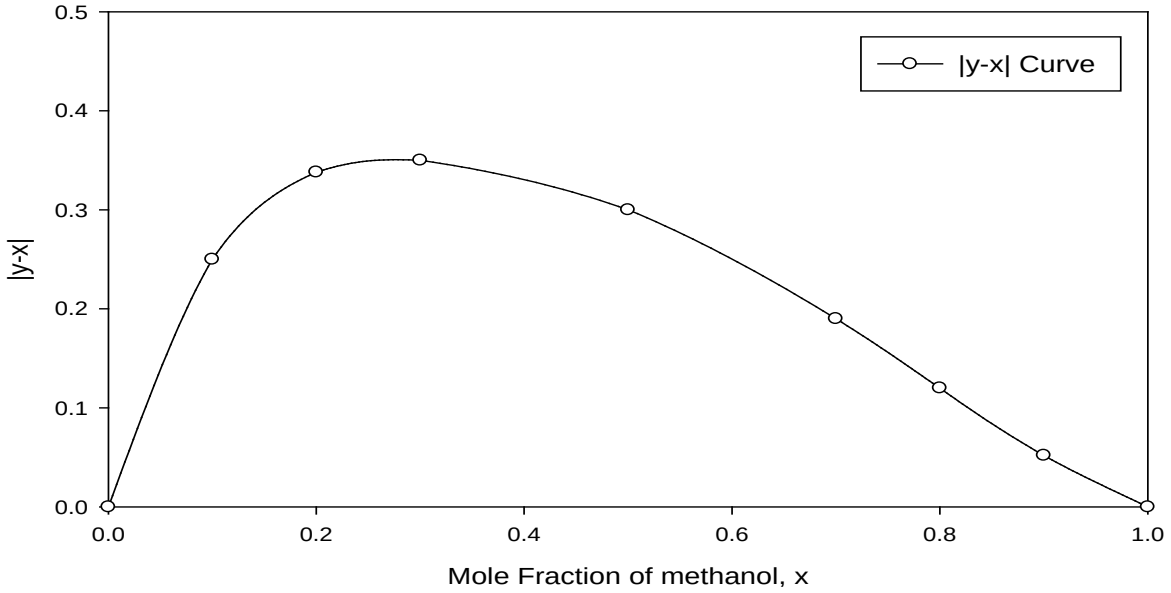

(a)

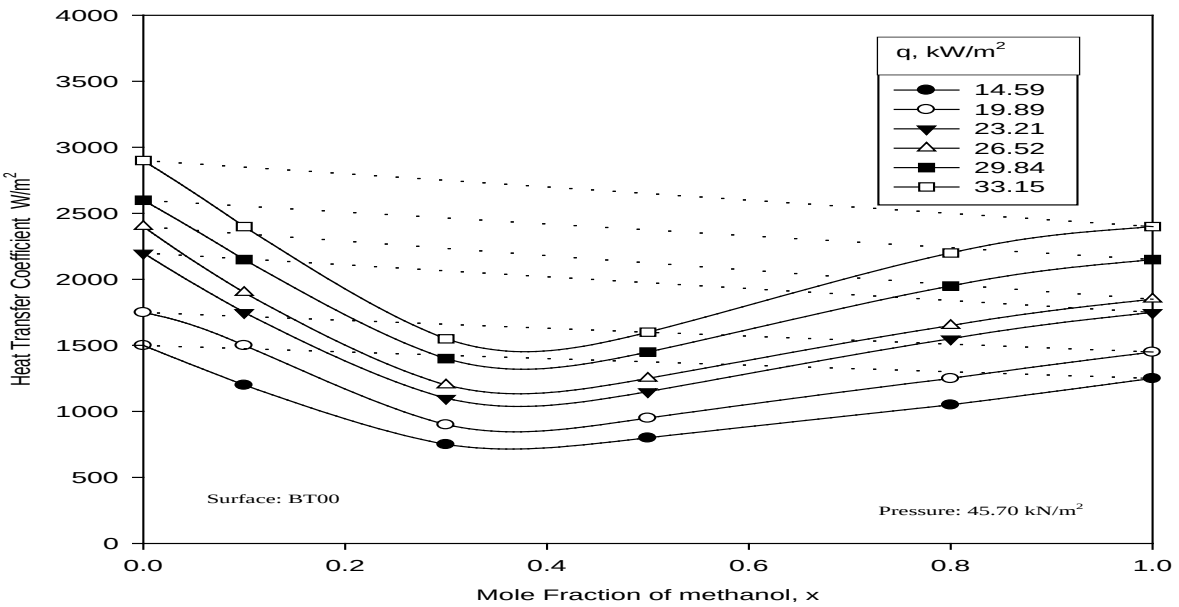

(b)

Figure 5.32 Variation of heat transfer coefficient, and |y-x| with mole fraction of methanol for methanol-distilled water mixtures on uncoated tube at 45.40 kN/m^2 pressure

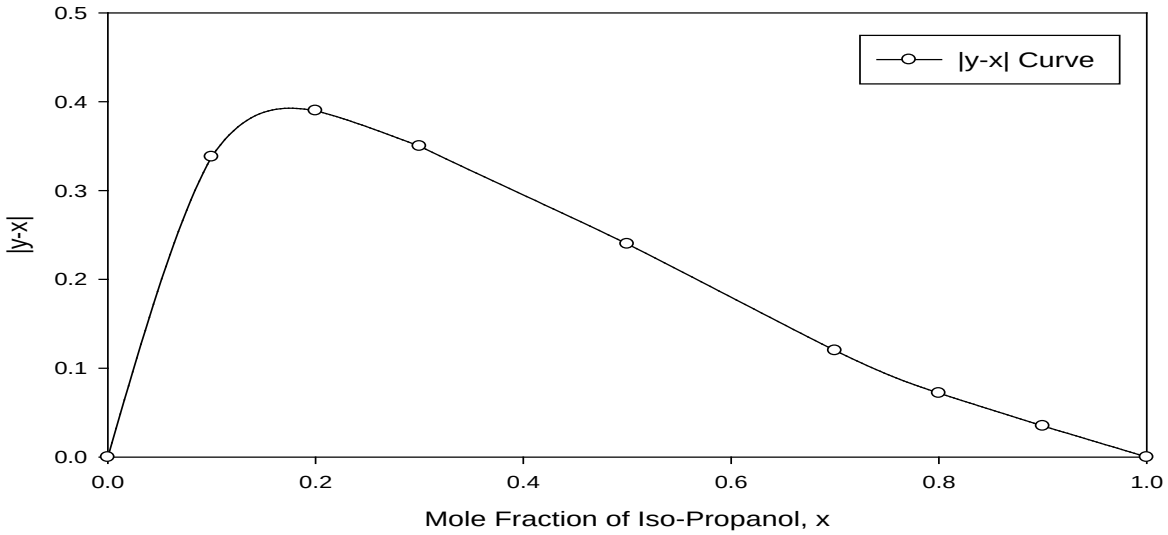

(a)

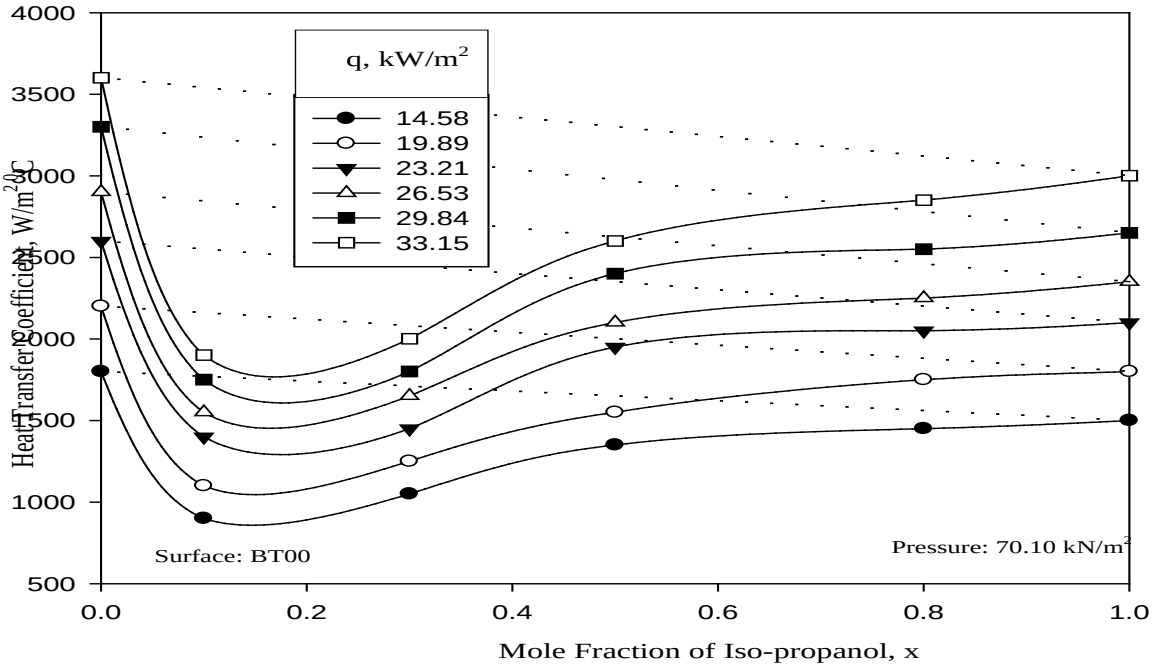

(b)

Figure 5.33 Variation of heat transfer coefficient, and |y-x| with mole fraction of Iso-propanol for Iso-propanol-distilled water mixtures on uncoated tube at 70.10 kN/m^2 pressure

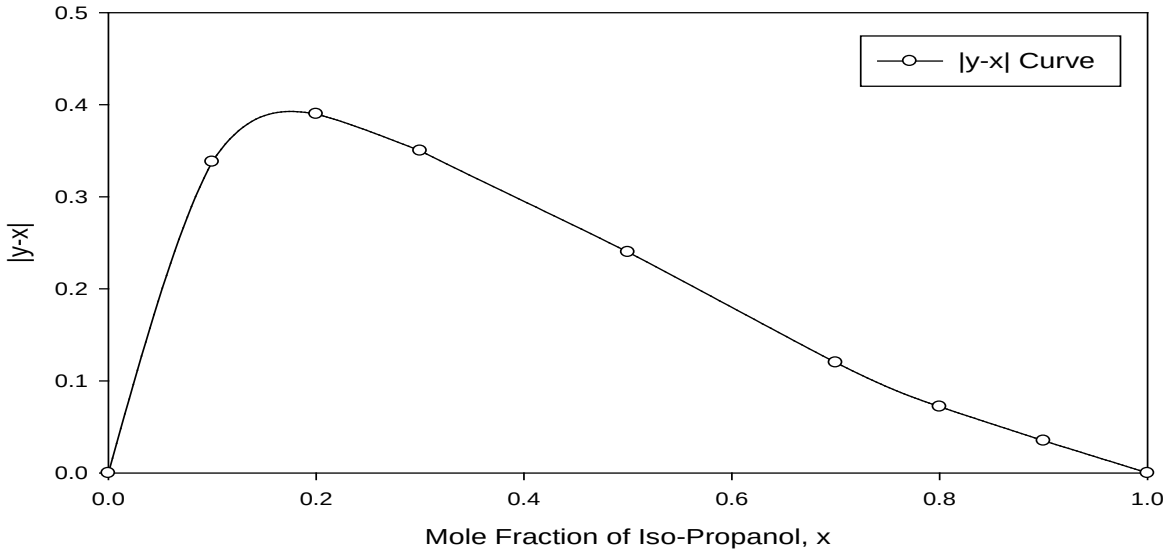

(a)

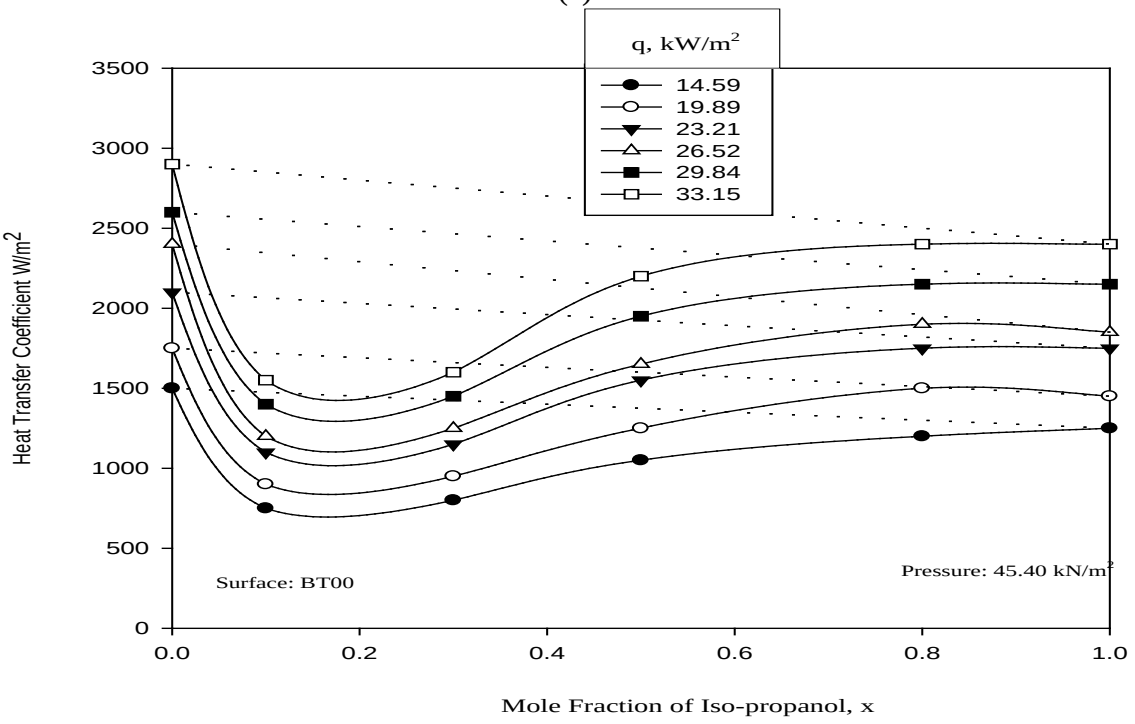

(b)

Figure 5.34 Variation of heat transfer coefficient, and |y-x| with mole fraction of Iso-propanol for Iso-propanol-distilled water mixtures on uncoated tube at 45.40 kN/m^2 pressure

additional vapour as bubbles grows. As a result, the local concentration of high volatile component in the liquid decreases and thereby the local boiling temperature of liquid rises. This, in turn, causes wall temperature to increase so heat transfer may occur at a constant rate. Hence, lower values of heat transfer coefficient which is based on bulk liquid temperature are found in case found in case of liquid mixture than that observed for single component liquids.

Boiling of a binary mixture involves simultaneous heat and mass transfer. In it, evaporation of liquid components occurs by the transfer of heat from heated surface to bubble via micro-layer existing beneath the bubble base. It is also accompanied by the diffusion of high volatility component from liquid bulk to bubble through bubble-bulk interface.

The diffusion of mass makes the boiling process in mixture to be different than that is single component liquid. Mass diffusion is a slow process as compared to that of heat diffusion. Hence, it is controlling the process of boiling of a liquid mixture. In other words, mass diffusion is an impedance to heat transfer and so heat transfer rate in the boiling of liquid mixtures is lower than that in single components liquids. The rate of mass diffusion depends upon the driving force which is the difference existing between equilibrium vapour and liquid mole fraction of high volatile component. It is represented by the term, (y^*-x). Higher the value of (y^*-x), more is the rate if diffusion of high volatile component into the bubble and lower is the heat transfer rate and hereby heat transfer coefficient.

The variation of (y^*-x) with high volatile component mole fraction, x is shown in **Fig 5.31(a)**. The feature of this plot is as follows:

For the boiling of a binary mixture the value of (y^*-x) increases continuously with an increase in liquid mole fraction, x, and this trend continues till the value of x reaches to 0.30. Thereafter, an increase in the value of x causes (y^*-x), to decrease and ultimately to vanish at unity value of mole fraction.

Both the above observations are self explanatory in nature and therefore called for no detailed analysis.

Hence, in the light of above discussion, it can be said that the variation of heat transfer coefficient of boiling binary mixture with mole fraction of high volatile component to alteration in the value of mass diffusion driving force, (y^*-x) in it. An addition of a

component to a liquid increases the value of driving force (y^*-x) which lower down heat transfer coefficient. This behavior has been observed till liquid mole fraction becomes 0.30. At this value driving force (y^*-x) becomes maximum and heat transfer coefficient minimum. Thereafter, reverse trend exists due to decrease in the value of (y^*-x).

A note –worthy point is that heat transfer coefficient of a boiling binary mixture is minimum for the value of x at which driving force (y^*-x) is maximum. This corroborates the findings of [A1, B6, C1, C13, F6, F7, J6, J7, P3, P4, S17, T5, T8,T10,] who have also noted similar behavior. However, some investigators [I2, S18, Z2] obtain a range of x for which heat transfer coefficient of a binary mixture reaches to its maximum value.

Above discussion has pointed out clearly that boiling of a binary; liquid, mixture is different than that of single component liquids owing to the association of mass transfer with heat transfer. Consequently, heat transfer coefficient of binary mixtures at atmospheric pressures is lower than that of its single component liquids. Hence, its value cannot be predicted by interpolation method. In fact, heat transfer coefficient varies with concentration and attains a distinct minimum value when boiling of a binary mixtures is carried out at a given heat flux at atmospheric and subatmospheric pressures. An increase in heat flux does not alter the nature of curve h verses x but merely shifts the curve upward implying higher value of heat transfer coefficient for the boiling of a liquid mixture of a given composition at atmospheric and subatmospheric pressures.

5.4 NUCLEATE POOL BOILING OF TERNARY MIXTURES ON A UNCOATED HEATING TUBE

Experimental data for the boiling of various compositions of distilled water-iso-propanol-methanol are tabulated in table's B.21 to B.26, of Annexure B. It includes the measured value of temperature of heating surface as well as liquid pool at top, two side and bottom and heat flux. It also include the calculated value of heat transfer coefficient of each composition at atmospheric and subatmospheric pressures, based on these data variation of surface temperature and heat transfer coefficient around the circumference of the heating tube and the effect of heat flux, pressure and composition on heat transfer coefficient for the boiling of ternary mixtures of distilled water-iso-propanol-methanol have been studied. Following section discuss these in details:

5.4.1 Variation of heat transfer coefficient along Circumference

Figures 5.35(a) to 5.35(f) depicts surface temperature profile for the boiling of various compositions of distilled water-iso-propanol-methanol ternary mixtures on an uncoated heating tube surface at atmospheric pressure. Heat flux is the parameter in each plot. Each plot contains a dotted line which represent boiling temperature of liquid mixture. A close examination of these plots reveals the following:

i. Surface temperature is found to increases continuously as moving from bottom, to side, side to top position of the tube at given heat flux.
ii. At a given circumferential position an increase in heat flux increase the value of surface temperature.
iii. Saturation temperature remains unchanged irrespective of heat flux and circumference position.

Above features have also been found to hold true for various composition of distilled water-methanol-iso-propanol mixture at subatmospheric pressure as clearly shown in **Figs. 5.36(a) to 5.36(f) and Figs. 5.37(a) to 5.37(f)**.

All the above features are same as observed in case of boiling of saturated liquids as well as their binary mixtures. It may be mentioned here that experimentally obtained saturation temperature of mixture was compared with the theoretical value calculate by NRTL in software Aspen-Plus [J4]. This comparison indicates an indiscernible difference between the two, as evident from **Fig. 5.38.** These are plots between the experimentally obtained values of saturation temperature with that of calculated values for distilled water-iso-propanol-methanol mixtures. Pressure is parameter in these plots.

Thus, it can be concluded that boiling characteristic of a given composition of distilled water-methanol- iso-propanol ternary mixtures are same as of an individual liquids. Hence, local heat transfer coefficient of ternary is likely to vary in the same way as that of liquids. Keeping this in view it has not been included here, but detail analysis of heat transfer coefficient with respect to heat flux, pressure and composition has been carried out.

5.4.2 Heat transfer coefficient for ternary mixtures

The average value of surface temperature of heating tube has been determined by taking the arithmetic mean of local surface temperature. Similar procedures have also been adopted for taking the average values saturation temperature of ternary liquid mixtures. Using these values heat transfer coefficient for boiling of various compositions of distilled water-methanol-iso-propanol ternary mixtures have been determined. The heat transfer

coefficients of ternary mixtures have been calculated as given in Annexure C, Sample Calculation.

Figure 5.39 describe a plot between heat transfer coefficient and heat flux for boiling 10 mol% methanol, 40 mol% iso-propanol and 50 mol% distilled water. In this plot pressure is a parameter. A close examination of this plot reveals the following features:

i. At a given pressure, heat transfer coefficient increases with increase of heat flux and the variation between the two can be described by power law $\boldsymbol{h \propto q^{0.67}}$.
ii. Rise in pressure increase the value of heat transfer coefficient of a mixture subject to given heat flux.

These features have also been observed for the boiling of other comparison of distilled water-iso-propanol-methanol ternary mixture at atmospheric and various subatmospheric pressures as can been from the plots in Figs. 5.40, to 5.42. Above mentioned features are same as

Figure 5.43 represents a plot between experimentally determined values of heat transfer coefficient and those calculated from **Eq. (5.10)** for the boiling of various compositions of distilled water-methanol-iso-propanol mixtures at atmospheric and subatmospheric pressures on an uncoated heating tube. This plot clearly reveals that the predicted values of heat transfer coefficient match excellently with experimental values within a maximum error of ±8.5 %.

Equation (5.10) is quite analogous to **Eq. (5.4)** which holds true for the boiling of pure saturated liquids. This equation also requires the experimentally determined values of constant, $\mathbf{C_3}$ for its applicability to determine heat transfer coefficient of a given composition of a ternary mixture from the known values of heat flux, (q) and pressure, (p). The constant, $\mathbf{C_3}$ is quite similar to constant, $\mathbf{C_1}$ of **Eq. (5.4)**. Hence, the strategy which has been followed to get rid of the constant in case of liquid is also used herewith. Hence, $h^* = (\frac{h}{q^{0.72}})$ is defined and following dimensionless correlation is obtained:

$$\frac{h^*}{h_1{}^*} = (\frac{p}{p_1{}^*})^{0.33} \qquad \textbf{(5.11)}$$

Where, Subscript, 1 refers to atmospheric pressure condition.

Figure 5.44 is a plot between $(\frac{h^*}{h_1{}^*})$ vs $(\frac{p}{p_1{}^*})^{0.33}$ for the boiling of various composition of distilled water-methanol-iso-propanol mixtures on an uncoated heating surface at atmospheric and subatmospheric pressures. It also contains experimental data for the boiling of methanol-1pentanol and ternary mixture of methanol/1-pentanol/ 1-2

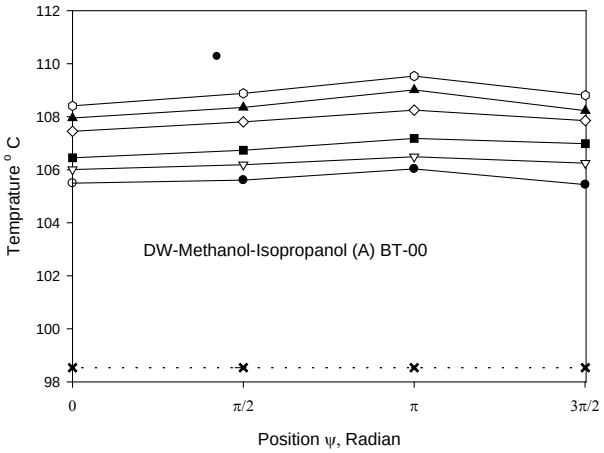

(a)

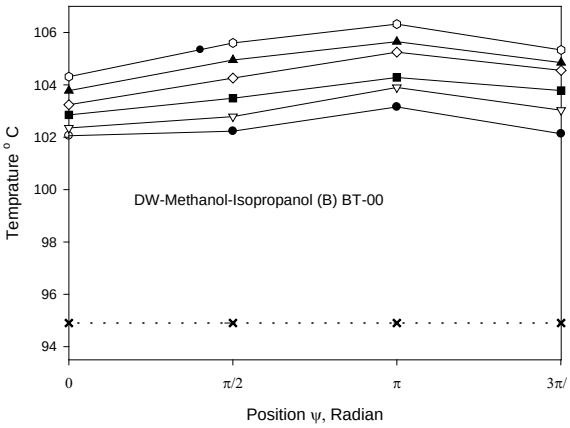

(b)

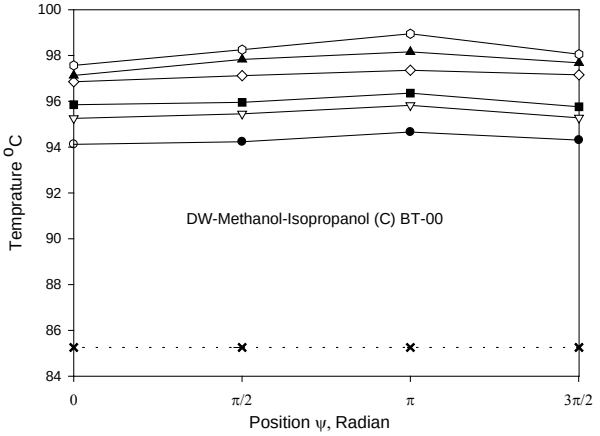

(c)

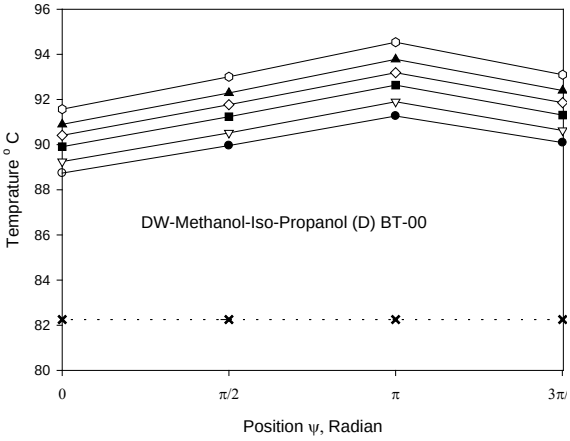

d)

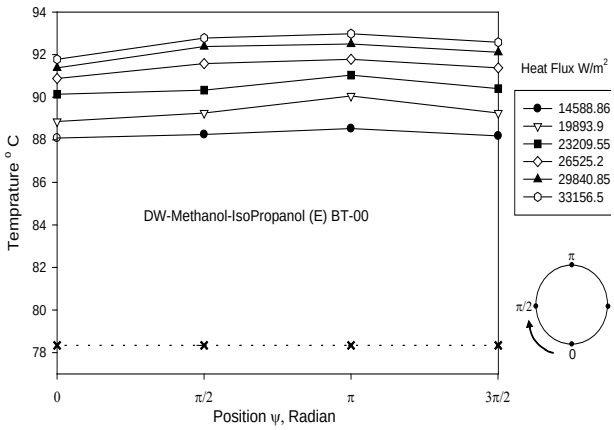

(e)

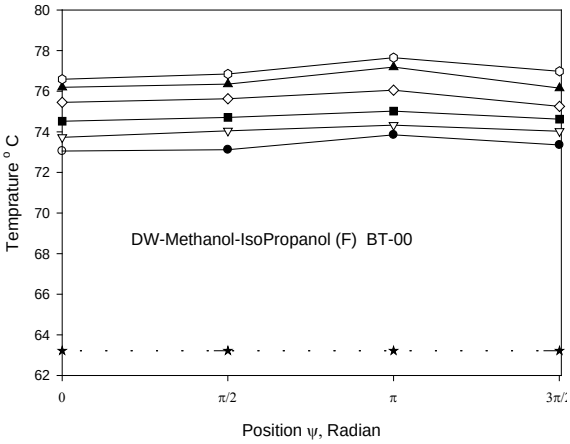

(f)

Figures 5.35 (a..f) Variation of liquid and surface temperature along circumference at bottom, two sides and top positions of uncoated heating tube with heat flux as a parameter for boiling of ternary mixture at atmospheric pressure

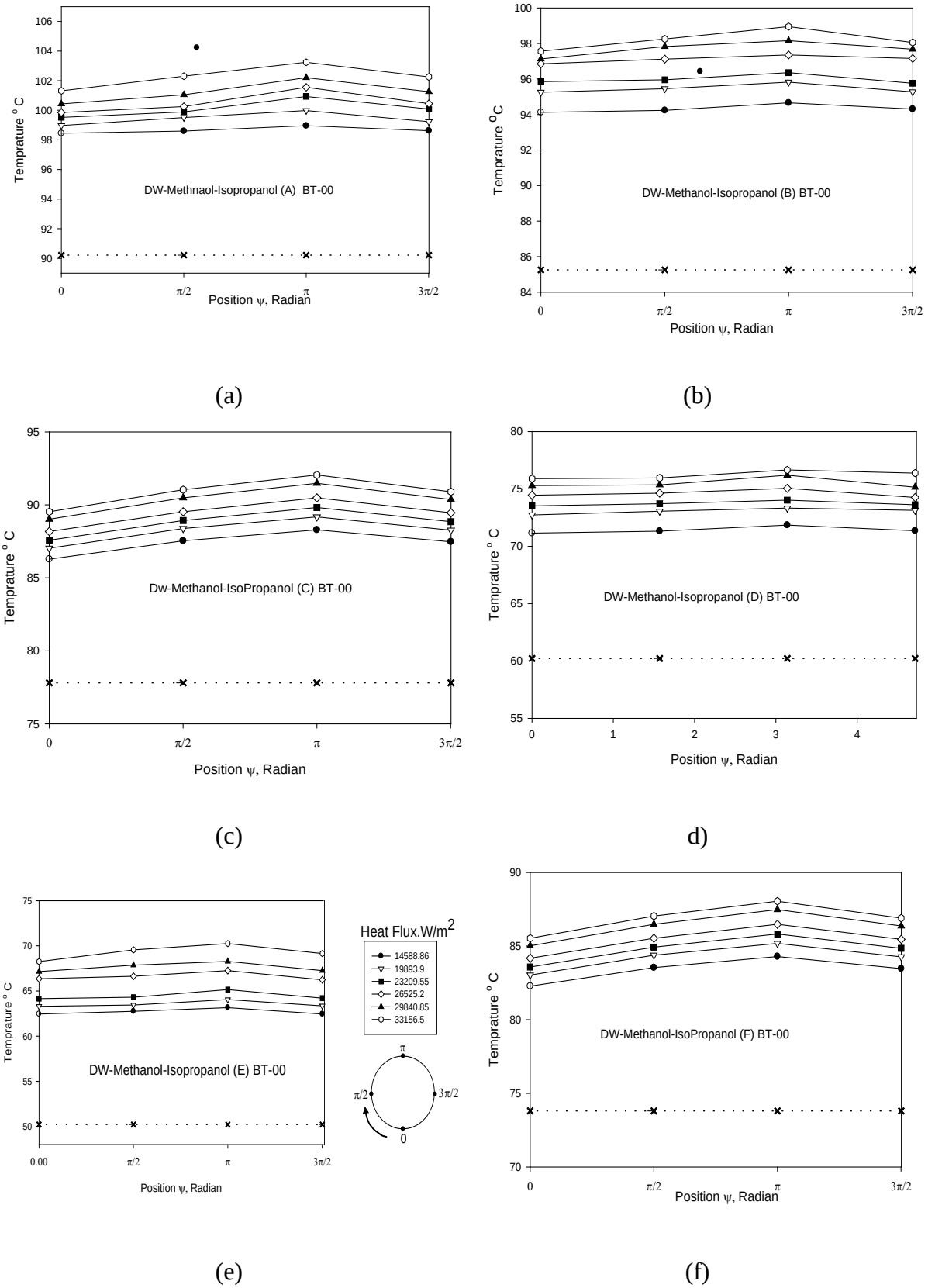

Figure 5.36(a..f) Variation of liquid and surface temperature along circumference at bottom, two sides and top positions of uncoated heating tube with heat flux as a parameter for boiling of ternary mixture at atmospheric pressure

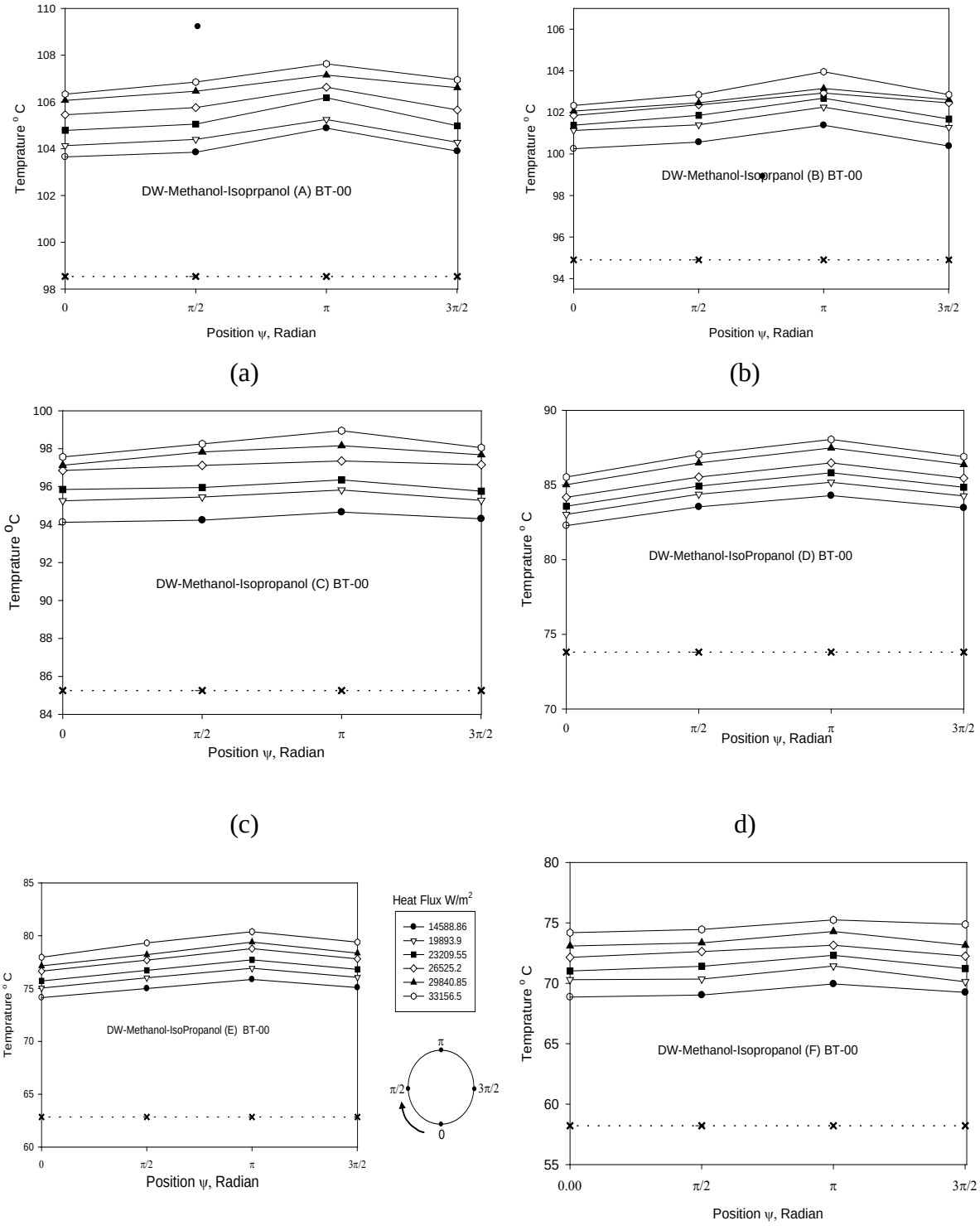

Figure 5.37(a..f) Variation of liquid and surface temperature along circumference at bottom, two sides and top positions of uncoated heating tube with heat flux as a parameter for boiling of ternary mixture at atmospheric pressure

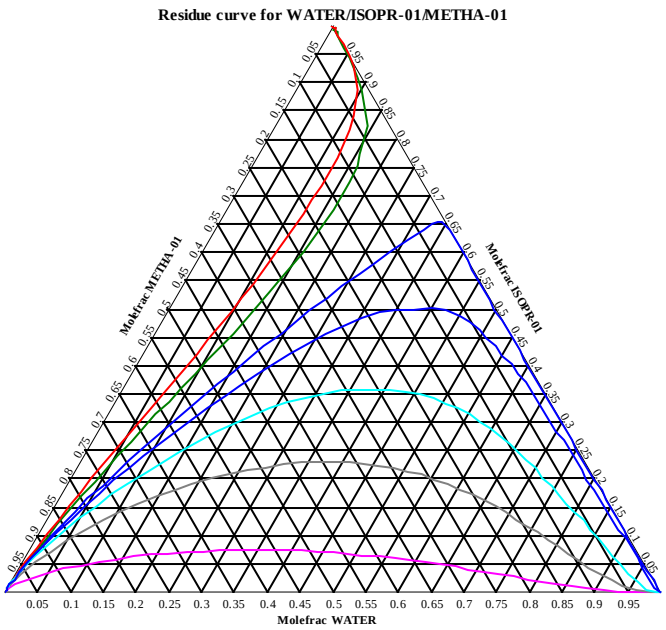

Figure 5.38 Liquid and vapour phase diagram for ternary mixture(A) and (B) at atmosphere and subatmospheric pressures

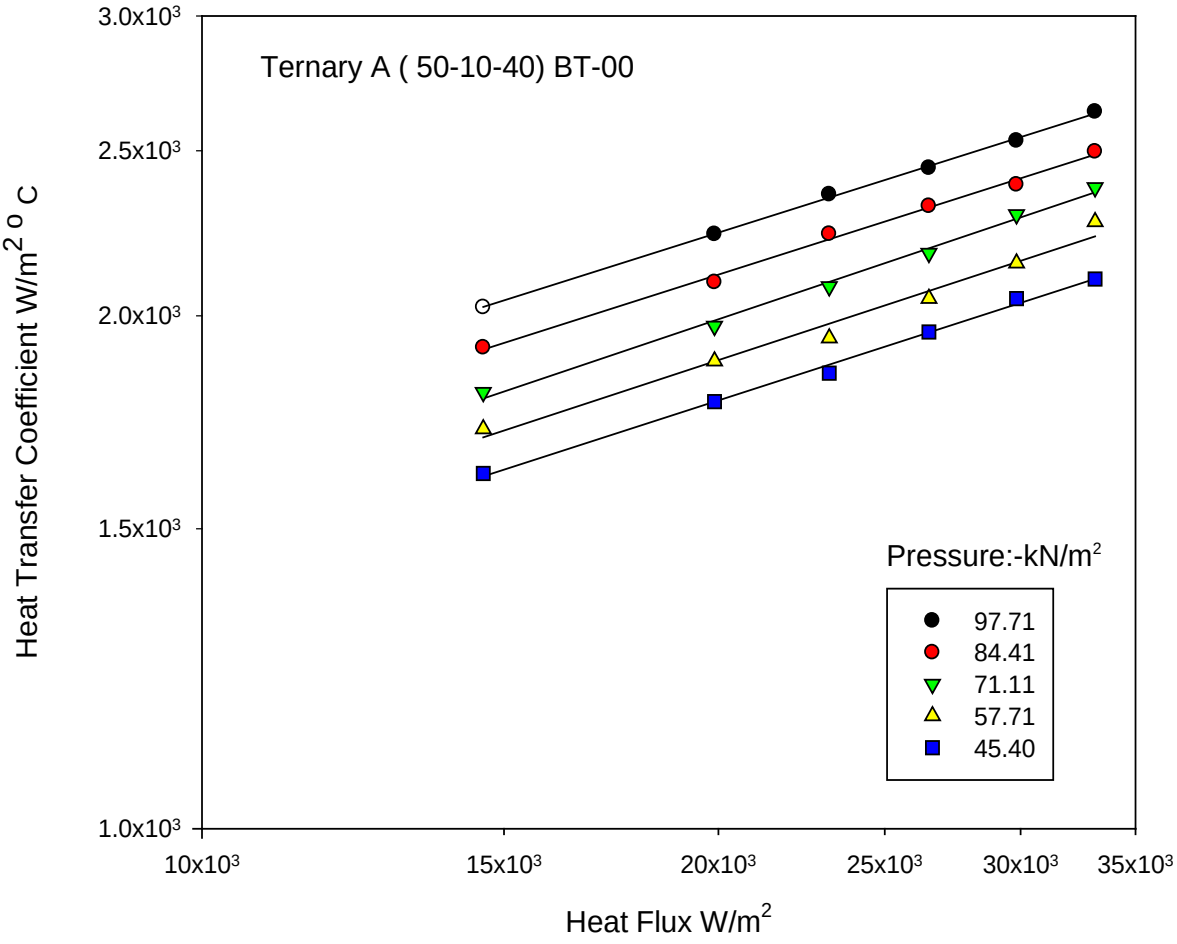

Figure 5.39 Variation of heat transfer coefficient with heat flux for boiling of 10% mole methanol, 40% mole Iso-Propanol and 50% distilled water ternary mixture on an uncoated heating tube

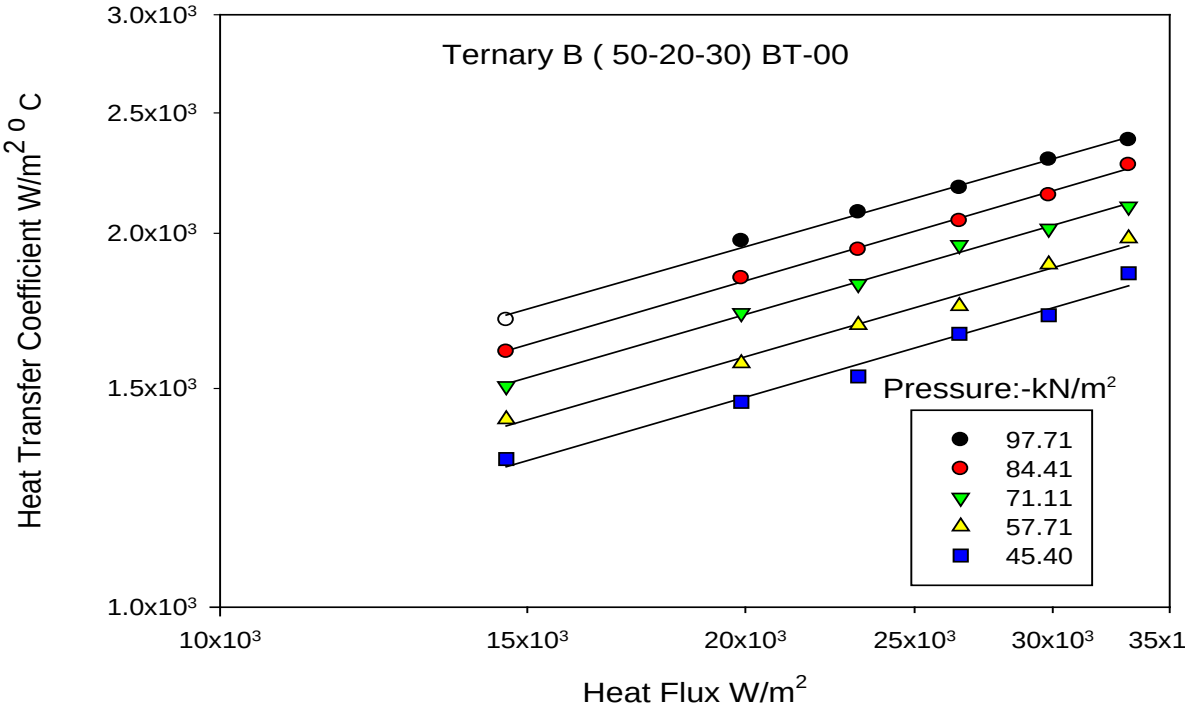

Figure 5.40 (a) Variation of heat transfer coefficient with heat flux for boiling of 20% mole methanol, 30% mole Iso-Propanol and 50% mole distilled water ternary mixture on an uncoated heating tube

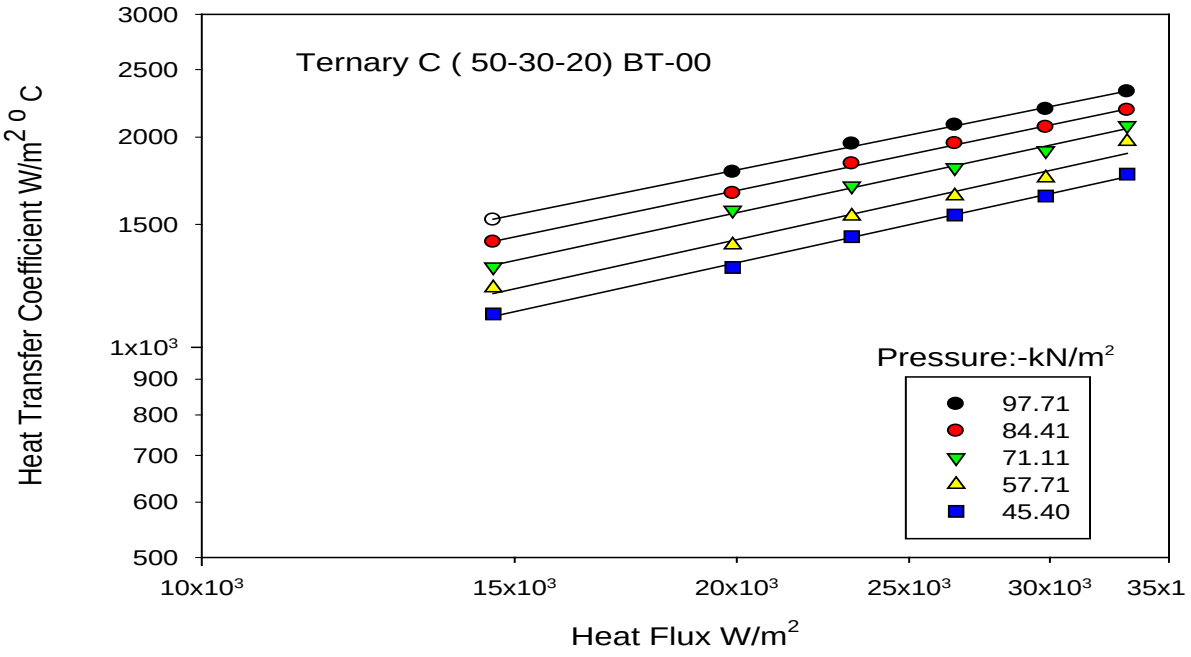

Figure 5.40 (a) Variation of heat transfer coefficient with heat flux for boiling of 30% mole methanol, 20% mole Iso-Propanol and 50% mole distilled water ternary mixture on an uncoated heating tube

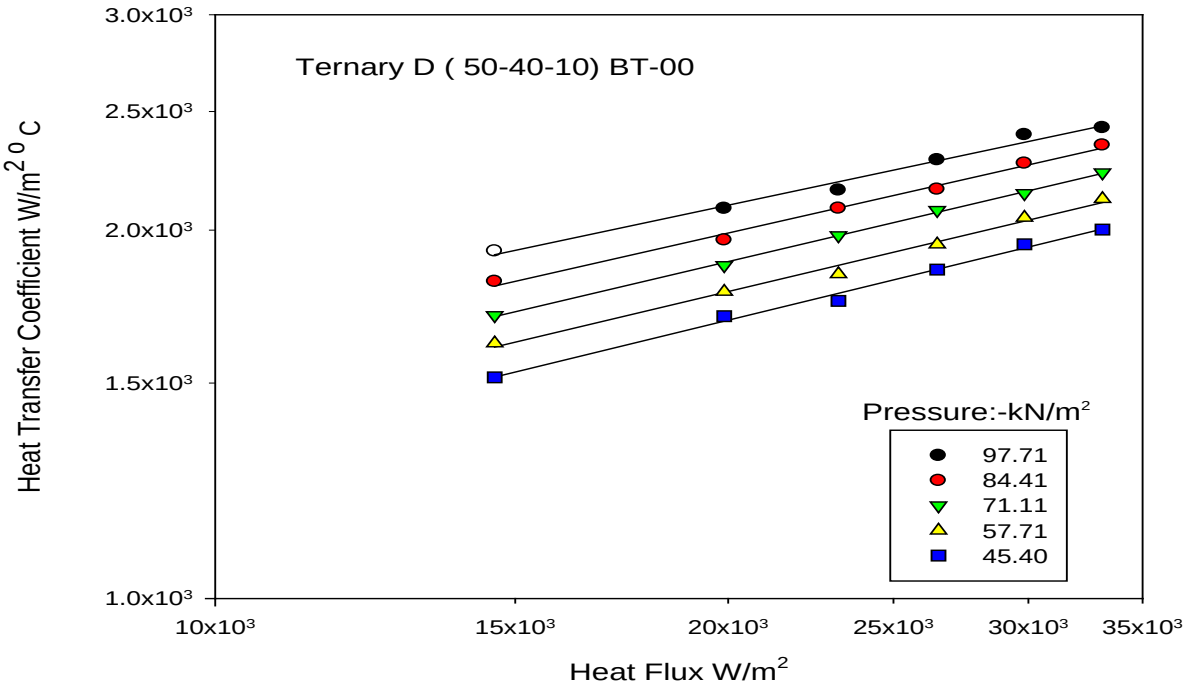

Figure 5.41 (a) Variation of heat transfer coefficient with heat flux for boiling of 40% mole methanol, 10% mole Iso-Propanol and 50% mole distilled water ternary mixture on an uncoated heating tube

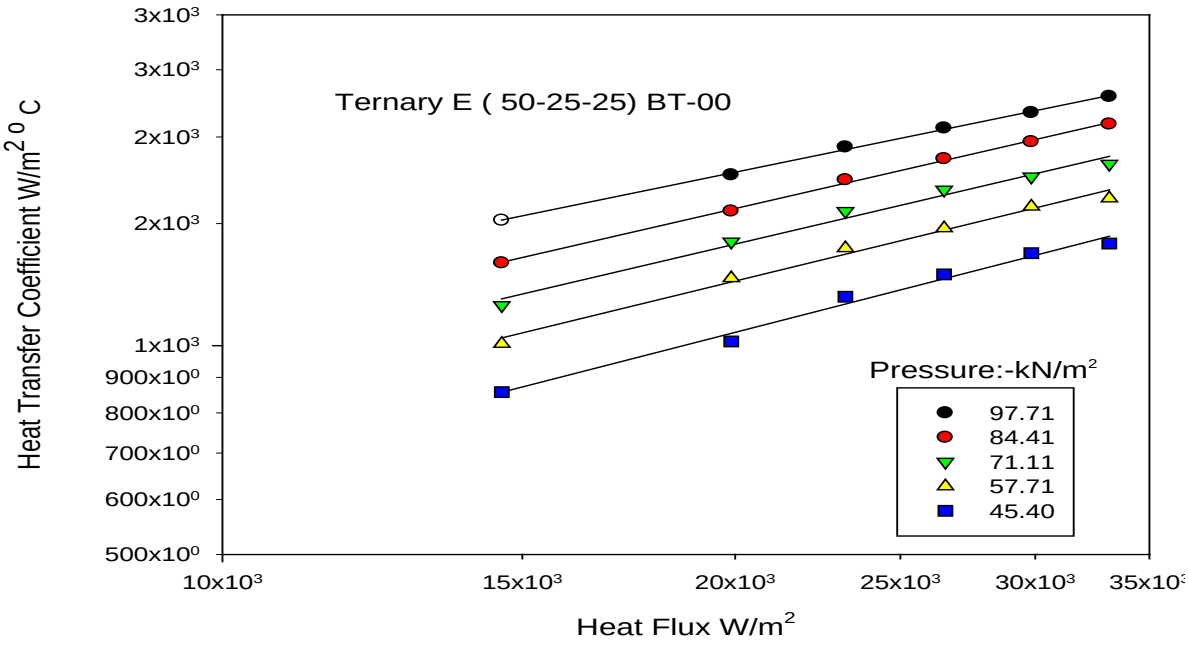

Figure 5.41 (a) Variation of heat transfer coefficient with heat flux for boiling of 25% mole methanol, 25% mole Iso-Propanol and 50% mole distilled water ternary mixture on an uncoated heating tube

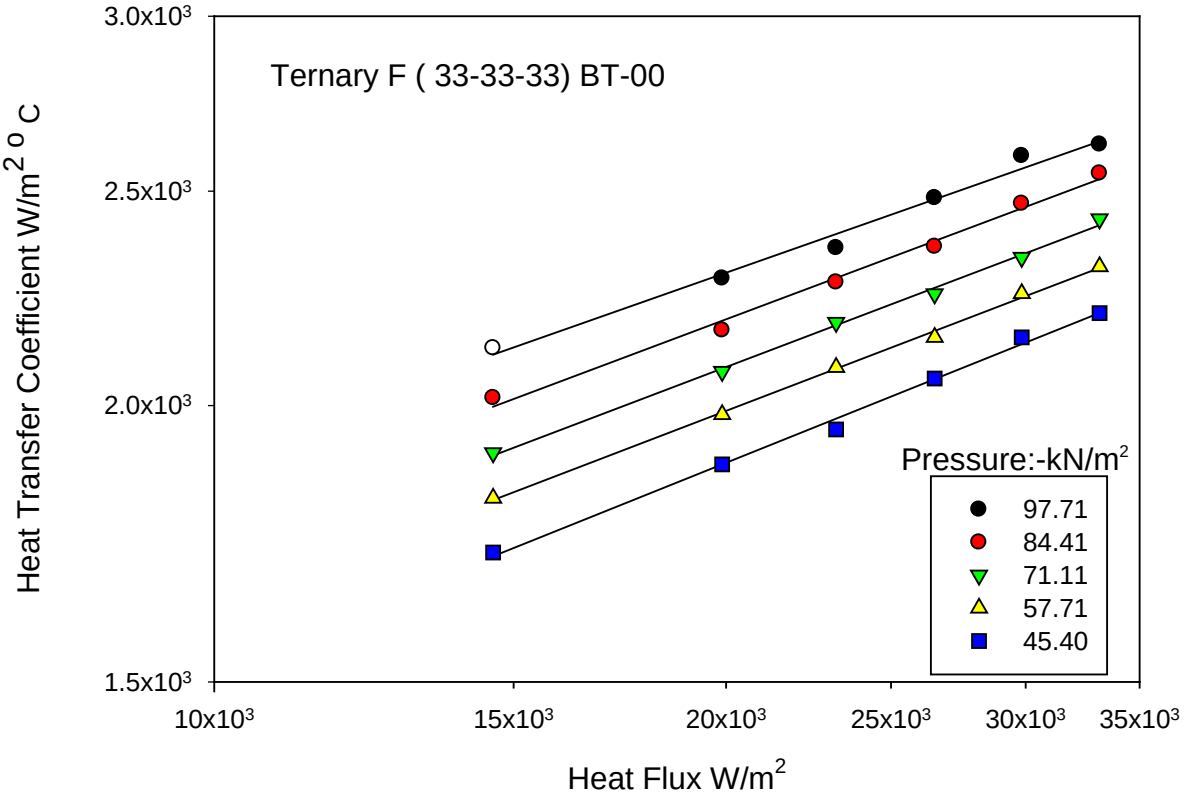

Figure 5.42 Variation of heat transfer coefficient with heat flux for boiling of 33% mole methanol, 33% mole Iso-Propanol and 33% mole distilled water ternary mixture on an uncoated heating tube

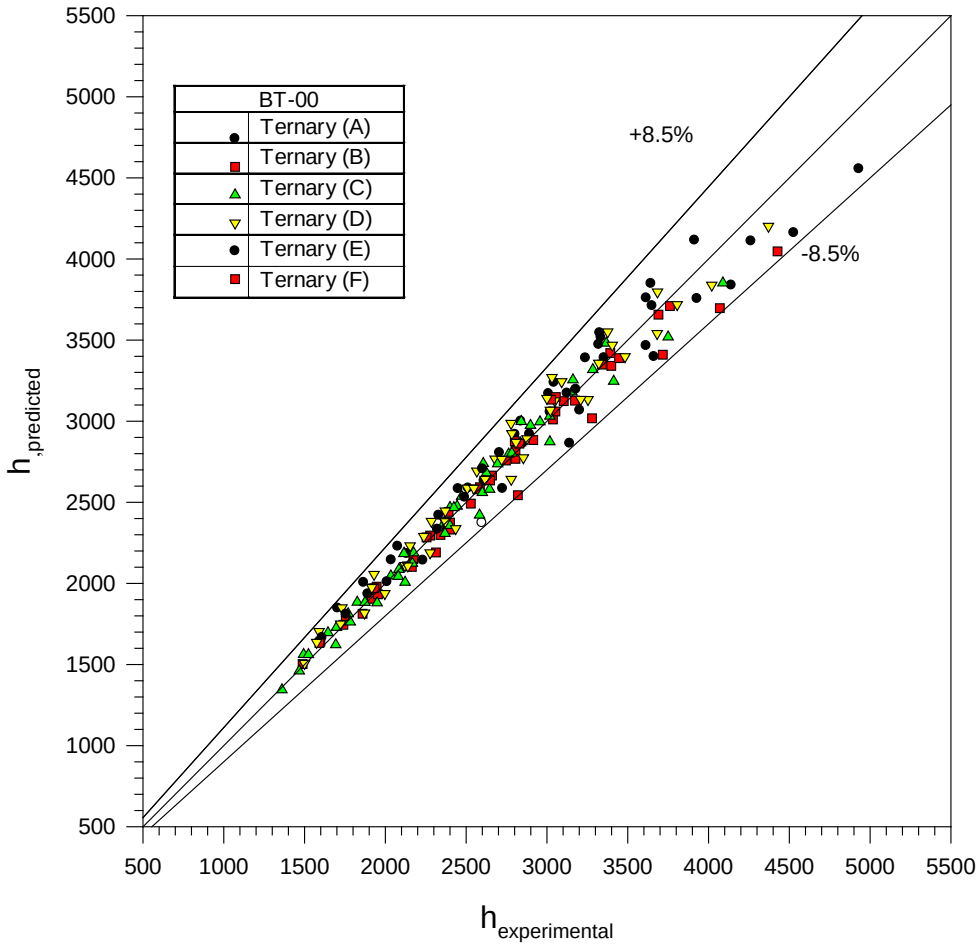

Figure 5.43 Comparison between Experimental heat transfer coefficient and predicted heat transfer coefficient from **Eq.(5.10)** of nucleate pool boiling of Distilled water-Iso-Propanol-Methanol Ternary mixture on an uncoated heating tube surface at atmospheric and subatmospheric pressures

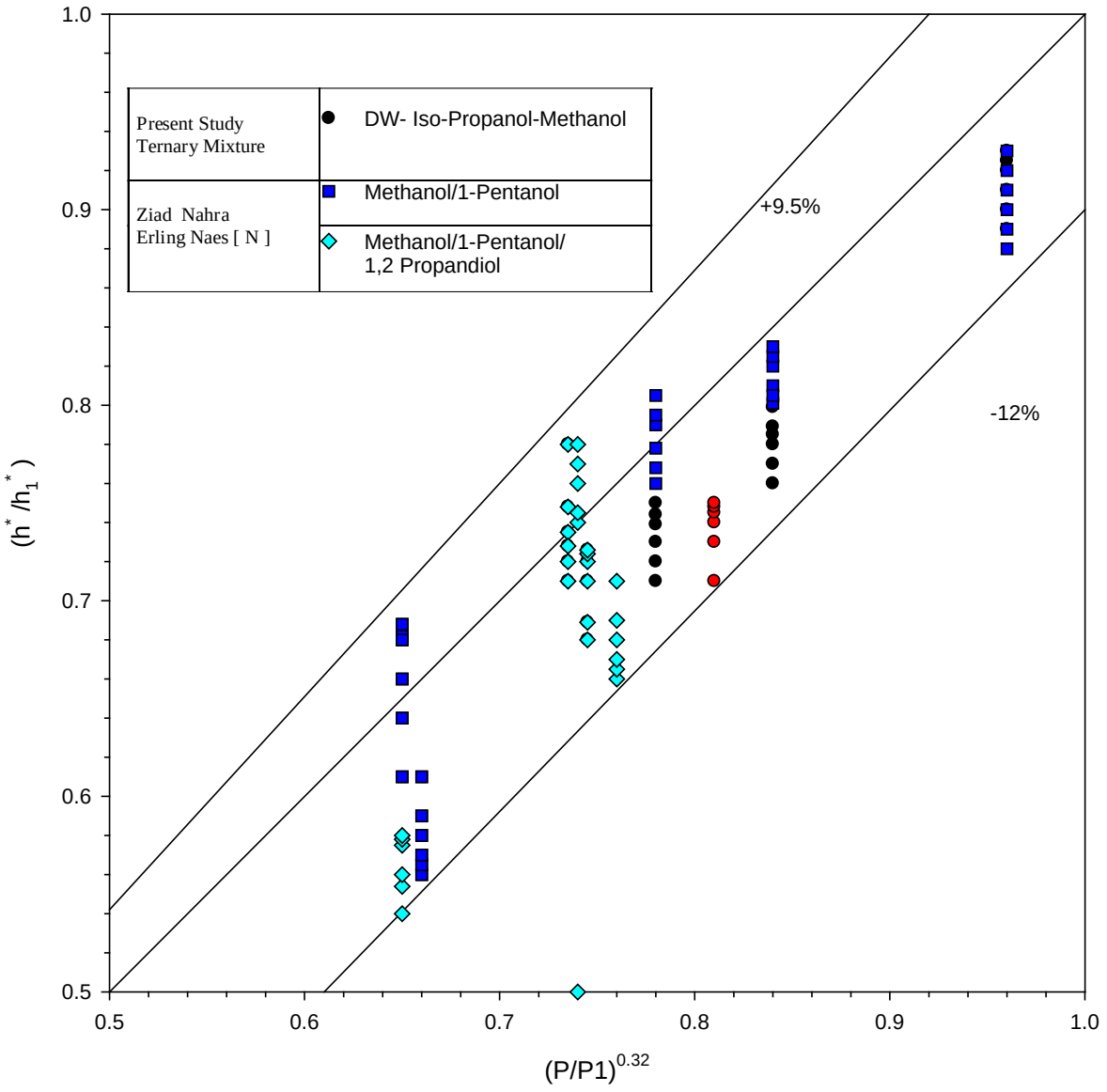

Figure 5.44 A plot between (h^*/h^*_1) and $(P/P_1)^{0.32}$ for the boiling of various composition ternary mixtures on an uncoated heating surface at atmospheric and subatmospheric pressures

Propanoldiol due to Nahara & Erling Naess [N1] on carbon steel surface at atmospheric pressure using different roughness of the heating surface. As can be noticed from this plot, all the data points of this investigation lie around a 45^0 diagonal line with the maximum deviation ranging from -12 to 9.5%. This indicates the validity of **Eq. (5.11)**. In this way **Eq. (5.11)** has been found to hold good for the boiling of a given composition of a ternary liquid mixture.

A close scrutiny of **Eq. (5.11)** reveals that it is free from surface-liquid combination factor $\mathbf{C_3}$. Therefore, it is applicable to any liquid mixture boiling on a surface. Further, it can be used to generate boiling heat transfer coefficient of liquid mixture at subatmospheric pressure from the knowledge of experimental data of one atmosphere pressure only. In other words, it requires experimentation only at atmospheric pressure. Another implication of above equation is that it can be used to test the consistency of experimental data of boiling heat transfer of ternary liquid mixture conducted on heating surfaces of varying characteristics at subatmospheric pressures.

5.4.3 Variation of heat transfer coefficient of ternary mixture of various composition

In previous section discussion has been restricted to a give composition of ternary liquid mixture at atmospheric and subatmospheric pressure. However it also been found that salient features during boiling of liquid mixture remain the same as those of single component liquid hence, it is quiet logical to determined boiling heat transfer coefficient of a given ternary mixture from the knowledge of individual component boiling heat transfer, keeping in the view, heat transfer coefficient of boiling ternary mixture has been computed by the following equation, Which represent the weighted mean of individual component of heat transfer coefficient.

$$\frac{1}{h_{id}} = \frac{\sum x_i}{h_i} \tag{5.12}$$

$$\frac{1}{h_{id}} = \frac{x_{lk}}{h_{lk}} + \frac{x_{hk}}{h_{hk}} \tag{5.13}$$

Where (*lk*) low key component (*hk*) high volatile component

Calculation of heat transfer coefficient has been made for various composition of a ternary mixture of distilled water, iso-propanol, methanol at atmospheric and subatmospheric pressure. The computed value so obtained, are compared as shown in **Fig. 45(b)**. This plot reveal that the predicted values represent by dotted curve do not match with the experimental firm

Figures 5.46(b) and. 5.47(b), plot between experimental heat transfer coefficient with mole fraction of highest volatile component in the bulk liquid of distilled water-iso-propanol- methanol at atmospheric and subatmospheric pressure. In this figure heat flux is a parameter; close examination of this figure reveals the following silent feature.

i. At a given heat flux, heat transfer coefficients of given composition of boiling mixture is lower than those of component implies that, heat transfer coefficient of a ternary mixture cannot be predicted by interpolation of heat transfer coefficients.
ii. Heat transfer coefficient decreases with increase highest volatile liquid and this trend continuous up to 30% of highest volatile component there after any further addition of methanol, iso-propanol concentration increase the heat transfer coefficients
iii. An increase of heat flux make the appearance of region depicting low heat transfer coefficients to be more pronounced.

Figures 5.48(b), 5.49(b), and 5.50(b), depict similar trend of heat transfer coefficient versus methanol mole fraction at (70.11kN/m^2, 45.12kN/m^2) subatmospheric pressure, respectively. These plots have essentially the same features as describe above, hence it is inferred that pressure does not change the nature of heat transfer coefficient of versus of composition of mixture.

Above observation are consistent and in agreement [B6], [F7], above features can be explain by the above.

A ternary mixture composes of three component of having different volatility they as single component liquid boil at different temperature. Hence, a ternary mixture boil over a range of temperature ranging from the boiling temperature of highest volatility to that lowest volatility one, it can be understood by the vapor liquid phase equilibrium and diagram at atmospheric and subatmospheric as shown in **Fig. 5. 45(b)** upper curve represent the vapor temperature, lower curve represents the liquid temperature, where the liquid boiling temperature as a function of highest volatile as fraction as can be seen from, equilibrium vapor mole fraction y^* is higher than that surrounding liquid mole fraction x give temperature, Van et al [V3] in bubble growing heated surface. So, in order to maintain equilibrium between phases more amount of high volatile component in the liquid mixture

to vapor to provide additional vapor as bubble grows.

As a result local concentration in the liquid decrease, local boiling temperature liquid rises this in term, wall temperature to increase so that heat transfer coefficient may occur at constant rate, as a result the concentration of highest volatile component in the liquid decrease, thereby liquid rise this, entire wall temperature to increase so that heat transfer may occur at constant rate hence lower values of heat transfer coefficient which based on bulk liquid temperature found in case of liquid mixture than that observed of single component liquids.

Heat transfer reduction was more pronounced in ternary mixture relative to binary mixture. The boiling of ternary mixtures involves simultaneous heat and mass transfer in the process of boiling evaporation of liquid components occurs by the transfer of heat from heated surface by micro layer existing beneath the bubble base during the boiling of liquid mixture, due to the vapor equilibrium vapor phase has a composition different that of composition of liquid phase, hence, micro layer is depleted of the light component and enriched in high component. Due to this mass diffusion of light component more diffusion occur due mass diffusion of light component from micro layer occur

As the rate of mass diffusion is much lower than that heat diffusion, mass transfer of light component to the bubble interface becomes the limiting process and a portion of driving force is utilized in overcoming the mass transfer rate resistance. The driving force is the difference between the equilibrium vapor and liquid composition $\left(y_i^* - x\right)$. Higher the value o $\left(y_i^* - x\right)$ more is the rate of diffusion of volatile components into the bubble and lower down the heat transfer coefficient.

Above discussion clearly reveals that boiling ternary mixture is different that of single component liquid owing to the association of heat and mass transfer. As a result of it, heat transfer coefficient of boiling ternary mixtures at atmospheric and subatmospheric pressure is lower than single components hence it value cannot be predicted by equation **Eq. (5.12).** In fact, heat transfer coefficient varies with concentration and attains a distinct minimum value, when boiling of a ternary mixture is carried out for a given heat flux at atmospheric and subatmospheric pressures. An increase in heat flux does not change nature of the curve h versus x but merely shift curve upward implies higher value heat transfer coefficient for boiling liquid mixture at atmospheric and subatmospheric pressures.

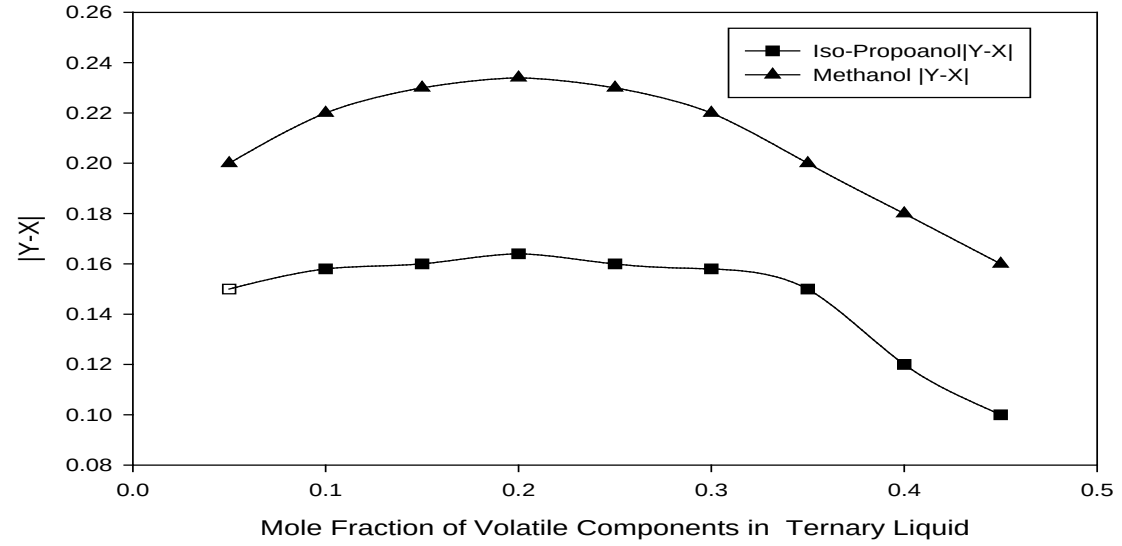

(a)

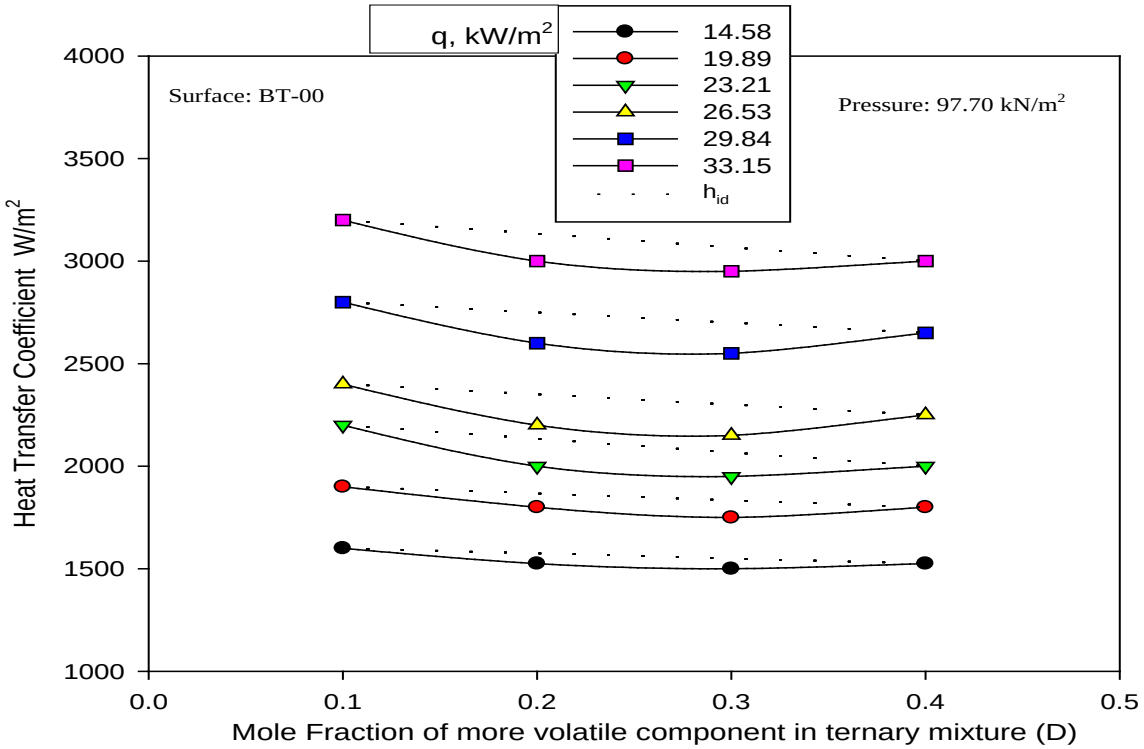

(b)

Figure 5.45 Variation of heat transfer coefficient with mole fraction of volatile component in ternary mixture (D) on uncoated heating tube at atmospheric pressure

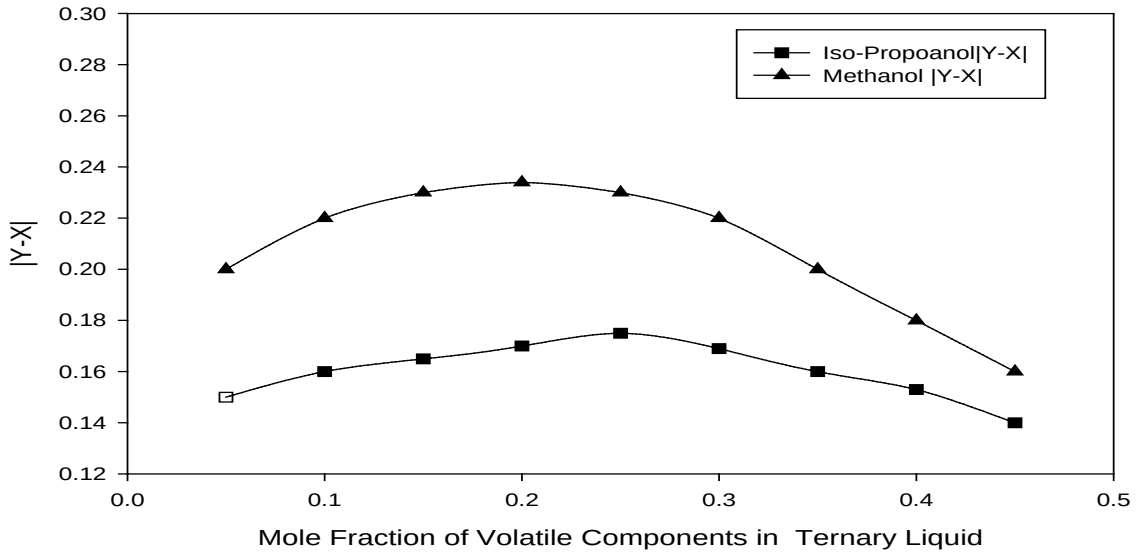

(a)

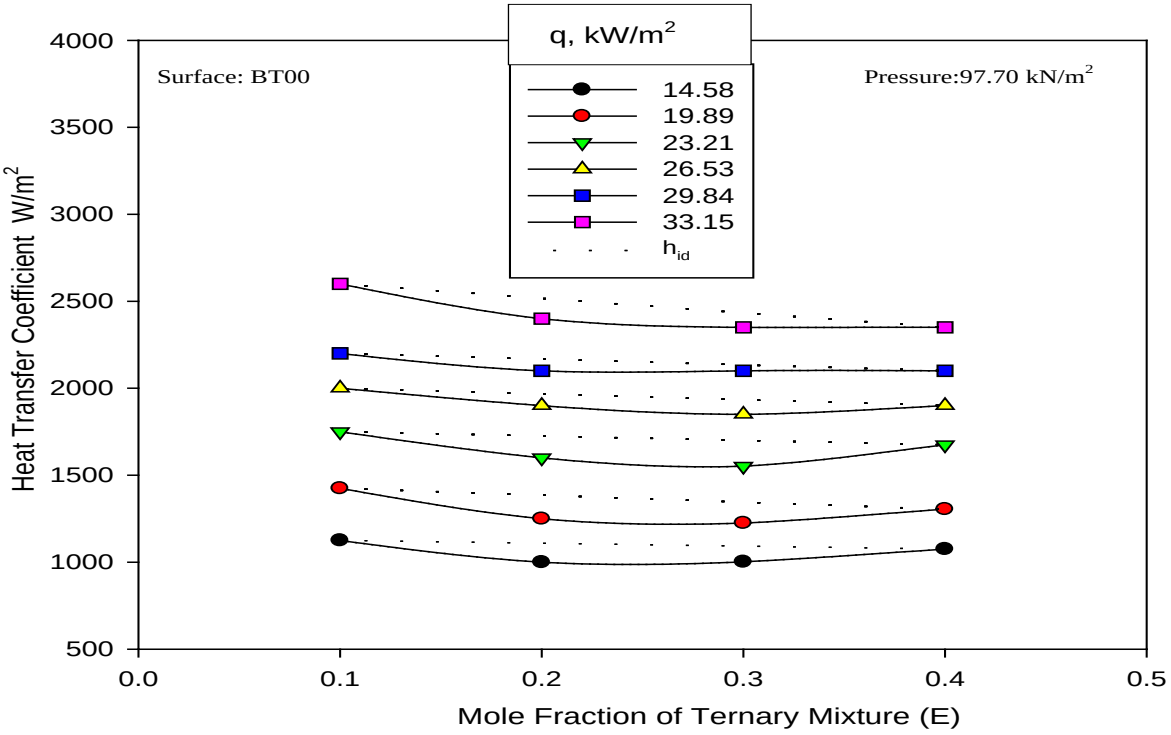

(b)

Figure 5.46 Variation of heat transfer coefficient with mole fraction of volatile component in ternary mixture (E) on uncoated heating tube at atmospheric pressure

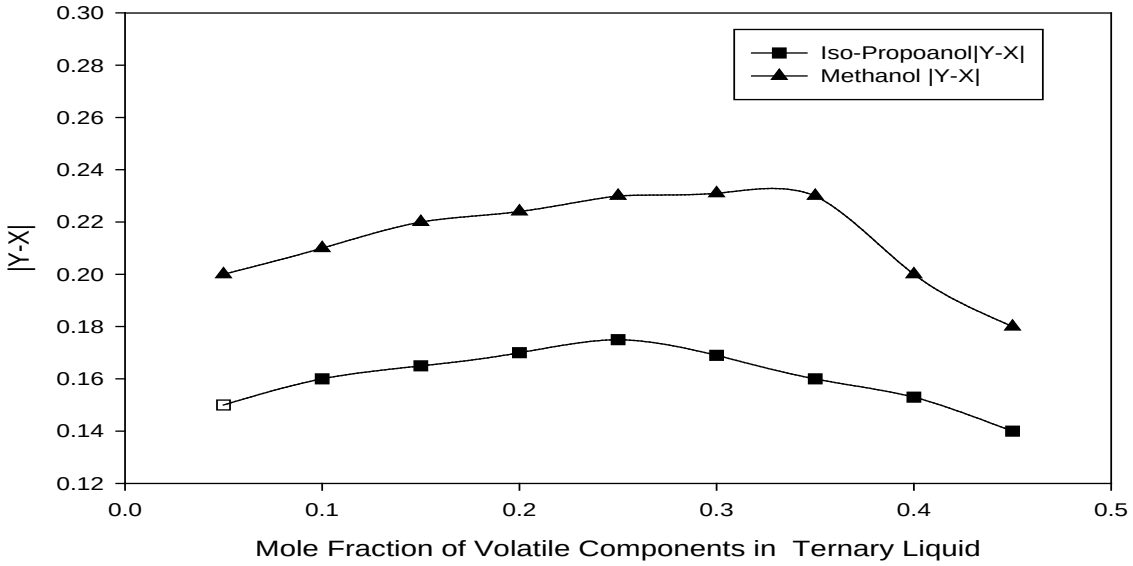

(a)

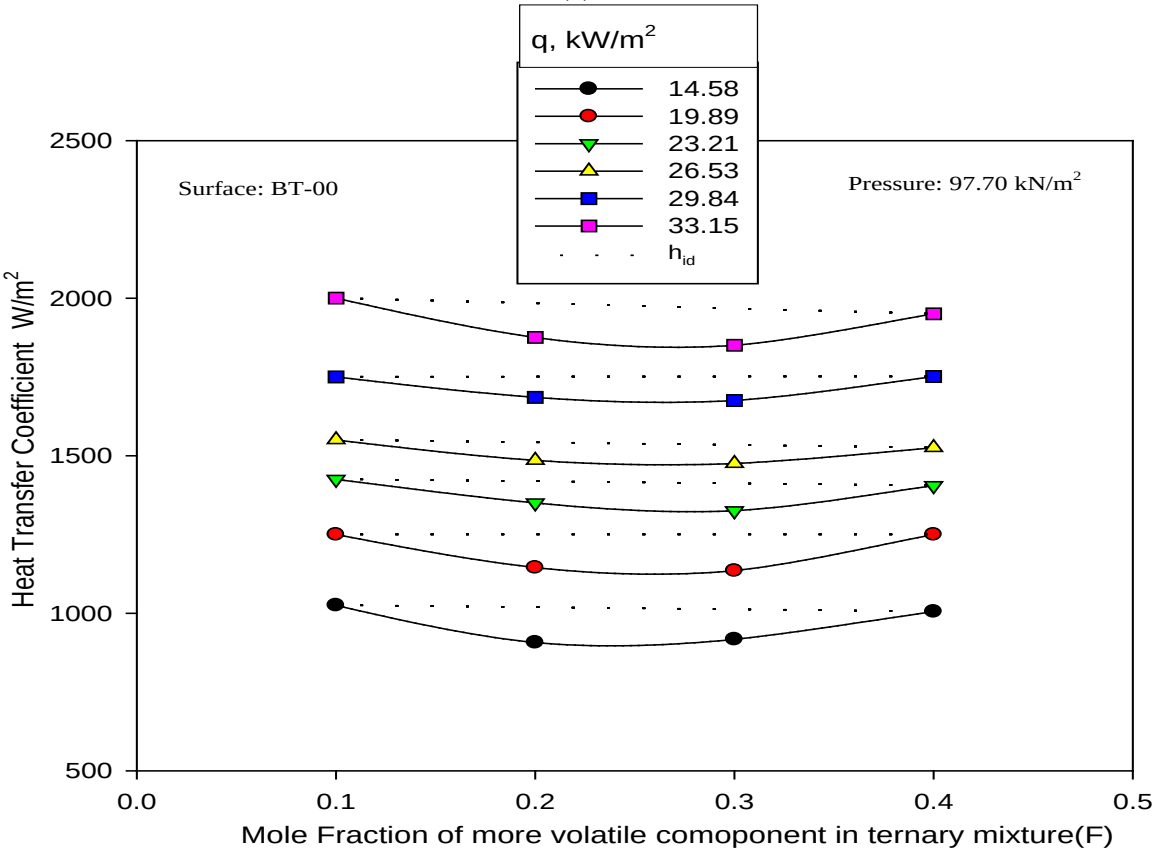

(b)

Figure 5.47 Variation of heat transfer coefficient with mole fraction of volatile component in ternary mixture (F) on uncoated heating tube at atmospheric pressure

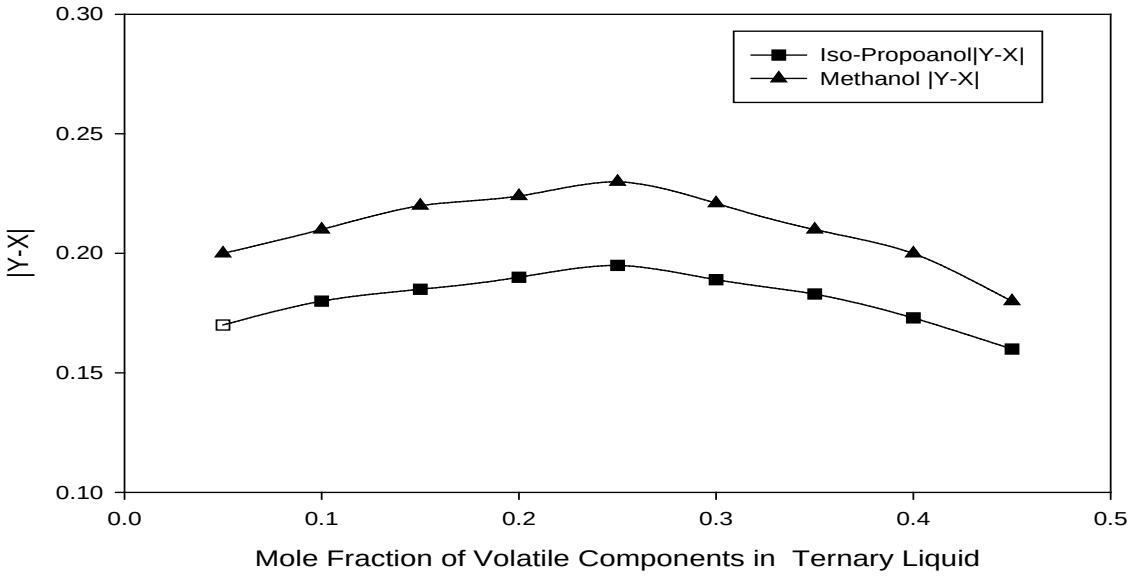

(a)

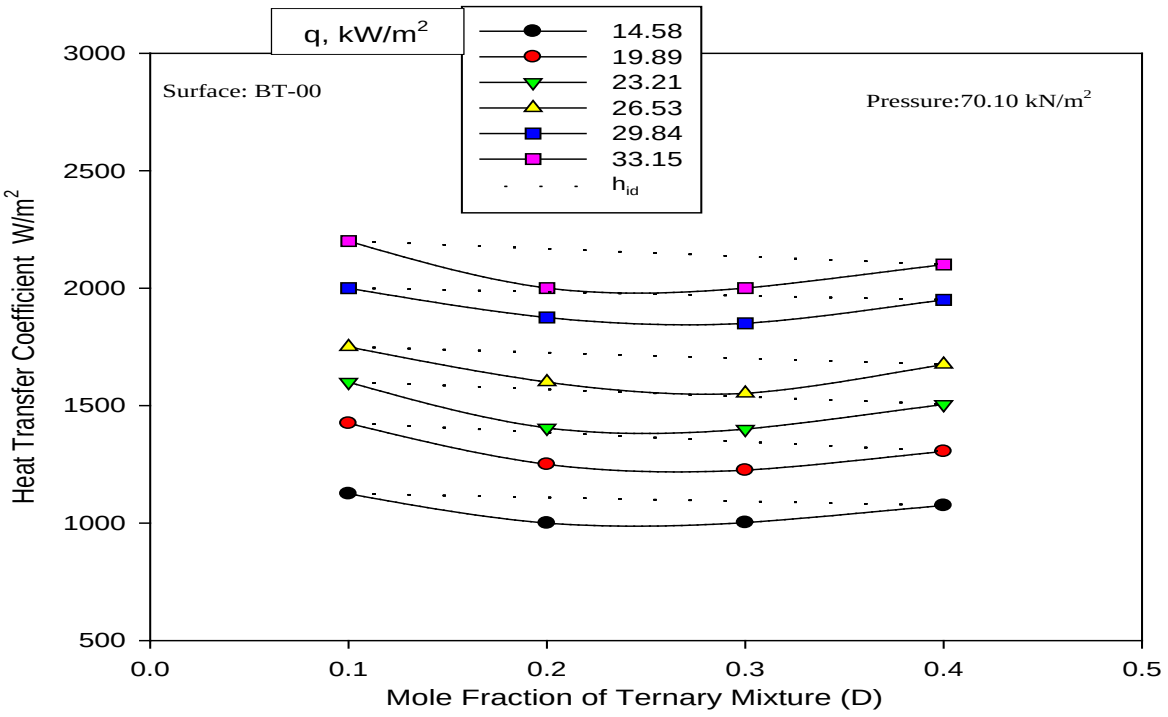

(b)

Figure 5.48 Variation of heat transfer coefficient with mole fraction of volatile component in ternary mixture (D) on uncoated heating tube at 70.10 kN/m^2 sub-atmospheric pressure

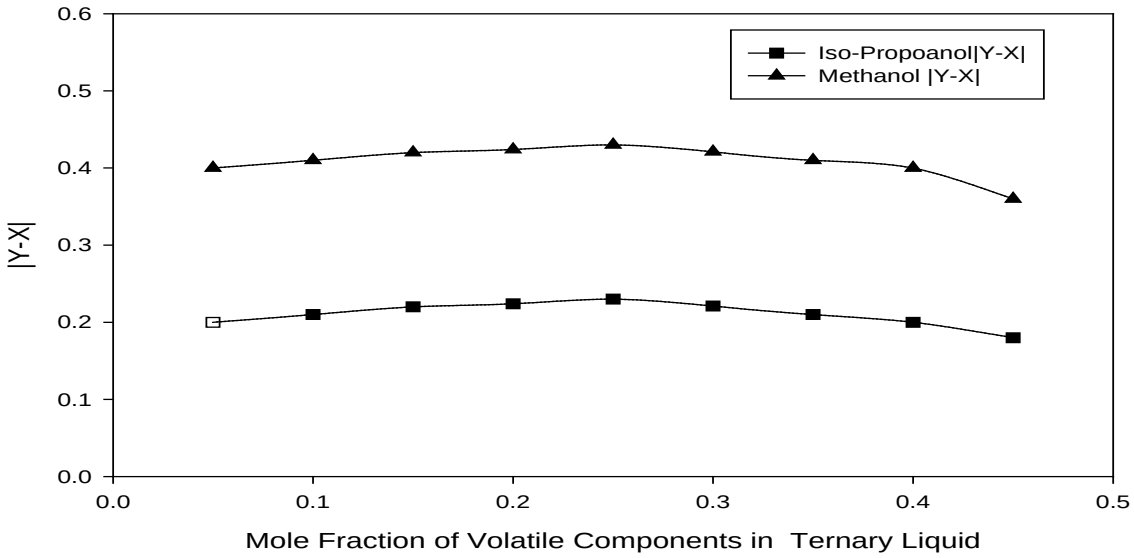

(a)

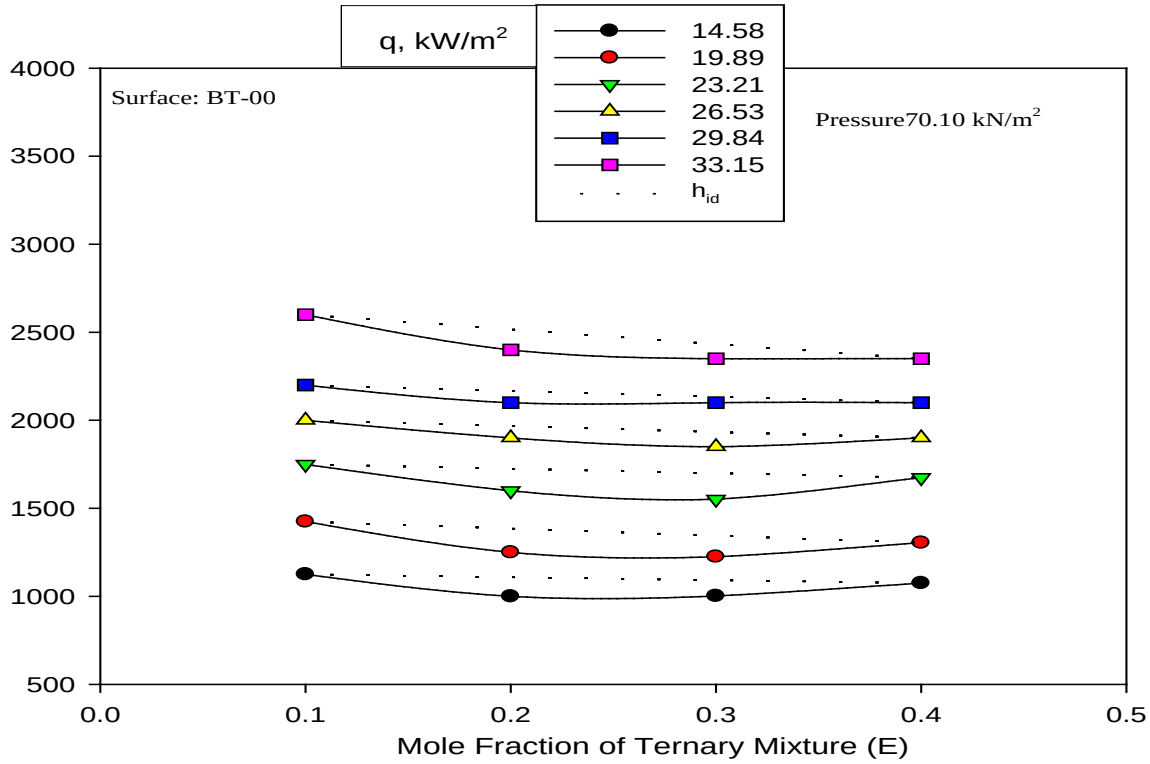

(b)

Figure 5.49 Variation of heat transfer coefficient with mole fraction of volatile component in ternary mixture (E) on uncoated heating tube at atmospheric pressure

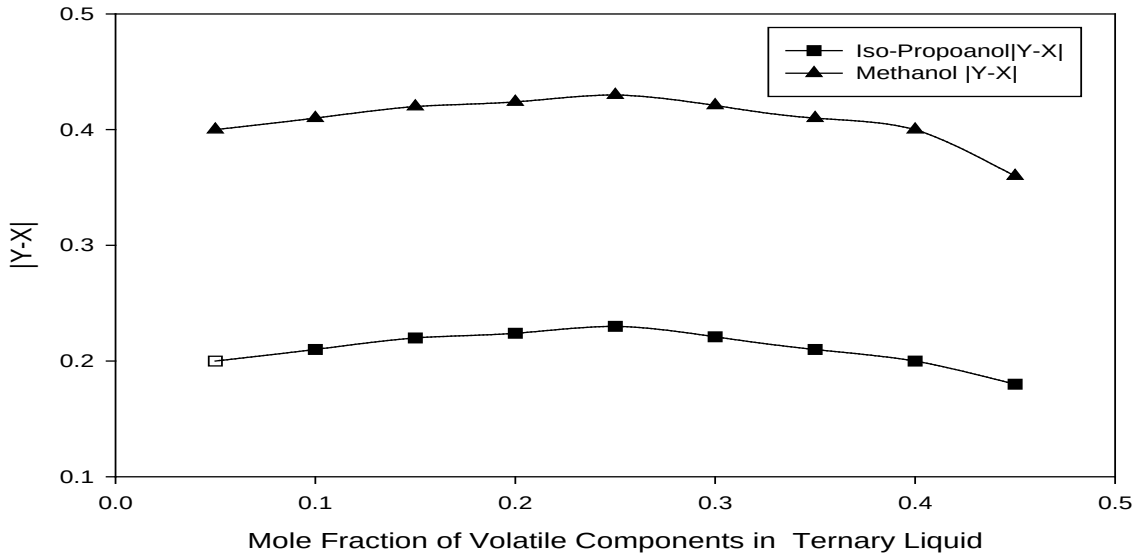

(a)

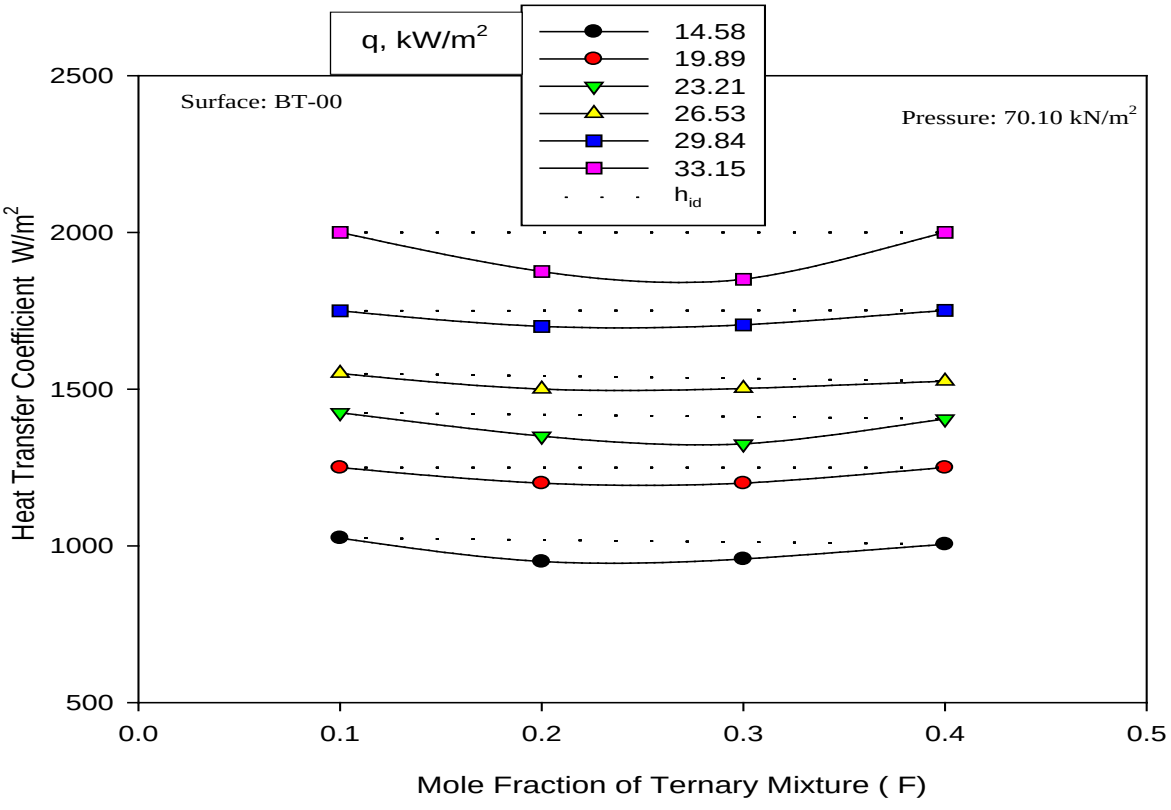

(b)

Figure 5.50 Variation of heat transfer coefficient with mole fraction of volatile component in ternary mixture (E) on uncoated heating tube at atmospheric pressure

5.4.4 Development of semi empirical correlation for heat transfer coefficient of ternary mixtures

In previous section it has been demonstrated that heat transfer coefficient for the binary and ternary mixtures at atmospheric and subatmospheric pressures cannot be calculated by weighted mean of heat transfer coefficient of individual components, **Eq. (5.13)**. This is due the fact that the mass transfer also occurs simultaneously only with heat transfer in the process of boiling of binary and ternary liquid mixtures. This calls for development of method which may be used to predict heat transfer coefficient of boiling of ternary mixture form the knowledge of measurable parameters such as heat flux, pressure concentration and physico thermal properties of the mixtures. This section devoted to it:

The boiling of ternary mixture is a simultaneous heat and mass transfer process. During the boiling of a liquid mixture, the vapour has a composition different than that of liquid phase owing to vapour-liquid phase equilibrium characteristic discussed above. Hence, as liquid mixture evaporators on the heating surface, the vapor contains more mole fraction of the high volatile component than that of low volatile one. This naturally affects the composition of micro layer and it is depleted of the high volatile component and is enriched in another i.e. low volatile component as a result of it, mass diffusion of high volatile components from the bulk to micro layer occurs. Since the rate of mass diffusion is much sluggish than heat diffusion, mass transfer of high volatile component to bulk interface becomes the limiting process and a portion of the driving force is utilized in overcoming the mass transfer resistance. As a result, an additional temperature driving force is required to obtain a given heat flux, q. Thus, wall superheat, ΔT is composed of effective temperature driving force, Δt_{id} and an additional temperature driving force, ΔT_a. So

$$\Delta T = \Delta T_{id} + \Delta T_a \tag{5.14}$$

Where, $q = h.\Delta T$

If there is no mass transfer, the mixture will behave as a hypo-theoretical pure liquid and the wall superheat will be lower than that required for the actual mixture for the same heat flux, Hence,

$$q = h_{id}.\Delta T_{id} \tag{5.15}$$

From Eq. 5.(9) And 5.(10)

$$\frac{h}{h_{id}} = \frac{\Delta T_{id}}{\Delta T} \tag{5.16}$$

Thus, one can determine, the value of heat transfer coefficient for a ternary liquid mixture from the knowledge of the ratio, $\left(\frac{\Delta T_{id}}{\Delta T}\right)$ and heat transfer coefficient of a hypo-theoretical pure liquid, h_{id}. As mentioned above, this pure liquid has some properties as the mixture but no mass transfer involved in it. Therefore, h_{id} represents heat transfer coefficient of an ideal mixture. It can be obtained from **Eq. (5.9)** which represents weighted mean temperature difference in a mixture. So its value can be calculated from the known values of heat transfer coefficients and mole fractions of individual components present in the primary mixture.

$\left(\frac{\Delta T_{id}}{\Delta T}\right)$ represents the ratio of temperature driving force for the case of no mass transfer to that in presence of mass transfer occurring along with heat transfer in the boiling of a liquid mixture. The driving force for mass transfer of high volatile component is the concentration difference, $\left(y_i - x_i\right)$. Its value is positive for high volatile component whereas negative for low volatile component. Hence, $\left|y - x\right|$ must find a place in defining the $(\frac{\Delta T_{id}}{\Delta T})$ .Further, as mass diffusion is rate controlling process so the term, $(\alpha/D)^{0.5}$ which represents a measure of the resistance to heat transfer, should also be included in it. Incorporation of above terms leads to the quantity, $\left[\sum_{i=1}^{n-1} /y_i - x_i/\left(\alpha / D\right)^{0.5}\right]$ which represents effective driving force in the boiling of a liquid mixture. Where (n) is the number of components present in the mixture, with this following correlation has been develop to correlation data of this investigation for the boiling of various compositions of iso-propanol-methanol-distilled water mixture at atmospheric and subatmospheric pressures.

$$\frac{h}{h_{id}} = \frac{\Delta T_{id}}{\Delta T} = \left[1 + \left|y_1 - x_1\right|\sqrt{\frac{\alpha_1}{D_1}} + \left|y_2 - x_2\right|\sqrt{\frac{\alpha_2}{D_2}}\right]^m \tag{5.17}$$

Where m = -(0.73x1 +0.36)

1= methanol

2= iso-propanol

This equation correlates all the data of this investigation within an error of ± 18% as can be seen for **Fig.5. 51**

Above equation has also been tested against the predicted data due to correlations of following investigators: Calus & Rice [C1], Fujita et al. [F5], Happel & Stephan [H3], Jungnickel et al. [J7], Schlunder[S6], Stephan & Korner[S15], Thome [T5], and Thome & Shakir [T7]. The comparision between experimentally obtained values of heat transfer coefficient and those predicted by above correlations and **Eq. (5.17)** of this investigation is shown in **Fig. 5.52.** As is clear from this figure, predictions have matched the experimental values within an average error of ±25%. Thus, it can be said that correlation, **Eq. (5.17)** for boiling of binary liquid mixture is capable of correlating experimental data for the boiling of liquid mixtures taken on different heating surface.

obtained for the boiling of liquids and their binary mixtures. Hence, same explanation was given in section 5.2.3 hold true in this case also.

Hence, boiling characteristic representing the variation of heat transfer coefficient of a ternary mixture with respect to heat flux and pressure remains the same as of individual liquids. It can be described by the following equation which has been obtained by regression analysis with an error of ± 4.21 %

$$h = C_3 q^{0.67} p^{0.33} \quad \textbf{(5.18)}$$

Where, $\mathbf{C_3}$ is a constant whose value depends upon the percentage composition of the mixture, and their surface characteristics. The values of constant, $\mathbf{C_3}$ as determined for various compositions of distilled water-iso-propanol-methanol mixtures are given in **Table 5.3**.

Table 5.3 Values of constant $\mathbf{C_3}$ of **Eq. (5.18)** for various compositions of distilled Water-Iso-propanol-Methanol

S.No.	Designations to mixtures	Compositions			
		Distilled Water	Methanol	Iso-Propanol	$\mathbf{C_3}$
1	Ternary (A)	50 Mol%	10 Mol%	40 Mol%	0.531
2	Ternary (B)	50 Mol%	20 Mol%	30 Mol%	0.501
3	Ternary (C)	50 Mol%	30 Mol%	20 Mol%	0.497
4	Ternary (D)	50 Mol%	40 Mol%	10 Mol%	0.467
5	Ternary (E)	50 Mol%	25 Mol%	25 Mol%	0.438
6	Ternary (F)	33.33 Mol%	33.33 Mol%	33.33 Mol%	0.431

An important implication of **Eq. (5.10)** is that heat transfer coefficient of a given composition of ternary mixture of distilled water-iso-propanol- methanol can be calculated from the knowledge of heat flux, (q) and pressure, (p) provided the value of constant, $\mathbf{C_3}$ appearing in **Eq. (5.10)** is experimentally known. It may be pointed out that above correlation, **Eq. (5.17)** is free from a surface-liquid combination factor, so this equation is applicable to the boiling of any liquid mixture irrespective of the characteristic of heating surface involved in it. Further, the value of heat transfer coefficient for the boiling of a binary and ternary liquid mixture can be calculated from the known values of heat transfer coefficients, diffusivity and relative volatility of the binary liquid mixture. It hold true for the boiling of non-azeotropic liquid mixtures as it has not been tested against boiling heat transfer data for azeotropic liquid mixtures.

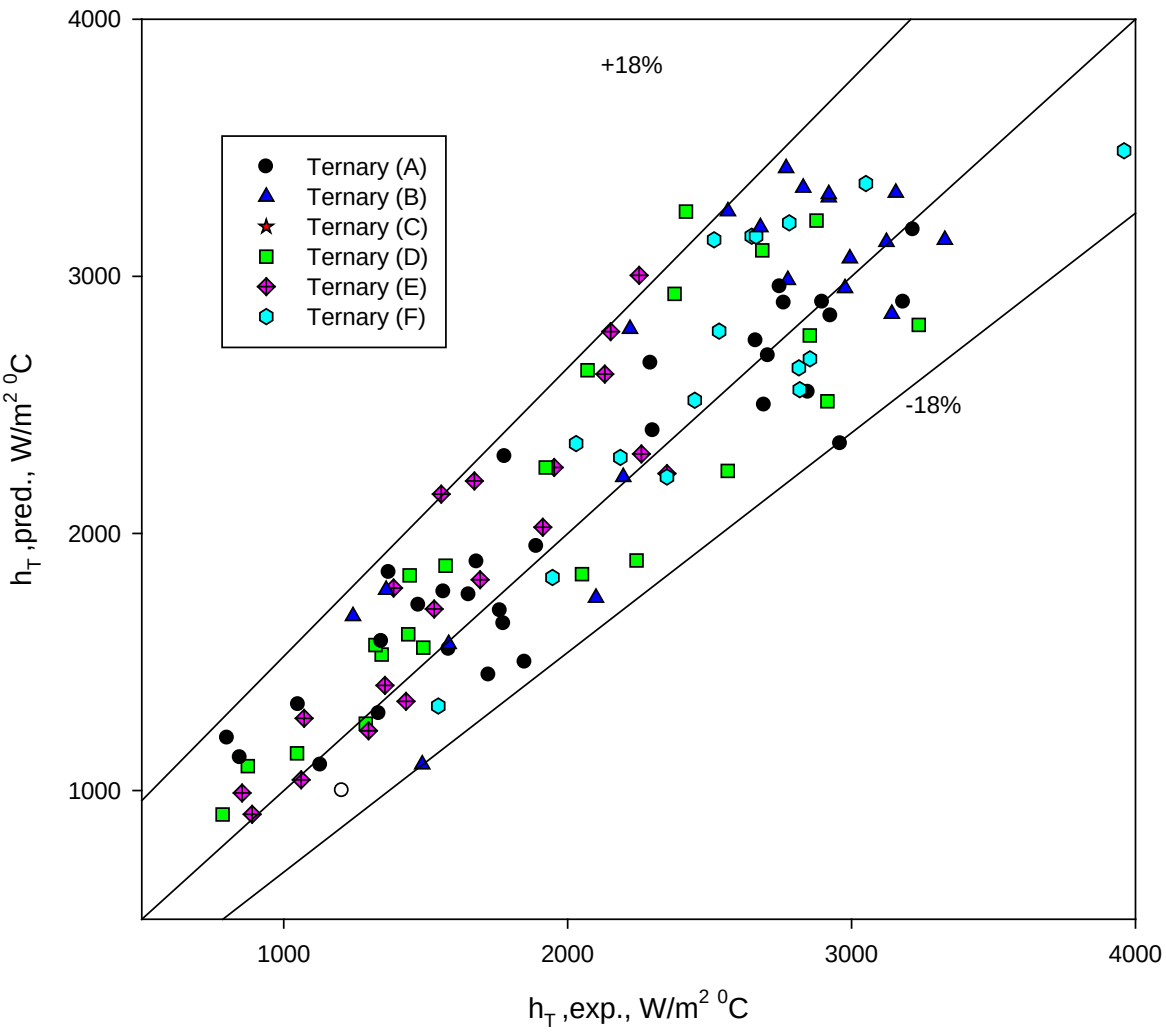

Figure 5.52 Comparison between Experimental heat transfer coefficient and predicted heat transfer coefficient from **Eq.(5.17)** of nucleate pool boiling of Distilled water-Iso-Propanol-Methanol Ternary mixture on an uncoated heating tube surface at atmospheric and subatmospheric pressures

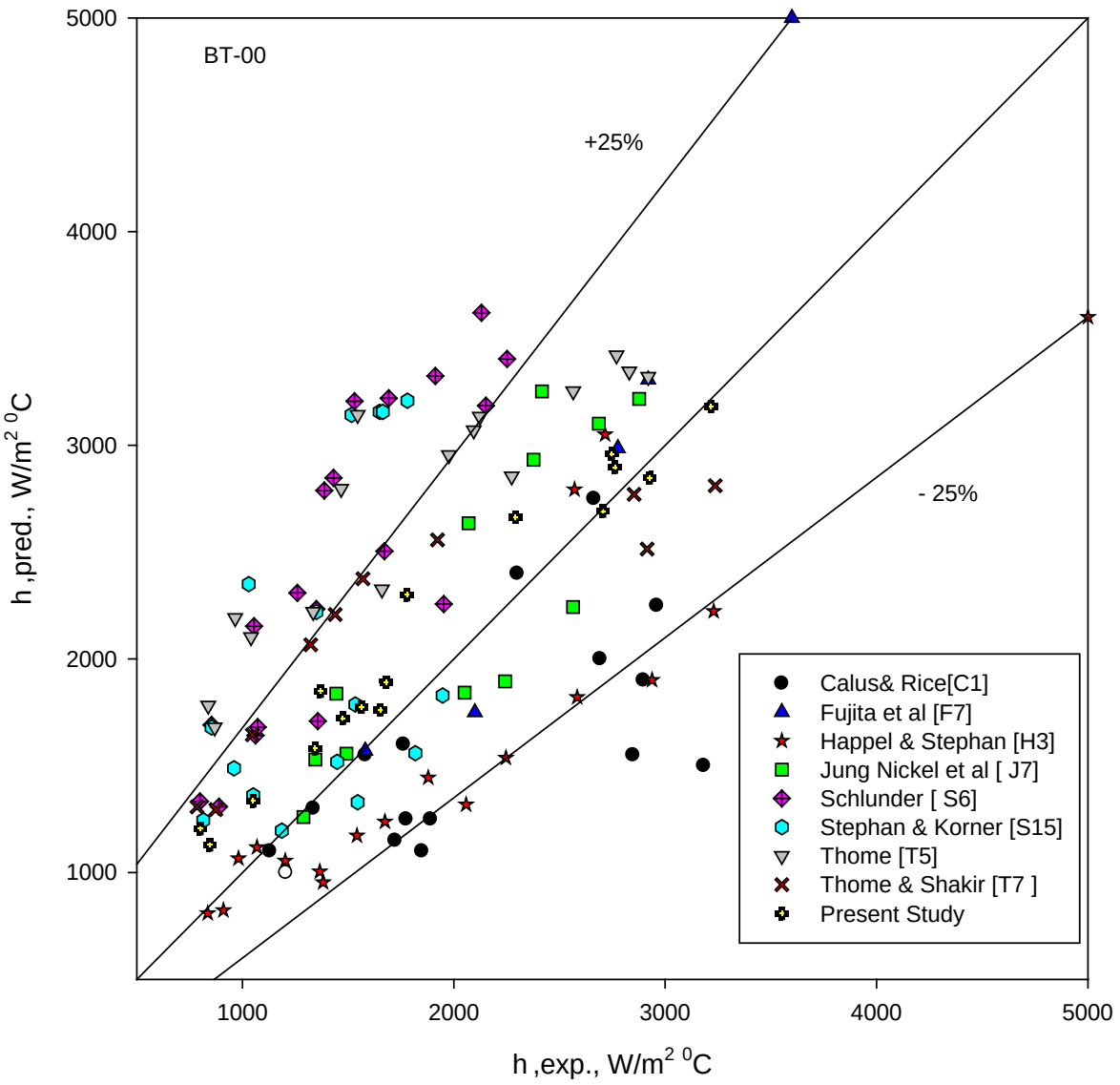

Figure 5.52 Comparison of experimental heat transfer coefficient with those predicted from **Eq. (5.17)** for boiling of methanol-distilled water and iso-propanol water mixture on an uncoated heating tube surface at atmospheric

SUMMARY

On the basis of above, it can be concluded that boiling heat transfer characteristics of ternary mixture are same as that of pure liquid. The functional relationship of heat transfer coefficient with heat flux, pressure is same as observed for liquids and their dimensional equation for the boiling ternary mixture ($h = C_3 q^{0.67} p^{0.33}$) at atmospheric and subatmospheric this equation has also give dimensionless correlation to estimated the heat transfer coefficient for the boiling of a liquid mixture on any surface irrespective characteristics however heat transfer coefficient of boiling ternary mixture cannot be calculated by method of interpolation of heat transfer coefficient of individual component present in mixture. In fact, heat transfer coefficient does not vary linearly with composition but depicts a minimum value corresponding minimum vapor composition of mixture. Such as composition of the minimum volatile liquid phases of vapor liquid equilibrium diagram of the mixture. This is due to the simultaneous the mass transfer and heat transfer process occur further analysis as resulted in an equation for prediction of heat transfer coefficient from known values physico-thermal properties, vapor- liquid phase equilibrium diagram, heat transfer coefficient and mole fraction of individual component present in ternary mixture, resultant equation has been found to correlate the experimental data of this investigation well as those of earlier investigators.

5.5 NUCLEATE POOL BOILING OF DISTILLED WATER ON COATED HEATING TUBE

Experimental data for boiling of distilled water on horizontal brass coated with copper of various thicknesses are given in Table B.2 to B.4 of Annexure B. In this investigation three thicknesses of copper coating viz. 15, 25 and 35 μm have been employed. It is worthwhile to mention here that procedure used for calculation of heat transfer coefficient in this case has been the same as that used for uncoated heating tube surface. The thickness of copper coating has not been used in calculation of heat transfer coefficient from heating tube surfaces. Hence, heat transfer coefficient on coated tube surface is based on substrate temperature only. This has been carried out for the sake of comparison of thermal behavior between coated and uncoated tube surface. The main objective of conducting experiment on three coated tube for distilled water was to identify the coating with maximum heat transfer coefficient for boiling of distilled water. Following subsections discuss the effect of heat flux, pressure and coating thickness on heat transfer coefficient during nucleate pool boiling of distilled water on coated heating surfaces.

5.5.1 Heat transfer coefficient on coating heating surface

Figure 5.53 describes a plot between heat transfer coefficient and heat flux for saturated boiling for distilled water on a brass heating tube coated with 15 μm thickness of copper by plasma spray deposition technique at atmospheric pressures. It also contains experimental data of various other investigators, namely, Cieslinski [C22] on stainless steel surface coated with 0.19 mm thickness of aluminum by modified gas flame spray technique, Afgan et.al. [A1] on Cr-Ni steel surface coated with 0.45 mm thickness of Cr-Ni by sintering, Mihir das. [M9] on a copper heating tube coated with copper 43 μm thickness coated by wire flame spraying technique, Bliss et.al. [B14] on stainless steel surface coated with 127 μm thickness of copper by electroplating technique and Siraj et. al. [A3]on stainless steel heating tube coated with copper with 63μm by electroplating technique. The experimental data for uncoated tube surface due to present investigation as well as of above mentioned investigators have also been including in it for the purpose of comparison between coated and uncoated tube surfaces. A close examination of this plot inferred the following salient feature:

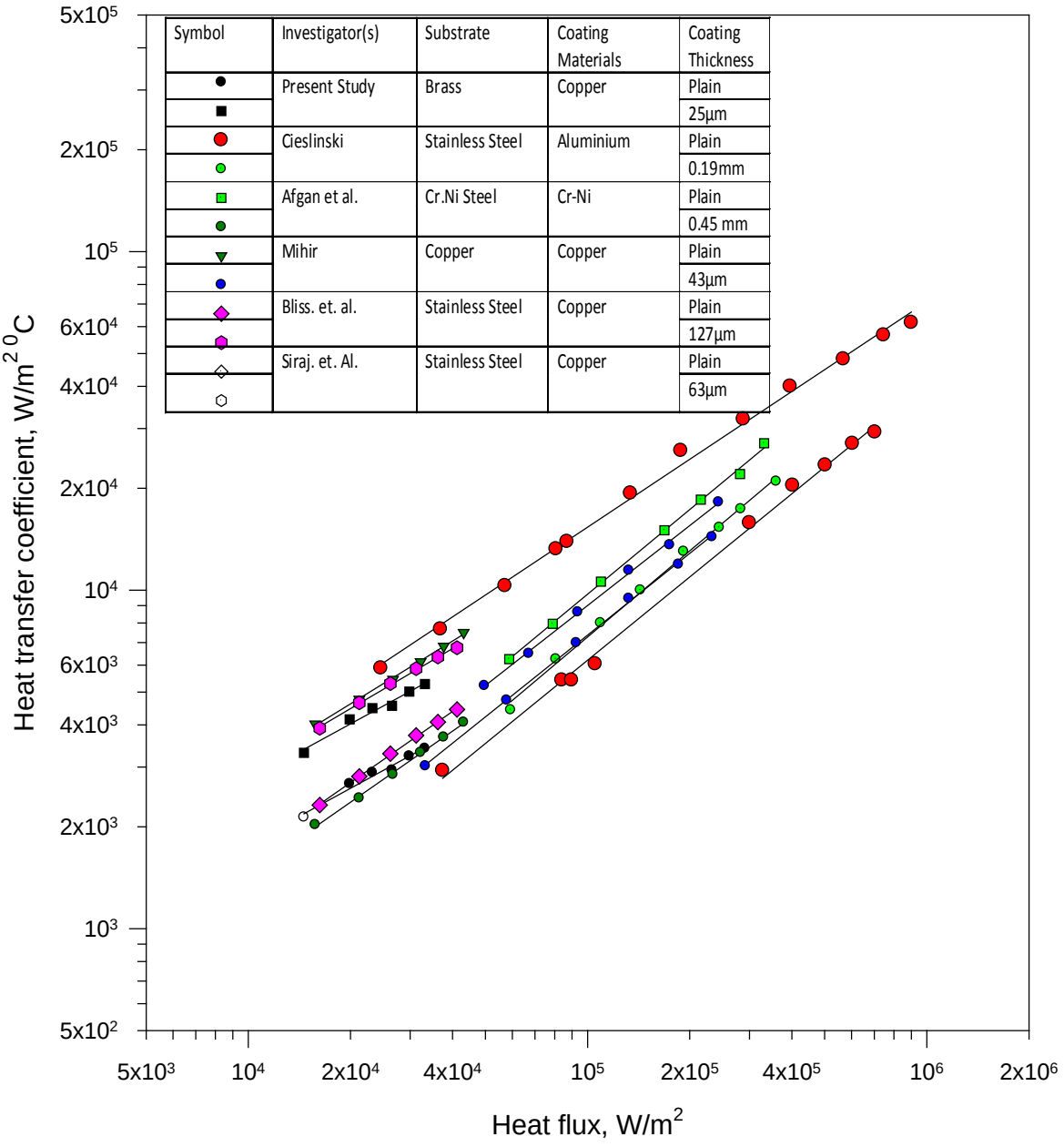

Figure 5.53 Variation of heat transfer coefficient with heat flux for saturated boiling of distilled water from plain surface and coated surfaces due to present and earlier investigators at atmospheric pressure

i. A substantial disagreement exists between data point of present investigation and those of others. Further, data of earlier investigators also do not match amongst themselves.

ii. At a given value of heat flux, coated heat transfer tube offers higher value of heat transfer coefficient than that of corresponding uncoated heating tube.

iii. The heat transfer coefficient of coated heating tube surface increases with increase in heat flux and can be represented by the relationship $\boldsymbol{h} \propto \boldsymbol{q}^{r}$, where value of exponent r differ from investigation to investigation. However, the value of exponent r is always found to be less than 0.7 which is usually observed in the case of boiling on an uncoated heating surface.

Above features are consistent and can be explained as follows:

As reported above, heating surfaces, employed in each of the above investigations have differed in material of substrate, quality of coating material, thickness of coating and the method of application of coat. Therefore, characteristics of heating surfaces are likely to differ from investigation to investigation and therefore, above noticed disagreement amongst data points of various investigations are bound to occur.

Application of copper coating on an uncoated heating tube leads to the formation of interwoven matrix consisting of various micro porous layers. Depending upon the method of application of coating some pores of inner layers are partially or fully exposed to distilled water. As a matter of fact, they entrap residual gas and act as nucleation sites for initiation and development of vapor-bubbles. In this way population of nucleation sites on a coated surface becomes more than that on an uncoated one. In addition, coating has also been found to affect contact angle significantly. In fact, it decreases with increase in thickness of coating, [A3, B11, B13, P8, P9, R1]. As contact angle effects surface tension directly, so coating on an uncoated tube surface decreases surface tension. Thus, coating on an uncoated tube surfaces produces two significant effects i.e. multiplies nucleation site and decreases surface tension. Both these factors contribute to activate nucleation sites of smaller size to form vapor-bubbles, as can be seen from **Eq. (5.2)**. Consequently, vapor-bubble population on a coated heating surface increases. In fact, at some stage population of vapor-bubbles on coated surface become so large that many of them combine together to form agglomerates which, in turn, lead to vapor blanketing and thereby, obstruct the process of nucleation and development of nucleation and formation of vapor-bubbles on

heating surface. At high values of heat flux, population of vapor agglomerates and thereby the magnitude of vapor blanketing becomes so large that heat removal occurs at a lower rate than that at low values of heat flux. Hence, heat transfer coefficient on a coated surface varies with the heat flux at a low rate than that on an uncoated heating surface. In other words, the value of exponent r in the relationship between h and q for boiling of distilled water on a coated heating tube surface is less than 0.7 which holds true for an uncoated heating surface. It may be mentioned here that almost all the investigators [A1, A3, B12, B14, C14, D1, P8, S9, V11] have reported the value of exponent r to be less than 0.7. Thus, experimental observations of this investigation substantiate the finding of earlier investigations too.

As mentioned above, coating on an uncoated tube surface multiplies nucleation sites and reduces surface tension. Hence, large number of small sized vapor-bubbles emit for heating surface with high emission frequency. In addition, coating also increases the magnitude of capillary action due to the formation of matrix structure over an uncoated surface. As a result, water from bulk rushes to inner layer with greater intensity and therefore, heat removal from uncoated surface takes place at a higher rate than that on an uncoated surface. Thus, for a given value of heat flux, heat transfer coefficient of coated surface is found to be more than that on a uncoated one.

5.5.2 Boiling of distilled water on copper coated tubes

Figure 5.54 represent variation of heat transfer coefficient with heat flux of the boiling of distilled water on a 15 μm thick copper coated heating tube surface. In this figure, pressure is a parameter.

i. Heat transfer coefficient increases with heat flux irrespective of pressure and variation between the two can be describe by relationship, $\mathbf{h \propto q}^{0.67}$
ii. At a given value of heat flux, heat transfer coefficient increases with rise in pressure.

Above features have also been, found for the boiling of distilled water on 25 and 35 μm thick coated tube as can seen from **Figs. 5. 55 (a and b)**, respectively. However, the value of exponent q in the functional relationship between h and q has been found to be different. It is 0.62 and 0.58 for 25 and 35 μm thick coated thick coated heating tubes surfaces, respectively.

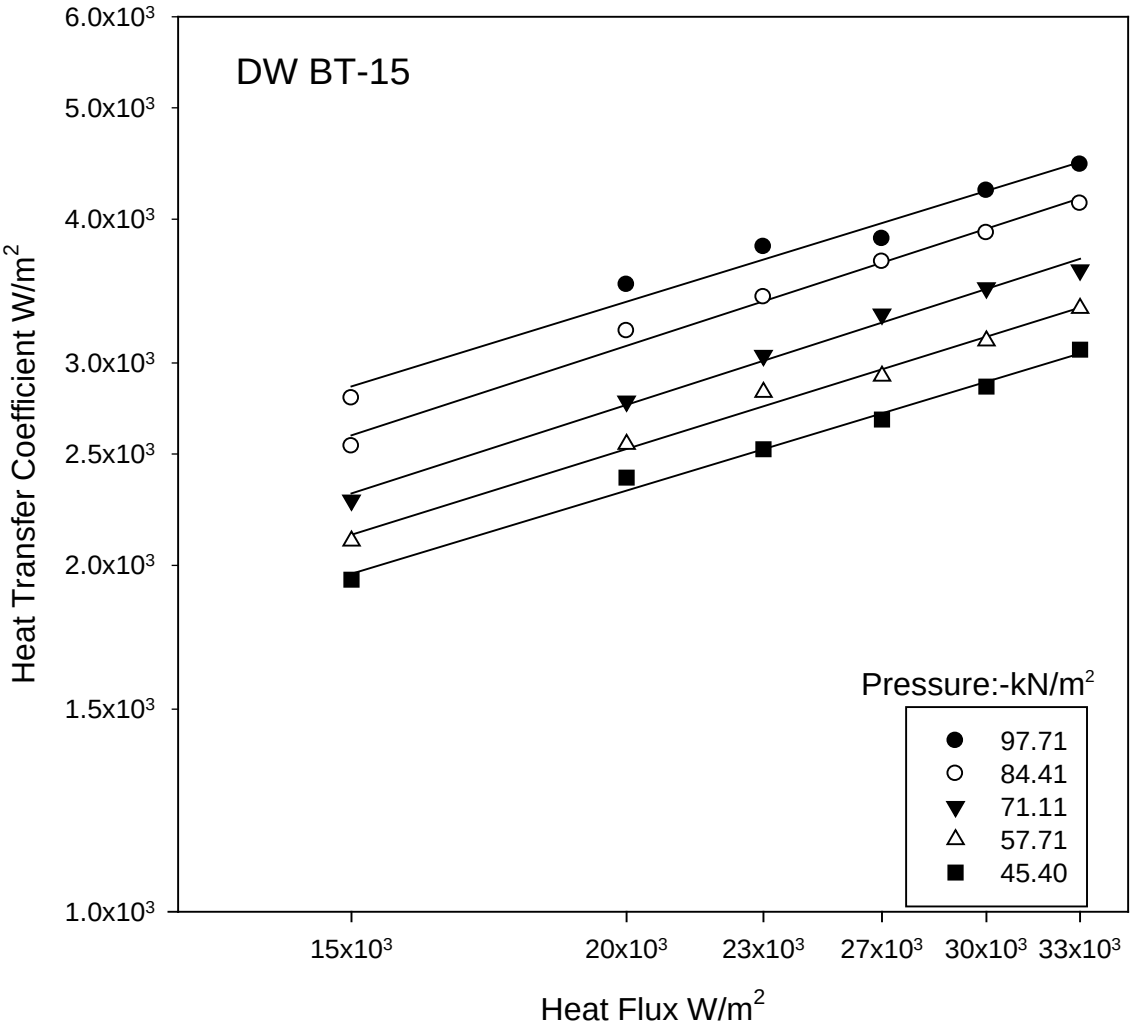

Figure 5.(54) Variation of heat transfer coefficient with heat flux for boiling of distilled water on coated tube BT-15 with pressure as a parameter

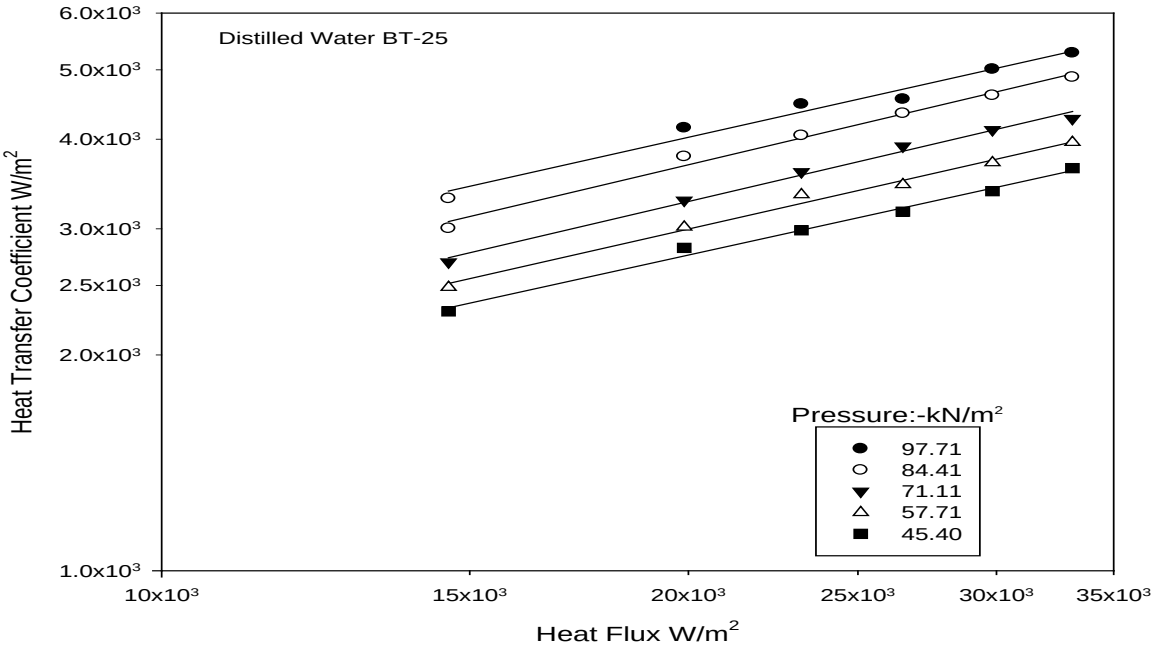

(a)

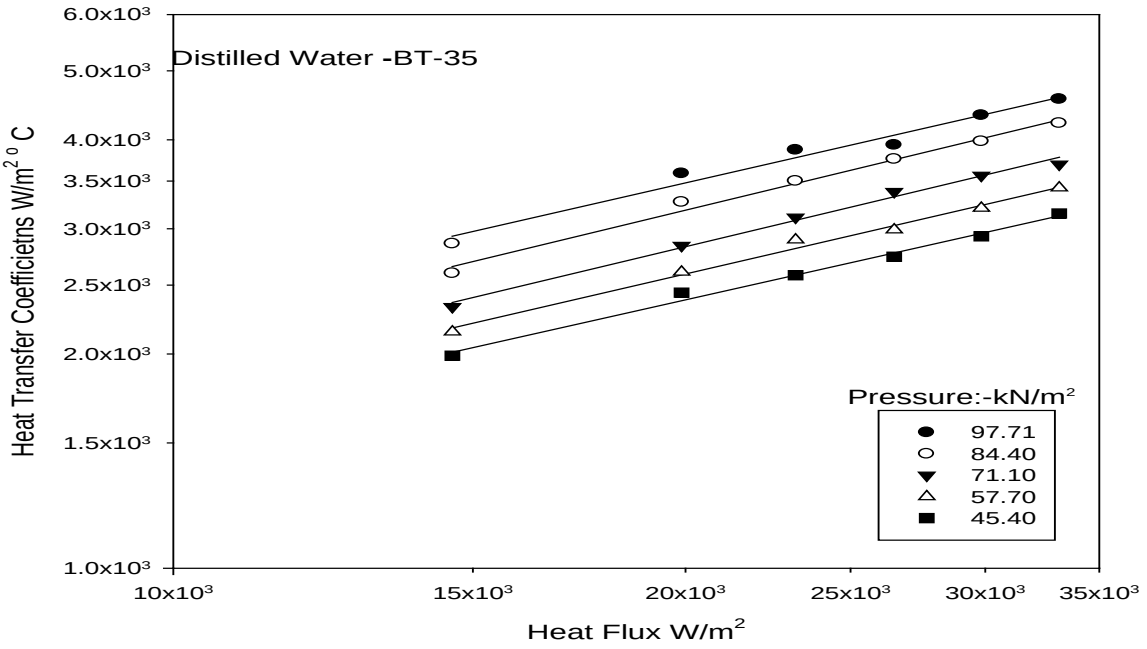

(b)

Figure 5.55 Variation of heat transfer coefficient with heat flux for boiling of distilled water on coated tube BT-25 and BT-35 with pressure as a parameter

Above features are same as discussed earlier. Hence, same explanation holds true in this case also. Thus, the value of exponents of q decreases with increase in thickness of coating on heating tube surface. This might be due to the following reason:

An increase in thickness of coating of copper on a heating tube increases the number of micro-porous layers in the matrix structure. Thus, in turn, multiplies the number of small sized nucleation sites on heating tube surface. As a consequence of increase in the population of nucleation sites, larger number of vapor-bubbles originates in interior portion of matrix of a higher coating thickness tube surface than that on a less coating thickness tube surface. However, many of them combine together to form agglomerates. As the number of small vapor-bubbles on higher coating thickness coated tube is more than that on less coating thickness coated tube, larger number of agglomerates form on the former than that on later one. Hence, area of heating tube surface covered by vapor- agglomerates increases with increase in thickness of coating. Besides this, it is also affected by the magnitude of heat flux. At high value of heat flux, it is more pronounced than that at low heat flux value. At high value of heat flux, the population of small sized vapor-bubbles is more. Hence, the formation of vapor agglomerates is more. As a result, heat transfer coefficient is affected by two parameters thickness of coating and heat flux in the same manner. Hence, heat removal rate for boiling of distilled water on a heating surface covered with copper decreases with increase in thickness of coating as well as with heat flux. Therefore, heat transfer coefficient-heat flux curve become steeper when thickness of coating is decreased. In other words, the slope of h versus q represented by exponent in relationship, $h \propto q^r$ decrease with increase in thickness of coating on a brass heating tube. That is way, the value of exponent of heat flux (q) is found to be smaller on higher coating thickness coated tubes than that observed on lesser coating thickness coated tubes.

5.5.3 Heat transfer coefficient-heat flux relationship for distilled water on coated tubes

The experimental determine values of heat transfer coefficient for the boiling of distilled water on a coated heating surface have been re-processed by regression analysis to obtain a correlation. Which is as follows:

$$h = C_6 q^{0.56} p^{0.36} \tag{5.18}$$

Where, constant, C_4 and exponents r and s depend upon the thickness coating on tube surface. The values of constants C_4 and exponents r and s for coated tubes for three coated tubes of investigation are given in **Table 5.4.**

Table 5.4 Values of constant, C_4 and exponents, r and s for boiling of distilled water using **Eq. (5.18)**

S.No.	Coated Tube	C_4	r	s
1	BT-15	1.01	0.67	0.54
2	BT-25	1.24	0.60	0.46
3	BT-35	2.69	0.58	0.47

Figure 5.56 shows a plot between experimentally-determined values of heat transfer coefficient and those predicted from **Eq.(5.18)** for the boiling of distilled water on coated heating tube surface at atmospheric and sub-atmospheric pressure. The plot clearly indicates that the predicted values have matched excellently with the experimental values within a maximum error of $\pm 3.50\%$. Thus Eq. (5.18) has succeeded to correlated experimental data of boiling heat transfer of distilled water on coated heating tubes surfaces and coefficient of correlation of this **Eq. (5.18)** is 0.975.

5.5.4 Comparison between coated and uncoated heating tube

In this section a comparison is shown to study the heat transfer characteristics of distilled water on brass tubes coated with copper of various thicknesses with that on an uncoated tube surface at atmospheric and subatmospheric pressure with an objective to obtain the effect of thickness of coating on boiling heat transfer coefficient.

Figure 5.57 depicts a plot between heat transfer coefficient and heat flux for saturated boiling of distilled water on brass tubes coated with copper of various thicknesses at atmospheric pressure. This plot also contains a curve for an uncoated tube surface to show comparison between the two. This figure reveals the following salient features.

i. At a given heat flux, an increase in thickness of coating increasing heat transfer coefficient up to a certain value and thereafter decreases
ii. Heat transfer coefficient on coated tube of various thicknesses is higher than that on an uncoated tube for a given value of heat flux.

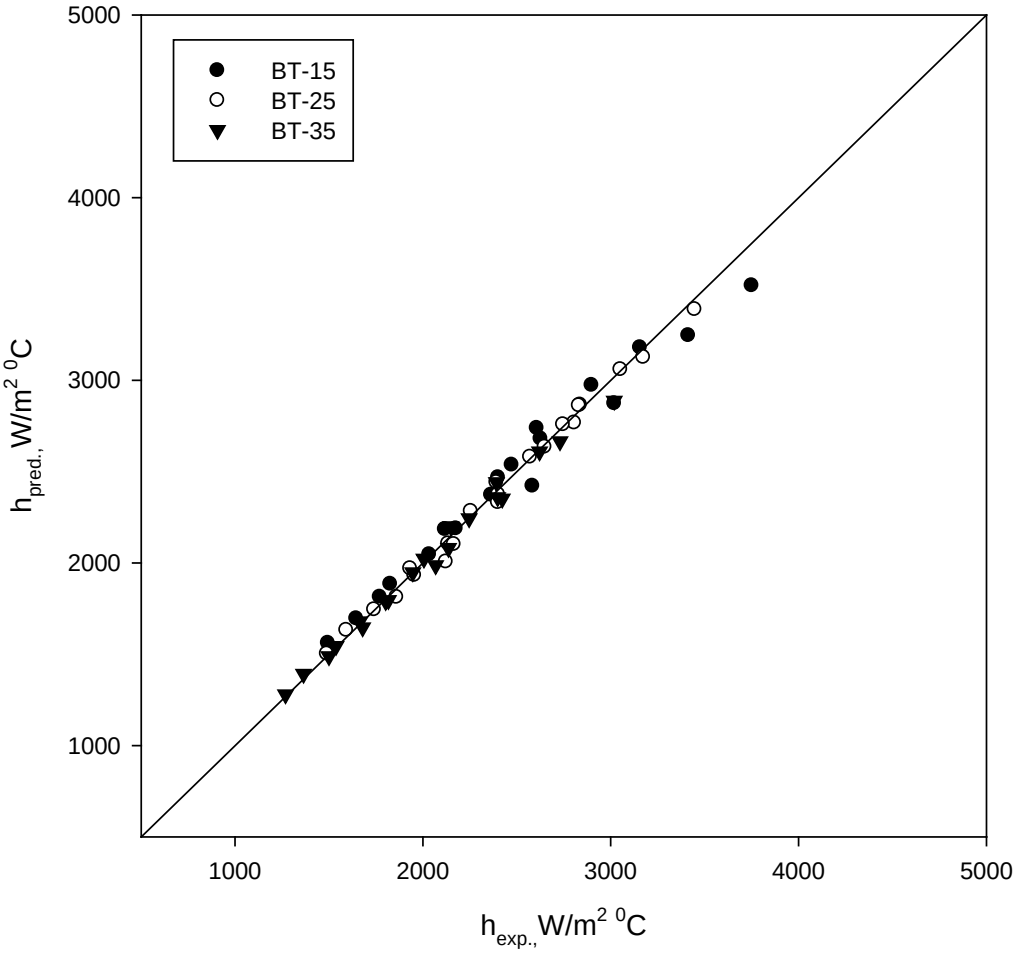

Figure 5.56 Comparison of experimental heat transfer coefficients with those predicted from **Eq. (5.20)** for boiling of distilled water on coated heating tube surfaces at atmospheric and subatmospheric pressures

Possible explanation for above behavior is as follows:

As explained in sub-section 5.5.1, coating of copper on an uncoated tube surface increases nucleation site density and reduces contact angle. Hence, number of small sized vapor-bubbles emitting from a coated heating surface increases. This increases the population of vapor-bubbles which causes coalescence leading to from vapor agglomerates. As a result, heat removal rate decreases. In addition, coating also increases the magnitude of capillary action which in turn, instigates liquid from pool to inner portion of matrix structure with greater intensity to fill void caused by the departure of vapor-bubbles from surface. In fact, it increases continuously with increases in coating thickness. This increases recirculation of liquid which leads to increase the intensity of turbulence near the heating surface and enhances heat removal rate. Thus, increases in thickness of coating produces two opposing phenomena reduction of heat removal rate due to the formation of vapor bubble-agglomerates and increases of heat removal rate owing to enhancement of capillary action. The resultant effect of coating thickness depends upon the magnitude of these phenomena. As a matter of fact, the effect of later seems to be more pronounced than that of former during initial stage of coating on a heating tube surface. That is why, heat transfer coefficient on a 15 μm thick coated surface is found to be more than that on an uncoated tube surface.

Above behavior also hold true when thickness of coating is increased from 15 to 25 μm. An increase in thickness of coating beyond 35 μm further enhances the population of vapor-bubbles and vapor agglomerates which are responsible to decrease heat removal rate. However, it is also accomplished with the decrease of heat flow rate by conduction from substrate surface to various layers of coating owing to continuous replacement of liquid by layer in matrix structure. Hence, heat removal rate decreases. Thus, both the above mentioned phenomena supplement each other to reduce heat removal rate from surface to liquid pool. No doubt, the intensity of recirculation rate due to capillary structure increase with thickness of coating, but its effect on heat removal rate does not seems to be as pronounced as that of vapor agglomerates. In other words, vapor agglomerates play a dominating role to effect heat transfer rate from coated surface. Since number of agglomerates increases with coating thickness, a reduction in heat removal rate and thereby heat transfer coefficient is bound to occur beyond a certain thickness of coating. In present

investigation heat transfer coefficient, at a given heat flux, is observed to beyond a thickness of coating of 25 μm i.e. for coating thickness of 35 μm.

An increase in heat flux on a coated surface affect above phenomena considerably. When boiling of distilled water occurs on a coated surface, increase in vapor-bubble population occurs on account of increases in number of nucleation sites formed by various layers of coating as well as heat flux. As a result, of its many of them combine together to from vapor agglomerate which effect heat transfer coefficient adversely. Therefore, heat transfer rate in the region of high heat flux does not increase with the same rate as it does in the region of low heat flux. Thus, as can be seen from **Fig.5.57**, slope of heat transfer coefficient-heat flux curve decrease with increase in coating thickness.

Figures 5.58 and 5.59 are typical plots depicting the effect of coating thickness on heat transfer coefficient for boiling of distilled water at various subatmospheric pressures. These plots have essentially the same features as that of plot in **Fig. 5.57,** for boiling of distilled water at atmospheric pressure.

Figure 5.60 is typical plot showing the percentage enhancement in heat transfer coefficient due to copper coating of various thickness of 15, 25 and 35 μm (BT-15, BT-25 and BT-35) brass heating tube surface. This plot reveals that percentage enhancement in BT-25 heating tube is the maximum to the of tune of 55% more than that of uncoated brass tube. Calculations of percentage enhancement have been carried out for all the pressures and found to be the same order.

On the basis of above, it can be said that coating of copper on an uncoated tube surface increases heat transfer coefficient of boiling liquids significantly. For a given value of heat flux, heat transfer coefficient increases with increase in coating thickness up to a certain value and thereafter decreases. However, increase in heat transfer coefficient is not proportional to increase in coating thickness. Further, the rate of variation of heat transfer coefficient with heat flux depends upon coating thickness. In fact, it decreases with increase in thickness of coating. This continues and therefore, a thick coated heating tube surface may provide heat transfer coefficient lower than that of an uncoated heating tube surface depending up on the value of heat flux and pressure. The increase in magnitude of heat transfer coefficient has differed due to difference in physico-thermal properties of other liquid and distilled water.

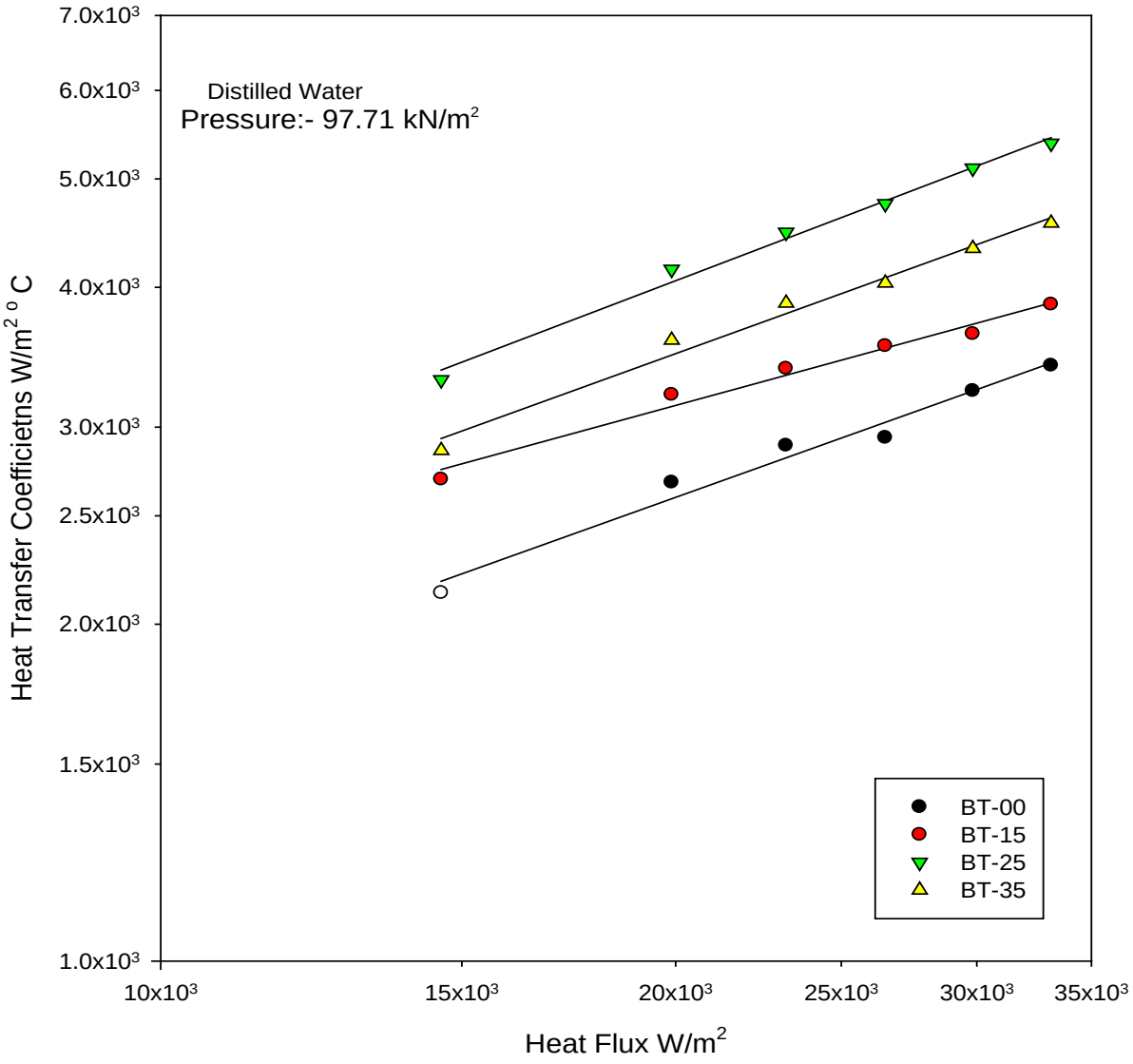

Figure 5.57 Variation of heat transfer coefficient with heat flux for boiling of distilled water on copper coated tubes and uncoated tube at atmospheric pressure

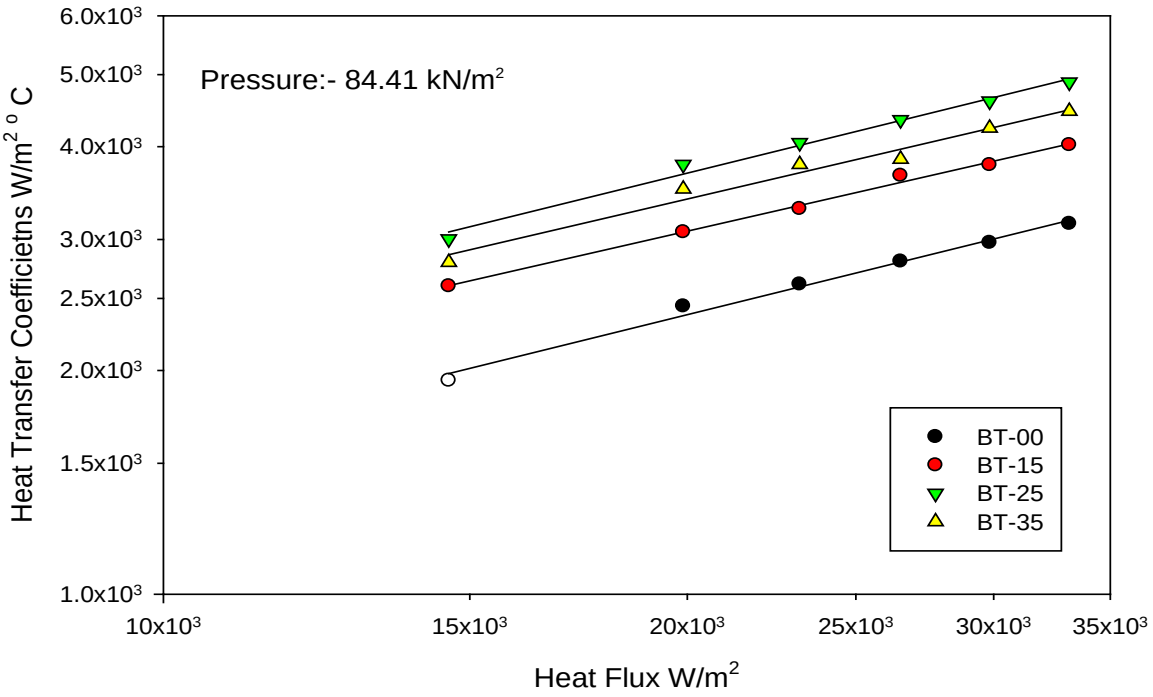

(a)

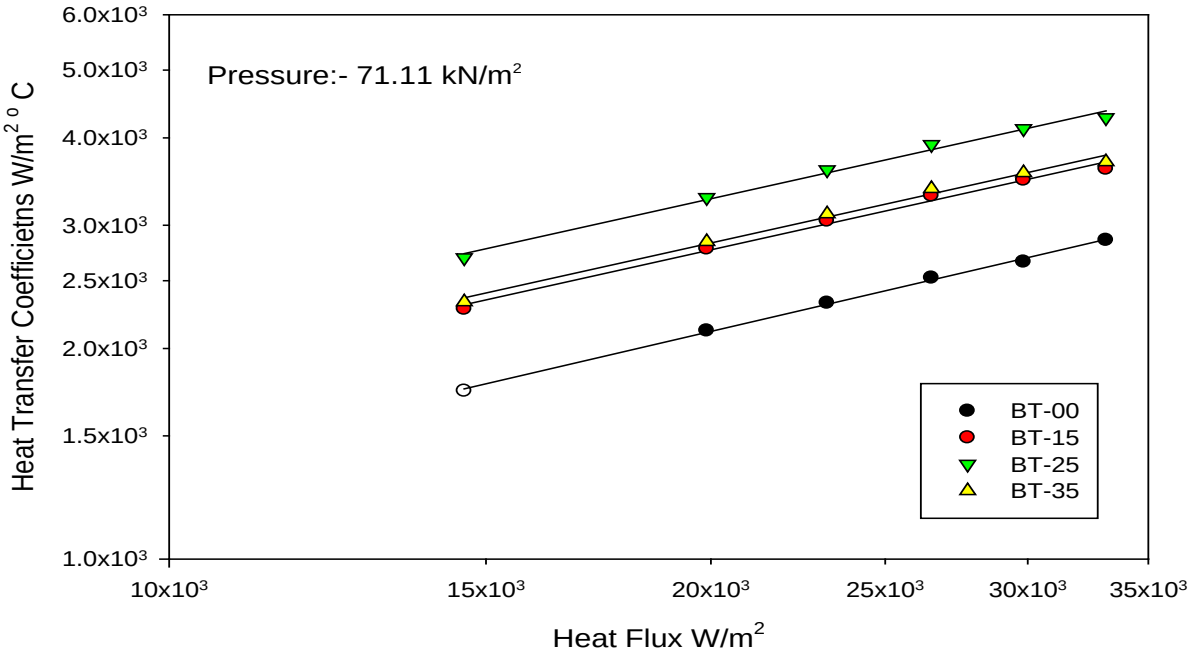

(b)

Figure 5.58 Variation of heat transfer coefficient with heat flux for boiling of distilled water on copper coated tubes and uncoated tube at 84.41kN/m^2 and 71.41kN/m^2.

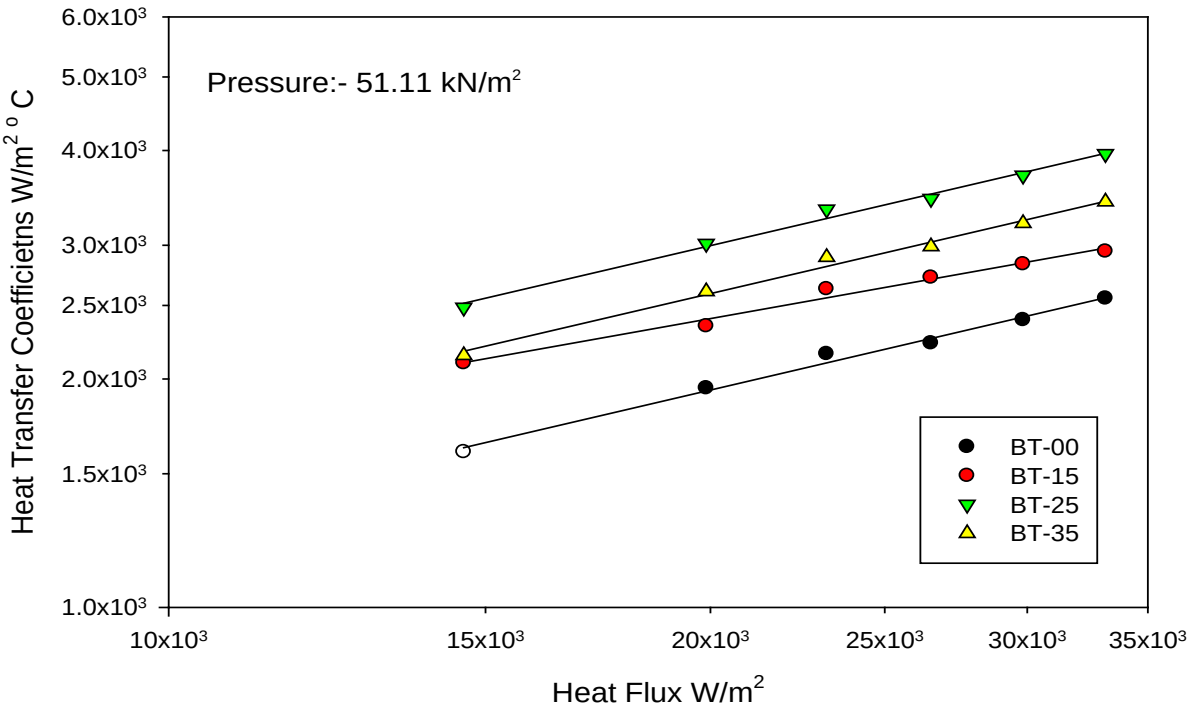

(a)

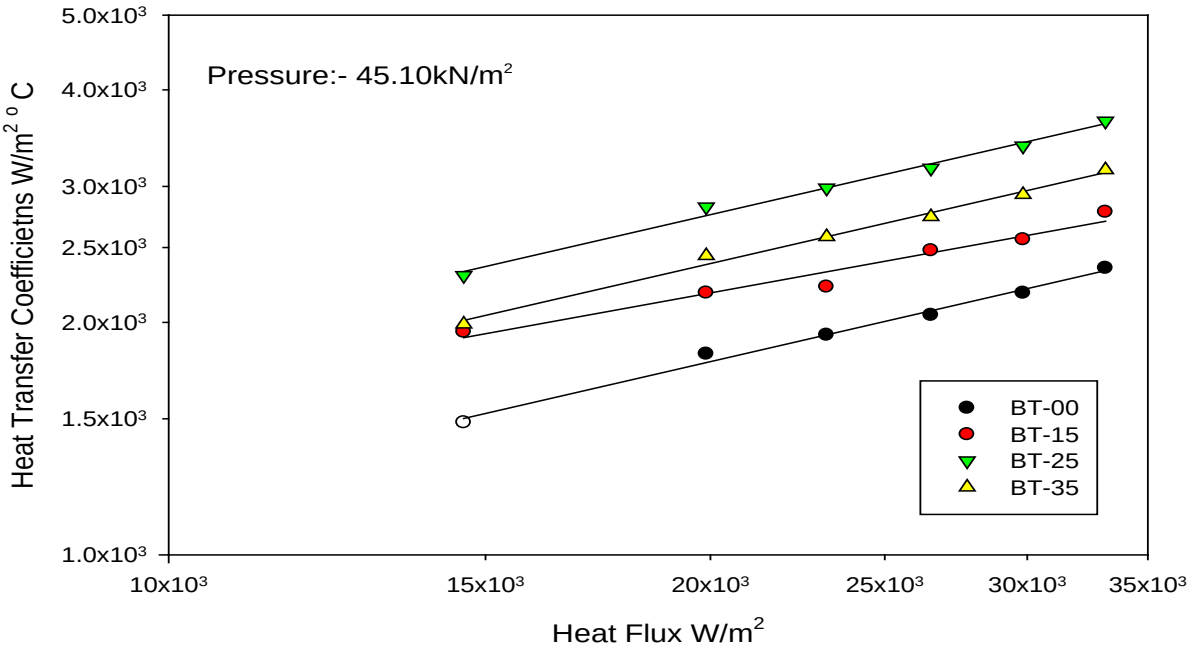

(b)

Figure 5.59 Variation of heat transfer coefficient with heat flux for boiling of distilled water on copper coated tubes and uncoated tube at 51.11kN/m^2 and 45.11kN/m^2.

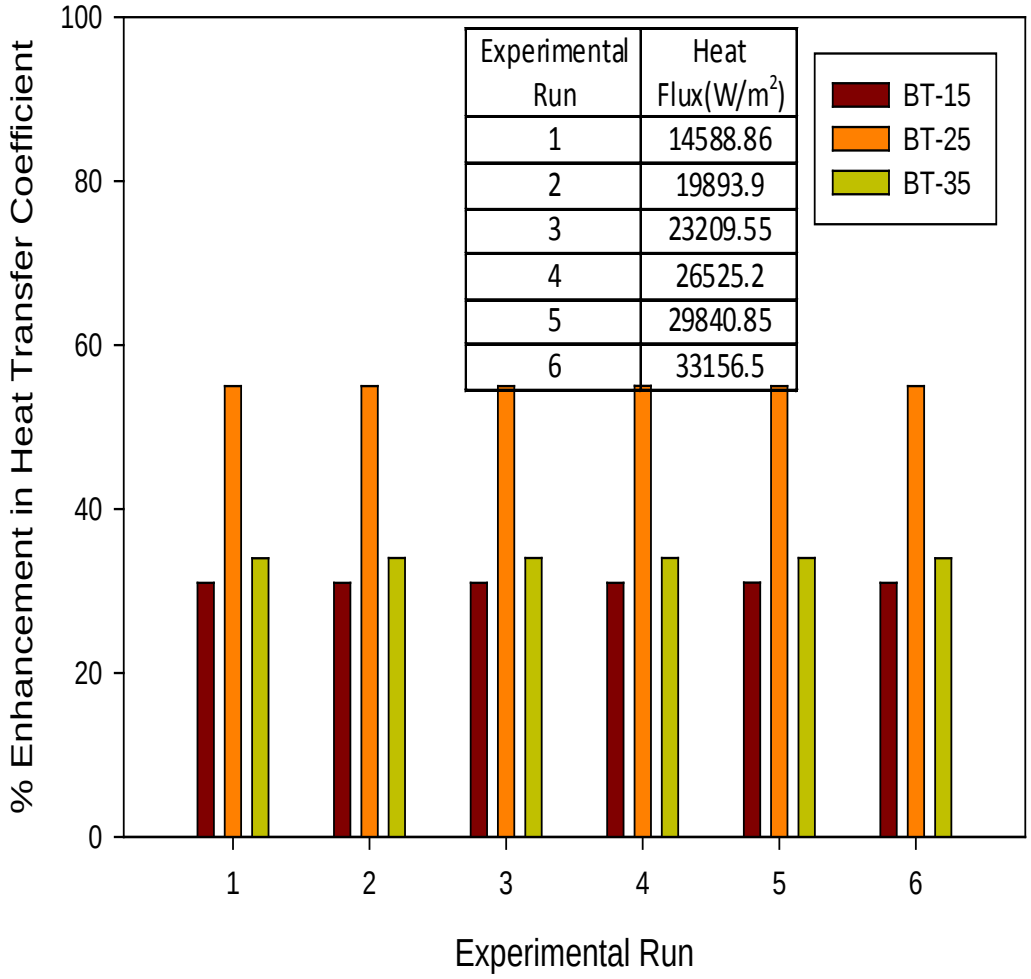

Figure 5.60 Percentage enhancement in heat transfer coefficient for different heat fluxes

5.6 NUCLEATE POOL BOILING OF ISO-PROPANOL AND METHANOL ON A COATED HEATING TUBE

As discussed in preceding section, coating of a copper on a horizontal brass tube increase heat transfer coefficient for the boiling of distilled water at atmospheric and subatmospheric pressure. However, there exists a thickness of coating at which enhancement of heat transfer coefficient is maximum. In the present investigation $25\ \mu m$ copper coated brass heating tube has been found to provide the more heat transfer coefficient than 15 and $35\ \mu m$ coated tubes to the on tune of 55% more than that uncoated tube. Thus, use of a $25\ \mu m$ thick coated tube is advantageous. Keeping this mind, it was considered adequate to investigate the pool boiling of saturated iso-propanol and methanol on a $25\ \mu m$ thick coated heating tube only. This was carried out due to constrain of time. Hence, following discussion pertains to the boiling of methanol, iso-propanol on a $25\ \mu m$ thick copper coated brass tube at atmospheric and subatmospheric pressures.

Experimental data for boiling of saturated methanol or iso-propanol on horizontal brass tube coated with copper of $25\ \mu m$ thickness at atmospheric and subatmospheric pressures are given in Tables B.6 and B7, respectively,of Annexure-B. Following subsections discuss the effect of heat flux and pressure on heat transfer coefficient for nucleate pool boiling of saturated iso-propanol and methanol on a coated heating surface.

5.6.1 Boiling heat transfer characteristics for iso-propanol and methanol on a coated tube

Figure 5.61(a and b) represent plots between heat transfer coefficient and heat flux for the boiling of methanol and iso-propanol on a $25\ \mu m$ thick coated heating tube surface. Pressure is a parameter in this plot. These plots reveal the following salient features:

i. At a given pressure, heat transfer coefficient increases with increase in heat flux and the variation between the two can be described by the relationship, $h \propto q^a$ where the value of exponents (a) are 0.58 and 0.56 for methanol and iso-propanol, respectively.

ii. At a given value of heat flux heat transfer coefficient increases with rise in pressure.

Above features are same as discussed earlier. Hence, same explanation hold true in this case also.

5.6.2 Heat transfer coefficient-heat flux relationship for iso-propanol and methanol on a coated tube

A discussed in the above the heat transfer coefficients of methanol, iso-propanol boiling on a 25 μm thick coated heating tube, is a function of heat flux and pressure. hence, experimentally determined values of heat transfer coefficient for boiling of methanol and iso-propanol on a 25 μm thick coated surface have been re-processed by regression analysis to obtain a correlation, which is as follows:

$$h = C_4 q^v p^w \tag{5.19}$$

Where, constant C_5 and exponent v and w depend upon type of liquid. The values of constant C_4 and exponents (v) and (w) for the boiling of methanol and iso-propanol on a 25 μm thick coated tube as listed in **Table. 5.5.**

Table 5.5 The values of constant C_4 and exponents v and w for boiling of methanol and iso-propanol

S.No.	Boiling liquid	C_4	v	w
1	Methanol	1.23	0.58	0.73
2	Iso-Propanol	1.33	0.56	0.76

Figure 5.62 show a plot between experimentally-determined values of heat transfer coefficient and these predicted from **Eq. (5.19)** for the boiling of methanol and iso-propanol on a 25 μm thick coated heating tube at atmospheric and subatmospheric pressure. The plot clearly indicates that the predicted values have matched excellently with the experimental values within a maximum error of $\pm 3.5\%$. Thus **Eq. (5.19)** has succeeded to correlate experimental data of boiling heat transfer of saturated methanol and iso-propanol on a 25 μm thick coated heating tube surface.

5.6.3 Comparison of boiling heat transfer characteristics on a coated and uncoated tube surface for a methanol and iso-propanol

This section has been devoted to show a comparative study of boiling heat transfer characteristics of methanol and iso-propanol on a 25 μm thick coated tube surface at

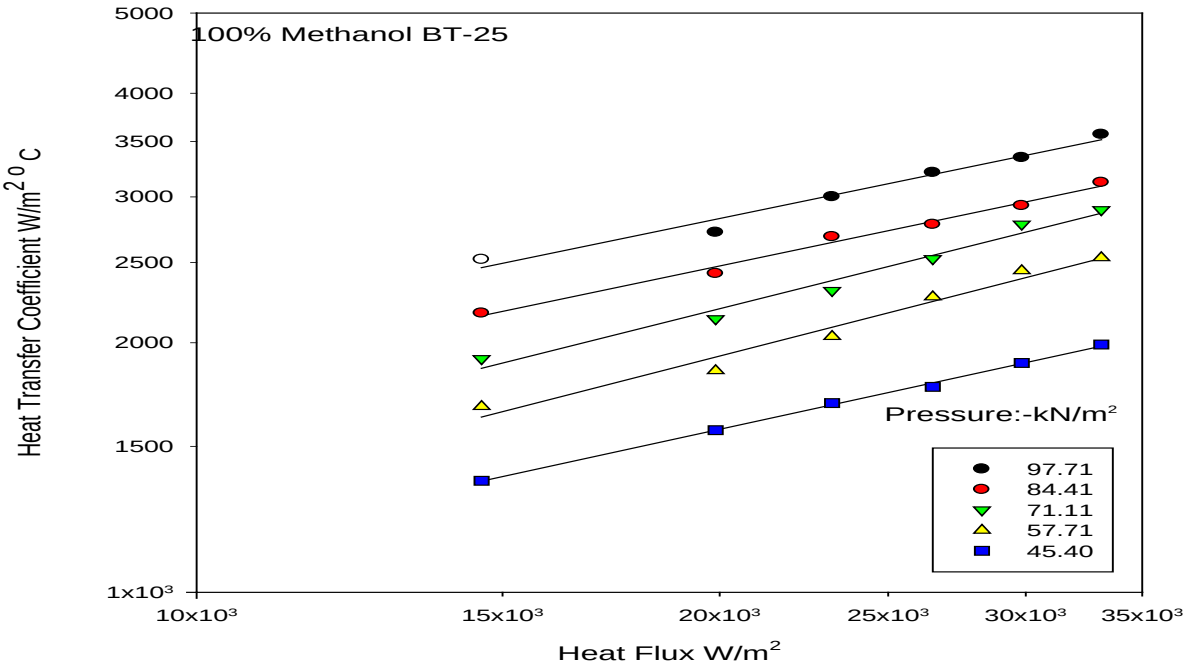

(a)

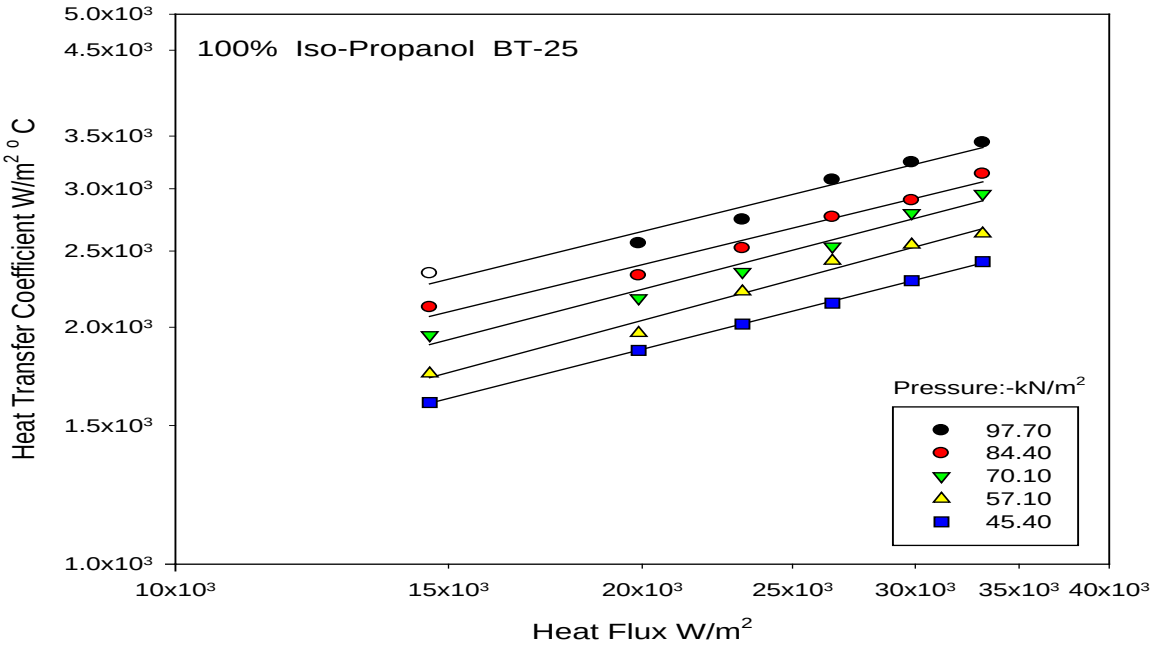

(b)

Figure 5.61 Variation of heat transfer coefficient with heat flux for boiling of methanol on a 25µm thick copper coated heating tube surface with pressure as a parameter

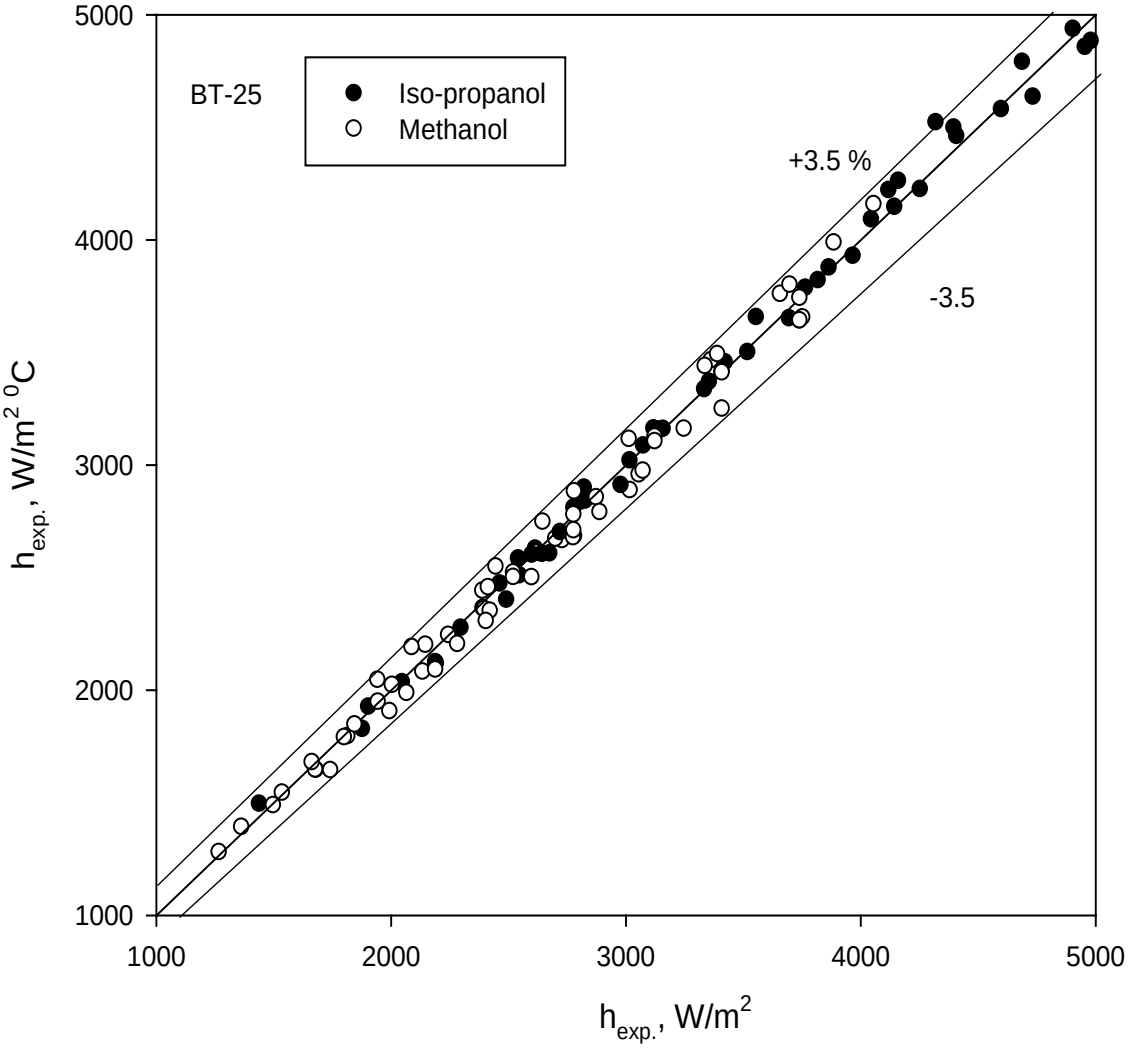

Figure 5.62 Comparison of experimental heat transfer coefficient with those predicted from **Eq. (5.19)** for boiling of Iso-propanol and methanol on 25 μm (BT-25) coated heating tube surfaces at atmospheric and subatmospheric pressures.

atmospheric and subatmospheric pressure with an objective to obtain the effect of coating on boiling heat transfer coefficients.

Figure 5.63(a, b) depict plots between heat transfer coefficient and heat flux for saturated boiling of methanol and iso-propanol on a tube coated with 25 μm thickness of copper at atmospheric and subatmospheric pressures, respectively. These plots also contain the curve for an uncoated tube surface for the sake of comparison. These plots reveals that heat transfer coefficients of methanol and iso-propanol on 25 μm thick coated tube are higher than that on an uncoated tube for a given value of heat flux.

Above features are similar as obtain for boiling of distilled water on a coated tube as discussed earlier. Hence, same explanation hold true in these cases also for coated tube.

Similar analysis for the comparison of heat transfer coefficient for saturated boiling of methanol and iso-propanol on a 25 μm thick coated tube with uncoated tube has been carried out for subatmospheric pressure. The analysis corroborate that heat transfer coefficient for the boiling of methanol and iso-propanol on coated tube is higher than that on uncoated tube for all the value of heat flux at all subatmospheric pressure.

On the basis of above, it may concluded that coating of copper on brass tube increases the heat transfer coefficient for boiling of saturated liquid distilled water, methanol and iso-propanol at atmospheric and subatmospheric pressure. However, enhancement on 25 μm thick coated tube has been found to be more than 15 and 35 μm thick coated tube for boiling of distilled water.

Figure 5.64 and 5.65 depict the percentage enhancement in heat transfer coefficient on 25 μm thick copper coated brass heating tube for the boiling of methanol and iso-propanol, respectively. These plots reveal that the percentage enhancement in both the cases for the boiling of methanol and iso-propanol is more than 50% for all pressure and heat flux.

5.7 NUCLEATE POOL BOILING OF BINARY MIXTURE ON A COATED TUBE

As discussed earlier 25 μm thick coated brass heating tube was also selected to investigate heat transfer characteristics for boiling of various composition of methanol-distilled water and iso-propanol- distilled water binary mixture at atmospheric and

subatmospheric pressure. Experimental data for boiling of 10, 30, 50, 70, 80, 90 mole percent of more volatile component in both the mixture on 25 μm thick coated brass heating tube are

listed in tables B.27 to B.32 and B.33 to B.38, respectively of Annexure B. Following sub section have been devoted to study the effect of heat flux, pressure and composition on heat transfer coefficient for boiling of these mixtures on a coated heating tube.

5.7.1 Boiling heat transfer characteristics for binary mixtures on a coated heating tube

Fig. 5.66(a), Fig. 5.66(b) depicts plots between heat transfer coefficient and heat flux for saturated boiling 10% methanol- distilled water and 10% iso-propanol- distilled water mixture on 25 μm thick copper coated heating tube surface, respectively. Pressure is a parameter in these plots. A close examination of these plots reveals the following salient features:

i. For a given pressure, heat transfer coefficient increase with heat flux and the variation between the two can be describe by functional relationship, $\boldsymbol{h \propto q^b}$, where exponent (b) is equal to 0.57 and 0.56 for 10%methanol-distilled and iso-propanol-distilled, respectively.
ii. At a given value of heat flux, heat transfer coefficient increases with increase in pressure.

Boiling of other composition of methanol- distilled water, iso-propanol-distilled water mixture on a 25 μm thick coated tube also resulted similar plots as shown in **Figs. 5.67, Fig. 5.70.** All the plots show similar features as mentioned above.

Thus, it may be concluded that boiling heat transfer characteristics of these binary mixtures on 25 μm thick coated brass heating tube surface are likely with those of their pure liquids. This is quiet synonymous with the behavior on uncoated tube surfaces.

5.7.2 Heat transfer coefficient-heat flux relationship for a binary mixture on a coated heating tube

As discussed above the heat transfer coefficient of methanol-distilled water and iso-propanol–distilled water binary mixtures boiling on 25 μm thick coated heating tube, is function of heat flux, pressure. Hence, experimentally determine values of heat transfer coefficients for boiling of these binary mixtures on a 25 μm thick coated surface have been

reprocessed by regression analysis to obtain a correlation, which is as follows: Where C_5 is a constant whose value depends upon the percentage composition of the mixture, and surface characteristic. The values of constants, as determined for various compositions of methanol-distilled water and iso-propanol-distilled water mixtures are given in **Table 5.6.**

Table 5.6 Value of constants C_5 of **Eq. (5.20)** for various compositions of methanol-distilled water and iso-propanol- distilled water mixtures

Iso-Propanol- Distilled Water		Methanol-Distilled Water	
Iso-Propanol Composition	$\mathbf{C_5}$	Methanol Composition	$\mathbf{C_5}$
10 Mol%	1.517	10 Mol%	1.471
30 Mol%	1.567	30 Mol%	1.421
50 Mol%	1.370	50 Mol%	1.351
70 Mol%	1.317	70 Mol%	1.385
80 Mol%	1.423	80 Mol%	1.401
90 Mol%	1.421	90 Mol%	1.429

Eq. (5.20) is simple and convenient equation for the prediction for heat transfer coefficient boiling of methanol-distilled water and iso-propanol-distilled water mixtures on a 25 μm thick copper coated brass heating surface from the knowledge heat flux and pressure provide C_5 constant is known.

Figure 5.71, and 5.72 presents plots between experimentally determined values of heat transfer coefficient and those calculated by **Eq. (5.20)** for the boiling of various concentrations on a 25 μm thick copper coated heating tube surface at atmospheric and subatmospheric pressure. These two plots reveals that, the prediction match the experimental values within an error of $\pm 7.5\%$ and $\pm 8.0\%$ only in the case of iso-propanol-distilled water and methanol-distilled water mixtures, respectively. Thus, it concluded that **Eq. (5.20)** can be used to determine heat transfer coefficient for the boiling of iso-propanol-distilled-water and methanol-distilled water mixtures on a 25 μm copper coated brass heating tube from the knowledge of heat flux and pressure provided the values of constant

$$h = C_5 q^{0.57} p^{0.36} \qquad (5.17)$$

5.7.4 Variation of heat transfer coefficient of binary mixture with composition for boiling on coated tube

Figure 5.81(b) represents a typical plot between heat transfer coefficient for the boiling of various composition of iso-propanol-distilled water mixture on 25 μm thick copper coated tube at atmospheric pressure to show the effect of concentration on heat transfer coefficient. Heat flux is a parameter in this graph. This plot reveals the following features:

i. Heat transfer coefficient decreases with increase in iso-propanol concentration irrespective of heat flux. This trend continue till 30 % of iso-propanol mole fraction thereafter, any further increase in concentration increase the value of heat transfer coefficient.
ii. For a given concentration heat transfer increases with increase in heat flux.

Figs. 5.82(b) and 5.83(b) represents variation of heat transfer coefficient on 25 μm thick coated tube for the boiling of various compositions of iso-propanol-distilled water mixture at subatmospheric pressures. Heat flux is a parameter in these plots. These plots also have the same features as discussed above except turn around concentration is 30 mole percent.

Further, **Figs. 5.84(b) to 5.86(b)** shows the variation of heat transfer coefficient on 25 μm thick coated tube for boiling for various composition of methanol-distilled water mixture at atmospheric and subatmospheric pressures. In these plots heat flux is a parameter. These plots also have the essential same feature as discussed above.

To explain the behavior of above plots, phase equilibrium diagram of iso-propanol-distilled water binary mixture. Fig 5.81(a) is consider it may be seen pin pointed here that experimental value |y-x| as obtained from the analysis of liquid and vapor samples during the boiling of various composition binary mixtures on coated surfaces have been found to be almost same at those obtained in case boiling on an uncoated tube. This is quite obvious, thus it is validate the correlations of experimental data taken on a coated tube. The variation of heat transfer coefficient with mole% iso-propanol and also the existence of the turnaround point for the boiling of binary mixture on an uncoated tube surface hold true in this case also found to be same 30 mole% methanol distilled water where slightly higher as 35% moles in the case iso-propanol which is differ in case of uncoated surface. Similar

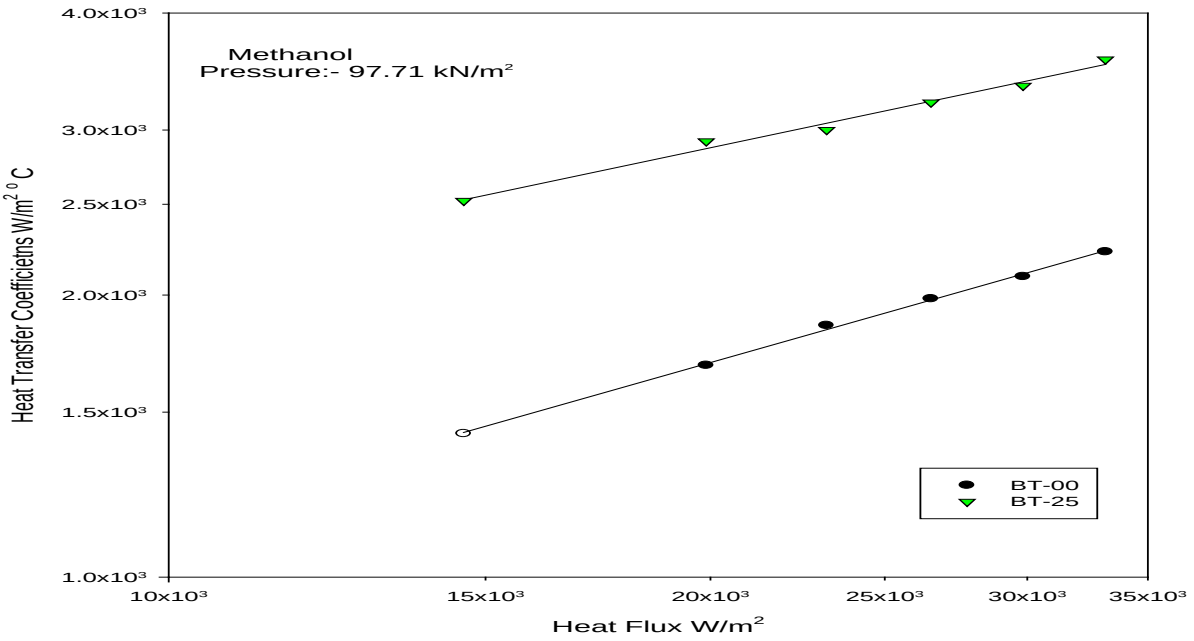

(a)

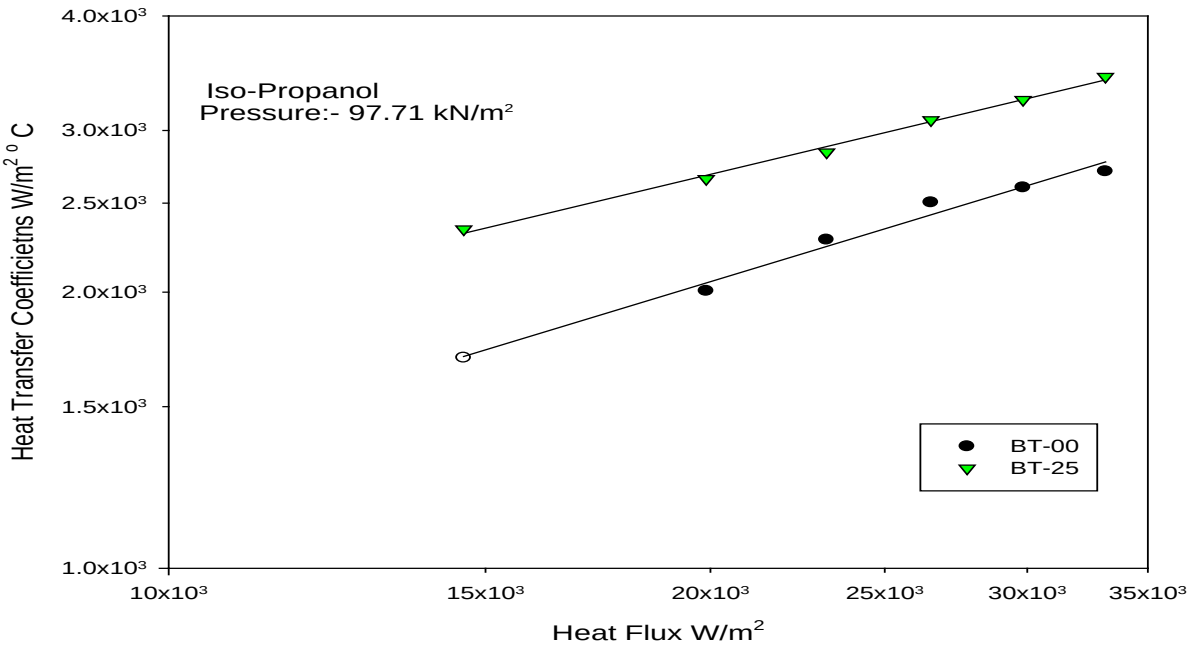

(b)

Figure 5.63 (a,b) Variation of heat transfer coefficient with heat flux for boiling for methanol and iso-propanol on a 25 μm thick copper coated tube and on an uncoated tube at atmospheric pressure

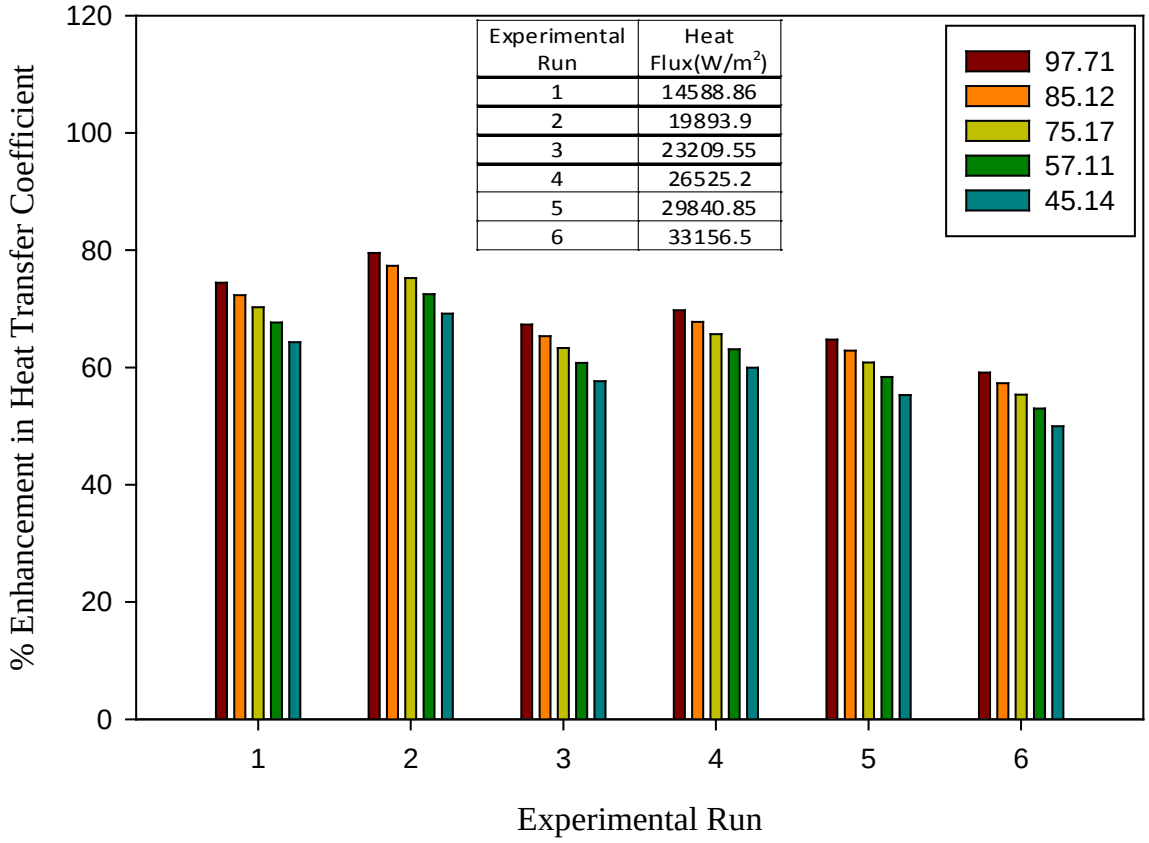

Figure 5.64 Percentage enhancement in heat transfer coefficient with heat flux for methanol on copper coated (BT-25)

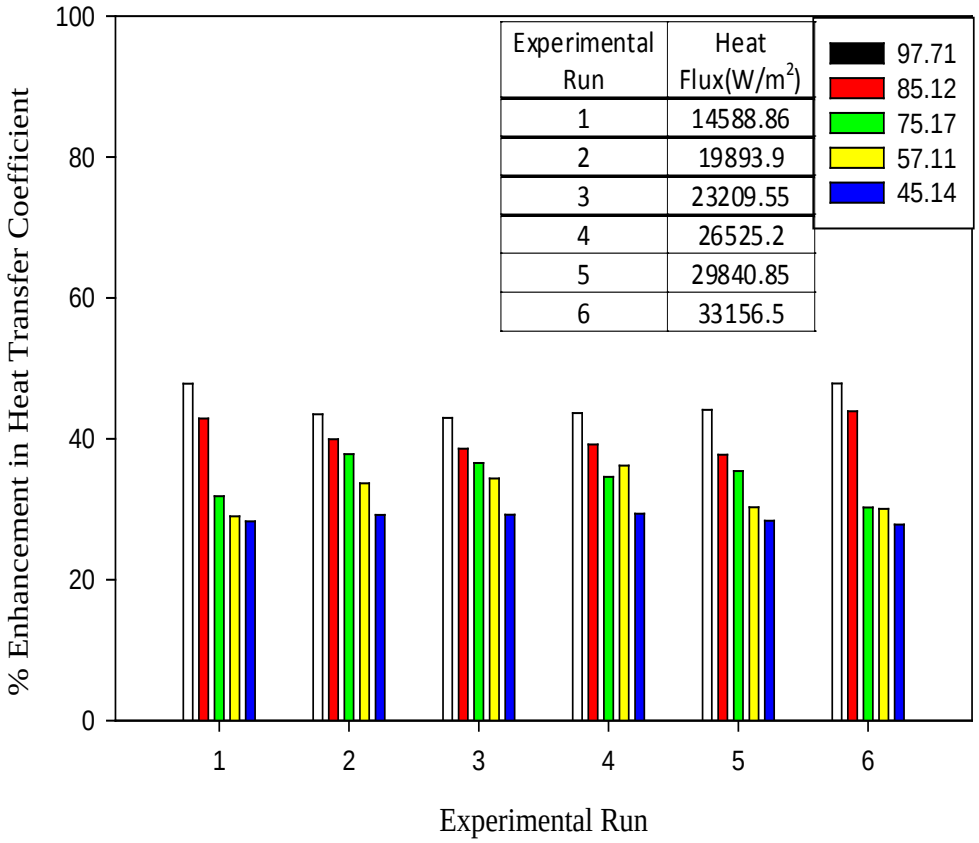

Figure 5.65 Percentage enhancement of heat transfer coefficient with heat flux for boiling of iso-propanol on BT-25

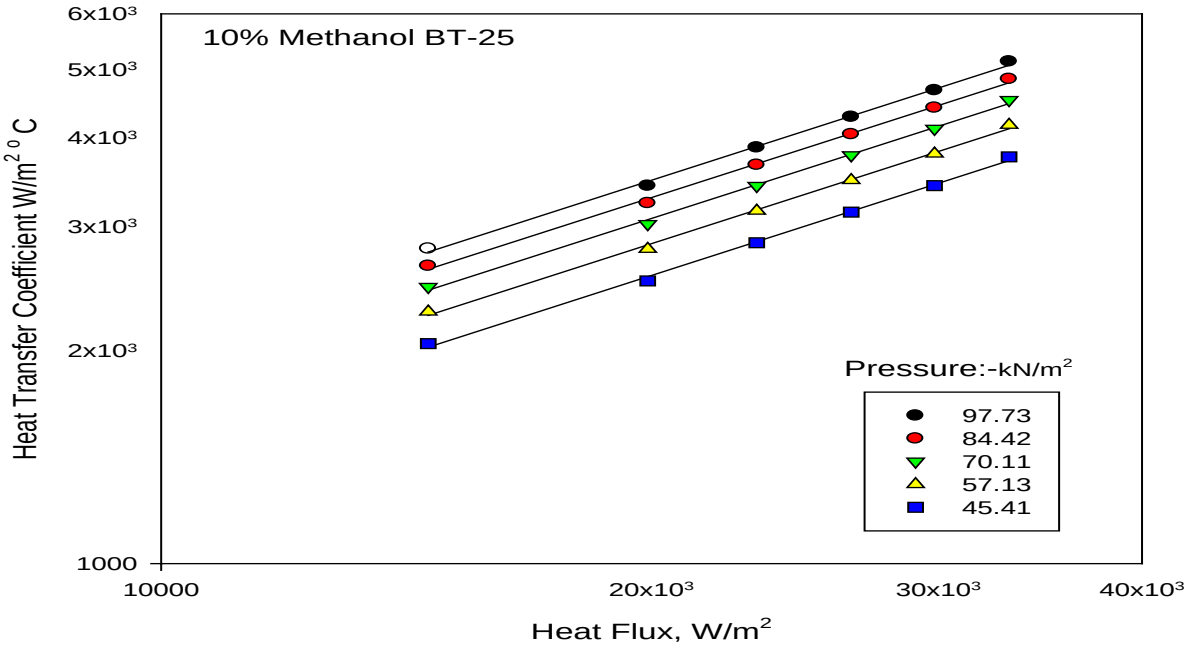

(a)

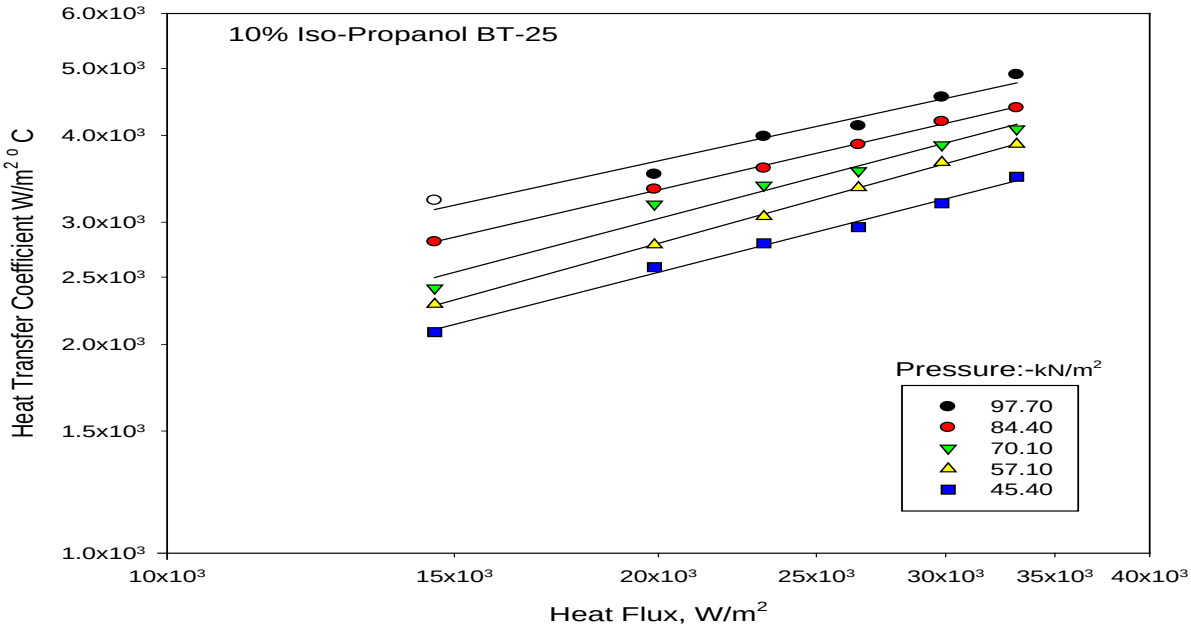

(b)

Figure 5.66 Variation of heat transfer coefficient with heat flux for boiling of 10% methanol-DW and 10% iso-propanol-DW mixture on a 25μm thick coated heating tube surface with pressure as parameter

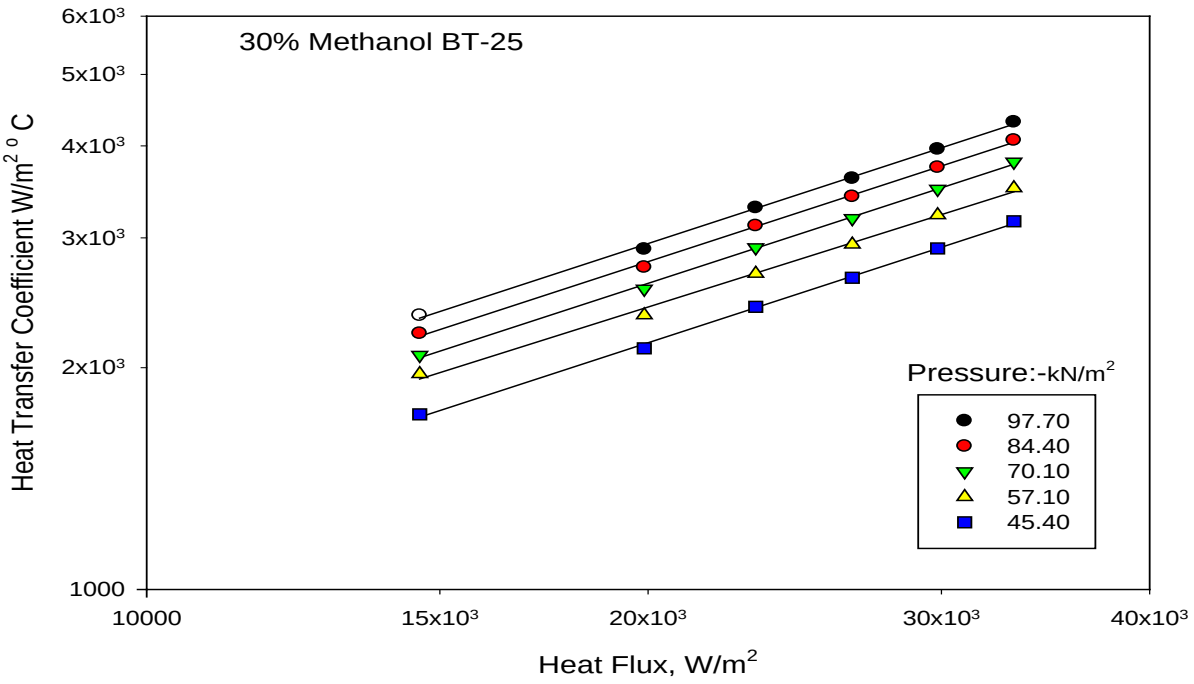

(a)

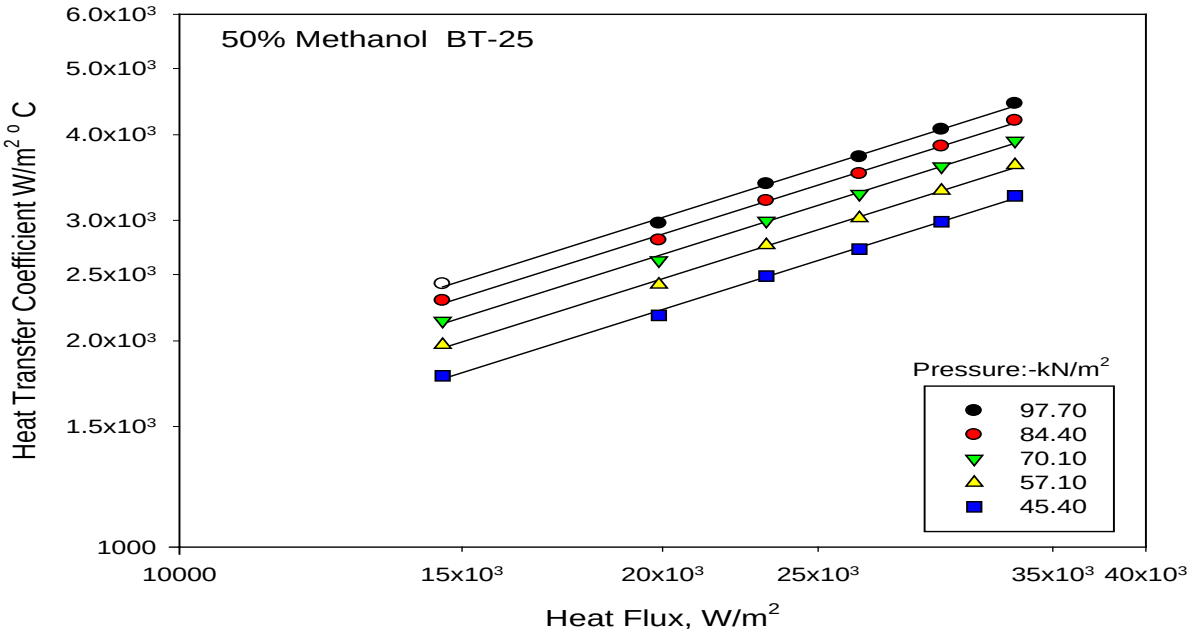

(b)

Figure 5.67 Variation of heat transfer coefficient with heat flux for boiling of 30% and 50%methanol-DW mixture on a 25μm thick coated heating tube surface with pressure as parameter

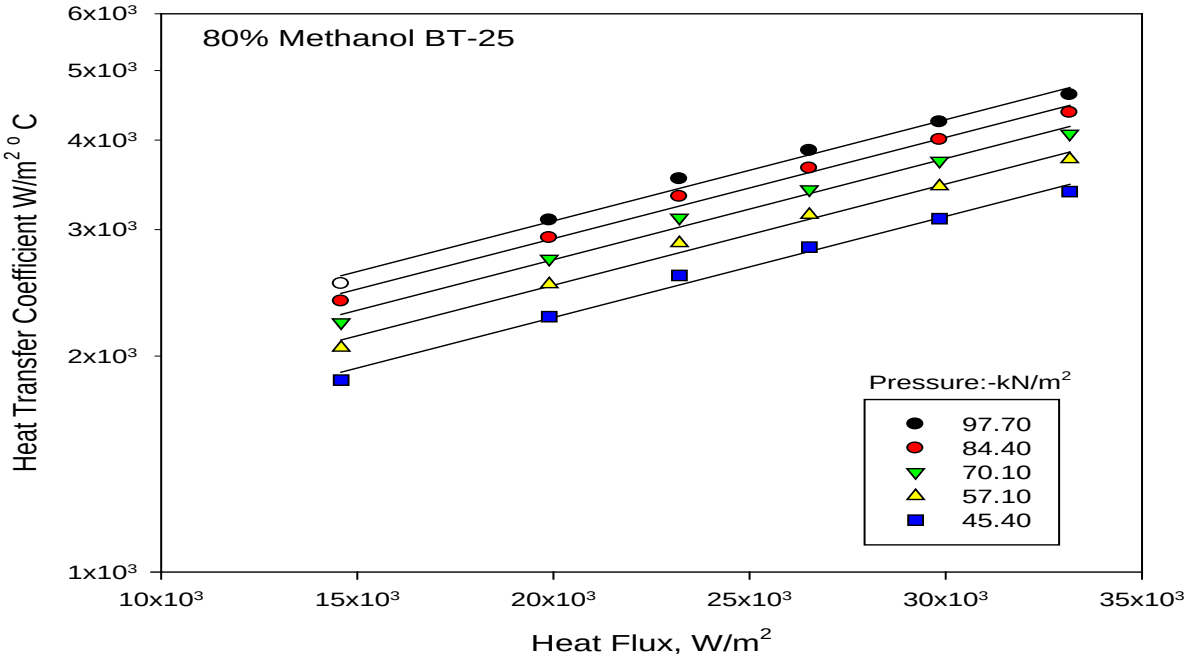

(a)

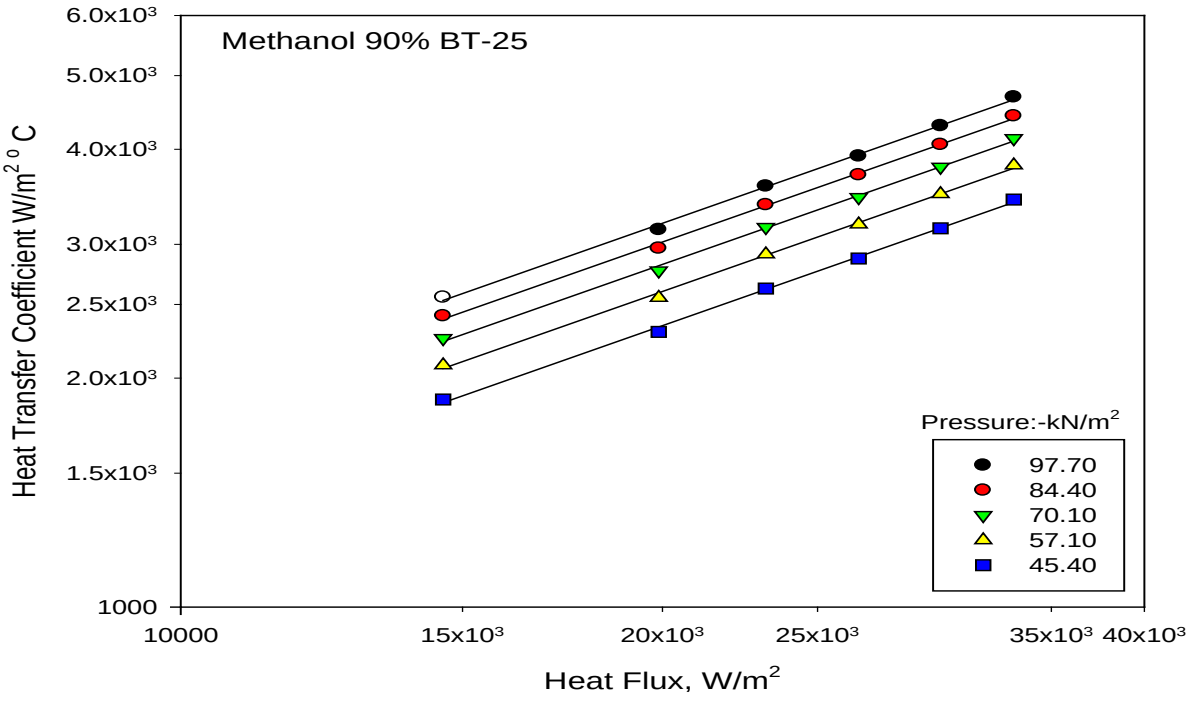

(b)

Figure 5.68 Variation of heat transfer coefficient with heat flux for boiling of 80% and 90%methanol-DW mixture on a 25µm thick coated heating tube surface with pressure as parameter

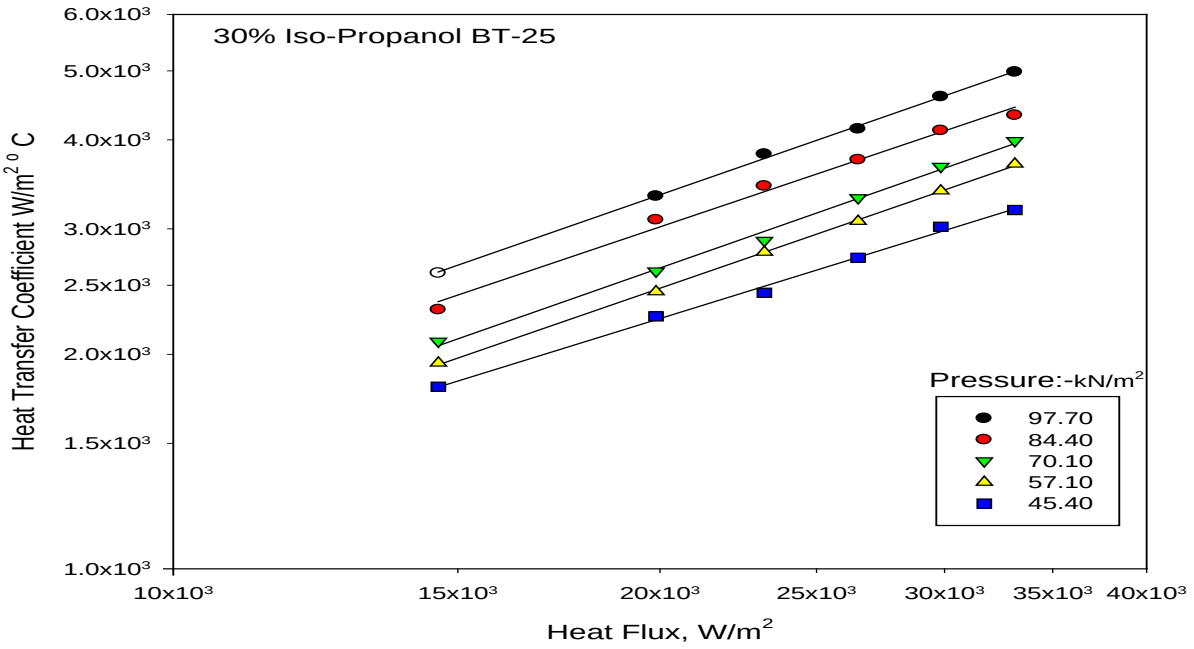

(a)

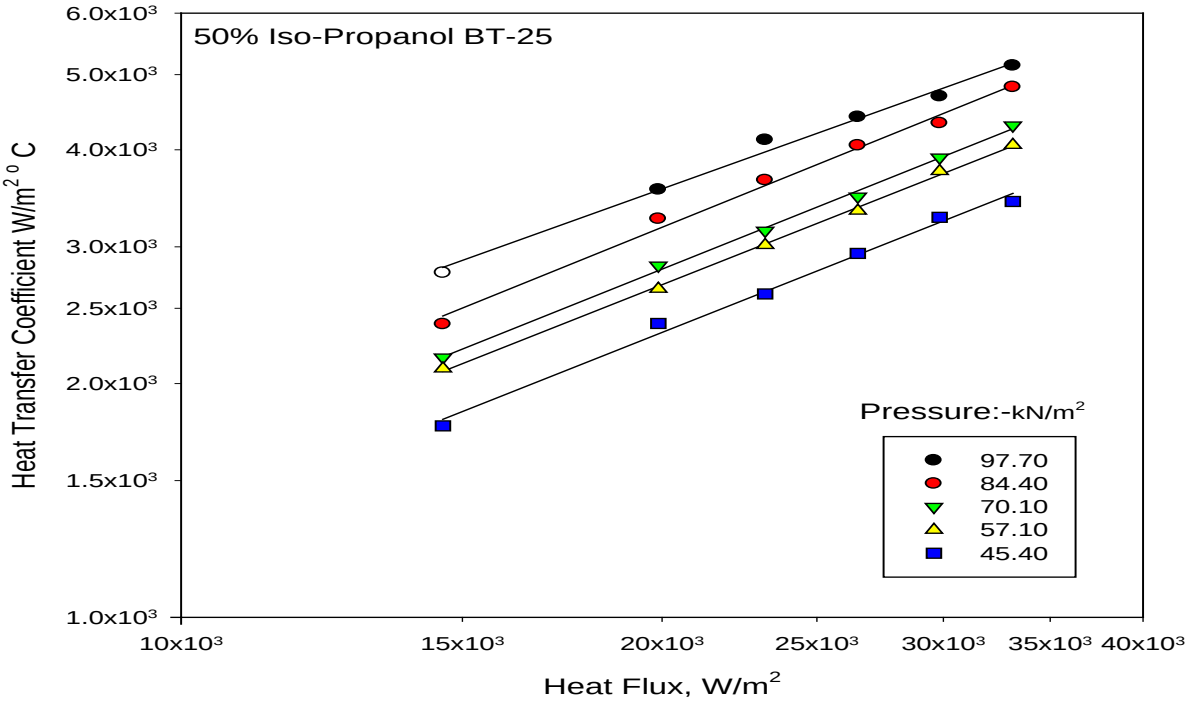

(b)

Figure 5.69 Variation of heat transfer coefficient with heat flux for boiling of 30% and 50% iso-propanol-DW mixture on a 25μm thick coated heating tube surface with pressure as parameter

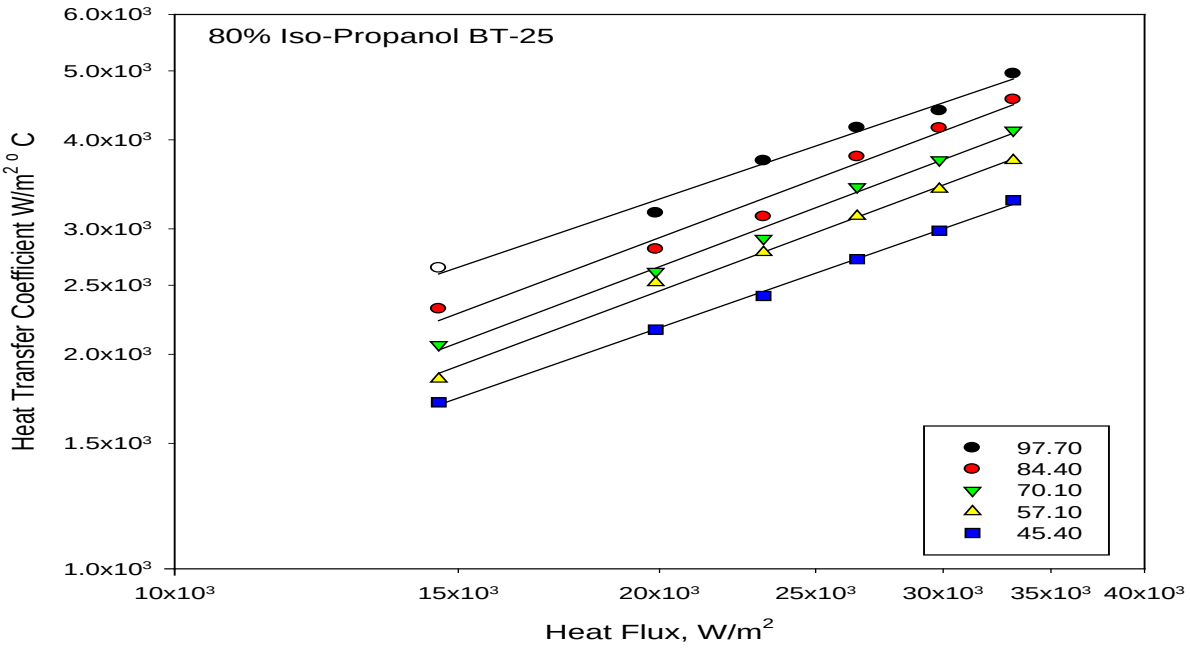

(a)

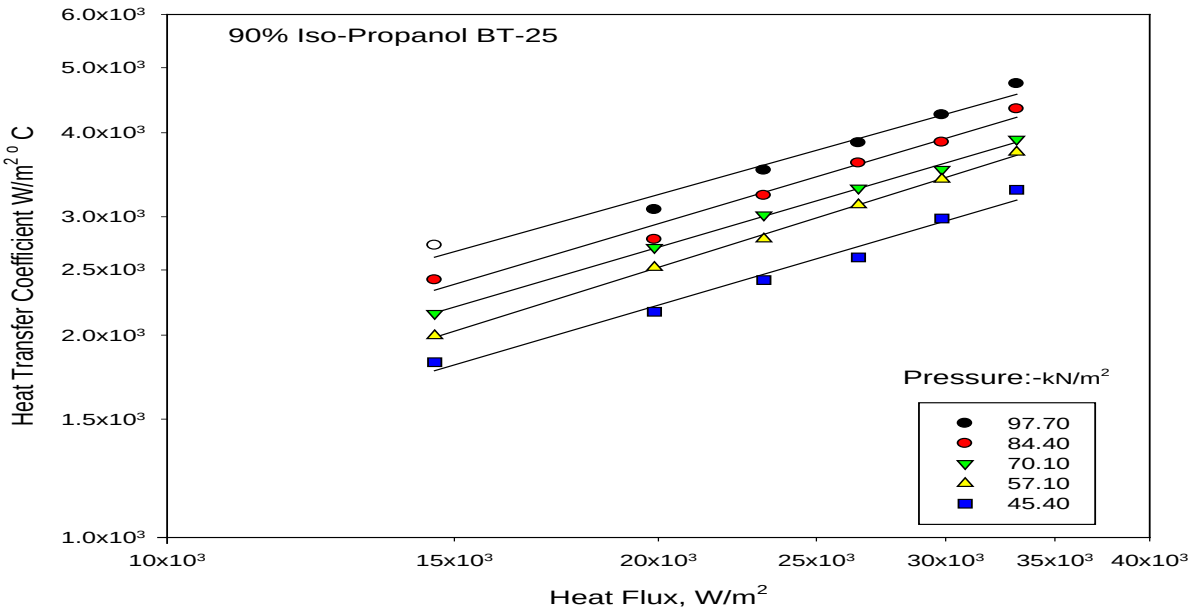

(b)

Figure 5.70 Variation of heat transfer coefficient with heat flux for boiling of 30% and 50% iso-propanol-DW mixture on a 25µm thick coated heating tube surface with pressure as parameter

C_5 are known.

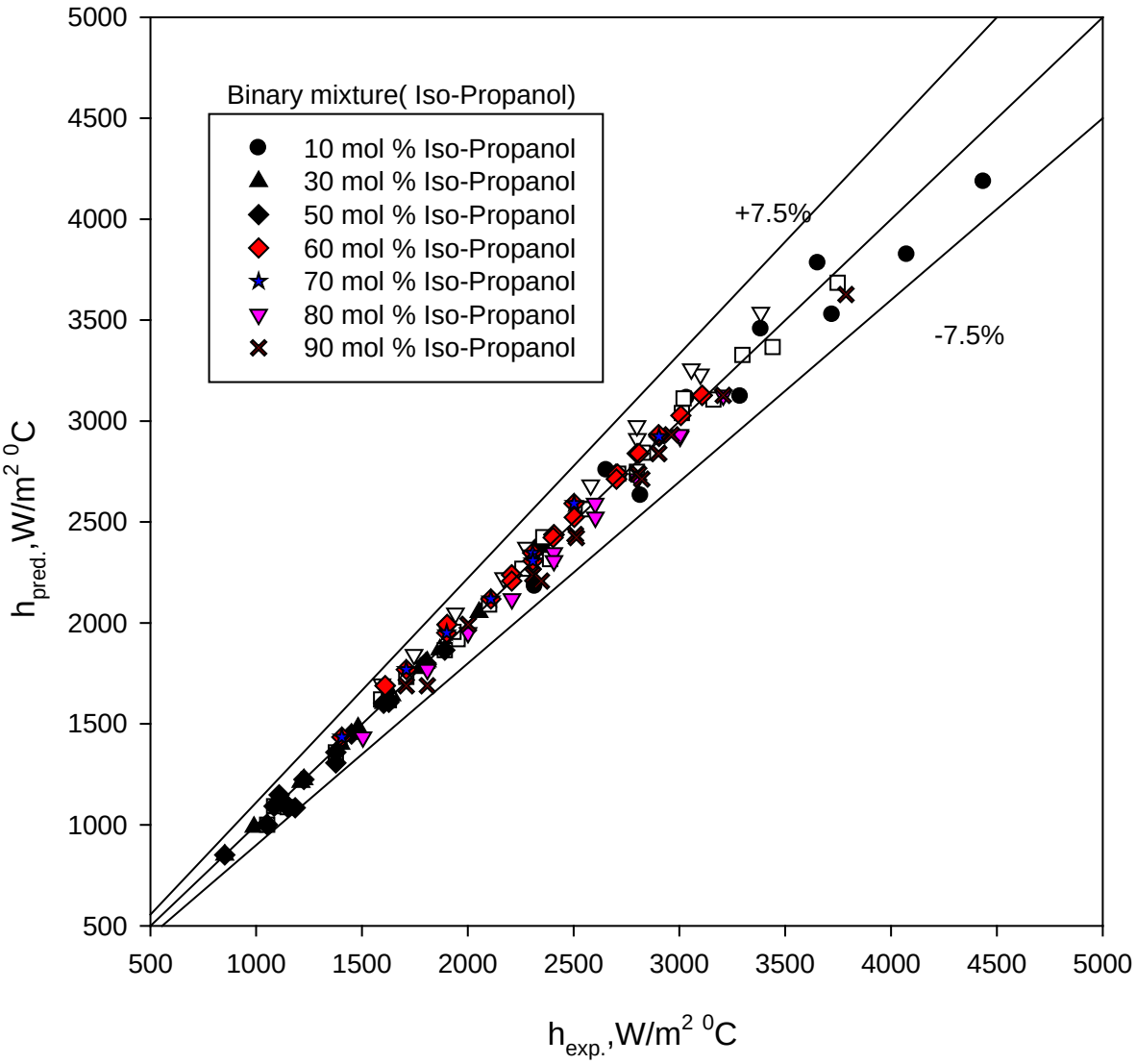

Figure 5.71 Comparison of experimental heat transfer coefficient with those predicted for **Eq.(5.20)** for boiling of iso-propanol-distilled water mixtures on a 25μm coated heating tube surface at atmospheric and subatmospheric pressures

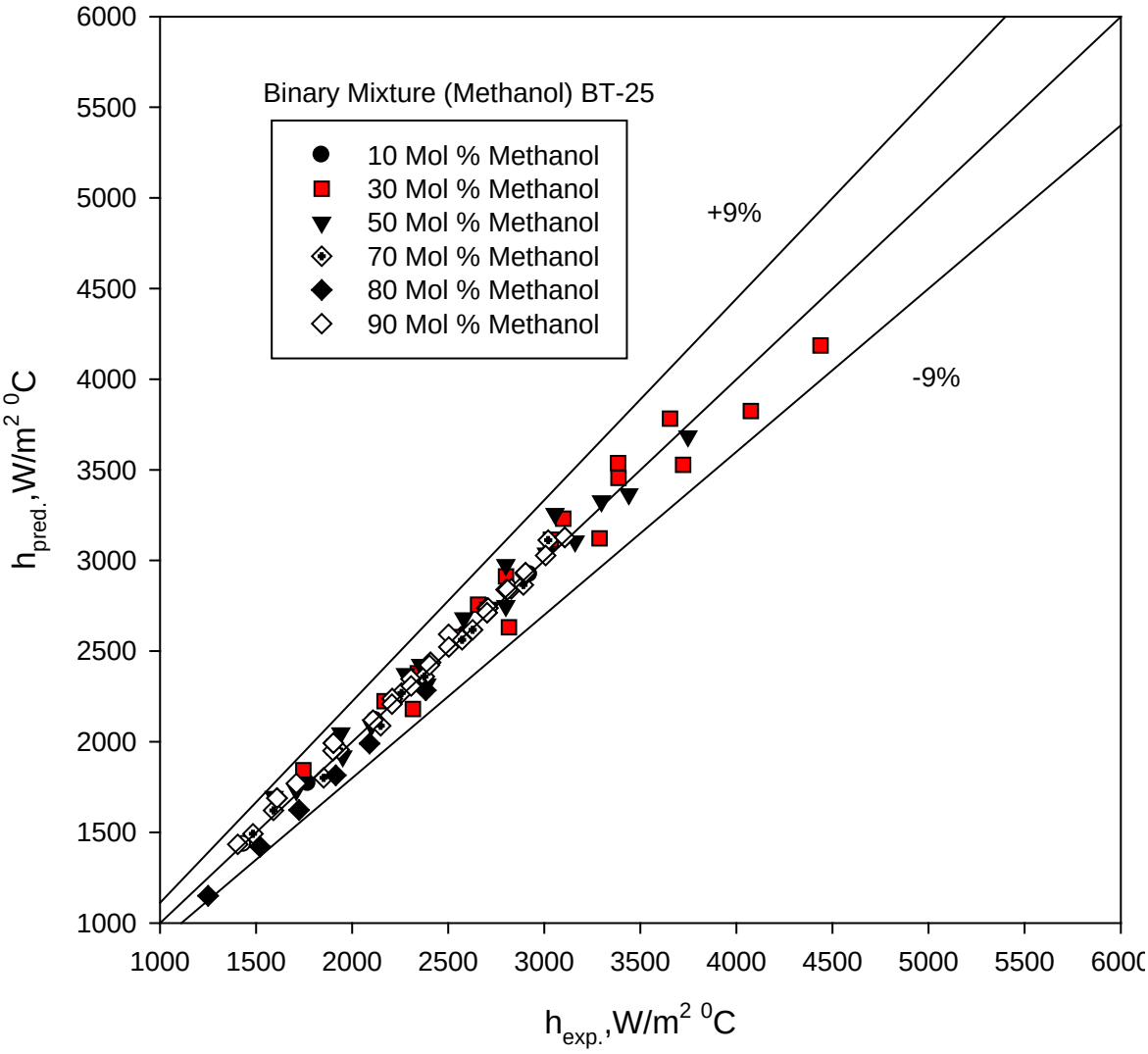

Figure 5.72 Comparison of experimental heat transfer coefficient with those predicted for **Eq.(5.20)** for boiling of iso-propanol-distilled water mixtures on a 25μm coated heating tube surface at atmospheric and subatmospheric pressures

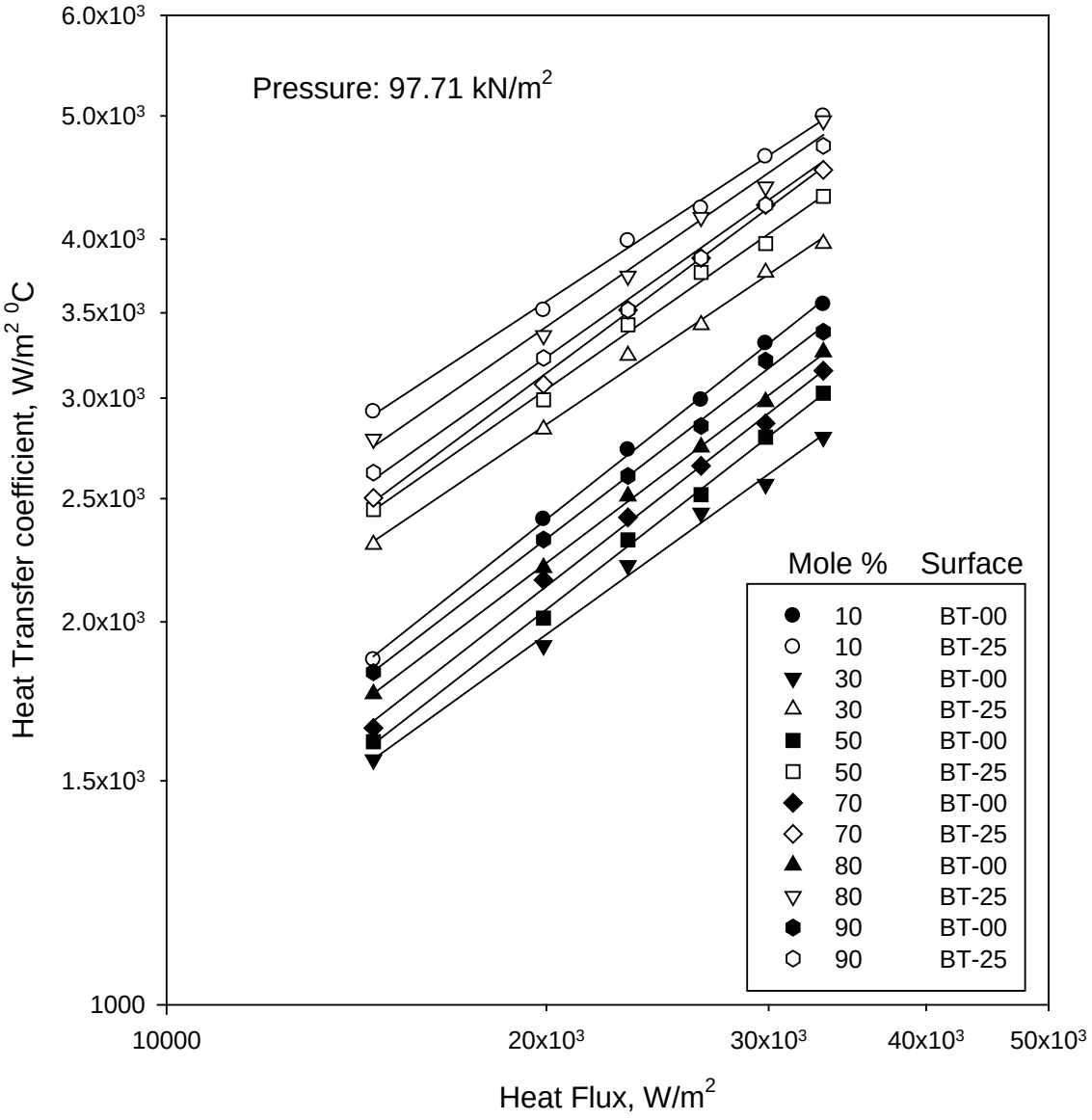

Fig. 5.73 Variation of heat transfer coefficient with heat flux for boiling of various iso-propanol-distilled water mixtures on a 25 μm thick copper coated tube and on an uncoated tube at atmospheric pressure

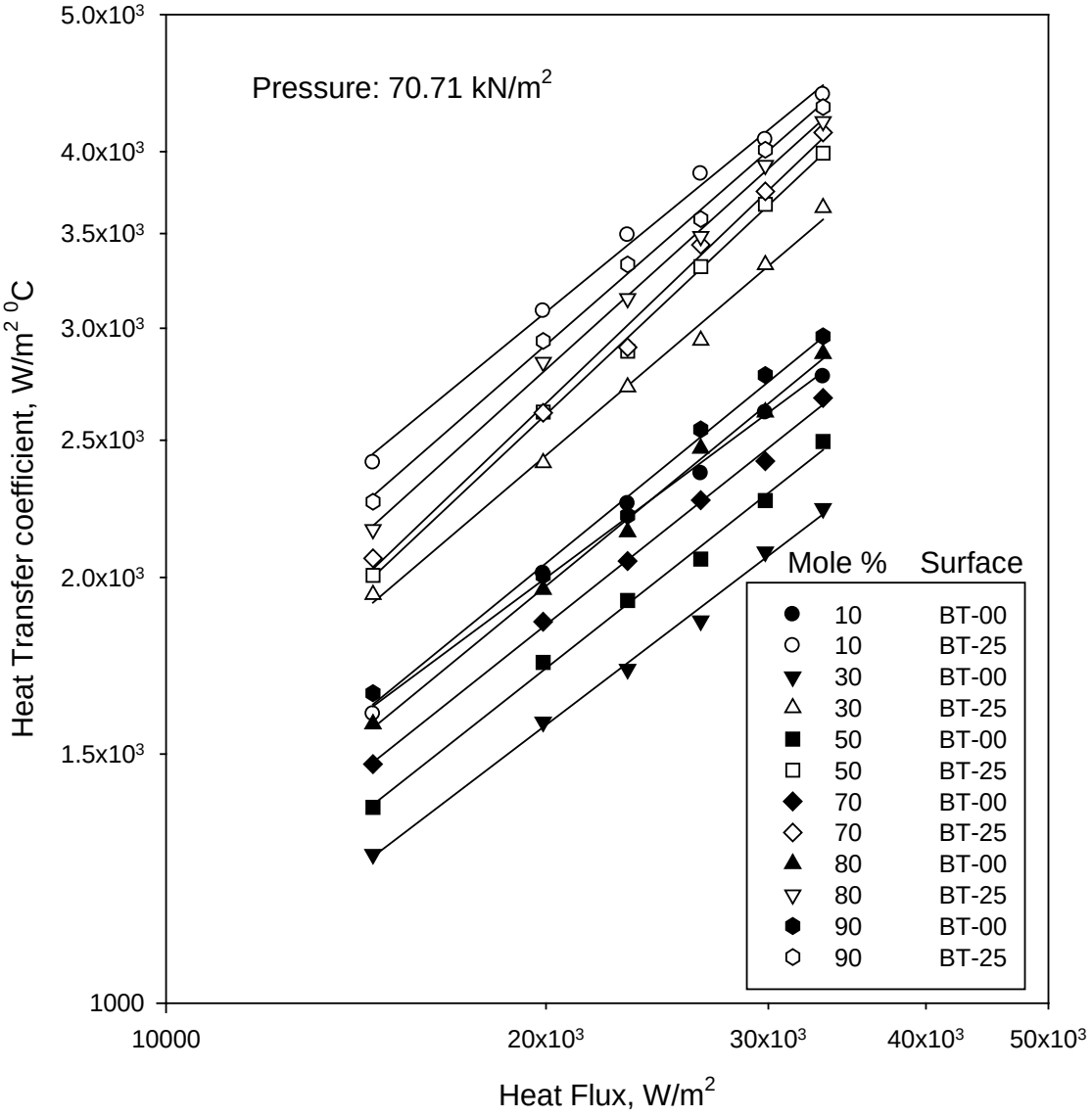

Fig. 5.74 Variation of heat transfer coefficient with heat flux for boiling of various iso-propanol-distilled water mixtures on a 25 μm thick copper coated tube and on an uncoated tube at 70.71 kN/m^2 pressure

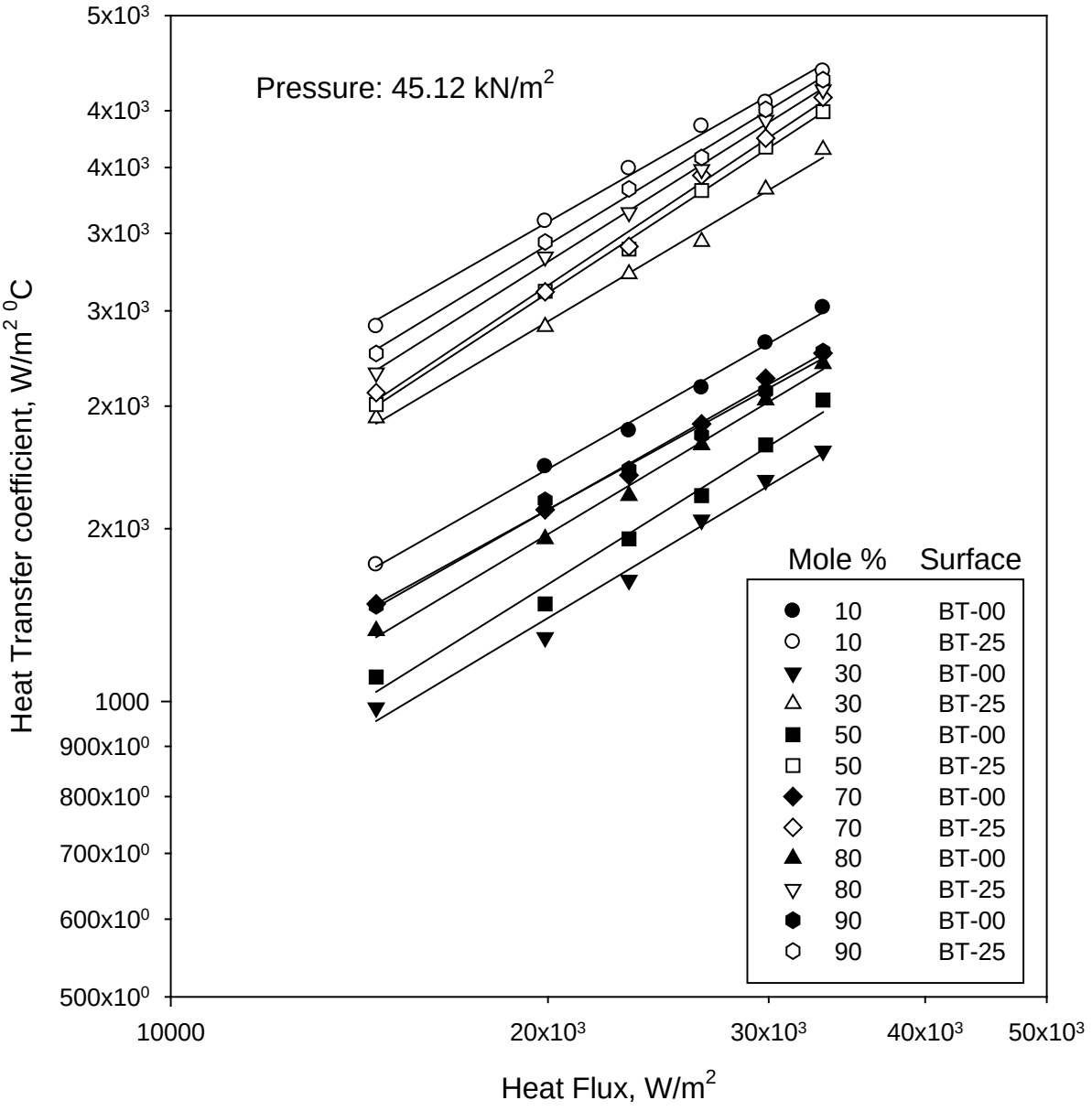

Fig. 5.75 Variation of heat transfer coefficient with heat flux for boiling of various iso-propanol-distilled water mixtures on a 25 μm thick copper coated tube and on an uncoated tube at 45.12 kN/m^2 pressure

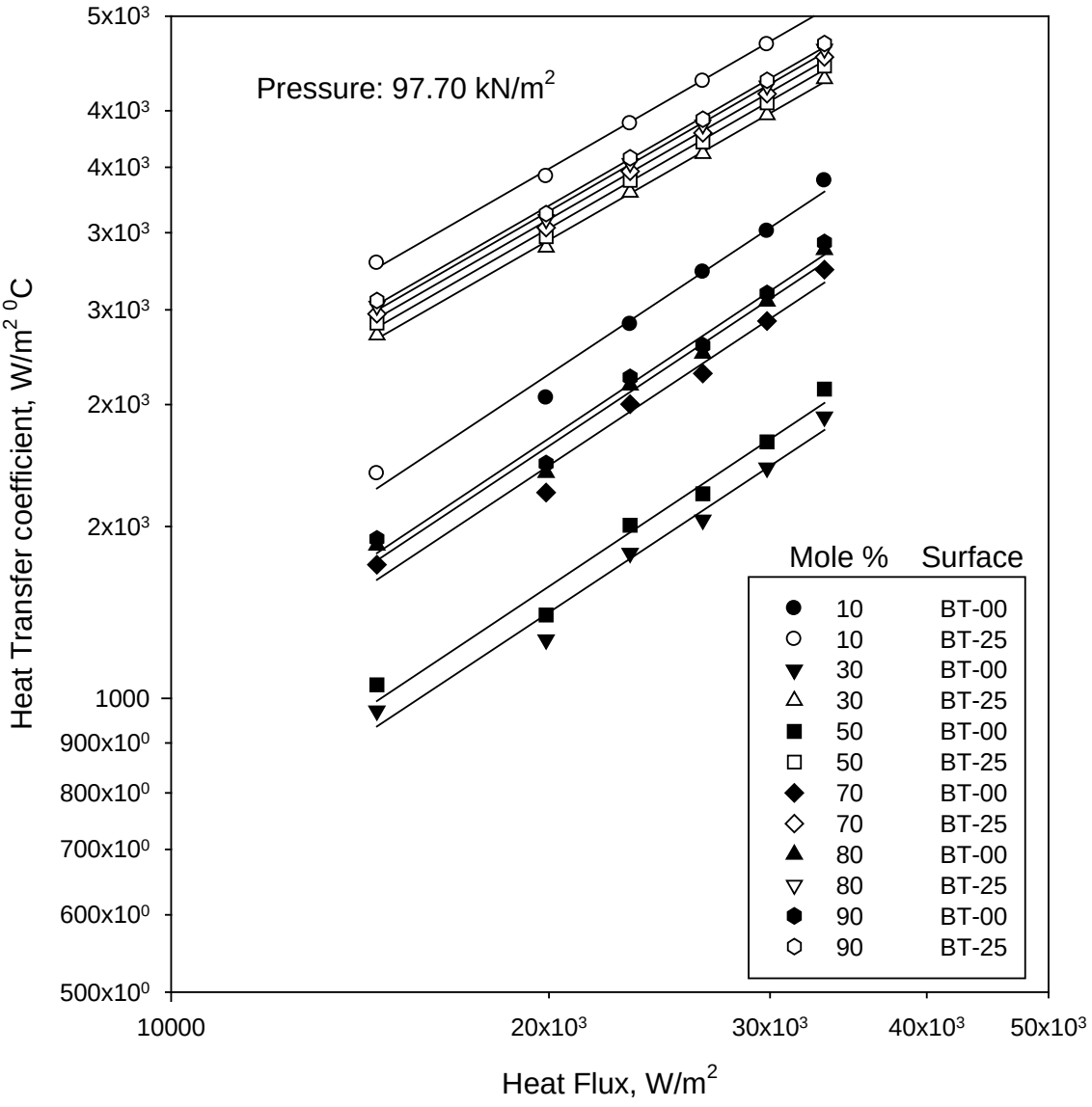

Fig. 5.76 Variation of heat transfer coefficient with heat flux for boiling of various methanol-distilled water mixtures on a 25 μm thick copper coated tube and on an uncoated tube at atmospheric pressure

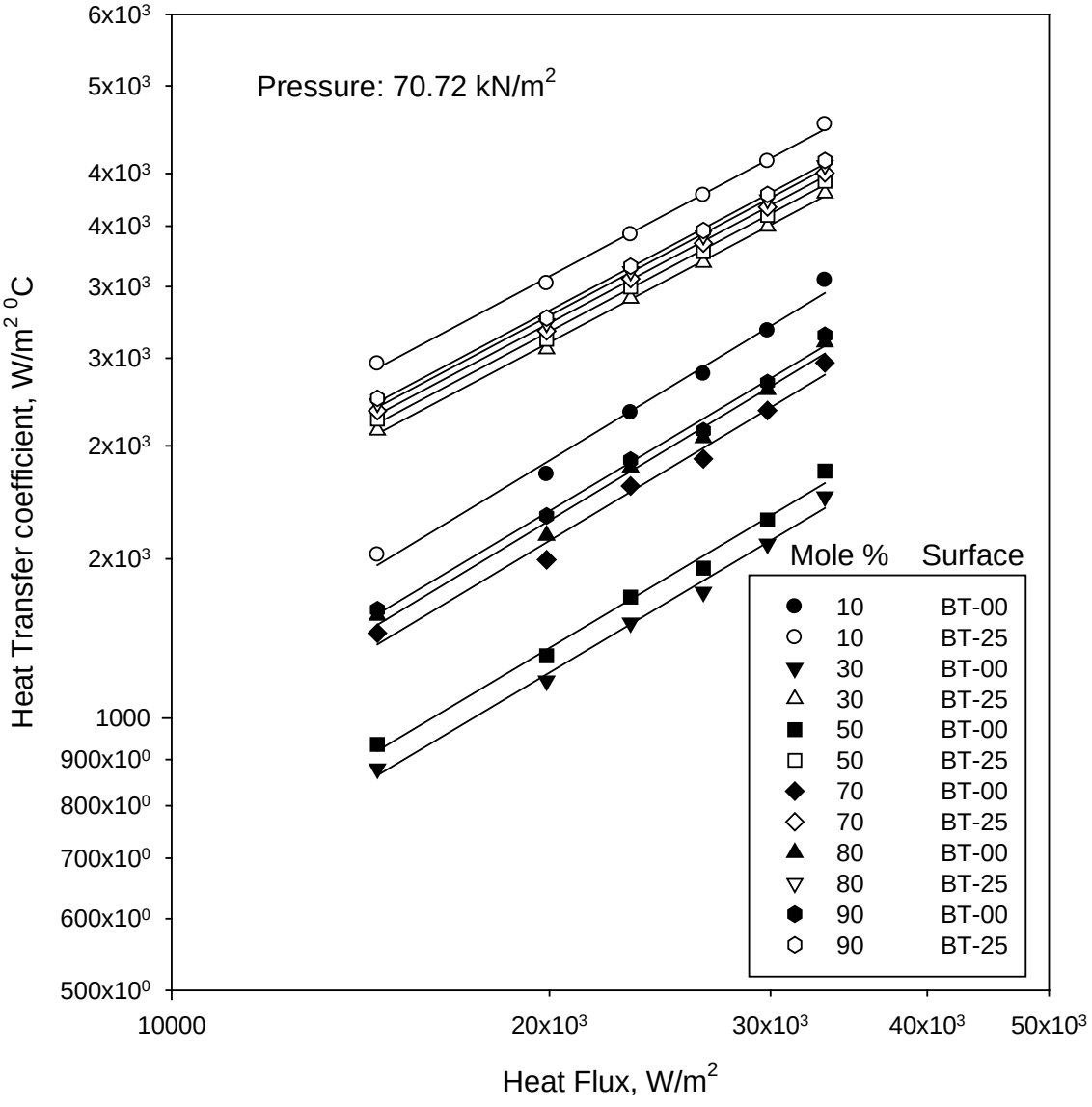

Fig. 5.77 Variation of heat transfer coefficient with heat flux for boiling of various methanol-distilled water mixtures on a 25 μm thick copper coated tube and on an uncoated tube at 70.72 kN/m^2 pressure

Z

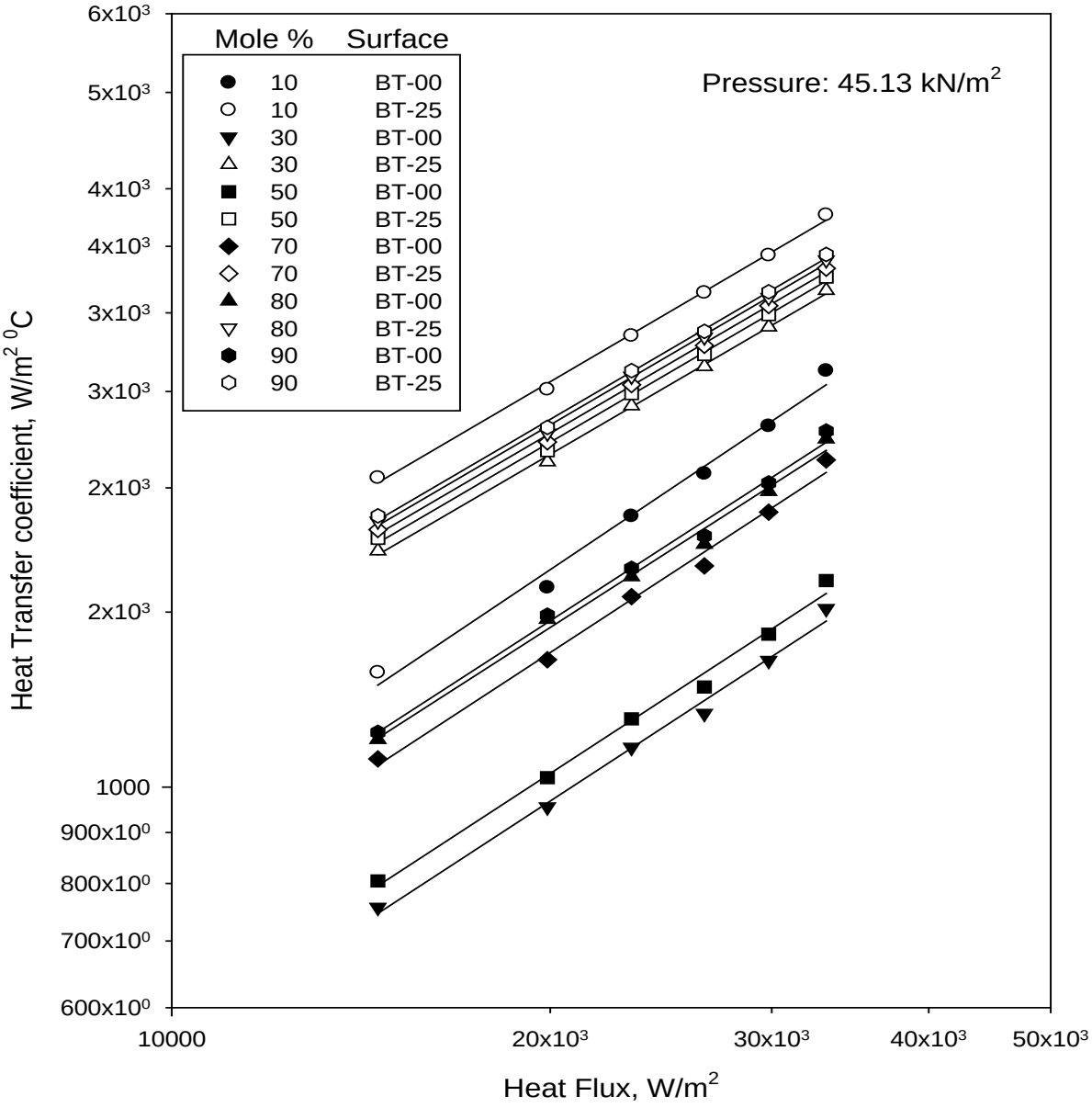

Fig. 5.78 Variation of heat transfer coefficient with heat flux for boiling of various methanol-distilled water mixtures on a 25 μm thick copper coated tube and on an uncoated tube at 45.13 kN/m^2 pressure

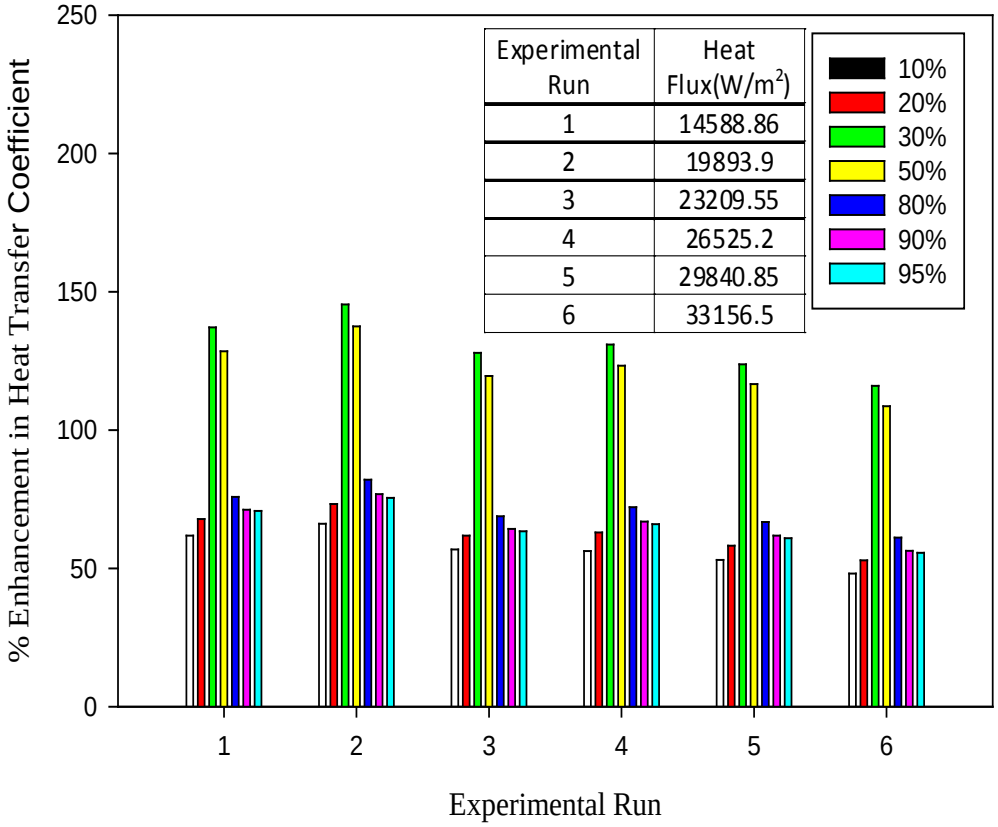

Fig.5.79 Percentage enhancement in heat transfer coefficient with heat flux for methanol-distilled water mixture for various compositions on copper coated (BT-25)

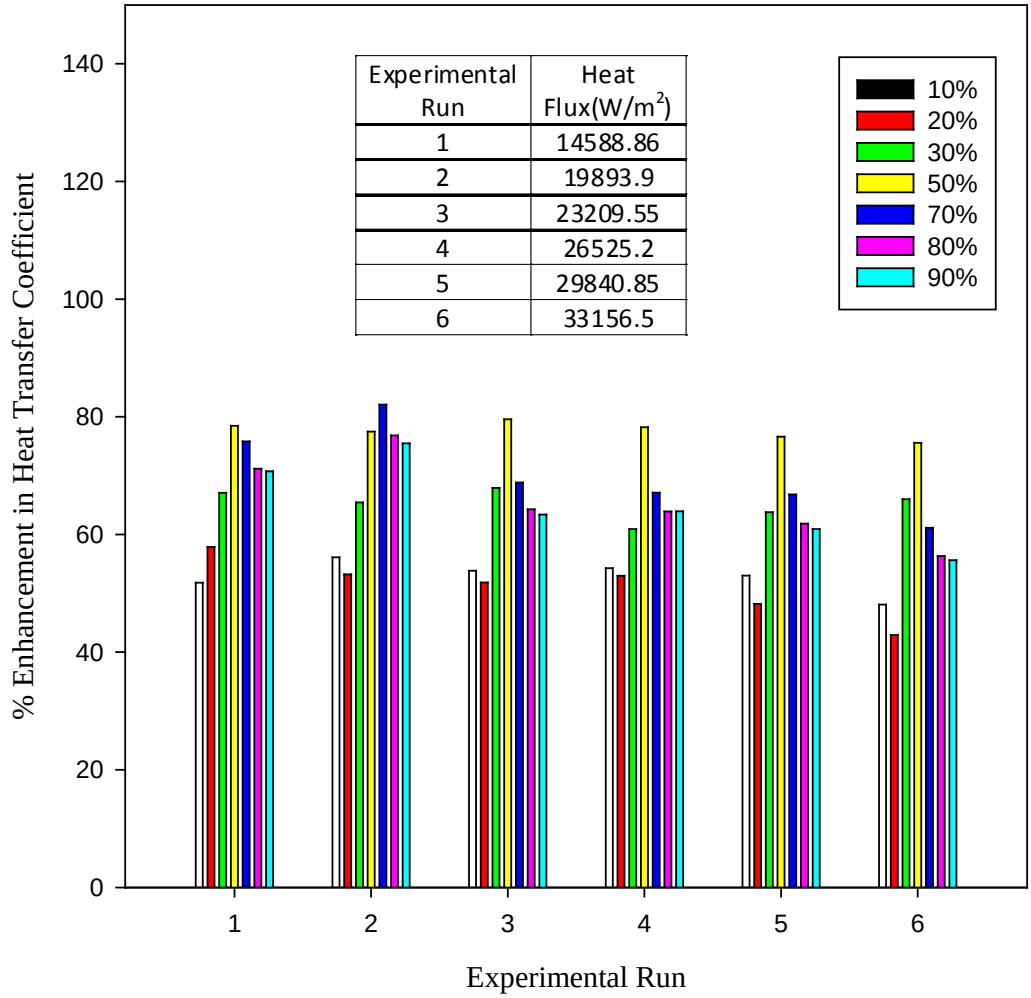

Fig. 5.80 Percentage enhancement in heat transfer coefficient with heat flux for isopropanol-distilled water mixture for various compositions on copper coated (BT-25)

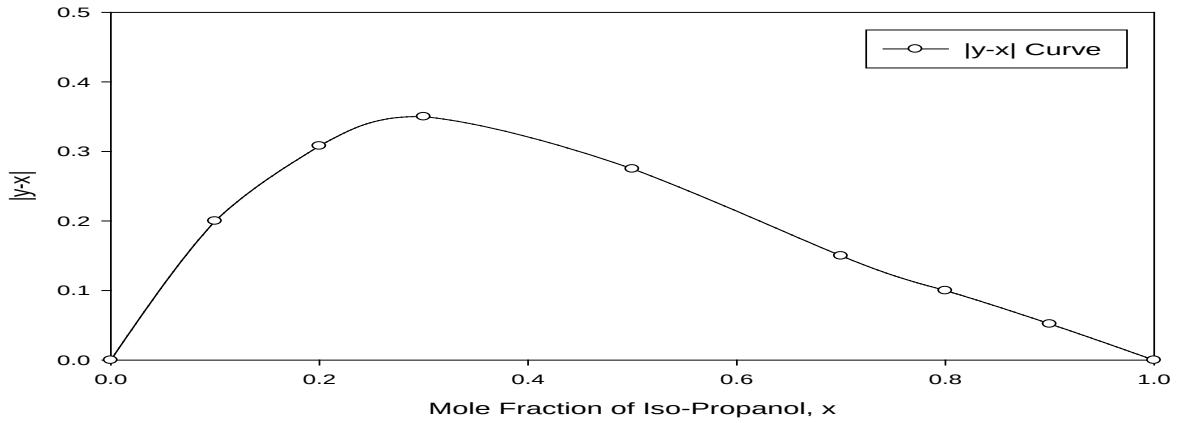

(a)

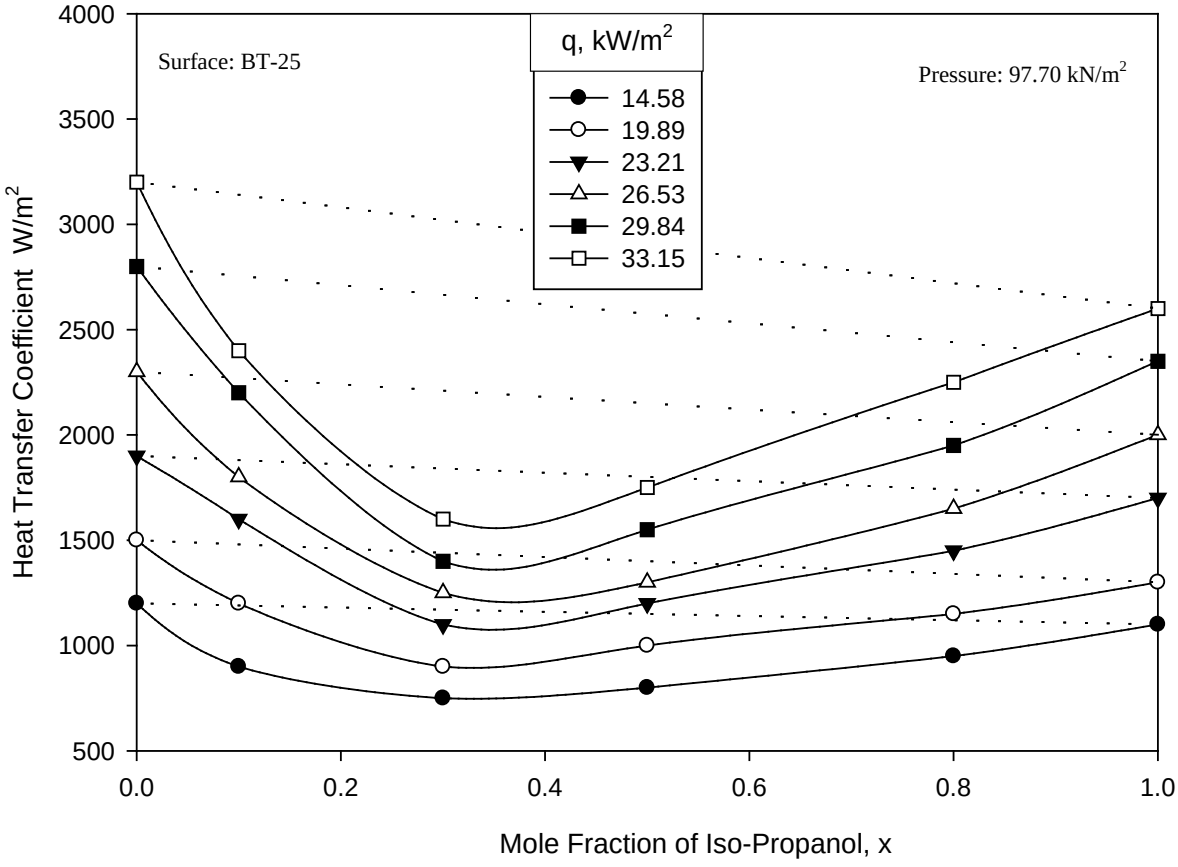

(b)

Figure 5.81 Variation of heat transfer coefficient, and |y-x| with mole fraction of methanol for iso-propanol-distilled water mixtures on coated tube at 97.10 kN/m^2 pressure

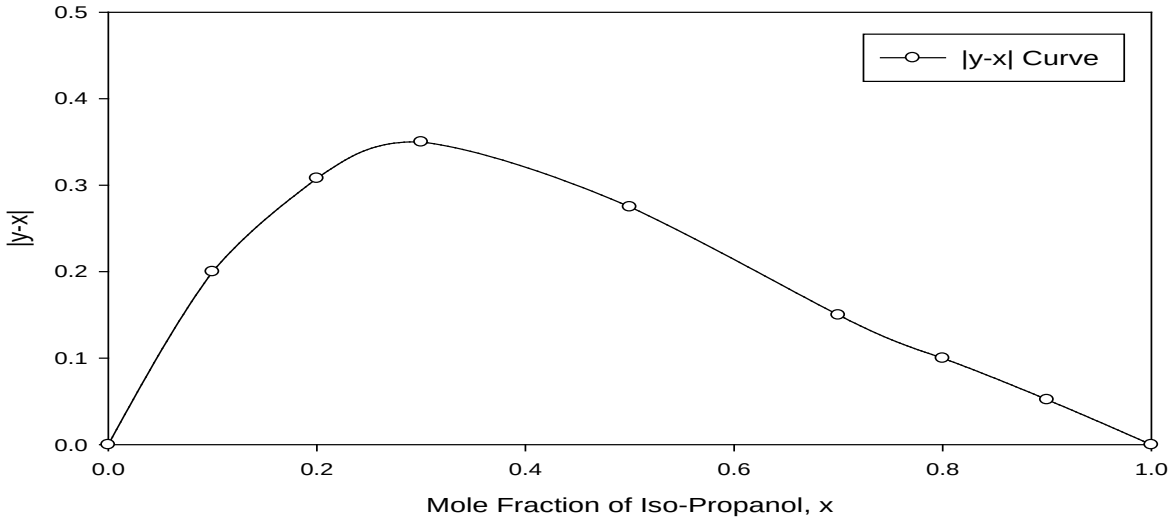

(a)

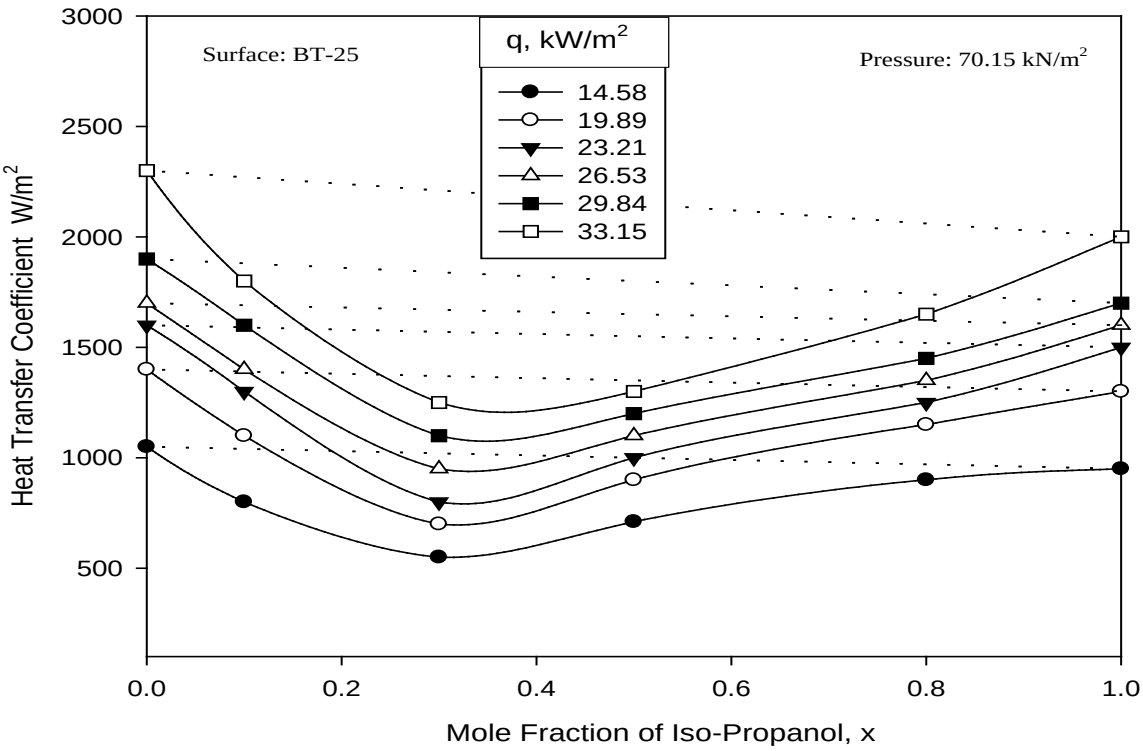

(b)

Figure 5.82 Variation of heat transfer coefficient, and |y-x| with mole fraction of methanol for isopropanol-distilled water mixtures on coated tube at 70.15 kN/m^2 pressure

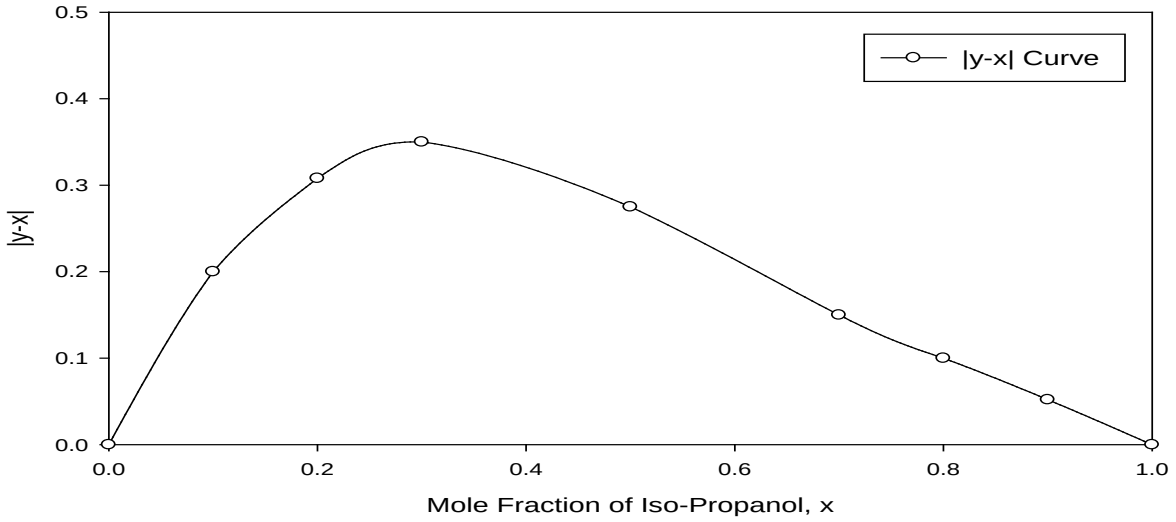

(a)

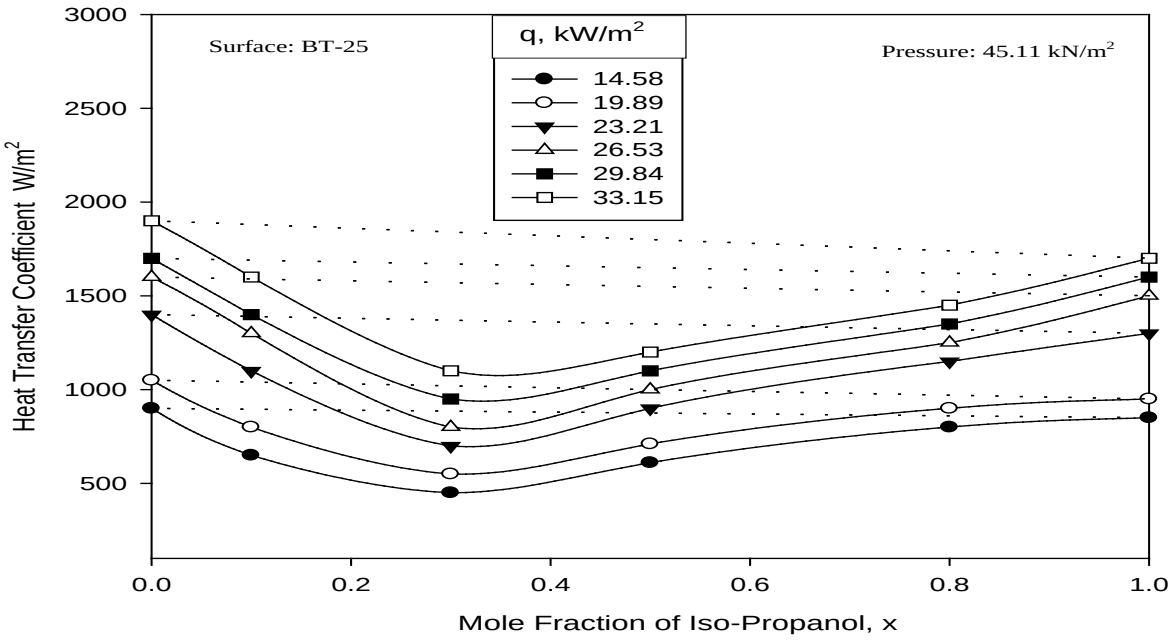

(b)

Figure 5.83 Variation of heat transfer coefficient, and |y-x| with mole fraction of methanol for iso-propanol-distilled water mixtures on coated tube at 45.11 kN/m^2 pressure

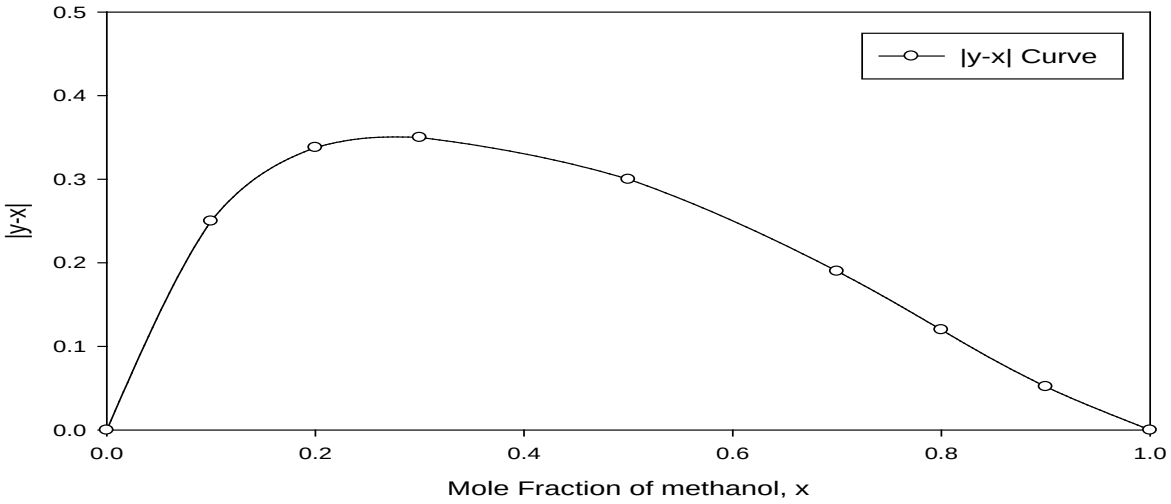

(a)

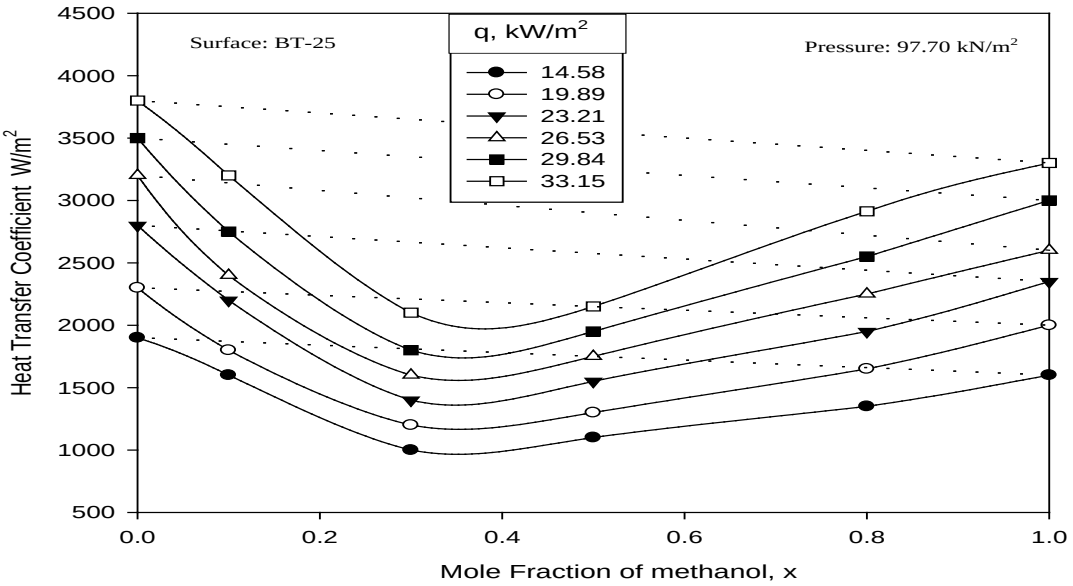

(b)

Figure 5.84 Variation of heat transfer coefficient, and |y-x| with mole fraction of methanol for methanol-distilled water mixtures on coated tube at 97.15 kN/m^2 pressure

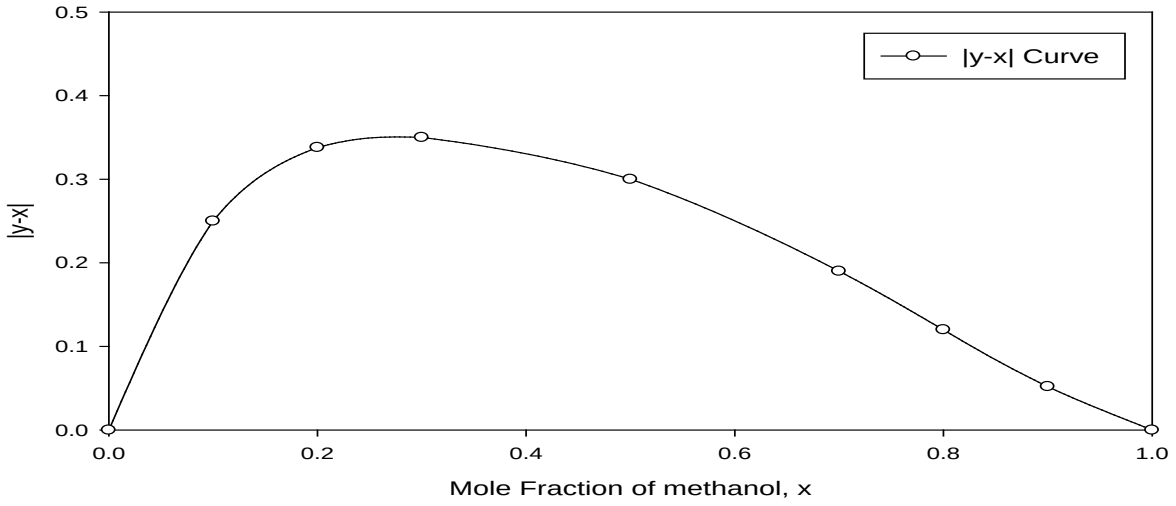

(a)

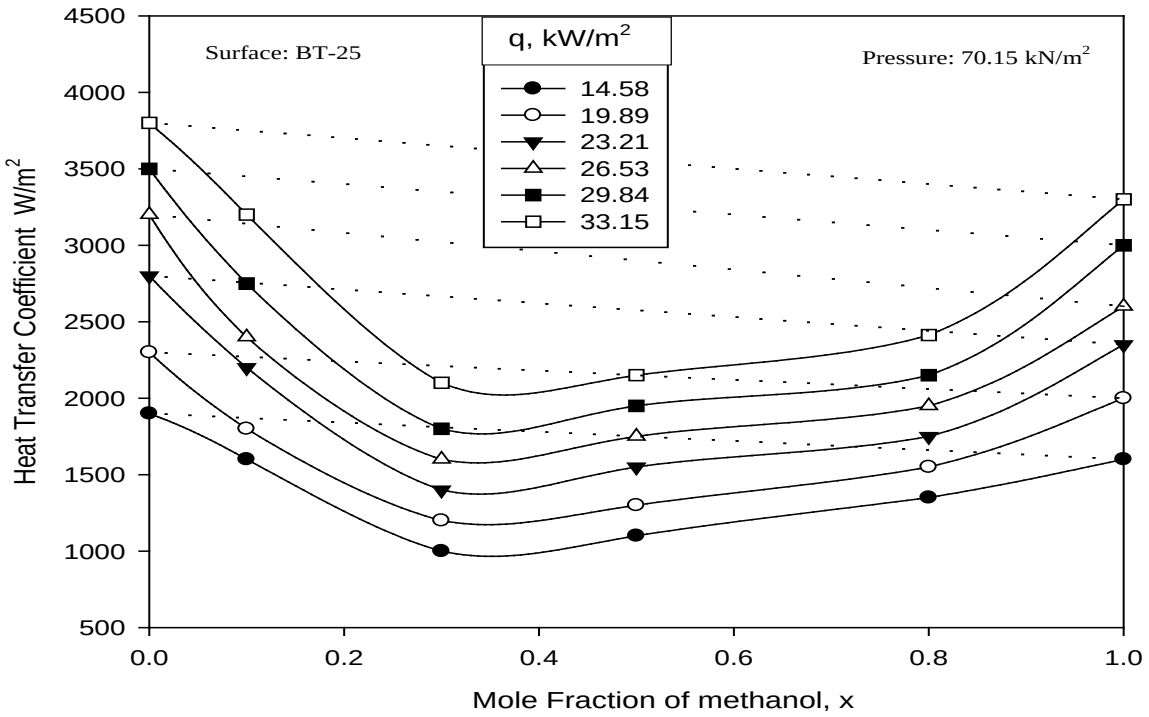

(b)

Figure 5.85 Variation of heat transfer coefficient, and |y-x| with mole fraction of methanol for methanol-distilled water mixtures on coated tube at 70.15 kN/m^2 pressure

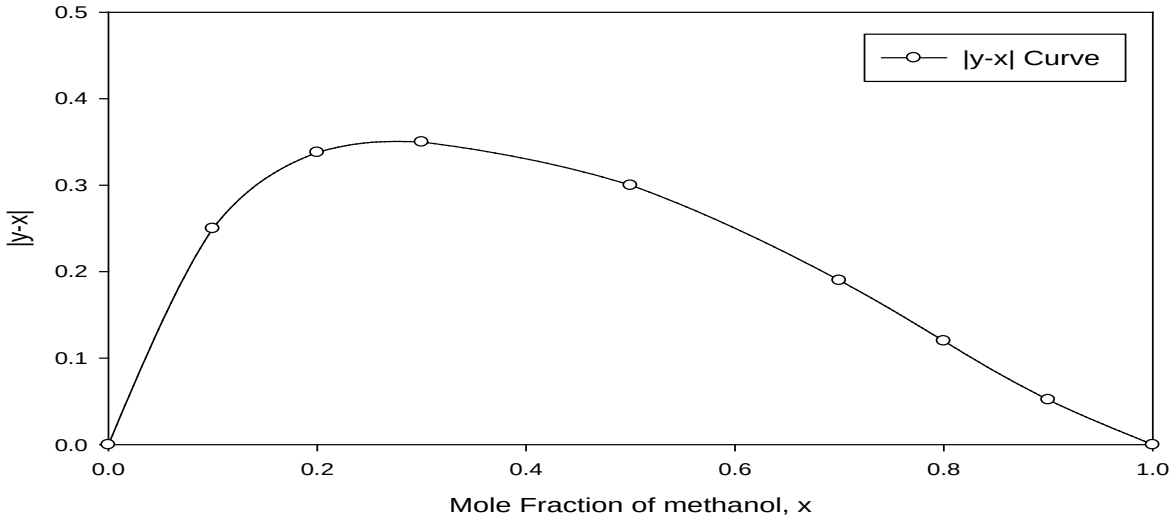

(a)

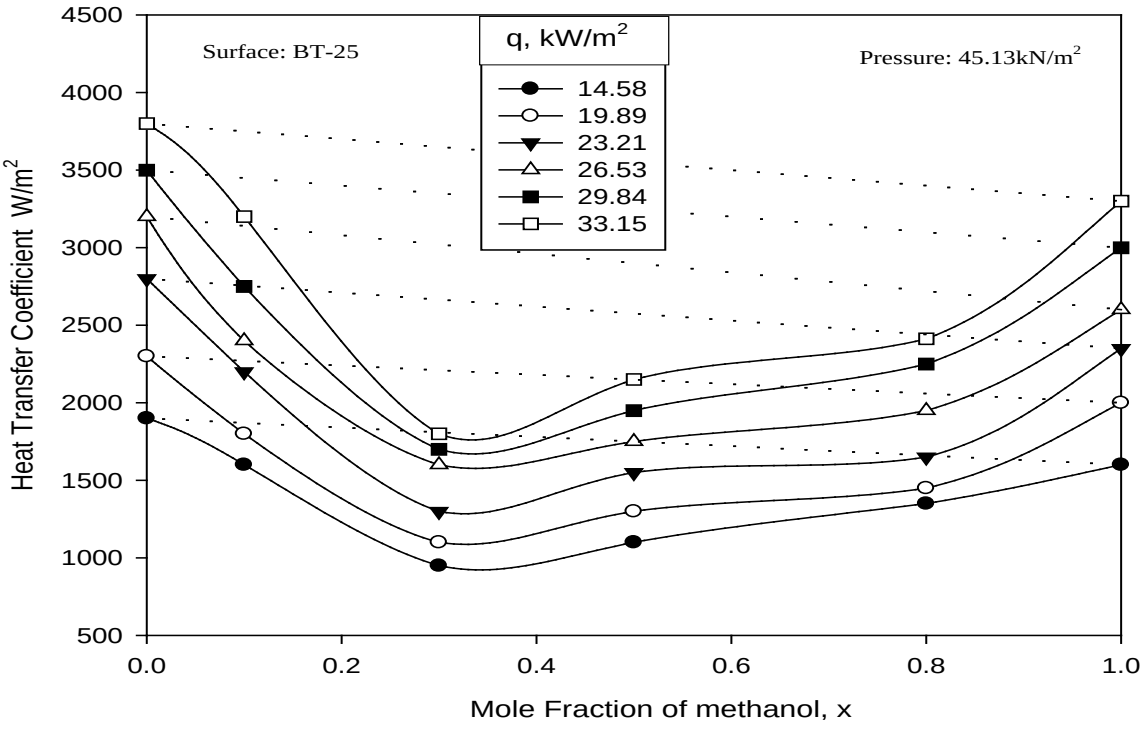

(b)

Figure 5.86 Variation of heat transfer coefficient, and |y-x| with mole fraction of methanol for methanol-distilled water mixtures on coated tube at 45.13 kN/m^2 pressure

results have also been obtained for various composition of iso-propanol- distilled water, and methanol-distilled water binary mixtures on coated surface at subatmospheric pressure. Based on this, it can be concluded that boiling of binary mixture on a 25 am thick copper coated brass heating tube surface is analogous to that on an uncoated brass heating tube surface at atmospheric and subatmospheric pressures. Hence, it is given by same phenomenon as in the case of uncoated tube. This included vaporization of unequal amount of high, low volatile component of the mixture, and so the occurrence of the heat and mass transfer involve in this process. This also responsible to vary potential and thereby heat transfer coefficient with concentration consequently, heat transfer coefficient for boiling of a given composition of binary mixture on coated heating tube surface at atmospheric and subatmospheric cannot be calculated by interpolation of heat transfer coefficient of the respective value of individual component liquids. This is quite similar to finding observed in uncoated heating tube surface.

5.8 NUCLEATE POOL BOILING OF A TERNARY MIXTURE ON A COATED HEATING TUBE

As pointed out earlier, 25 μm copper coated heating tube also selected to investigate heat transfer characteristics for the boiling of various composition of distilled water-methanol-iso-propanol ternary mixture at atmospheric and subatmospheric pressures. Distilled water has been kept constant as 50% and other highest volatile component concentration varies from (10, 20, 30, 40) mole percent. The experimental data of these run of ternary mixtures on 25 μm copper coated brass heating tube are listed in B.39 to B.44 of Annexure B. Following sub sections describe the effect of heat flux, pressure and composition on heat transfer coefficient for boiling of mixture on a coated heating tube.

5.8.1 Boiling heat transfer characteristics for a ternary mixture on a coated heating tube

Figure 5.87 depicts a typical plot between heat transfer coefficient and heat flux for the boiling of 10 Mole % highest volatile components in a ternary mixture on 25 μm thick copper coated brass heating tube surface. Pressure is a parameter in this plot. This reveals the following features:

i. For a given pressure, heat transfer increases with heat flux and variation between the two can be described by functional relationship $h \alpha q^t$.

ii. An increase in pressure increase heat transfer coefficient at a given value of heat flux.

Boiling of other compositions of ternary mixture on a 25 μm coated tube surface also resulted similar plots as evident in **Figs. 5.88** to **Fig. 5.89**. All of them have similar features as discussed above.

The above mentioned behavior is same as has been observed for the boiling of mixture on an uncoated tube surface. Further, the concentration (30) at which turn around phenomenon is observed is same as found in the case of uncoated tube. Thus, coating oftube surface does not seem to change the behavior and also the turnaround concentration.

It is concluded that boiling heat transfer characteristics of ternary mixture on 25 μm thick copper coated heating surfaces are alike those of methanol, iso-propanol, distilled water and their binary mixture. This is quite synonymous with the behavior of an uncoated heating surface.

5.8.2 Heat transfer coefficient - heat flux relationship for a ternary mixture on coated heating tube

A dimensional correlation amongst heat transfer coefficient, heat flux and pressure has been developed by regression analysis by using the experimental data for boiling of various compositions of distilled water–methanol–iso-propanol ternary mixture at a 25 μm thick copper coated brass heating tube surface at atmospheric and sub-atmospheric pressures, which is as follows:

$$h = C_6 q^{0.59} p^{0.36} \tag{5.21}$$

where, C_6 is constant whose values depends upon the percentage composition of the mixture and surface characteristics. The values of constant C6 as determined for various composition of distilled water–methanol–iso-propanol mixture are given in **Table 5.7**.

Eq. (5.21) is simple and convenient equation for the calculation of heat transfer coefficient for boiling of distilled water – methanol – iso-propanol mixture on a 25 μm thick copper coated heating tube surface from the knowledge of heat flux and pressure provided the value of C_6 is known.

Figure 5.90 shows a plot between experimentally determined value of heat transfer coefficient and those calculated by **Eq. (5.21)** for the boiling of various concentrations on a 25 μm thick copper coated brass heating tube surface at atmospheric and sub-atmospheric pressures. This plot reveals that the prediction match the experimental values excellently with an error of $\pm$18%. Thus, it is concluded that **Eq. (5.21)** can be used to calculate heat transfer coefficient for the boiling of distilled water – methanol – iso-propanol ternary mixture on a 25 μm thick copper coated brass heating tube, from the knowledge of heat flux and pressure provided the value of constant C_6 are known.

Table 5.7 Values of constant C_6, **Eq. (5.21)** for various compositions of distilled Water-Iso-propanol-Methanol

S.No.	Designations to mixtures	Compositions			
		Distilled Water	Methanol	Iso-Propanol	C_6
1	Ternary (A)	50 Mol%	10 Mol%	40 Mol%	1.367
2	Ternary (B)	50 Mol%	20 Mol%	30 Mol%	1.401
3	Ternary (C)	50 Mol%	30 Mol%	20 Mol%	1.451
4	Ternary (D)	50 Mol%	40 Mol%	10 Mol%	1.460
5	Ternary (E)	50 Mol%	25 Mol%	25 Mol%	1.421
6	Ternary (F)	33.33 Mol%	33.33 Mol%	33.33 Mol%	1.431

5.8.3 Comparison of Boiling Heat Transfer characteristics on a coated and uncoated tube surface for ternary mixture

These plots clearly represents that at a given value of heat flux, heat transfer coefficient on a coated tube is higher than that on an uncoated one. Similar features have also been obtained for the boiling of mixtures at atmosphere and sub-atmospheric pressures, as evident from plot containing **Figs. 5.91, and 5.93.** Reason for this behavior is same as discussed earlier in case of pure liquid and binary mixtures.

Keeping above in view, it may be concluded that coating of copper on brass heating tube enhances heat transfer coefficient for boiling of distilled water – methanol – iso-propanol at all pressures. **Fig. 5.94** represents the percentage of enhancement in heat transfer coefficient for boiling of these mixtures for various compositions of highest volatile component in the mixture for various experimental runs. This plot reveals that percentage enhancement in heat transfer coefficient varies from and the maximum enhancement is observed at turn around concentration.

5.8.4 Variation of heat transfer coefficient of ternary mixture with composition for boiling on a coated tube

Figure 5.95(b) depicts a typical plot between heat transfer coefficients for the boiling of various compositions of distilled water – methanol – iso-propanol ternary mixture on a 25 μm thick copper coated heating tube at atmospheric pressure to show the effect of concentration on heat transfer coefficient. Heat flux is the parameter in plots. Following important point emerge out from this plot:

i. For a given value of heat flux, heat transfer coefficient decreases with increase in the highest volatile component (methanol). This trend continues till the concentration is 30 mole percent. Therefore, any further increase in concentration increases the value of heat transfer coefficient.

ii. At a given concentration heat transfer coefficient increases with the increase in heat flux. **Fig. 5.96(b) and 5.97(b**) represent variation of heat transfer coefficient on a 25 μm thick copper coated heating tube as a function of concentration at 70.71 kN/m^2 and 45.41 kN/m^2, pressures, respectively. These plots also have essentially the same behavior as discussed above.

To explain the behavior of above graph, phase equilibrium diagram of ternary mixture as shown in **Fig 5.95(a)** is examined. It may be pinpoint here that the experimental values |y-x| as obtained from the analysis of liquid and vapor sample taken during the boiling of various composition of ternary mixture on coated surfaces have been found to be almost same as those obtained in the case of boiling on an uncoated tube. This is quite natural, thus it validates the correctness of experimental data on coated surfaces. The validation of heat transfer coefficient with mole percent of highest volatile component (methanol) and also the existence of turnaround point is given in section 5.4.3 for the boiling of ternary mixture on an uncoated tube surface holds true in this case also, the concentration at which turnaround in heat transfer coefficient occurs is also found to same 30%. Similar results have also been obtained for the boiling of various composition of distilled water – methanol

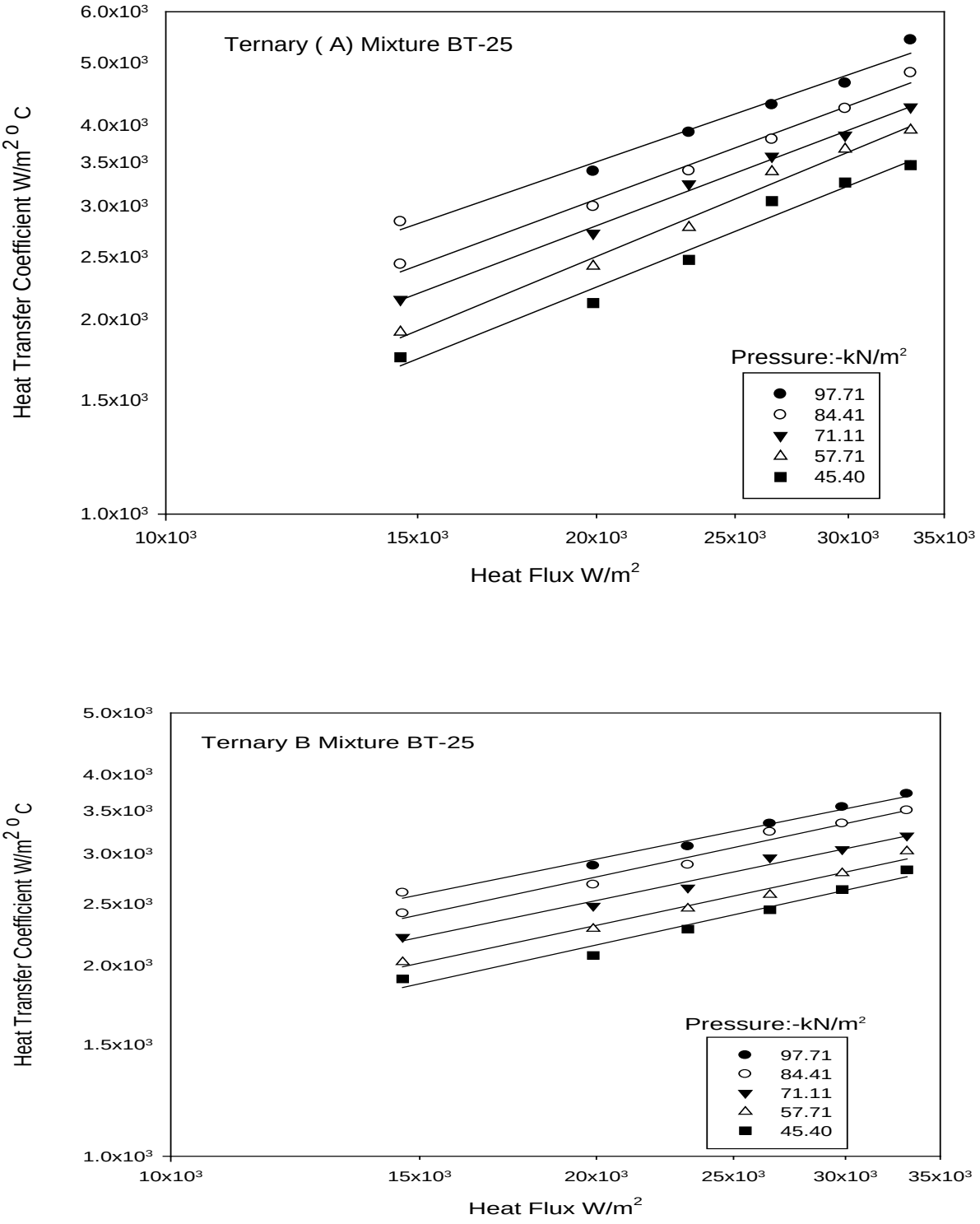

Figure 5.87 Variation of heat transfer coefficient with heat flux for boiling of ternary (A) and ternary (B) mixture on a coated heating tube with pressure as a parameter

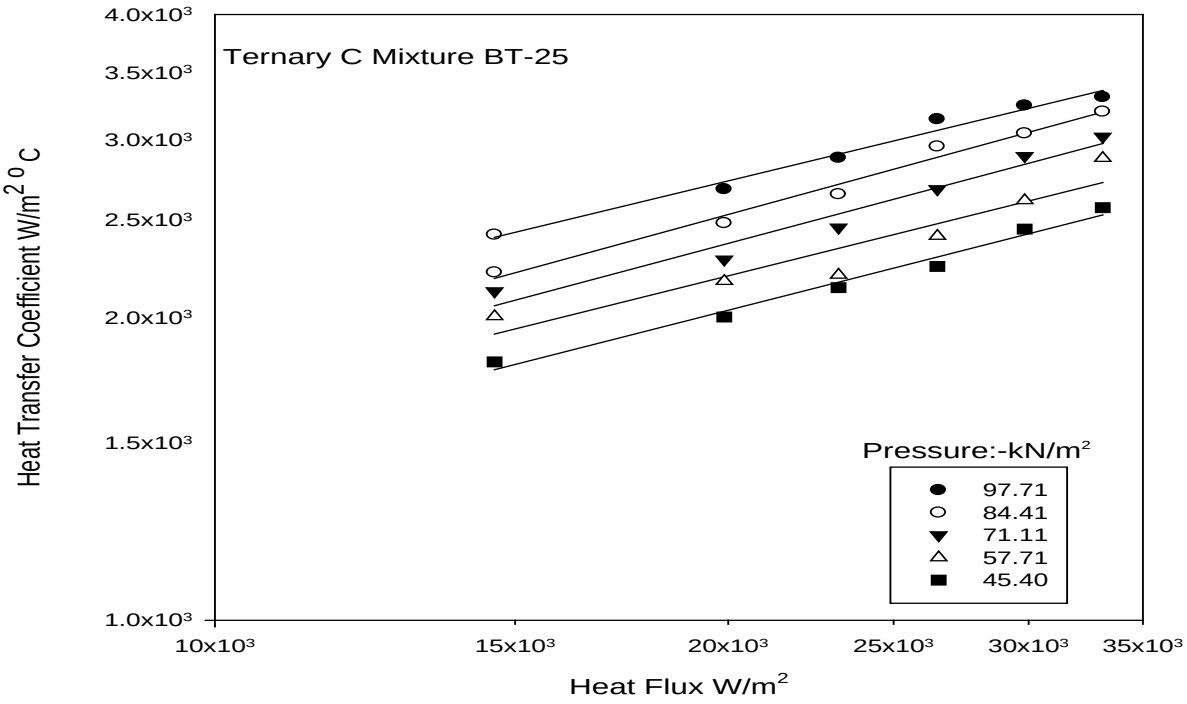

(a)

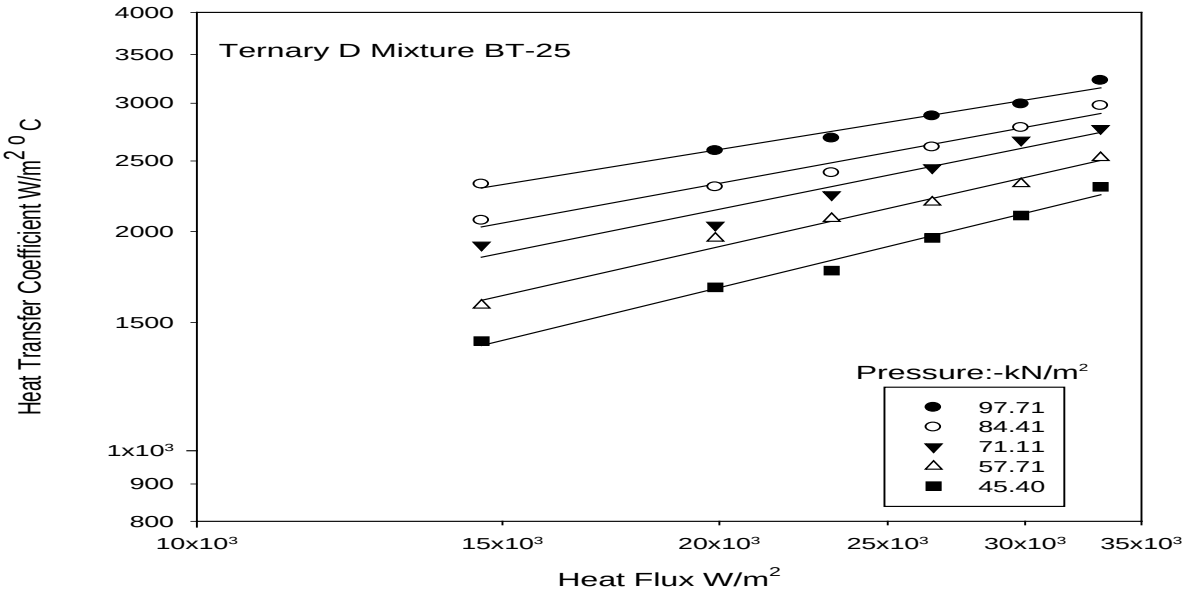

(b)

Figure 5.88 Variation of heat transfer coefficient with heat flux for boiling of ternary (C) and ternary (D) mixture on a coated heating tube with pressure as a parameter

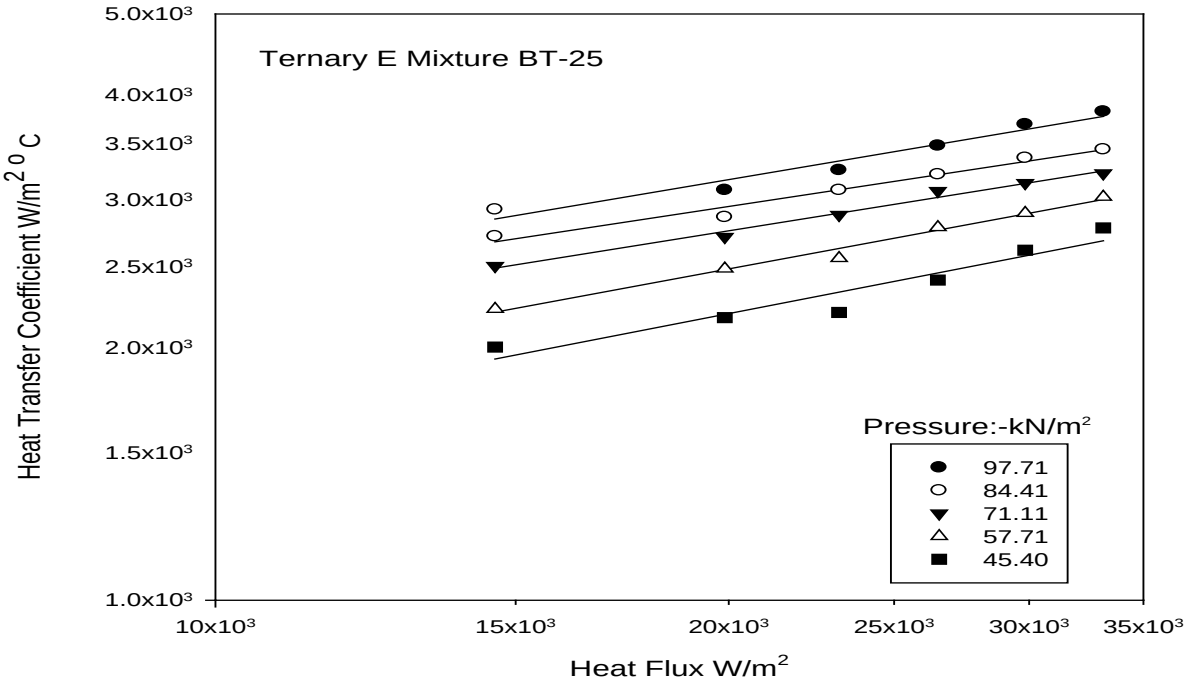

(a)

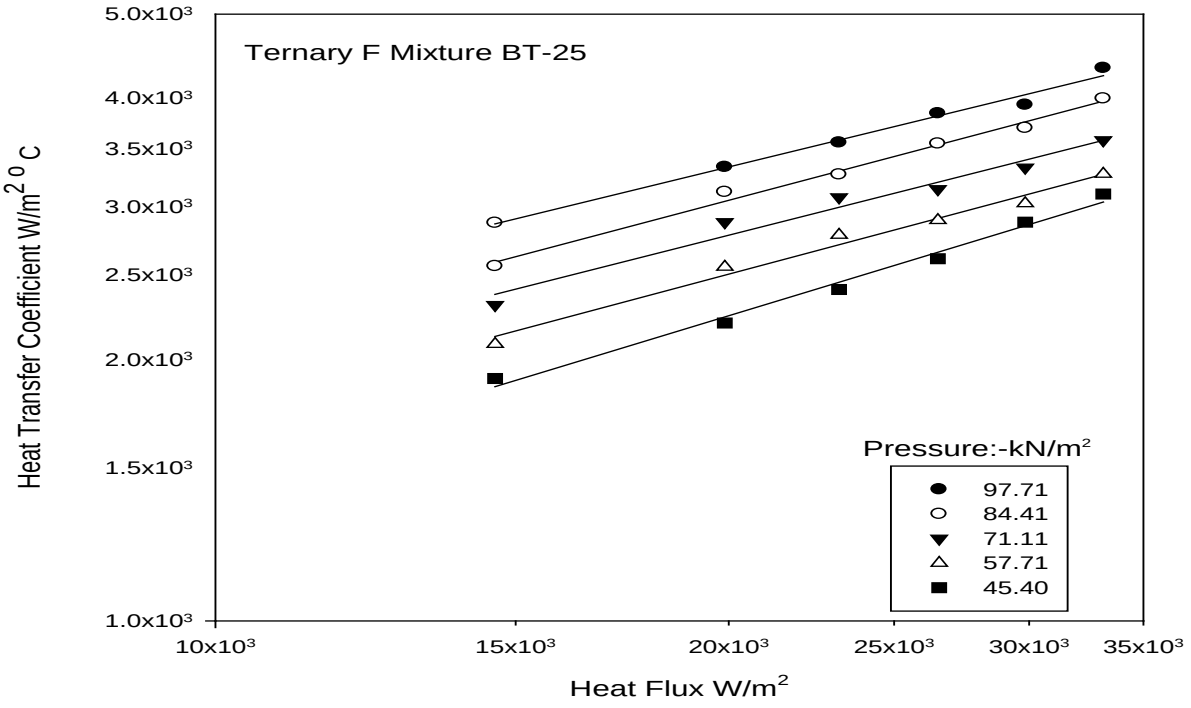

(b)

Figure 5.89 Variation of heat transfer coefficient with heat flux for boiling of ternary (E) and ternary (F) mixture on a coated heating tube with pressure as a parameter

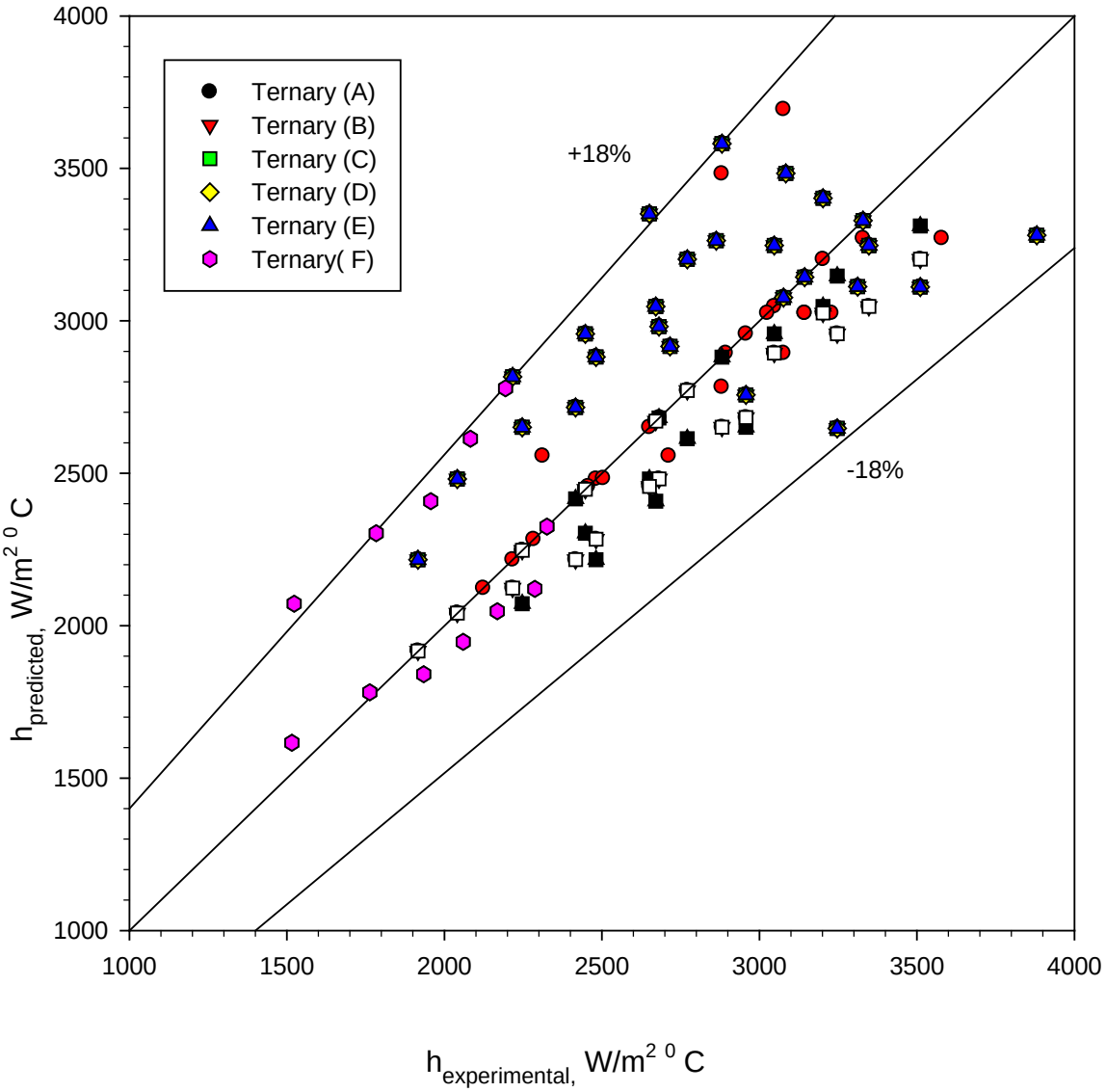

Figure 5.90 Comparison of experimental heat transfer coefficient with those predicted **Eq.(5.21)** for boiling of ternary mixture on a 25µm copper coated heating tube surface at atmosphere and subatmospheric

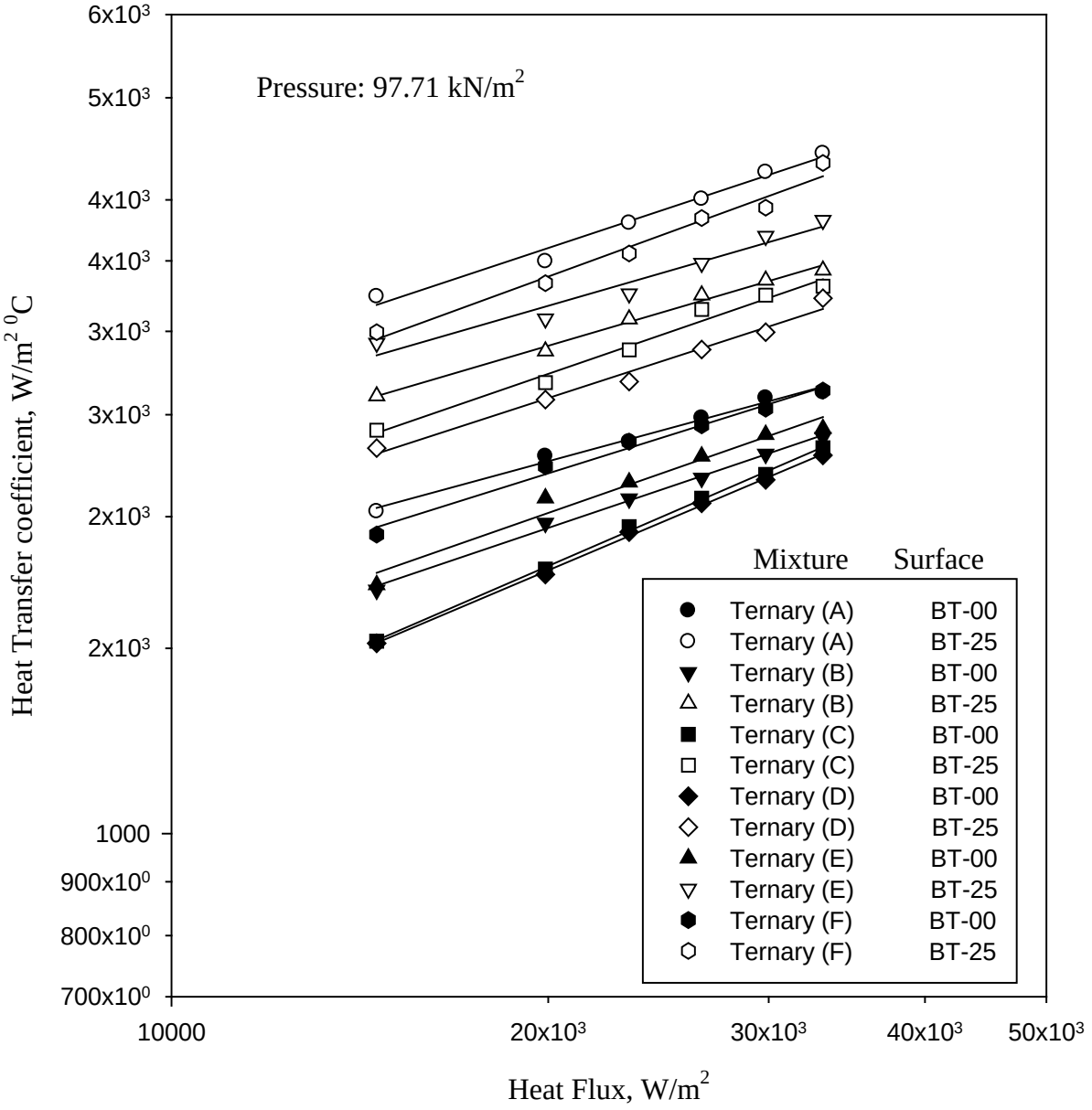

Figure 5.91 Comparison of heat transfer coefficient for various composition of ternary mixture on a coated BT-25 and uncoated BT-00 tube at atmospheric pressure

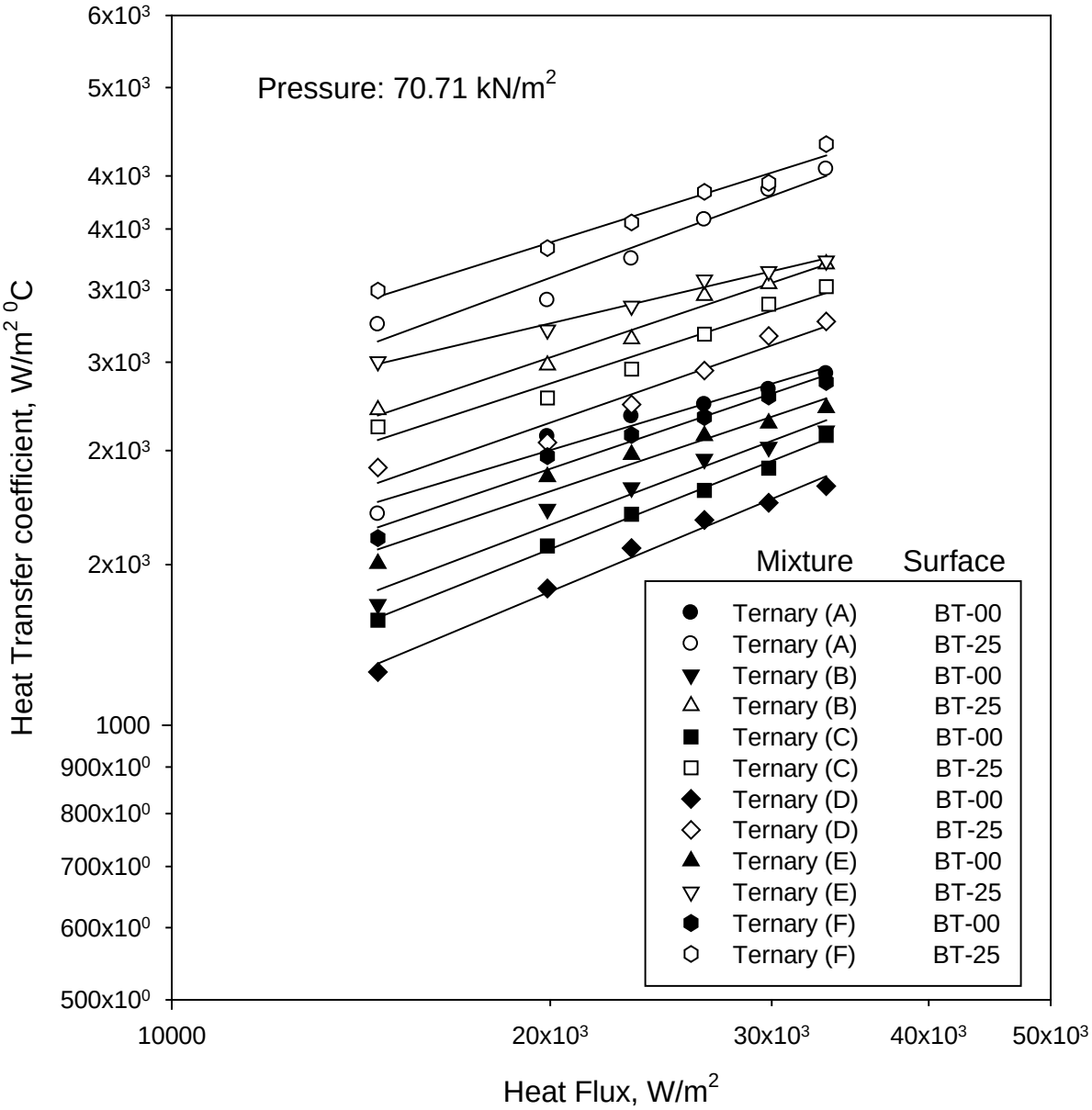

Figure 5.92 Comparison of heat transfer coefficient for various composition of ternary mixture on a coated BT-25 and uncoated BT-00 tube at 70.71 kN/m^2

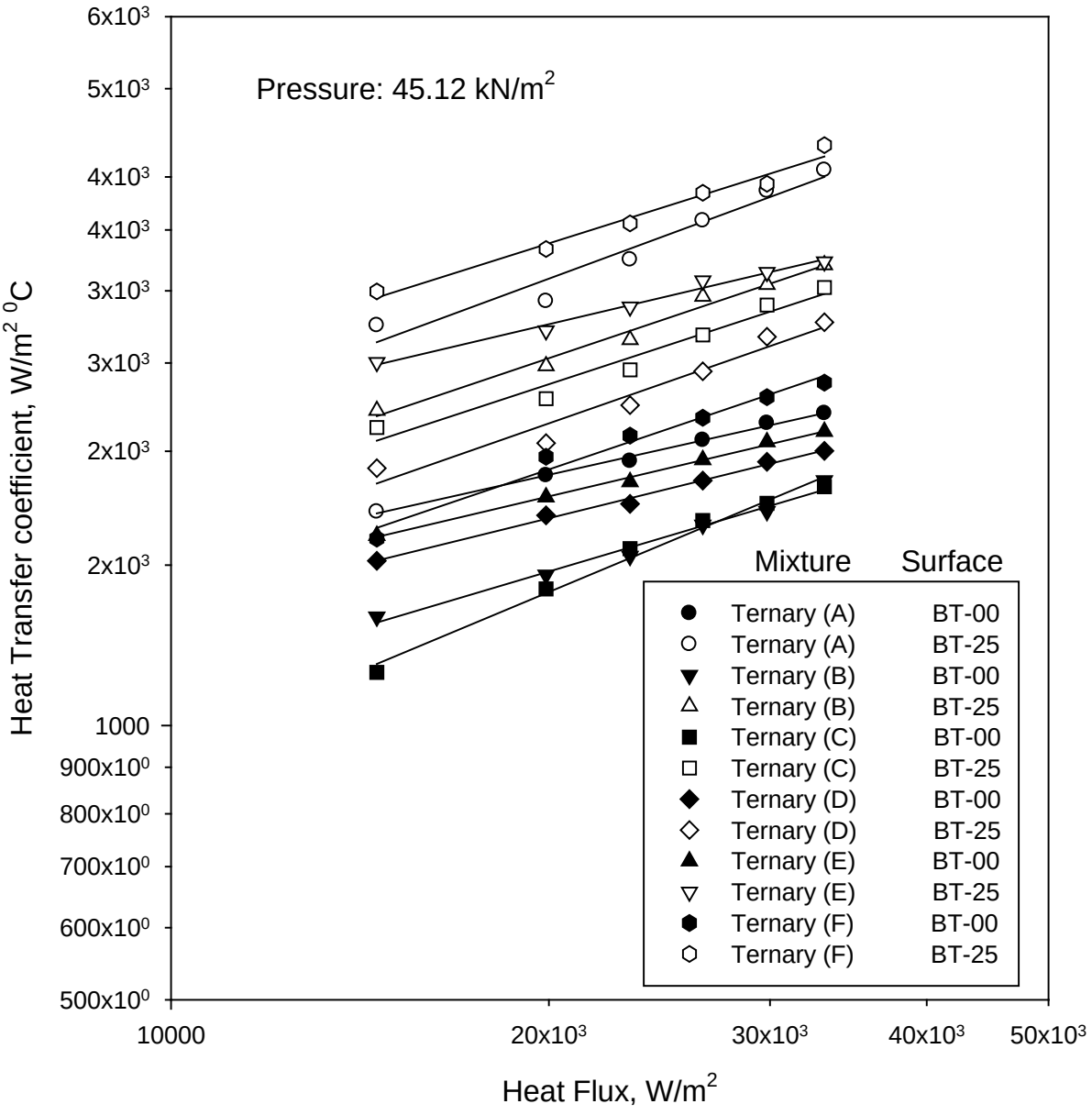

Figure 5.93 Comparison of heat transfer coefficient for various composition of ternary mixture on a coated BT-25 and uncoated BT-00 tube 45.12 kN/m^2

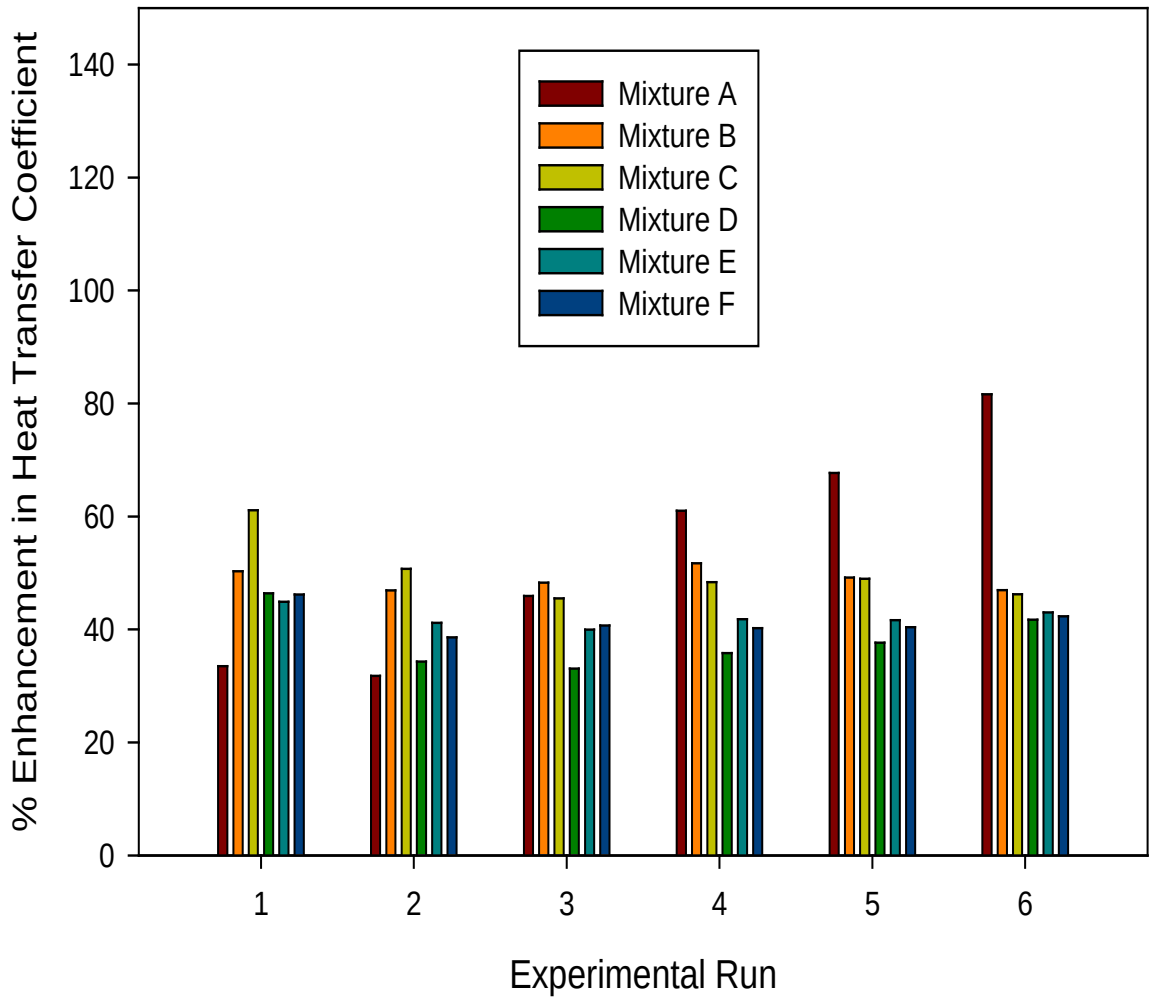

Figure 5.94 Percentage enhancement in heat transfer coefficient with heat flux for distilled water-methanol-iso-propanol mixtures for various compositions on copper coated (BT-25)

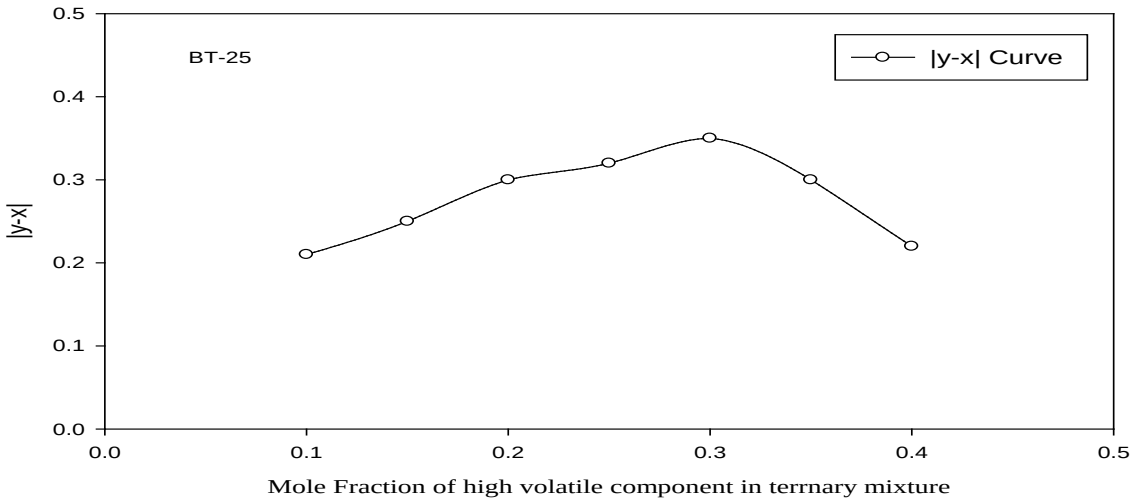

(a)

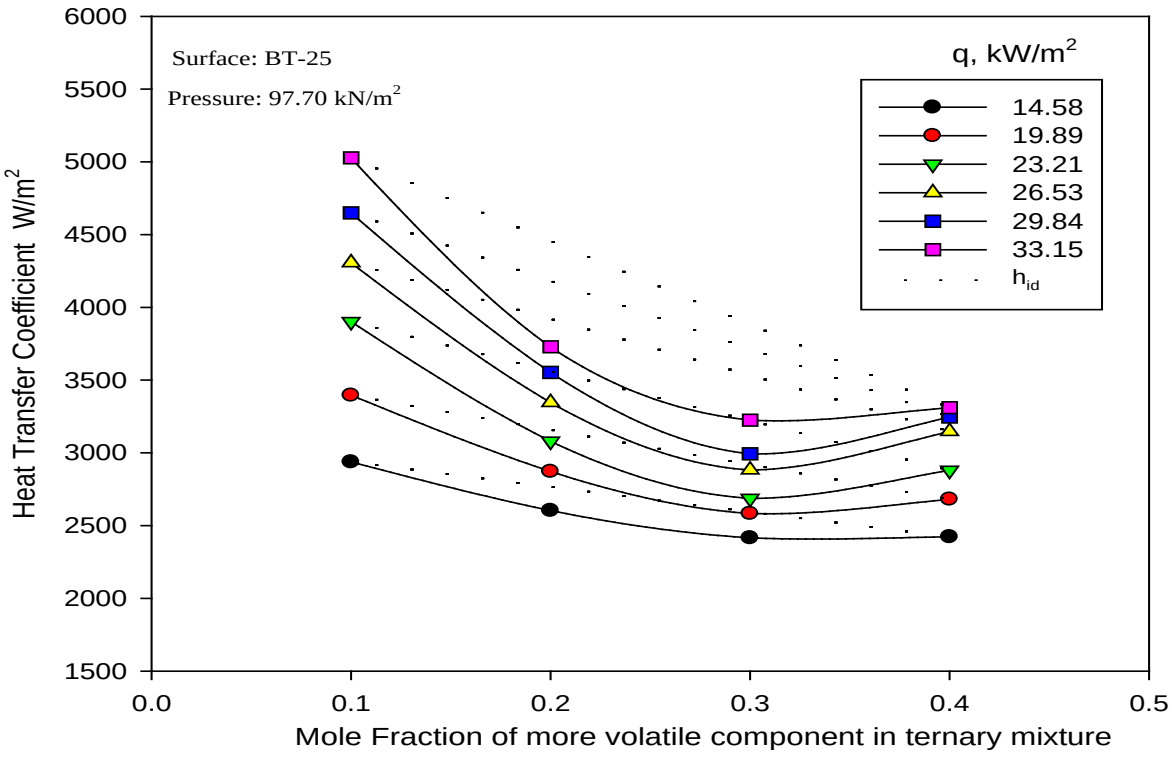

(b)

Figure 5.95 Variation of heat transfer coefficient, and |y-x| with mole fraction of high volatile component of ternary mixture on coated tube at atmospheric pressure

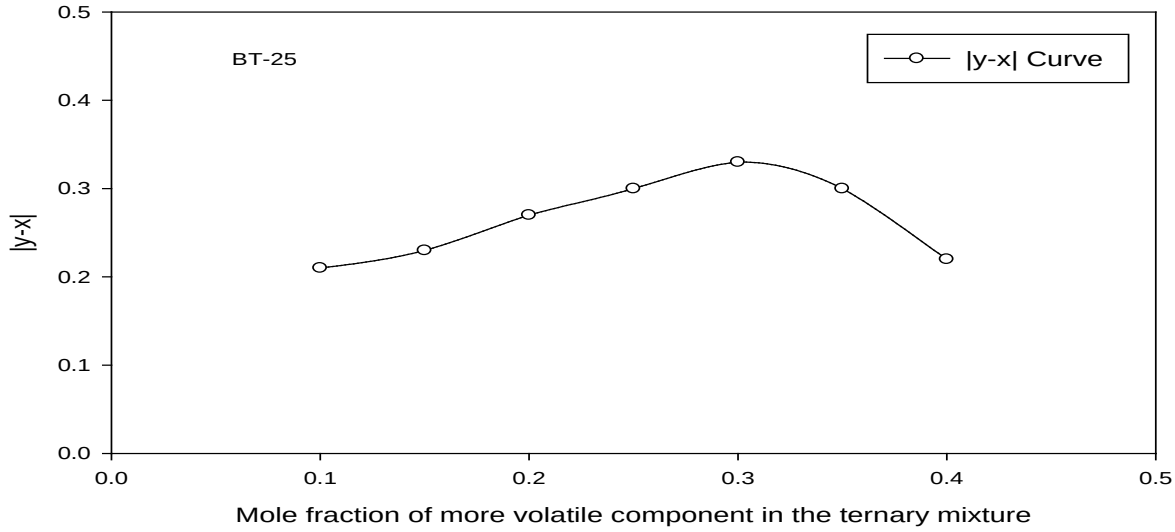

(a)

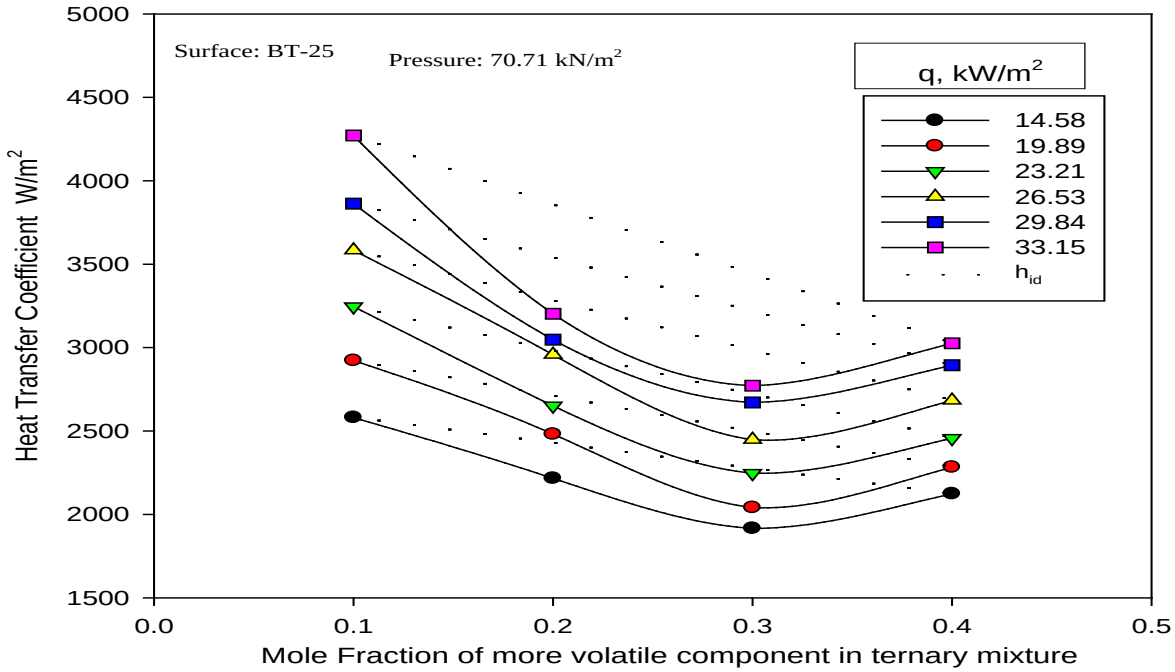

(b)

Figure 5.96 Variation of heat transfer coefficient, and |y-x| with mole fraction of high volatile component of ternary mixture on coated tube at 70.71 kN/m^2 pressure

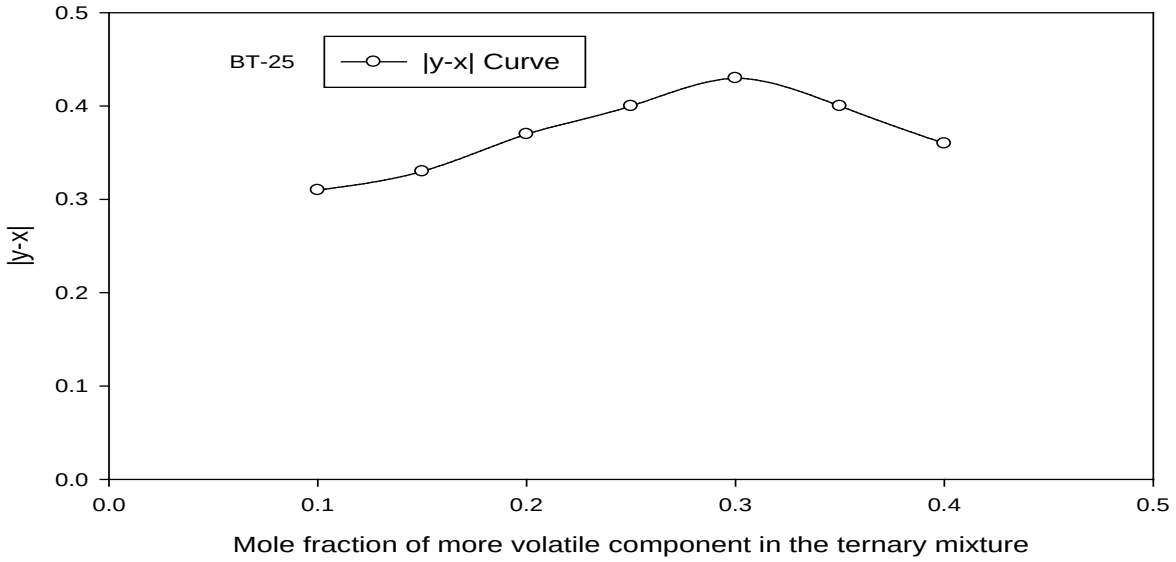

(a)

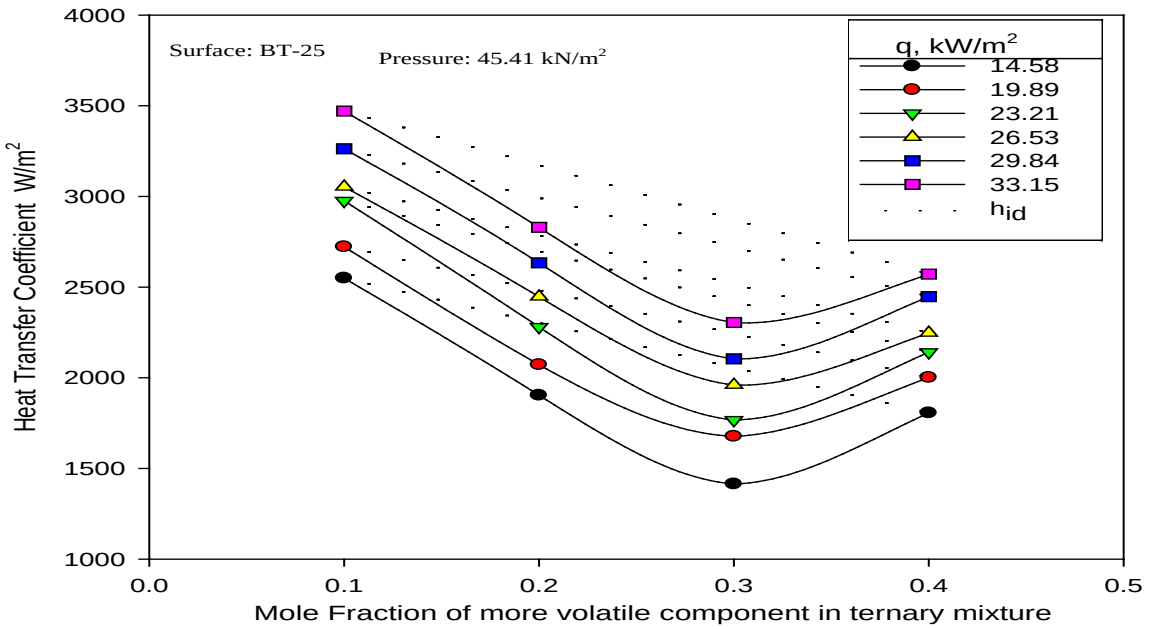

(b)

Figure 5.97 Variation of heat transfer coefficient, and |y-x| with mole fraction of high volatile component of ternary mixture on coated tube at 45.41 kN/m^2 pressure

– iso-propanol ternary mixture on a brass coated tube surface at atmospheric pressure. Based on the above it can be concluded that the boiling of various compositions of ternary mixture on 25 μm copper coated heating tube surface is quite analogous to that on an uncoated surface at atmospheric and sub atmospheric pressure. Therefore, it is governed by same phenomenon in the case of an uncoated tube surface. This includes of vaporization of unequal amount of high and low volatile component of mixture, so simultaneous heat and mass transfer take place. This is also responsible to vary potential and thereby heat transfer coefficient with concentration. Hence, heat transfer coefficient for boiling of given compositions of ternary mixtures on a coated heating tube surface cannot be determined by weighted mean of individual component heat transfer coefficient. This observation is quite similar to that obtained in case of an uncoated tube surface.

Above discussion has clearly shown that of heat transfer coefficient of ternary mixture on coated heating tube surface cannot be determined by weighted mean of individual component of heat transfer coefficient of this observation is quite similar to that obtained in case of an uncoated tube surface. Further, heat transfer coefficient on a coated tube has also been found to follow same pattern as that of an uncoated tube. In other words coating of tube does not change the trend of h v/s x curve. Hence, it was thought to examine **Eq. (5.17)** for its validity on coated tube surface also. For convenience **Eq. (5.17)** is reproduced here below:

$$(h / h_{id}) = (\Delta T_{id} / \Delta T) = [1 + | y_1 - x_1 | \sqrt{\alpha_1 / D_1} + | y_2 - x_2 | \sqrt{\alpha_2 / D_2}\,]^{-(0.73x1+0.36)} \qquad (5.17)$$

Fig.5.98 represents plots between heat transfer coefficients calculated by the **Eq. (5.17)** and experimentally determined the value for various compositions of distilled water – methanol – iso-propanol ternary mixture on a thick copper coated heating tube surface at atmospheric pressure. The computed values of heat transfer coefficient have been obtained by determining h_{id} by using the respective values of heat transfer coefficient determine experimentally for boiling methanol, iso-propanol and distilled water on 25 μm thick copper coated heating tube surface and then by using **Eq. (5.17)**. This plot clearly reveals that predicted values matches with the maximum value error ±18%.Hence, **Eq. (5.17)** has succeeded to predict heat transfer coefficient of a ternary mixture boiling on a 25 μm copper coated heating tube surface. Similar Analysis has been performed for ternary mixture at various sub atmospheric pressure as shown in **Fig.5.99**. In this case also predicted values have match excellently within maximum error of ±20%.Therefore, above

correlation holds true for sub atmospheric pressures range also. Thus it may be concluded that heat transfer coefficient of boiling of distilled water – methanol – iso-propanol mixture can be determined by using **Eq. (5.17)** for both the cases viz. uncoated and coated tube surface. This makes **Eq. (5.17)** to be of general applicability. Above observation is quite obvious by a relook of **Eqs. (5.13)**, and **(5.17)**. Both of them consider mole fraction of highest volatile component (methanol). Physico-thermal properties and phase equilibrium diagram for the mixture only. In fact they do not include any factor which depends on heating surface characteristics. Hence, **Eq. (5.13)** and **Eq. (5.17)** are applicable for the boiling of a liquid mixture irrespective of the heating surface involed in the boiling.

At this juncture it may be recalled that in sections 5.5.3, 5.6.3, 5.7.3 and 5.8.3; **Eqs. (5.17)., (5.19), (5.20),** and **(5.21)** have been developed for the prediction of heat transfer coefficient for the boiling of distilled water , methanol, iso-propanol and their binary and ternary mixtures on a 25 μm copper coated brass heating tube surface. Therefore, above equation may also be used in **Eq. (5.13)** to obtain h_{id} . However, it cautioned that **Eqs. (5.17)**, **(5.19), (5.20), and (5.21)** can be used only when the value of constant appearing in them is known experimentally. In other words the use of **Eq. (5.17)** requires experimentation for single component liquid mixtures viz. distilled water, methanol, iso-propanol on a coated surface to determine boiling heat transfer coefficient of ternary mixture on the surface.

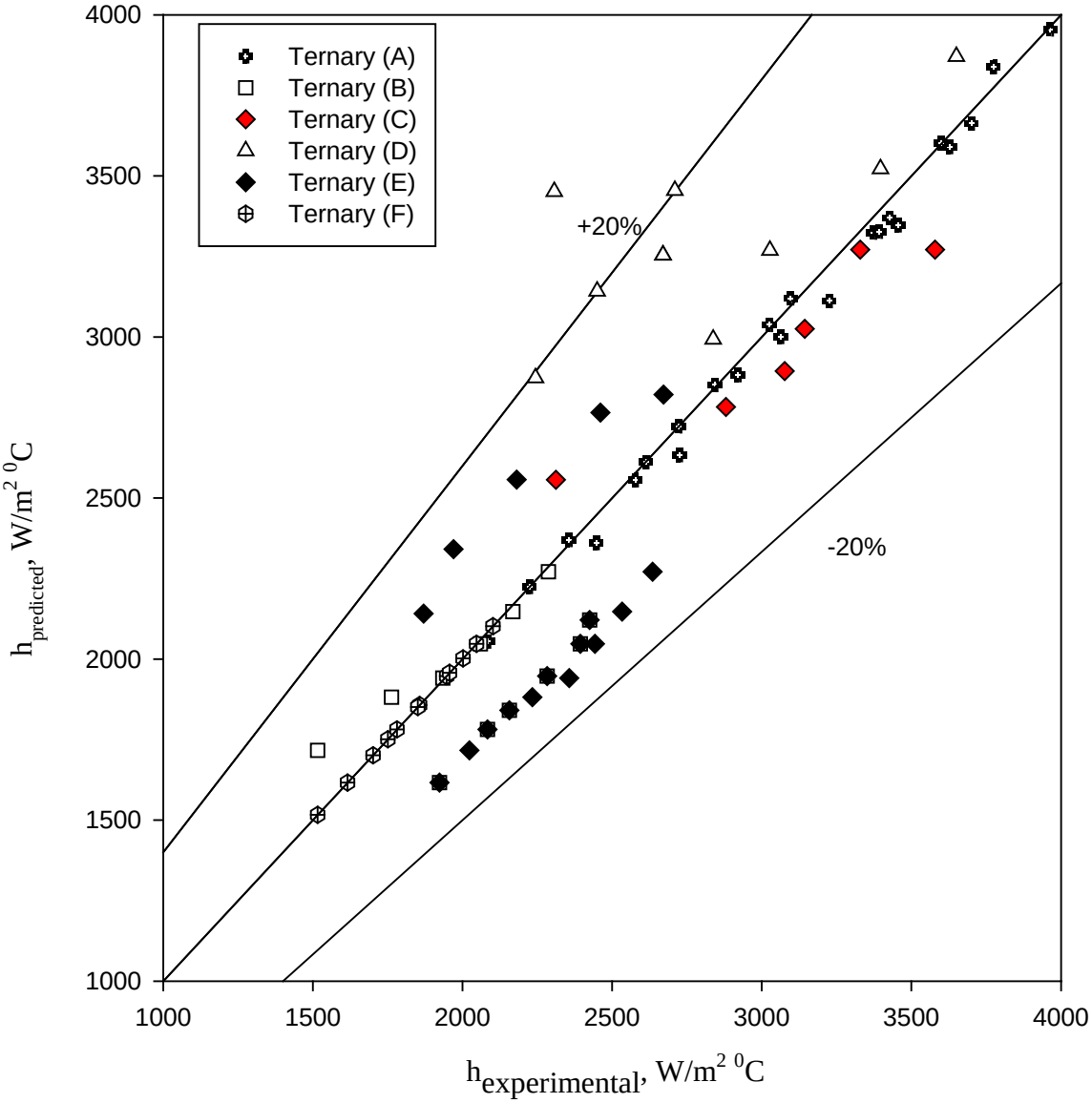

Figure 5.98 Comparison of experimental heat transfer coefficient with those predicted **Eq.(5.17)** for boiling of ternary mixture on a 25μm copper coated heating tube surface at atmospheric

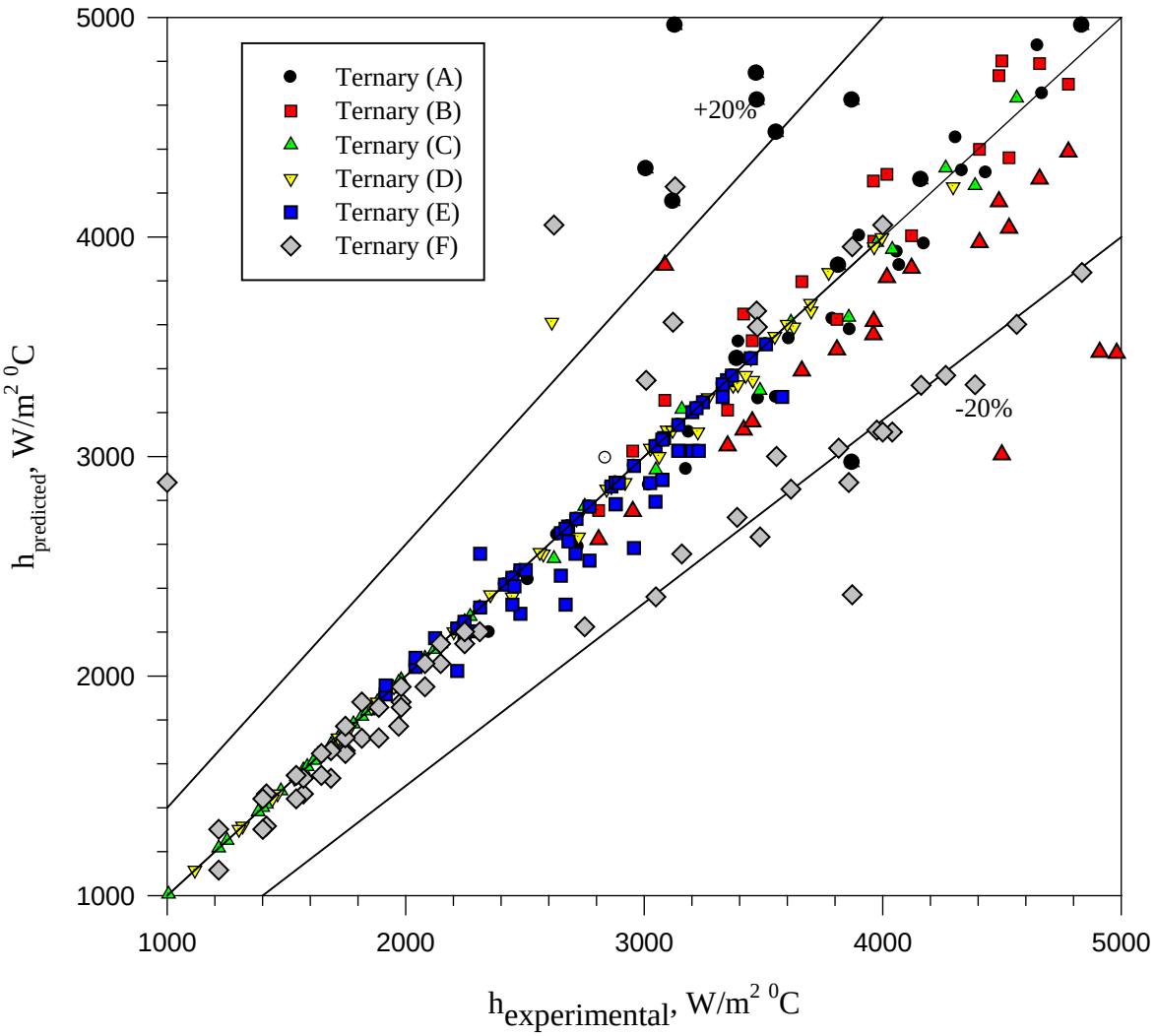

Figure 5.99 Comparison of experimental heat transfer coefficient with those predicted **Eq.(5.17)** for boiling of ternary mixture on a 25μm copper coated heating tube surface at subatmospheric

Remarks:- Above discussion is based on data for boiling of distilled water – methanol – iso-propanol ternary mixture at atmospheric pressure and sub-atmospheric pressure on 25 μm copper coated heating tube surface. Although, no study has been carried out on other similar ternary mixtures and on other coated surfaces. Yet the arguments advanced above clearly support that it should be valid for any ternary mixture having same characteristics (Non-azeotropic and non-ideal) also for a surface irrespective of thickness of coating on it. Therefore, no attempt should be made to extend the validity of above beyond its range of applicability i.e. non-azeotropic and non-ideal liquid mixture, similar to distilled water – methanol – iso-propanol mixture; atmospheric and sub-atmospheric pressures and copper coating on a brass heating tube surface.

Summary: Boiling of ternary mixtures of distilled water- methanol- iso-propanol on a copper coated heating tube surface at atmospheric and sub-atmospheric pressure has resulted in a similar behavior as that on an uncoated tube surface as regardless of the variation of heat transfer coefficient with respect to heat flux, pressure and concentration. Hence, heat transfer coefficient cannot be predicted from weighted mean of respective value of heat transfer coefficient of single component liquid. However, it can be calculated from the correlation, **Eq. (5.17)** developed above. These findings are quite similar to those obtained for uncoated heating tube surface. Hence, it can be concluded that boiling characteristics of a ternary mixture remains unchanged irrespective of heating surface being coated or not.

Chapter – 6

CONCULSIONS AND RECOMMENDATIONS

6.1 CONCLUSIONS

As a result of present investigation, following important conclusions emerge out:

1. Experimental data for nucleate pool boiling of distilled water, methanol and iso-propanol on an uncoated heating tube surface have been generated for wide range of heat flux at atmospheric and subatmospheric pressures. Analysis of data showed that surface temperature for a given value of heat flux, increases from the bottom to side, to top position and thus value of local heat transfer coefficient increases continuously from top to side, side to bottom position. The value of local heat transfer coefficient at a given circumferential position has been found to vary with heat flux according to power law relationship, $h \alpha q^{0.7}$ for various values of pressure of this investigation. An equation between local heat transfer coefficient, heat flux and pressure has been develop by regression analysis with in an error of ±8%
2. The average heat transfer coefficient of a liquid boiling on an uncoated tube at atmospheric and subatmospheric pressures has been found to vary with heat flux according to power law relationship $h \alpha q^{0.7}$. Further, heat transfer coefficient improves with the rise in pressure. Thus, heat transfer coefficient has been expressed as a function of heat flux and pressure by the relationship $h = C_1 q^{0.7} p^{0.32}$, where C_1 is a constant representing surface liquid concentration factor. Furthermore, this equation has been reduced into a non dimension form: $(h^* / h_1^*) = (P / P_1)^{0.32}$ where h^* refer $(h / q^{0.7})$ and subscript 1 denotes atmospheric pressure condition. Above equation is tested against experimental data for the boiling of distilled water, iso-propanol and methanol on an uncoated surface of this investigation: of water, methanol and iso-propanol and carbon-tetrachloride and n- butanol on a brass tube surface by Cryder and Finalborgo [C22]; of n-heptane on a copper plate surface by Cichelli & Bonilla [C13]; of distilled water, methanol, ethanol and iso-propanol on a brass tube surface by

Vittala et al. [V12]; of distilled water on a stainless steel tube surface by Bansal [B2]; of distilled water, benzene and toluene on a stainless steel surface by Bhaumik [B12]; of distilled water on mild steel heating tube surface by Alam et al. [A2]; of methanol on mild steel heat tube surface by Prasad et al.[P8]; and of iso-propanol on a mild steel heat surface by Prasad et al. [P8] and found to correlate them excellently with in an error of ranging -9% to +11 %.

Further, this non-dimension equation can be used to generate heat transfer coefficient for boiling of liquid at sub atmospheric pressure without conducting experimentation from the knowledge of experimentally determined value of heat transfer coefficient at atmospheric pressure only. Another important point is that it can also be used to examine the consistency of heat transfer data taken for the boiling of various liquids of heating surface of differing surface characteristics at atmospheric and sub atmospheric pressures.

3. Experimental data for the pool boiling of binary mixture of iso-propanol-distilled water and methanol- distilled water at atmospheric and subatmospheric pressure has resulted in analogous boiling characteristics as that of individual liquids. Hence, the variation of average heat transfer coefficient of binary liquid mixture with respect to heat and pressure remains the same as that of an individual liquid. It can be shown by relationship $h = C_2 q^{0.7} \mathrm{p}^{0.32}$, which has been obtained by regression analysis with in an error of ±8%; where C_2 is constant whose values depend upon composition of mixture and surface characteristic. Further, above equation has been reduced into a non-dimensional form: $(h^* / h_1^*) = (P / P_1)^{0.32}$. It has been tested against experimental data for the boiling of various composition of methanol-distilled water and iso-propanol-distilled water mixtures on a uncoated brass heating surface at atmospheric and subatmospheric pressures of this investigation, and of methanol-distilled water mixtures, ethanol-water mixtures and iso-propanol water mixtures due to Pandey [P3]; methanol-distilled water due to Alam [A3], on a plain stainless steel surface at atmospheric and subatmospheric pressures and found to correlate them with the maximum deviation ranging from -11 to +21%.
4. The experimental data for pool boiling of distilled water-methanol-iso-propanol ternary mixture at atmospheric and sub atmospheric pressures has resulted same boiling characteristics as that of individual liquids and their binary mixture.

Hence, variation of average heat transfer coefficient of a ternary liquid mixture with respect to heat flux and pressure can be represented by the relationship $h = C_3 q^{0.67} p^{0.33}$, which has been obtained by regression analysis with in an error of ± 8.5%, where C_3 is a constant whose value depends upon composition and surface characteristics. Further, above equation has been reduced into an non-dimensional form $(h^* / h_1^*) = (P / P_1)^{0.33}$. This equation has been tested against experimental data for the various compositions of ternary mixtures at atmospheric and subatmospheric of this investigation; and of methanol-1pentanol and ternary mixture of methanol/1-pentanol/ 1-2 Propanoldiol due to Nahara & Naess [N1] on carbon steel surface at atmospheric pressure using different roughness of the heating surface and found to correlate them with maximum deviation ranging from -12 to +24%.

5. Heat transfer coefficient of ternary mixture has been found to decrease with increase in concentration of highest volatile component (methanol and attains a distinct minimum turn around 30 mole percent of methanol concentration. Beyond this concentration of methanol heat transfer coefficient increases with increase in concentration of methanol. Further, increase in pressure has lead to increase the value of heat transfer coefficient of the mixture but does not change the turnaround concentration. Based on this, a correlation,

   $$(h / h_{id}) = (\Delta T_{id} / \Delta T) = [1 + | y_1 - x_1 | \sqrt{\alpha_1 / D_1} + | y_2 - x_2 | \sqrt{\alpha_2 / D_2}]^{-(0.73x1+0.36)}$$

   has been developed to determine heat transfer coefficient of ternary mixture from the knowledge of heat transfer coefficients of individual liquids, phase equilibrium data and physico thermal properties of the mixture. This equation has correlated all the experimental data of this investigation with an error of ±18% as well as those predicted by other [C1, F5, H3, J7, S15, T5, T7] with an error of ±25%.

6. Experimental data of nucleate boiling of distilled water on brass tubes coated with various thicknesses of 15, 25 and 35 μm copper coating have been generated for different value of heat flux. Analysis of data showed that heat transfer coefficient is found to vary according to power law relationship $h \alpha q^r$, where the value of exponent (r) depend on the thickness of copper coating, in fact, the value of exponent (r) is always less than 0.7, which generally holds true, for

boiling of liquids on an uncoated surface. Further, it has also been found to decreases with increase in thickness of coating. Thus, heat transfer coefficient of distilled water has been found to increase with coating. This phenomenon continues up to a particular value of the coating thickness and thereafter decreases with further increase in coating thickness. Enhancement on 25 μm coated tube is the highest to the tune of 55% more than that of uncoated brass tube. A dimensional relationship $h = C_4 q^r p^s$ has been developed to correlate heat transfer coefficient for boiling of distilled water on coated surface with heat flux and pressure. The value of constant C_4 and exponent (r) and (s) depend upon thickness of coating and heating surface characteristics. Similar observations have also been obtained for the boiling of methanol, iso-propanol on 25 μm thick copper coated heating tube surface. A dimensional relationship, $h = C_4 q^v p^w$ have been developed to obtain heat transfer coefficient for boiling of methanol, iso-propanol on a 25μm thick coated tube surface, where constant C_4 and exponent (v) and (w) depends upon the boiling liquids.

7. Experimental data for pool boiling of methanol-distilled water and iso-propanol-distilled water binary mixtures at atmospheric and subatmospheric pressures on a 25μm copper coated tube have resulted in similar trend as obtained for the boiling liquids and their mixtures on a uncoated tube. A functional relationship among heat transfer coefficient, heat flux and pressure, on 25μm copper coated brass tube has been obtained by regression analysis as $h = C_5 q^{0.57} p^{0.36}$, where the value of C_5 depend upon the concentration of high volatile component in the mixture and heating surface characteristics.
8. The experimental data of pool boiling distilled water-methanol-iso-propanol a ternary mixtures at atmospheric and subatmospheric pressure on 25μm copper coated tube has shown the same trend as observed for boiling of liquids and their binary and ternary mixtures on an uncoated tube. A functional relationship amongst heat transfer coefficient, heat flux and pressure on a 25 μm copper coated brass tube has been developed and shown as $h = C_6 q^{0.58} p^{0.36}$, where the value of constant C_6 depends upon concentration of highest volatile component it the ternary mixture and heating surface characteristics.

9. It has been observed that application of copper coating on brass heating tube surface does not change the turnaround concentration of highest volatile component (methanol) in a ternary mixture. In equation addition, the correlation $(h/h_{id}) = (\Delta T_{id}/\Delta T) = [1+|y_1 - x_1|\sqrt{\alpha_1/D_1} + |y_2 - x_2|\sqrt{\alpha_2/D_2}]^{-(0.73x1+0.36)}$ has been developed for boiling of mixture on an uncoated tube is also valid for boiling of liquid mixture on a 25μm thick copper coated tube as well. This correlation has been compared with the experimental data for boiling of ternary mixture of this investigation on a 25μm thick copper coated tube and found to match very well with ±20%

6.2 RECOMMENDATIONS

1. The present investigation has been confined to saturated pool boiling of water, methanol, iso-propanol and their binary and ternary liquid mixtures on an uncoated brass tube surface for various values of heat flux at atmospheric and subatmospheric pressures. Hence, correlation developed in this investigation is valid for operating condition of this investigation. It is desirable that more experimental data should be generated at pressure higher than one atmosphere. Further, investigation should also include other industrial liquids like refrigerants, hydrocarbons, cryogenics, solvents, etc. to obtain generalized inferences.
2. In the present investigation the effect of thickness of copper coating on a brass tube for the boiling liquid and their mixture has been determined. However, it will be worthwhile to investigate the effect of other metallic coating materials such as silver, molybdenum, cadmium, zinc, aluminum etc on boiling heat transfer characteristics.
3. Measurement of contact angle made by liquid droplet over a uncoated as well as coated tube surfaces could not be made in this investigation due to lack of instrumental facility. However, it is desirable to include such studies as it likely to provide strength to arguments advanced for phenomena occurring thenin.
4. Plasma technique is employed in this investigation for coating of copper on brass tube. It is recommended that other techniques such as thermal spray,

sintering, spurting etc, should be investigated to obtain there role in enhancement of boiling heat transfer coefficient on coated tubes.

5. This investigation has been confined for boiling of distilled water, methanol, iso-propanol and their binary and ternary mixture only. It is recommended that experiments on other industrially important liquid binary their ternary mixtures such as water-acetic acid, water-acetone, and other multicomponent liquids mixtures should also be used for investigation to obtain the generalized conclusions.